PROJECT SERV FINAL REVIEW

PHASE A SPACE SHUTTLE STUDY

CONTRACT NAS8-26341 MSFC-DRL-214 DRD MA-077-U3

JULY 1, 1971

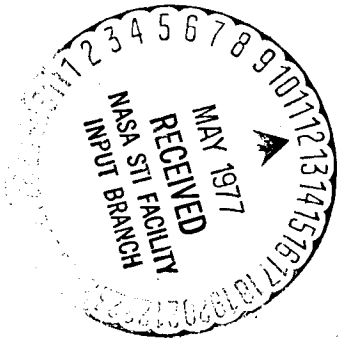

Approved by: C.E. Tharratt

C.E. Tharratt, Manager - Project SERV

Prepared by:

CHRYSLER CORPORATION SPACE DIVISION – POST OFFICE BOX 29200 – NEW ORLEANS, LA. 70129

PROJECT SERV

SPACE SHUTTLE FEASIBILITY STUDY

FINAL REVIEW

Contract NAS8-26345

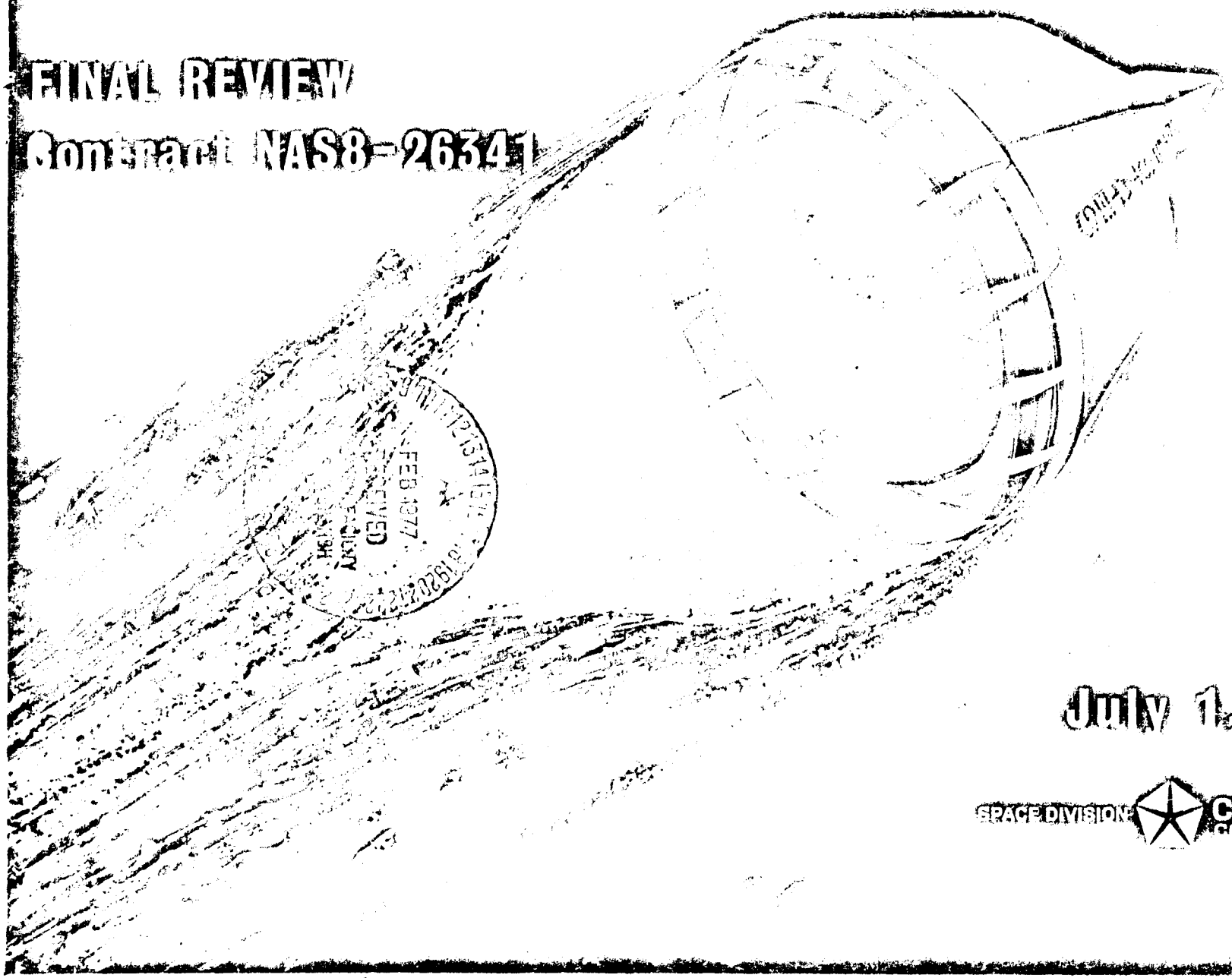

July 15, 1971

SPACE DIVISION CHRYSLER CORPORATION

15541

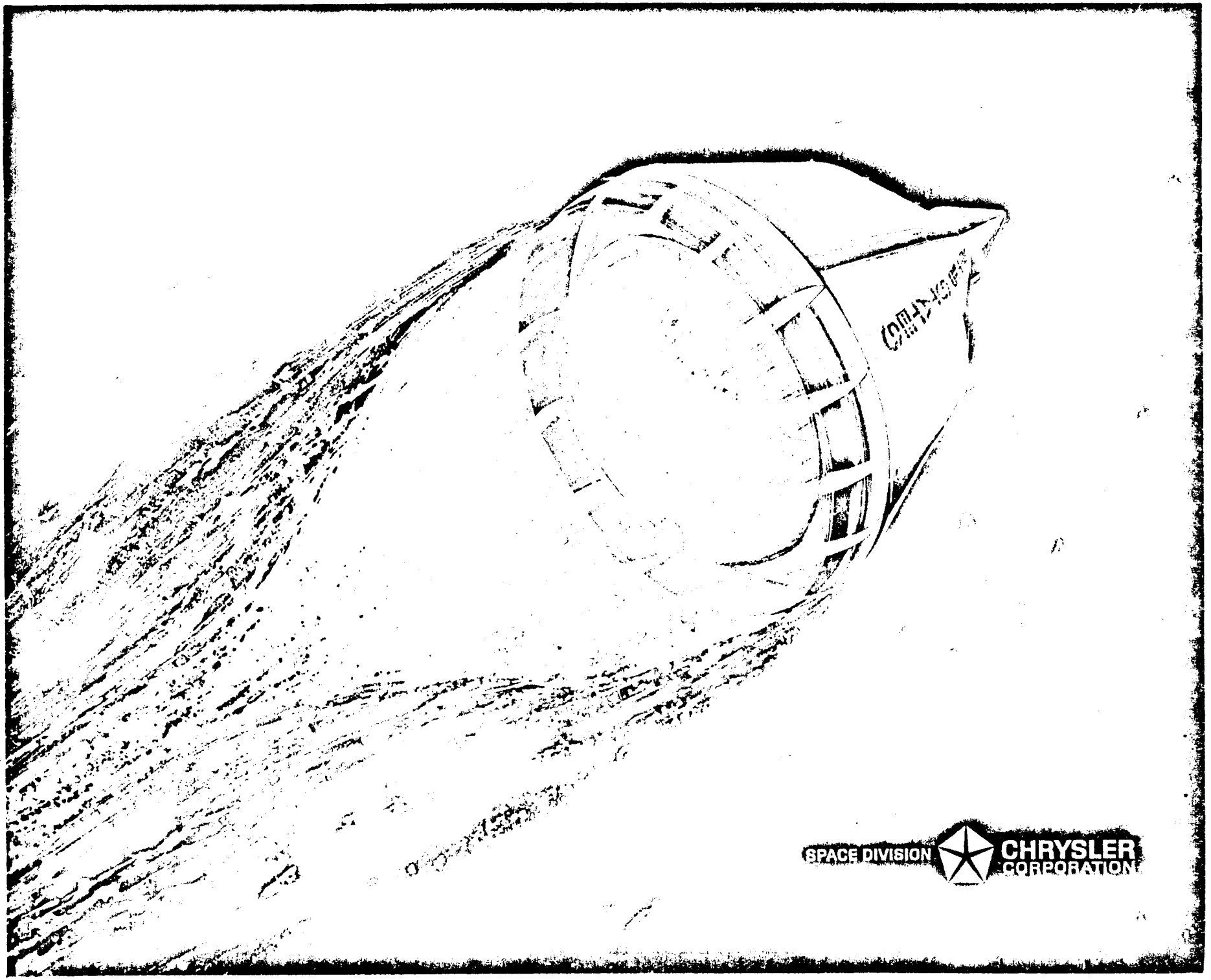
SPACE DIVISION
CHRYSLER
CORPORATION

FOREWORD

This final review document is submitted in accordance with DRD requirements of Contract NAS8-26341, the feasibility study of a Single-stage, Earth-orbital Reusable Vehicle (SERV). The final review is a description of work accomplished under all study tasks, with primary emphasis on results of the vehicle and program definition effort completed after the mid-term review. Questions concerning this study material should be directed to the following persons:

National Aeronautics and Space Administration
George C. Marshall Space Flight Center
Marshall Space Flight Center, Alabama 35812

R. J. Davies 205-453-0480

Chrysler Corporation Space Division
Post Office Box 29200
New Orleans, Louisiana 70129

C. E. Tharratt 504-255-2385
W. R. Baldwin 504-255-2385

TABLE OF CONTENTS

TABLE OF CONTENTS (continued)

TABLE OF CONTENTS (continued)

TABLE OF CONTENTS (continued)

AGENDA

- INTRODUCTION
- FINAL CONFIGURATION DEFINITION
- VEHICLE FLIGHT PERFORMANCE
- AEROSPIKE PROPULSION PERFORMANCE
- AERODYNAMIC CHARACTERISTICS
- THERMAL PROTECTION CHARACTERISTICS
- FLIGHT CONTROL CHARACTERISTICS
- SUBSYSTEM DESIGN
- OPERATIONS AND FACILITIES
- SCHEDULES AND COSTS
- CONCLUSIONS AND RECOMMENDATIONS

INTRODUCTION

Section 1
INTRODUCTION

1.1 STUDY APPROACH

The potential advantage of the SERV concept could become reality if the feasibility of the concept can be established. Previous Chrysler in-house studies indicated the concept was feasible within the limitations of available data; however, it was recognized that certain technical aspects for determining feasibility required inputs of higher quality data than those available before the concept can progress to a preliminary definition phase. It was planned to obtain the improved data during the course of this study contract.

1.1.1 STUDY OBJECTIVE AND EXPECTED RESULTS

The study objective was to further assess the feasibility of the SERV concept by selecting an appropriate configuration, determining the feasibility of the large diameter aerospike engine to meet the SERV requirements, and performing a more definitive design and weight analysis to support the necessary single-stage mass fraction requirements.

Study effort was divided into seven tasks, the output of which form the expected results. A brief synopsis of these expected results is as follows:

1) The development of the vehicle configuration to be used as the initial or preliminary baseline for the study, including a detailed comparison with previous single-stage-to-orbit vehicles.

2) Determination of base flow characteristics, and the determination of ascent and reentry static stability and drag characteristics for the baseline vehicle.

3) Substantiation of baseline concept, including the aerospike engine, through trade studies and parametric vehicle sizing analysis.

4) A point design of a selected configuration and its aerospike engine, including concept sensitivities.

5) Minimum definition of operations, plans, schedules and costs.

STUDY OBJECTIVE AND EXPECTED RESULTS

OBJECTIVE – FURTHER ASSESS SERV CONCEPT FEASIBILITY

- SELECT APPROPRIATE CONFIGURATION
- DETERMINE FEASIBILITY OF SERV AEROSPIKE ENGINE
- PERFORM MORE DEFINITIVE DESIGN AND WEIGHT ANALYSES

EXPECTED RESULTS

- DEVELOP BASELINE VEHICLE CONFIGURATION
- DETERMINE BASE FLOW AND AERODYNAMIC CHARACTERICS
- PERFORM TRADE STUDIES AND PARAMETRIC SIZING STUDIES
- DEVELOP POINT DESIGN OF SELECTED CONFIGURATION
- IDENTIFY REQUIRED RESOURCES FOR SERV PROGRAM

1.1.2 PRINCIPAL GROUND RULES

The NASA-approved ground rules were patterned after those of the other shuttle studies wherever possible to ensure the best possible comparison.

PRINCIPAL GROUND RULES

- FULLY REUSABLE SINGLE-STAGE-TO-ORBIT VEHICLE, SPACECRAFT STUDY EXCLUDED
- VERTICAL TAKE OFF AND LANDING
- REFERENCE MISSION IS LOGISTICS RESUPPLY OF SPACE STATION
- DESIGN REFERENCE ORBIT IS 270-NM CIRCULAR BY 55-DEG INCLINATION FROM 28.5 DEGREES NORTH LATITUDE
- 25,000 LB OF GROSS CARGO TO 55-DEG 270-NM ORBIT AND RETURN
- MAXIMUM PAYLOAD CAPABILITY TO POLAR ORBIT AND TO LOW INCLINATION ORBIT TO BE IDENTIFIED
- CARGO HOLD SIZED FOR A MINIMUM CLEAR VOLUME OF 15-FT DIA X 60-FT LONG
- BASELINE ASCENT MAIN PROPULSION IS AN INTEGRAL AEROSPIKE ROCKET ENGINE
- BASELINE LANDING PROPULSION IS AN ARRAY OF JET ENGINES USING JP-4 FUEL
- INTACT ABORT CAPABILITY TO BE PROVIDED
- PEAK ACCELERATION AND DECELERATION NOT TO EXCEED 3G
- RETURN TO PRESELECTED SITE MINIMUM OF ONCE EVERY 24 HOURS
- VEHICLE LIFE OF 10 YEARS AND 100 MISSIONS

1.1.3 CONTRACTOR PARTICIPATION

Two major subcontracts were awarded for the SERV study, both to the Rocketdyne Division of North American Rockwell Corporation. The first subcontract was to manufacture a 2.5 percent scale model of the SERV for cold-flow (air) testing in the 16-foot Propulsion Wind Tunnel at AEDC. This effort consisted of fabrication, assembly, test, and calibration, including a mounting system with forward sting. The second subcontract provided for cold-flow model design, cold-flow testing support, propulsion analysis and design for baseline vehicle development and trade studies, and an aerospike engine point design.

In addition, two smaller subcontracts were awarded, one to Standard Tool and Die, Incorporated, for manufacture of aerodynamic force models and one to Microcraft, Incorporated, for manufacture of a cold-flow pilot test model.

Acknowledgement is made to the Space Division of North American Rockwell Corporation for providing available data for the MURP spacecraft. Acknowledgement is also made to the Detroit Diesel Allison Division of General Motors Corporation for furnishing available data on direct-lift gas turbine engines and providing valuable technical assistance. In addition, acknowledgement is made to the AVCO Systems Division for providing available data on thermal protection materials.

CONTRACTOR PARTICIPATION

NR ROCKETDYNE DIVISION	• SUBCONTRACTED TO MANUFACTURE 2.5 PERCENT COLD FLOW MODEL • SUBCONTRACTED FOR MODEL DESIGN, TEST SUPPORT, AEROSPIKE ENGINE PARAMETRIC DATA AND DESIGN
STANDARD TOOL & DIE, INC.	• SUBCONTRACTED TO MANUFACTURE ASCENT AND DESCENT FORCE MODELS
MICROCRAFT, INC.	• SUBCONTRACTED TO MANUFACTURE COLD-FLOW PILOT MODEL
NR SPACE DIVISION	• PROVIDED AVAILABLE DATA ON MURP SPACECRAFT
GM ALLISON DIVISION	• PROVIDED AVAILABLE DATA ON DIRECT LIFT GAS TURBINE ENGINES
AVCO (SYSTEMS DIVISION)	• PROVIDED AVAILABLE DATA ON THERMAL PROTECTION ALTERNATES

1.1.4 CURRENT STUDY SCHEDULE

A summary of the study schedule identifying the critical path is presented to indicate the final status of the study contract.

CURRENT STUDY SCHEDULE IDENTIFYING CRITICAL PATH

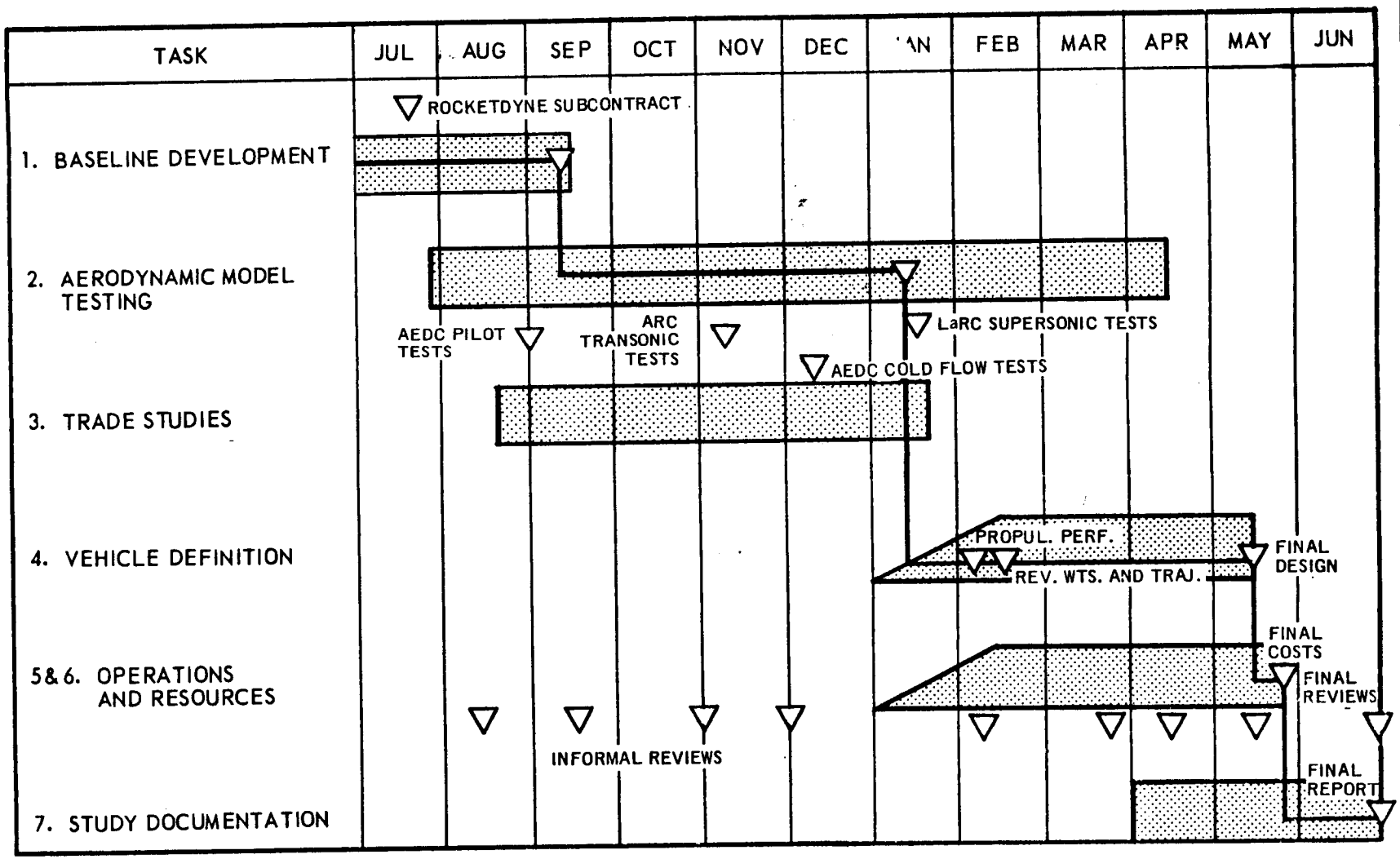

SPACE DIVISION CHRYSLER CORPORATION

1.2 BASELINE DEVELOPMENT

Because SERV has unorthodox features, NASA directed that Task 1 of this study be mainly devoted to researching past single-stage-to-orbit (SSTO) studies to ensure that accumulated experience and desirable system characteristics identified in those studies were incorporated in the development of a baseline vehicle. This baseline SERV was to form the starting point of all further study effort. Nine SSTO vehicles, including SERV, were examined. They varied from SASSTO to NEXUS; a range in gross liftoff weight of approximately 220 thousand to 24 million pounds. The diverse nature of the nine configurations ranged from the non-recoverable MLLV (most efficient SSTO due to its low drag ascent profile) through several partially recoverable concepts that are not appropriate for current NASA requirements, to several vehicles that could be considered or adapted to be fully reusable.

1.2.1 PRIMARY CONSIDERATIONS

From these investigations, it was established that the most important considerations in vehicle subsystem characteristic selection were the study ground rules, ascent propulsion, reentry and landing mode, external shape and internal arrangement. Of these considerations, study ground rules were the most influential. The SERV study ground rule of 3g maximum deceleration during reentry greatly influenced, or essentially dictated, the external configuration. The characteristics of SERV were recognized as a compromise between ascent and reentry performance; the former, requiring a slim, low drag, ascent profile; the latter a low weight, large frontal area, high drag profile of low reentry ballistic factor (W/C_DA).

The internal arrangement was demonstrated to be greatly influenced by the need to package the ascent and landing propulsion and propellant tanks within the mission-dictated external shape in as small a volume as possible.

The trade study baseline was not changed as a result of these investigations.

PRIMARY CONSIDERATIONS IN BASELINE DEVELOPMENT

SERV/SSTO COMPARISON:

- GROUND RULES
- ASCENT PROPULSION
- REENTRY AND LANDING MODES
- EXTERNAL SHAPE
- INTERNAL ARRANGEMENT

CONCLUSIONS:

- SERV EXTERNAL SHAPE DICTATED BY GROUND RULES
- INTERNAL ARRANGEMENT INFLUENCED BY PROPULSION AND PROPELLANT TANK PACKAGING
- NO CHANGE TO BASELINE VEHICLE AS RESULT OF SSTO COMPARISON

1.2.2 TRADE STUDY BASELINE

The baseline vehicle for trade study consideration and aerodynamic model tests is presented here. Key features are identified and changes are summarized under trade study results.

This vehicle has a liftoff weight of 4.5 million pounds, a liftoff thrust of 5.4 million pounds, and boosts 88,060 pounds to the baseline mission parking orbit of 100 nautical miles at 55 degrees inclination. Vehicle diameter is 90 ft and the cargo hold dimensions are 23 feet in diameter by 60 feet in length. The 12-module LO_2/LH_2 integral aerospike engine is 88.7 feet in diameter by 8.2 feet in length and has a sea-level and vacuum specific impulse of 346.7 seconds and 469.5 seconds, respectively. An installation of 28, JP-4 fuelled turbo jet lift engines provides deceleration and landing propulsion.

BASELINE VEHICLE ARRANGEMENT

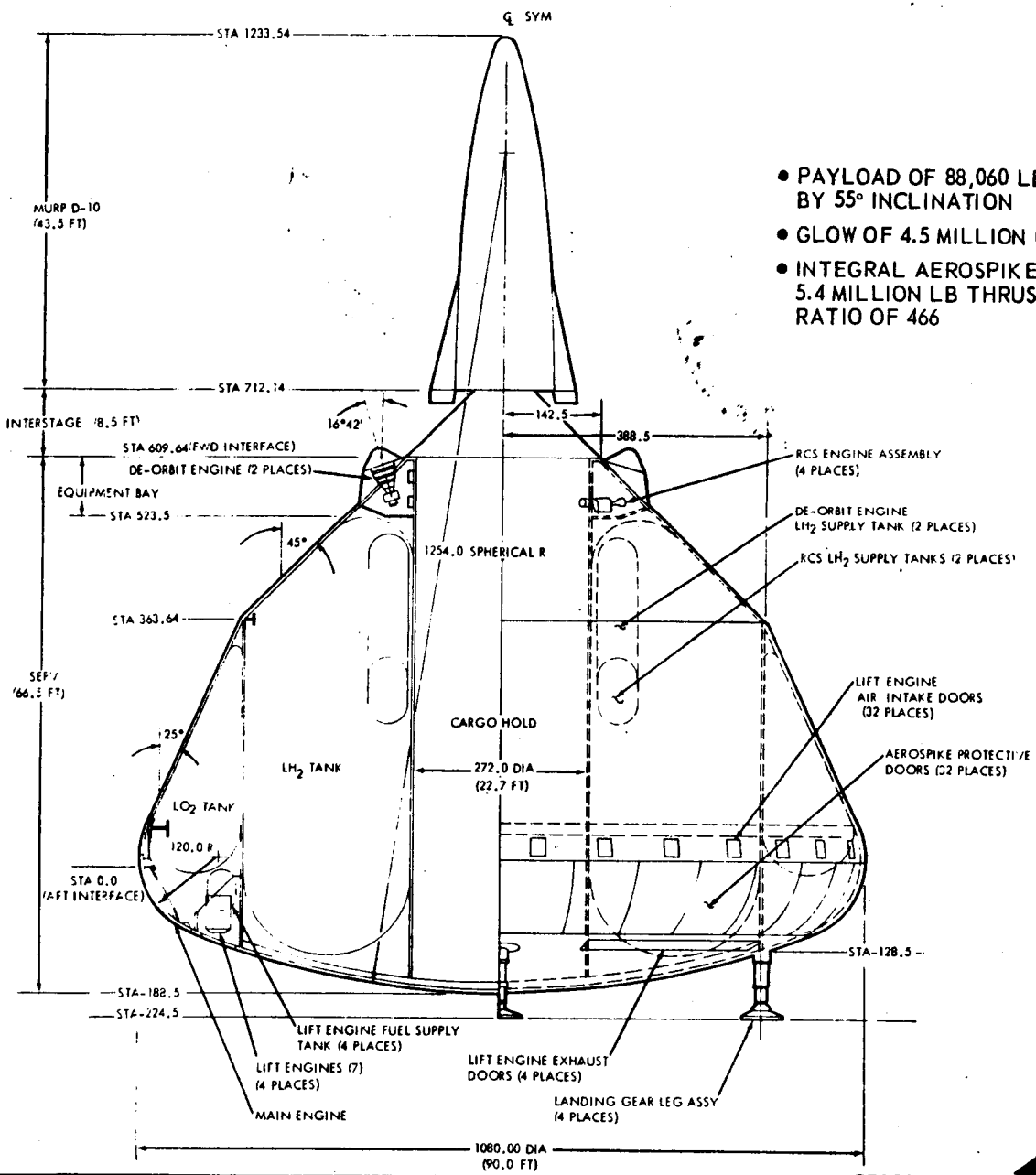

- PAYLOAD OF 88,060 LB TO 100 N MI BY 55° INCLINATION
- GLOW OF 4.5 MILLION LB
- INTEGRAL AEROSPIKE ENGINE WITH 5.4 MILLION LB THRUST AND AREA RATIO OF 466

7

SPACE DIVISION CHRYSLER CORPORATION

1.2.3 SERV OPERATION

SERV is propelled to earth orbit by the thrust of an integral aerospike rocket engine. In operation, the SERV with a spacecraft and a cargo module as its payload takes off vertically from the Kennedy Space Center (KSC) and goes to a 100 nm orbit in the plane of a space station. The spacecraft then extracts the cargo module from SERV and transfers the cargo to the space station in higher orbit. Following a transfer of cargo to and from the space station, the spacecraft returns with the cargo module and docks to SERV in lower orbit. If an optional winged spacecraft is used, the spacecraft disengages after docking the cargo module and returns to earth using swing wings in the lower atmosphere. Due to a relatively high hypersonic L/D it has a cross range capability of 1800 nm.

SERV remains in low earth orbit until required to reenter and return to KSC. To accomplish this reentry, SERV reorients itself to the familiar Apollo command module reentry attitude and reenters the atmosphere semiballistically. With SERV, however, the target landing point is on land instead of water, and more specifically, within operational distance from the Vertical Assembly Building (VAB) at KSC. Using current Apollo reentry navigation and guidance technology, SERV will be within 4 miles of the landing pad when it is at 25, 000 ft. Before this point, SERV will be tracked by radar, and a ground based command transmitter will be transmitting SERV landing site coordinate data. At 25, 000 ft altitude, air intakes and doors for exhaust efflux open and ignition of four quadrants of direct lift gas turbine engines occurs.

The landing phase begins at approximately 15, 000 ft with the gas turbine thrust being used to horizontally translate and decelerate the vehicle to a hover above the landing pad. The landing gear is deployed and a controlled descent to the landing pad is initiated. Final descent and touchdown is similar in operation to that of a helicopter.

SERV OPERATION

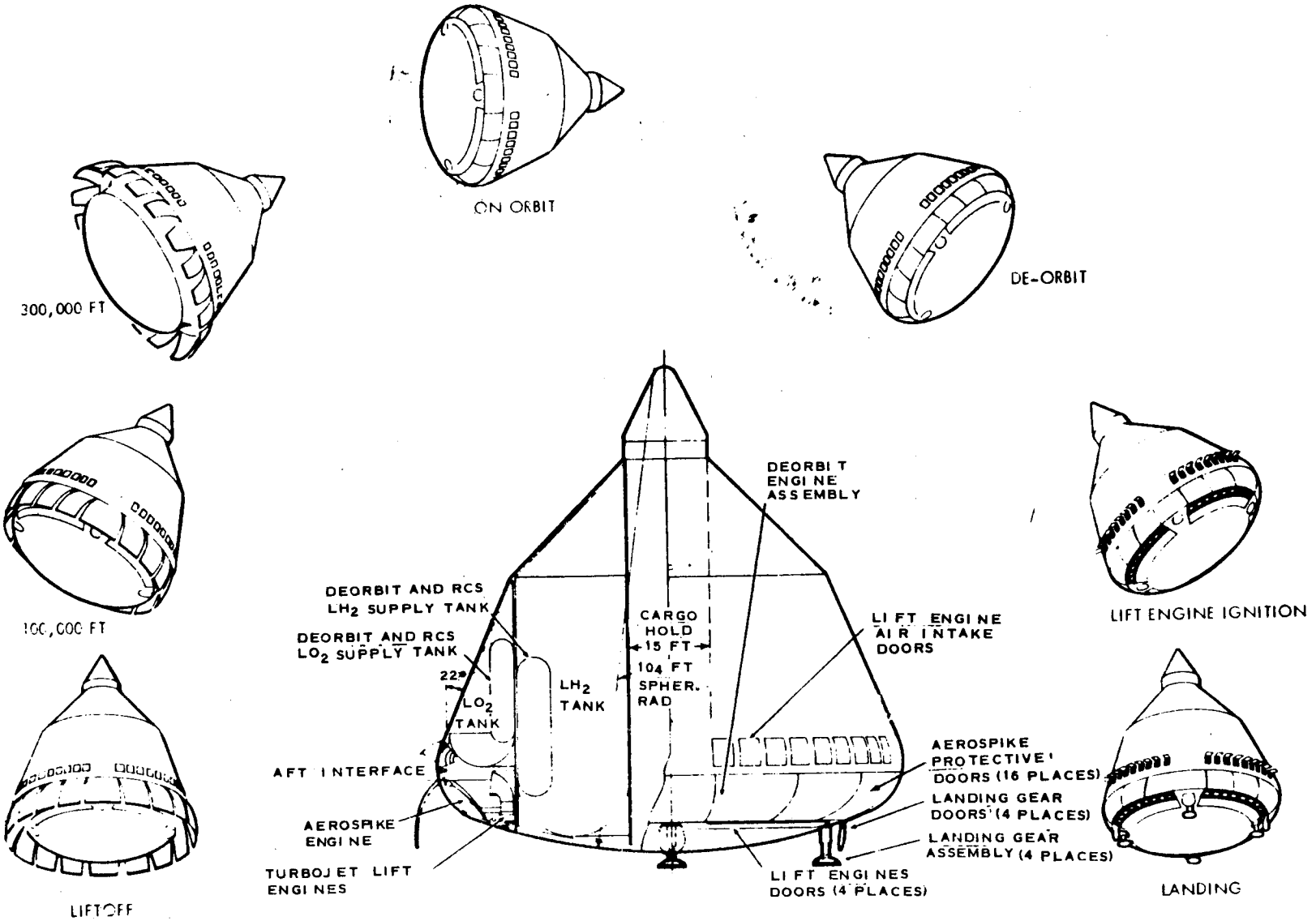

1.3 TRADE STUDY RESULTS

Trade study results were described in detail in the November 30th Status Review and the February 10th Mid-Term Review, and only a brief summary is presented here.

1.3.1 KEY FEASIBILITY ISSUES

The potential of SERV depends chiefly on the satisfactory solution of six key issues affecting concept feasibility. These issues are arranged on the chart with respect to their affect on the ascent and descent SERV configurations. Engine performance, aerodynamic drag, and subsystem weights have a decisive collective influence on vehicle ascent performance; i.e., the ability to meet mission objectives. The method and type of thermal protection during the reentry environment, descent aerodynamic characteristics, and landing method, determine the attractiveness of SERV as a recoverable and reusable space shuttle. These subjects were investigated during the trade study period, with incorporation of results from supporting aerodynamic model tests.

KEY FEASIBILITY ISSUES

ASCENT CONFIGURATION

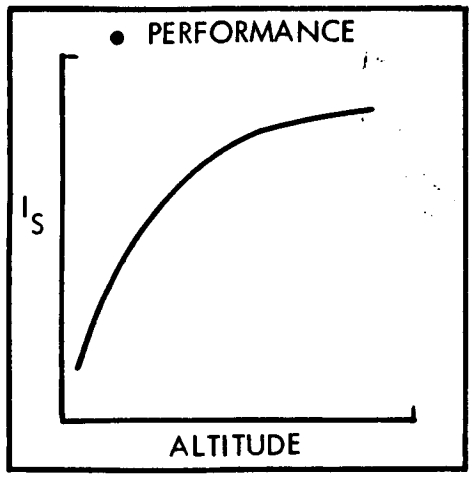

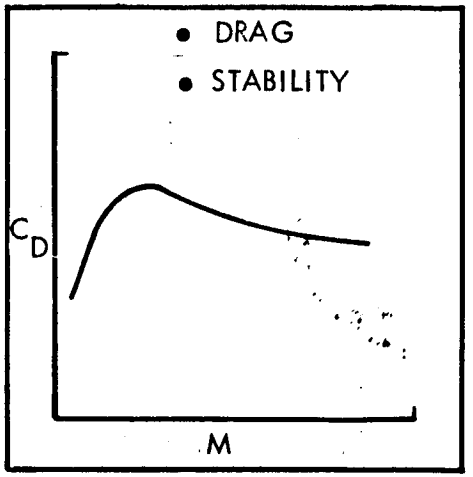

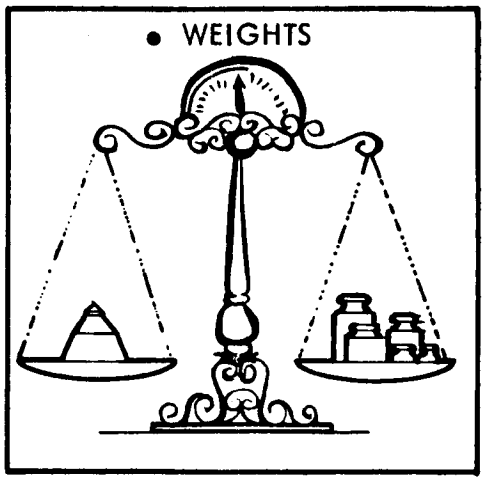

DESCENT CONFIGURATION

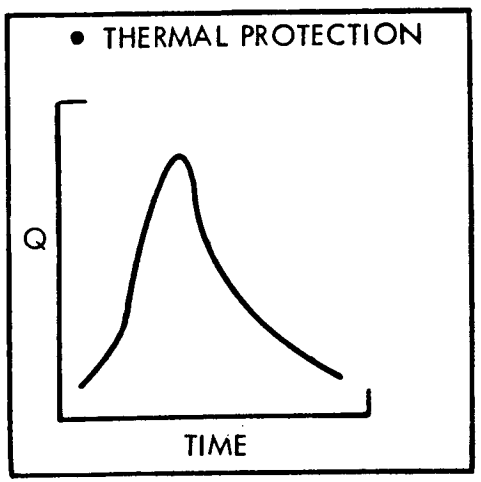

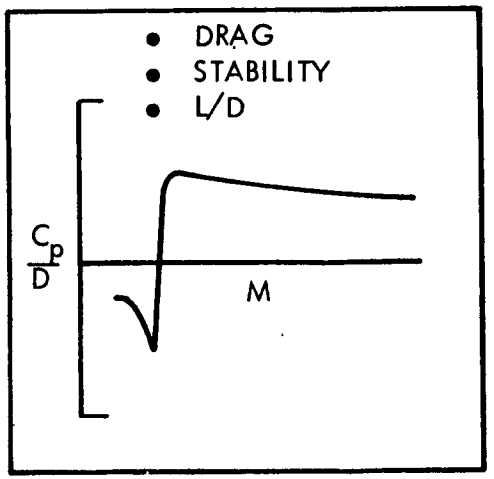

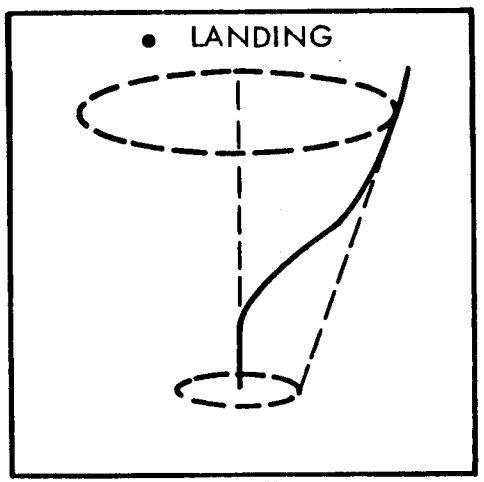

1.3.2 CONCEPT EVALUATION AREAS

Subsystem trade analyses were performed in seven areas, as indicated on the chart: ascent configuration, structural and vehicle arrangement, descent configuration, avionics, auxiliary propulsion, ascent propulsion, and landing propulsion. The results of these analyses were reflected as changes to the vehicle dry weight.

CONCEPT EVALUATION AREAS

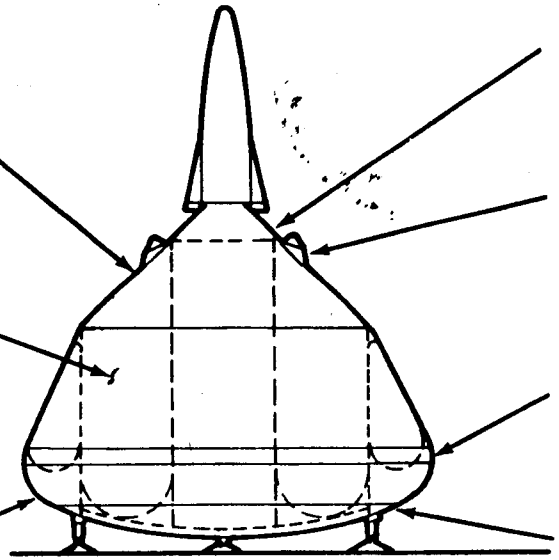

ASCENT CONFIGURATION

- ALTERNATE PAYLOAD SHAPES
- AEROSPIKE DOOR SHAPE AND OPERATION
- THERMAL PROTECTION
- VEHICLE SIZING

STRUCTURAL AND VEHICLE ARRANGEMENT

- PRIMARY STRUCTURE ALTERNATIVES
- STRUCTURAL MATERIAL ALTERNATIVES
- AEROSPIKE AND TURBOJET INSTALLATION
- HIGH-PRESSURE BELL ENGINE INSTALLATION
- PROPELLANT TANK INSULATION
- THERMAL PROTECTION DOOR INSTALLATION
- LANDING GEAR INSTALLATION
- BASE HEAT SHIELD INSTALLATION
- VEHICLE SIZING

DESCENT CONFIGURATION

- L/D AND W/C_DA CONFIGURATION ALTERNATIVES
- INSULATION MATERIALS
- HEAT SHIELD DESIGN ALTERNATIVES
- HEAT SHIELD DOOR SEALS AND OPERATION
- AEROSPIKE PROTECTION DOOR ALTERNATIVES
- LANDING GEAR ALTERNATIVES
- VEHICLE SIZING

AVIONICS

- GN&C
- POWER
- COMMUNICATIONS

AUXILIARY PROPULSION

- PITCH-YAW CONTROL ALTERNATIVES
- ROLL CONTROL ALTERNATIVES
- DEORBIT ALTERNATIVES

ASCENT PROPULSION

- ENGINE COMPARTMENT ARRANGEMENT
- AEROSPIKE INTERNAL ARRANGEMENT
- AEROSPIKE DUAL COMBUSTOR ALTERNATIVE
- PROPELLANT TANKAGE ARRANGEMENT
- HIGH-PRESSURE BELL ENGINE ALTERNATIVE

LANDING PROPULSION

- TURBOJETS VERSUS TURBOFANS
- LANDING ROCKET VERSUS TURBOJET
- AEROSPIKE RESTART VERSUS TURBOJET
- JP-4 VERSUS HYDROGEN FUEL
- JET INLET AND OUTLET GEOMETRIES

FINAL CONFIGURATION DEFINITION

11

SPACE DIVISION CHRYSLER CORPORATION

Section 2

FINAL CONFIGURATION DEFINITION

2.0 GENERAL

In this section the SERV configuration evolution and sizing criteria, and final definition are discussed.

2.1 SERV CONFIGURATION EVOLUTION

The chart traces the evolution of SERV during the study. The trade studies commenced with a baseline SERV of 90-ft diameter and a 4.5 million pound GLOW. Incorporation of results obtained from wind tunnel tests to establish the aerodynamic characteristics and to determine the aerospike engine performance, plus more definitive evaluation of structural, mechanical, and propulsion subsystem requirements initiated a resizing of the vehicle. During this activity it was decided to size a SERV capable of transporting a MURP spacecraft plus propulsion adaptor and cargo to orbit and returning a personnel module (PM) plus propulsion adaptor and cargo to earth. The weights of these ascent and reentry payloads have a significant influence on vehicle size. Thus the 88-ft diameter "hybrid" SERV evolved with a GLOW of 4.733 million pounds.

The 88-ft diameter "hybrid" SERV, shown on the chart, was used as a baseline for point design analyses. During these analyses the LH_2 propellant tank bulkhead was raised to provide additional space for tank sumps, additional thermal protection was incorporated to reduce the effect of thermal gradients across the primary structural shell, the propulsion subsystem weights were revised, and the results of a detailed stress analysis were incorporated. A final sizing of the vehicle was initiated to incorporate these changes. At the same time final aerospike engine performance data was used and the propellant tanks were increased in size to accommodate a minimum CEI performance of the aerospike engine. The output of this final sizing was a revised baseline 96 ft in diameter and 6.049 million pound GLOW.

SERV CONFIGURATION EVOLUTION

TRADE STUDY
BASELINE
(SERV-MURP)

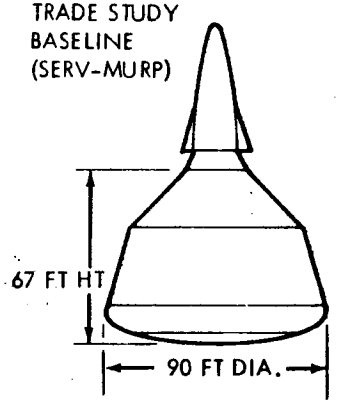

VEHICLE DEFINITION
HYBRID BASELINE
(SERV-PM CONFIGURATION)

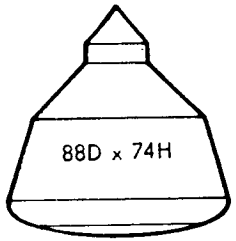

VEHICLE DEFINITION
HYBRID BASELINE
(SERV-MURP CONFIGURATION)

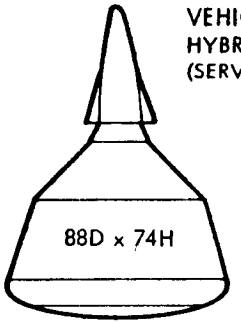

RECOMMENDED HYBRID
CONFIGURATION FROM
FINAL SIZING

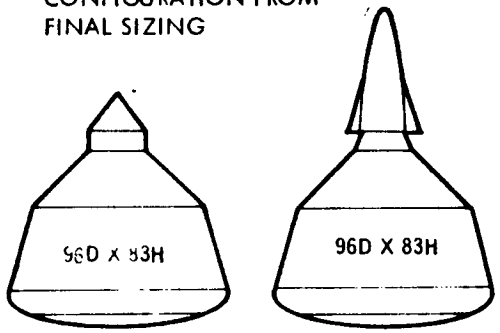

SPACE DIVISION CHRYSLER CORPORATION

2.2 PAYLOAD CRITERIA FOR SIZING HYBRID CONFIGURATIONS

Basic dimensions and summary weight breakdowns are given here for the two spacecraft under consideration. These two spacecraft were specified for study to evaluate the effect of long and short cross-range reentry vehicles aboard SERV.

Note that the hybrid SERV configurations are sized by the MURP mission payload during ascent and PM mission payload for landing.

PAYLOAD CRITERIA FOR SIZING HYBRID CONFIGURATIONS

HYBRID CONFIGURATIONS SIZED BY MURP MISSION
DURING ASCENT AND PM MISSION FOR LANDING

ASCENT

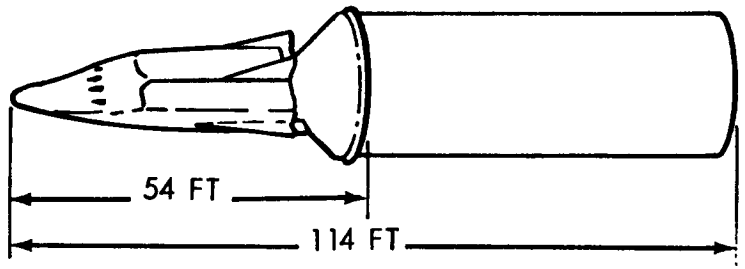

MURP SPACECRAFT (LB)		50,525
REENTRY VEHICLE	29,800	
PROPULSION ADAPTER	7,700	
ABORT SUBSYSTEM	6,300	
CONTINGENCY (10%)	4,385	
EXPENDABLES	2,340	
MANEUVERING PROPELLANTS		10,775
GROSS CARGO WEIGHT		25,000
TOTAL PAYLOAD (LB)		86,300

LANDING

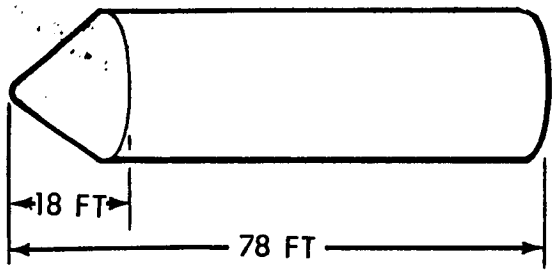

PM SPACECRAFT (LB)		21,758
PERSONNEL COMPARTMENT	7,912	
PROPULSION COMPARTMENT	7,668	
ABORT SUBSYSTEM	4,200	
CONTINGENCY (10%)	1,978	
EXPENDABLE (332 LB)	EXPENDED	
MANEUVERING PROPELLANTS		EXPENDED
GROSS CARGO WEIGHT		25,000
TOTAL PAYLOAD (LB)		46,758

2.3 MISSION PROFILES

This chart shows schematically the mission profiles for the two spacecraft concepts examined. The profiles apply to the 55-degree inclination, space station cargo delivery, reference mission. For both spacecraft profiles the injection altitude is 50 nm.

For the SERV-PM, both the SERV and spacecraft go into a high altitude (260 nm) phasing orbit. Terminal rendezvous and docking of the personnel module and cargo are accomplished using a propulsion system in the personnel module. Upon mission completion, the personnel module with its return cargo rejoins SERV. The SERV, plus cargo and spacecraft, reenters and lands as a unit. Alternate mission profiles for SERV-PM that yield higher cargo transfer will be discussed later.

In the SERV-MURP profile, the SERV with its payload establishes a circular orbit at a low altitude (110 nm). The MURP, plus cargo, proceeds to the space station while the SERV remains in the lower orbit. At mission completion the MURP rejoins SERV and transfers the return cargo. The MURP then separates, reenters, and lands, while the SERV, plus cargo, reenters and also lands.

These mission profiles are not exclusively used by the PM or MURP because alternate modes exist. For example, the SERV-PM profile could be used by SERV-MURP under emergency rescue conditions when with additional ascent propellants substituted for cargo.

MISSION PROFILES

SERV-PM

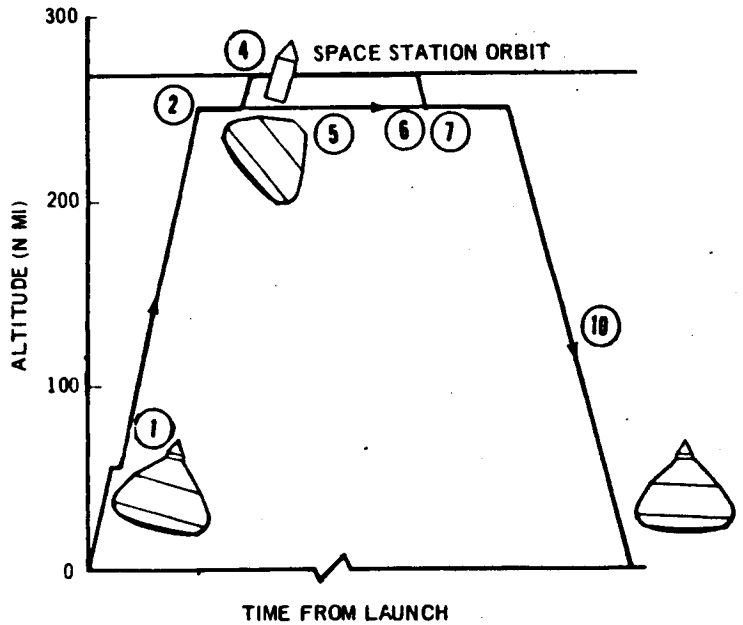

1. LAUNCH FROM KSC INTO PERIGEE OF TRANSFER ELLIPSE
2. CIRCULARIZE AT PARKING ORBIT ALTITUDE
3. SEPARATE AND TRANSFER TO 110×260 PHASING ORBIT
4. RENDEZVOUS AND DOCK WITH SPACE STATION AT 270 N MI ORBIT

SERV-MURP

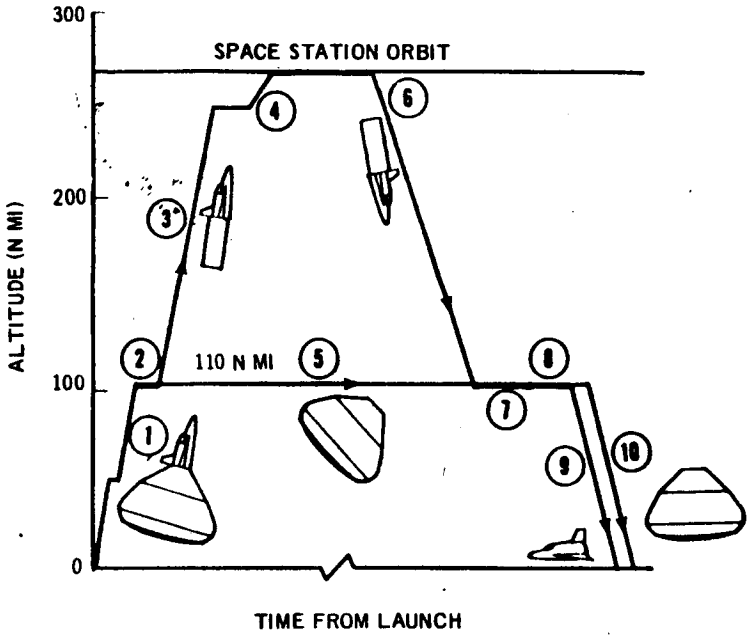

5. MAINTAIN PARKING ORBIT ALTITUDE
6. SEPARATE, CHANGE PLANE AND TRANSFER TO PHASING ORBIT
7. RENDEZVOUS AND DOCK WITH SERV
8. TRANSFER CARGO AND SEPARATE FROM SERV
9. DEORBIT AND REENTER (MURP)
10. DEORBIT AND REENTER (SERV OR SERV-PM)

2.4 FINAL VEHICLE SELECTION

Analysis of the alternative configurations for SERV led to the conclusion that the MURP configuration was capable of performing the PM mission except for the return payload requirement imposed by having the Personnel Module return on the SERV together with the cargo. A composite vehicle was therefore sized with the MURP ascent capability coupled with the PM return requirements. The composite vehicle delivers 27,300 pounds of cargo to the space station for a MURP mission, and 25,000 pounds for the PM mission.

FINAL VEHICLE SELECTION

ITEM	SPACECRAFT/PROFILE DESCRIPTION	
	PM (260 x 55)	MURP (110 x 55)
PAYLOAD WEIGHT (LB)	50,900	88,900
CARGO WEIGHT TO 270 x 55 (LB)	25,000	27,300
LIFTOFF THRUST (LB)	7,454,000	7,454,000
GLOW (LB)	6,046,000	6,049,000
VEHICLE DRY WEIGHT (LB)	494,249	
• PRIMARY STRUCTURE	200,018	
• AEROSPIKE ENGINE	110,804	
• TURBOJET ENGINES	48,845	
• THERMAL PROTECTION	24,695	
• ALL OTHER SUBSYSTEMS	64,955	
• CONTINGENCY (10%)	44,932	

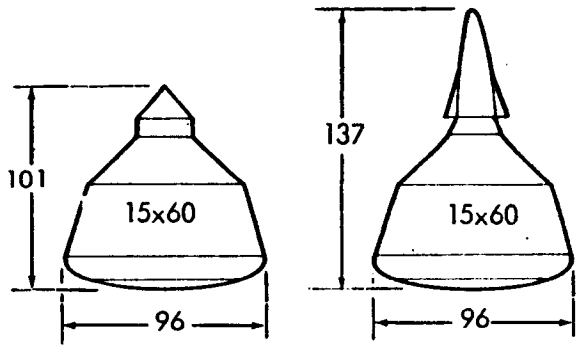

2-9

2.4.1 MAIN PROPULSION SUBSYSTEMS

Key features of the main propulsion subsystems are shown on this chart.

The SERV incorporates an integral aerospike engine comprising 12 interconnected modules for ascent propulsion. A one-turbopump-out capability is provided.

The landing propulsion is provided by turbojet lift engines which operate at a thrust efficiency of 80 percent. A one-engine-out capability is provided.

MAIN PROPULSION SUBSYSTEMS

ASCENT	LANDING
GENERAL: • 12-MODULE AEROSPIKE ENGINE • LOX/LH AT 6:1 MIXTURE RATIO • 2000 PSI CHAMBER PRESSURE • TURBOPUMP OUT CAPABILITY	GENERAL: • TURBOJET LIFT ENGINES • JP-4 FUEL • F/W RANGE OF 17 TO 20 • ENGINE OUT CAPABILITY
FINAL CONFIGURATION: • THRUST OF 7.45M LB SL, 9.72M LB VAC • I_S OF 348 SEC SL, 467 SEC VAC • NOZZLE EXPANSION RATIO OF 409	FINAL CONFIGURATION: • 40 ENGINES • 20,759 THRUST EACH • F/W OF 17

2.4.2 FINAL VEHICLE ARRANGEMENT

Major dimensions and key configuration features for the final configuration are shown in this chart. The standard vehicle has a PM spacecraft that returns to earth on SERV. The alternate MURP spacecraft is also shown. SERV is designed for fully automatic unmanned operation. For this mode of operation a nose cone of the PM external configuration would be installed in lieu of the spacecraft.

Differential corner radii have been incorporated in the aerospike protection doors on the vehicle maximum diameter. This feature, when combined with a horizontal cg offset, ensures that the desired trim angle of attack and lift-to-drag (L/D) ratio can be achieved during reentry.

FINAL VEHICLE ARRANGEMENT

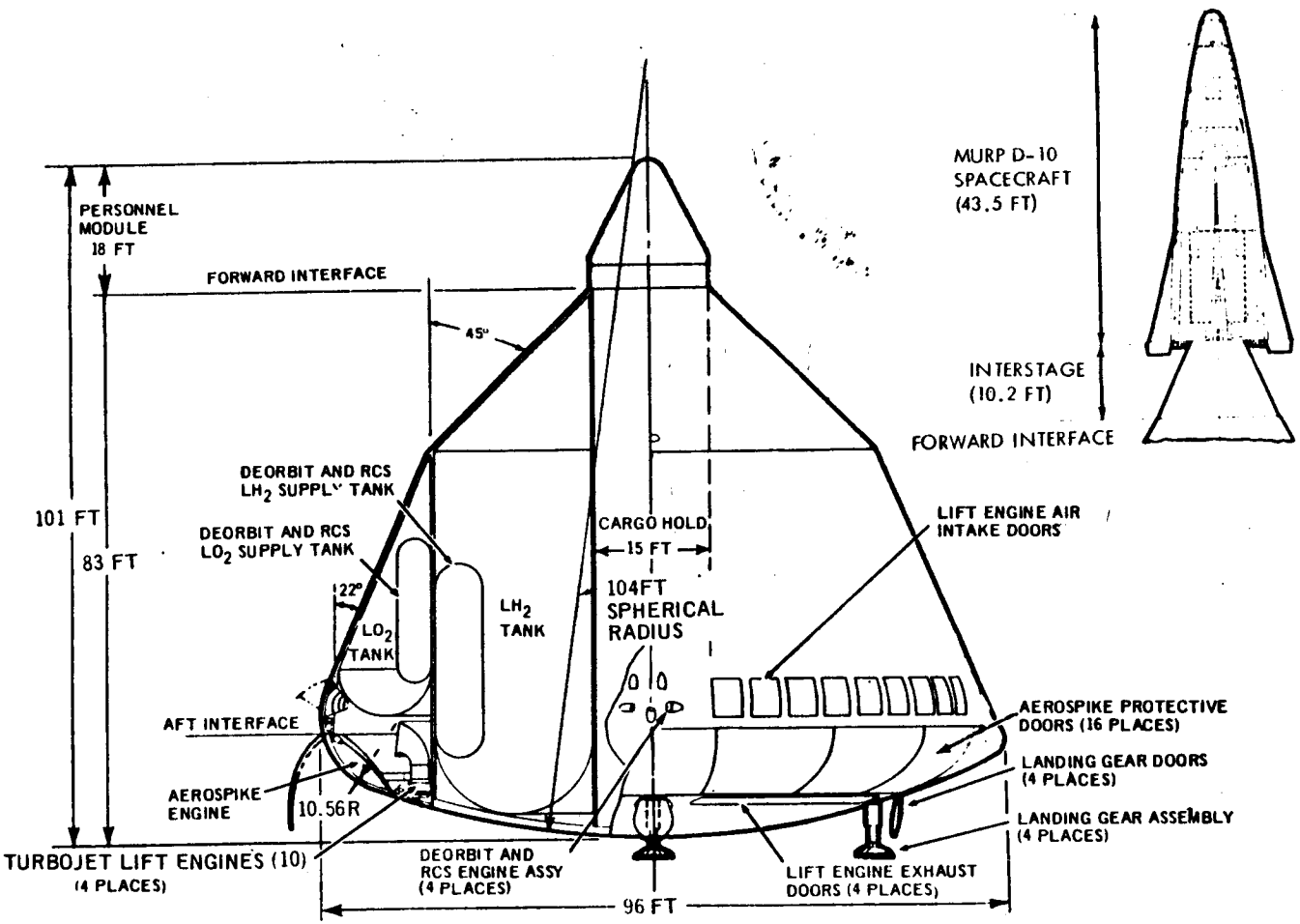

2.4.3 FINAL CONFIGURATION HORIZONTAL PROFILE

This chart shows the horizontal profile with key dimensions and major configuration features. Locations of the gas turbine lift engines, aerospike protective doors, and landing gear are shown. Note the location of lift engine fuel supply and diametrically opposite ballast tanks.

CONFIGURATION HORIZONTAL PROFILE

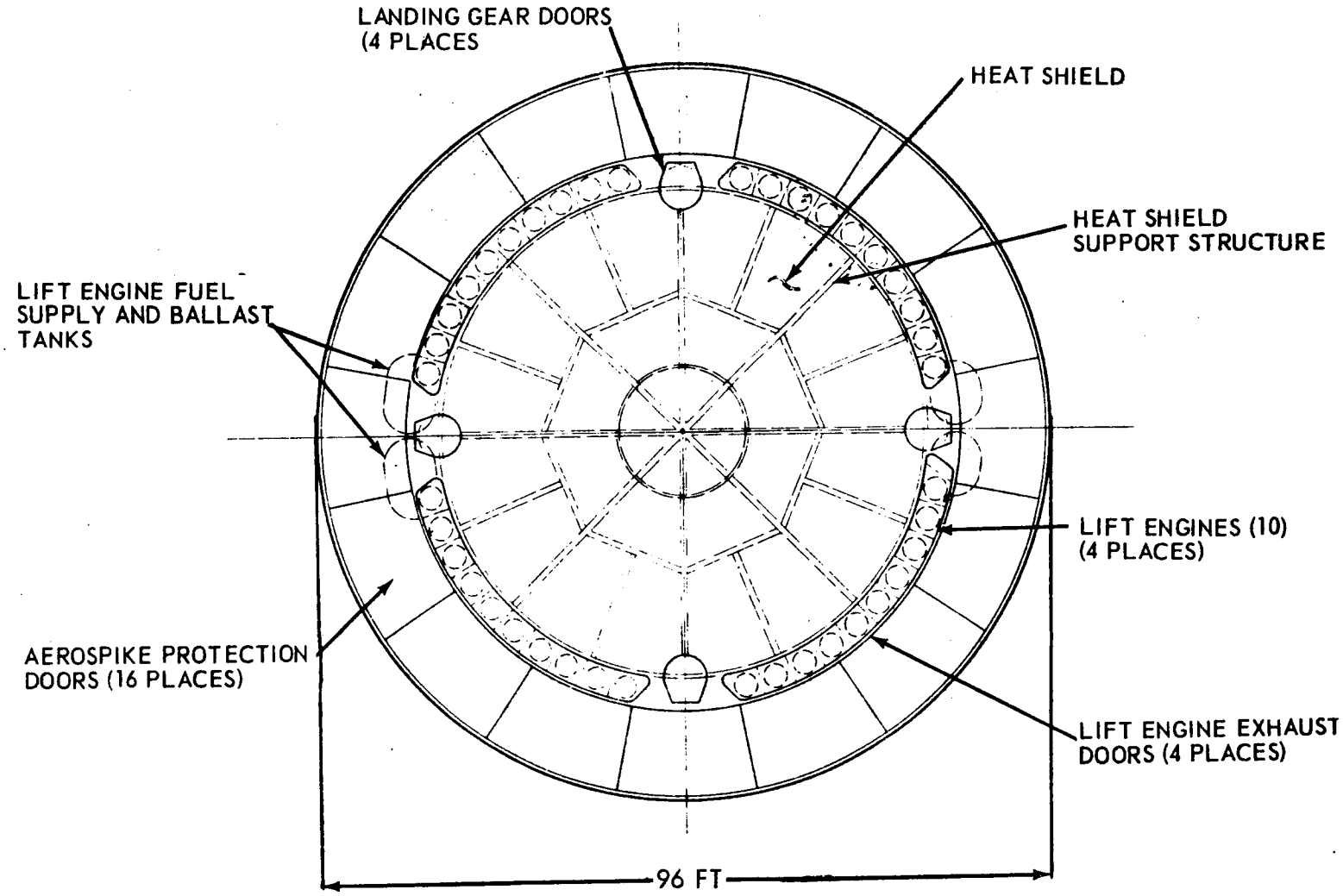

VEHICLE FLIGHT PERFORMANCE

Section 3

VEHICLE FLIGHT PERFORMANCE

3.0 GENERAL

The general scope of work for the mission and performance analyses subtask during the vehicle definition phase of the study is outlined on the chart.

MISSION AND PERFORMANCE ANALYSES

NOMINAL PERFORMANCE AND MISSION ANALYSES

- GENERAL ASCENT PERFORMANCE
- MISSION PROFILE SELECTION

HAZARDS AND ABORT

- ENGINE OUT IMPLICATIONS
- ABORT MODES

FINAL PERFORMANCE

- MISSION/PAYLOAD SPECTRUM
- FIXED HARDWARE SENSITIVITIES

3.1 MISSION PROFILES AND TIME LINES

The SERV as currently defined is capable of operating in two basic modes. In Mode A, following injection into an elliptical orbit using the mainstage propulsion system, required post-injection maneuvers are accomplished using the SERV auxiliary system only, with the payload (spacecraft plus cargo) as a passive unit. In Mode B, both the SERV auxiliary system and the propulsive capability of the spacecraft are used for on-orbit maneuvering.

Mission profiles for the space station cargo delivery mission using these two modes are illustrated schematically on the chart. The required post-injection maneuvers associated with each profile are also shown. The mission time lines associated with each mode are indicated on the chart.

MISSION PROFILES AND TIME LINES

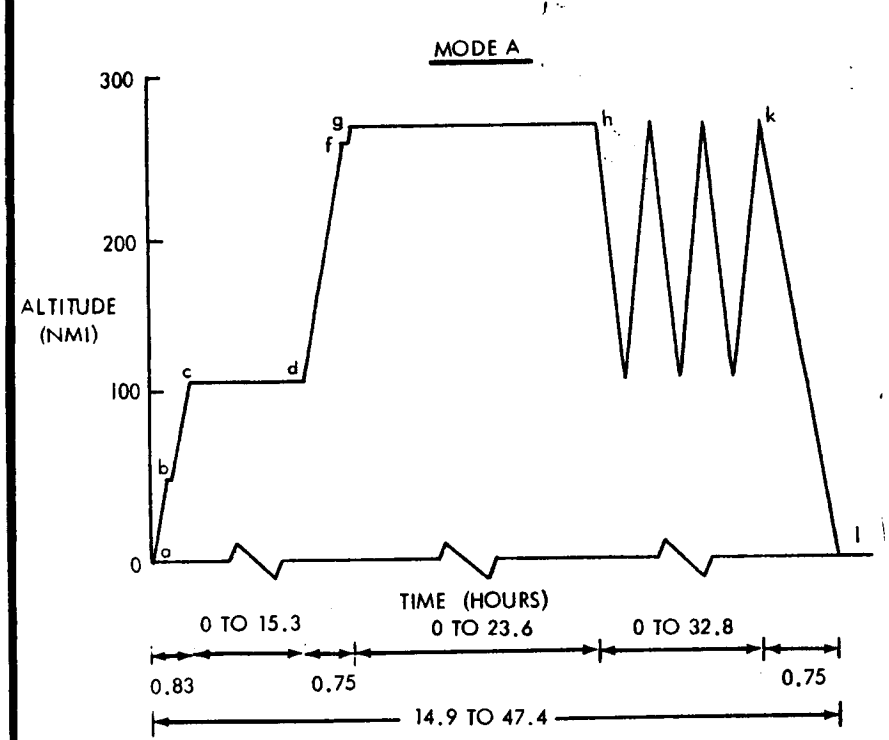

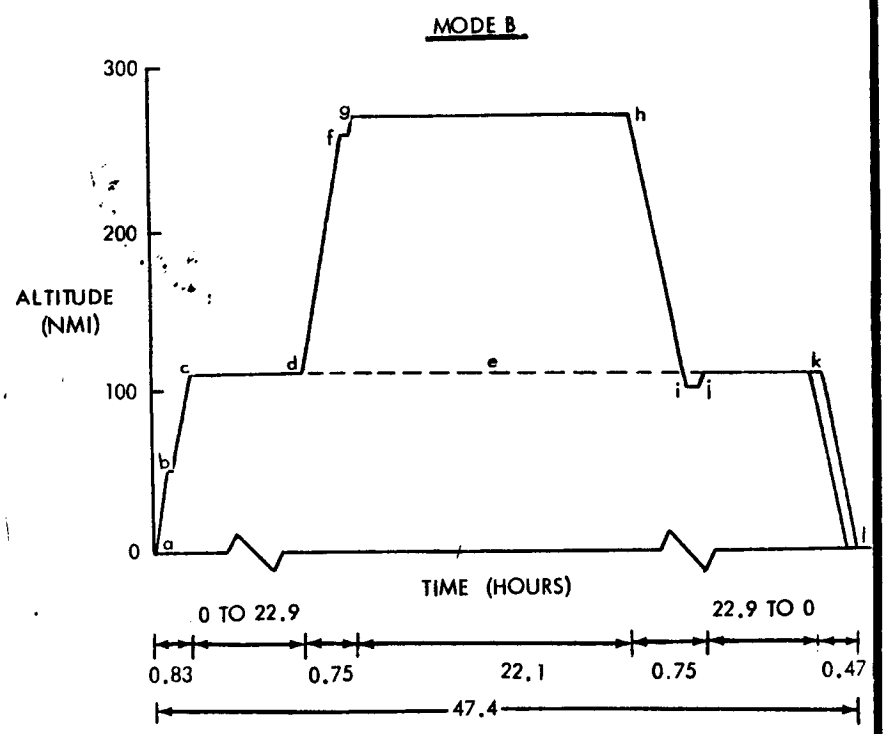

a. LAUNCH
b. INJECTION
c. CIRCULARIZE IN PARKING ORBIT
d. TRANSFER TO FINE PHASING ORBIT
e. SERV MAINTAINS PARKING ORBIT
f. CIRCULARIZE IN FINE PHASING ORBIT
g. RENDEZVOUS AND DOCK WITH SPACE STATION
h. TRANSFER TO PHASING ORBIT
i. CIRCULARIZE PHASING ORBIT
j. RENDEZVOUS AND DOCK WITH SERV
k. DEORBIT
l. LAND

SPACE DIVISION CHRYSLER CORPORATION

3.1.1 MODE A MISSION PHASING REQUIREMENTS

The central angle of the space station shown on this chart is defined as the angle formed by a line within the plane of the space station orbit from the center of the earth to the ascending node and a line from the center of the earth to the space station. This angle is measured when the plane of the space station orbit contains the launch site. The total minimum time from launch through landing is presented on the chart for SERV only, Mode A operation, as a function of space station central angle orientation. The combination of launch and landing direction yielding the minimum total time for a particular space station central angle region are shown. The total times are made up of four categories relating to the specific operational phases of ascent, orbital stay time available prior to descent phasing initiation, descent, and reentry. The times attributable to each phase are identified by different shading patterns. For a specific space station central angle, the stay time shown indicates the time measured from rendezvous when phasing must be initiated. If the required stay time at the orbit for a particular mission exceeds the time shown on this chart, approximately 24 hours or 15 orbits of the space station must pass before an opportunity to return recurs. The mission times that result from this operational mode range from 14.9 to 47.4 hours throughout the space station central angle range. For this profile it would be desirable to orient the space station within the 14.9 hour mission time range to allow minimum reaction time under emergency conditions. The time required in parking orbit for ascent phasing never exceeds 15.3 hours throughout the central angle range. This number is of interest in evaluating the velocity requirements for parking orbit maintenacce in the total velocity budget.

MODE A MISSION PHASING REQUIREMENTS

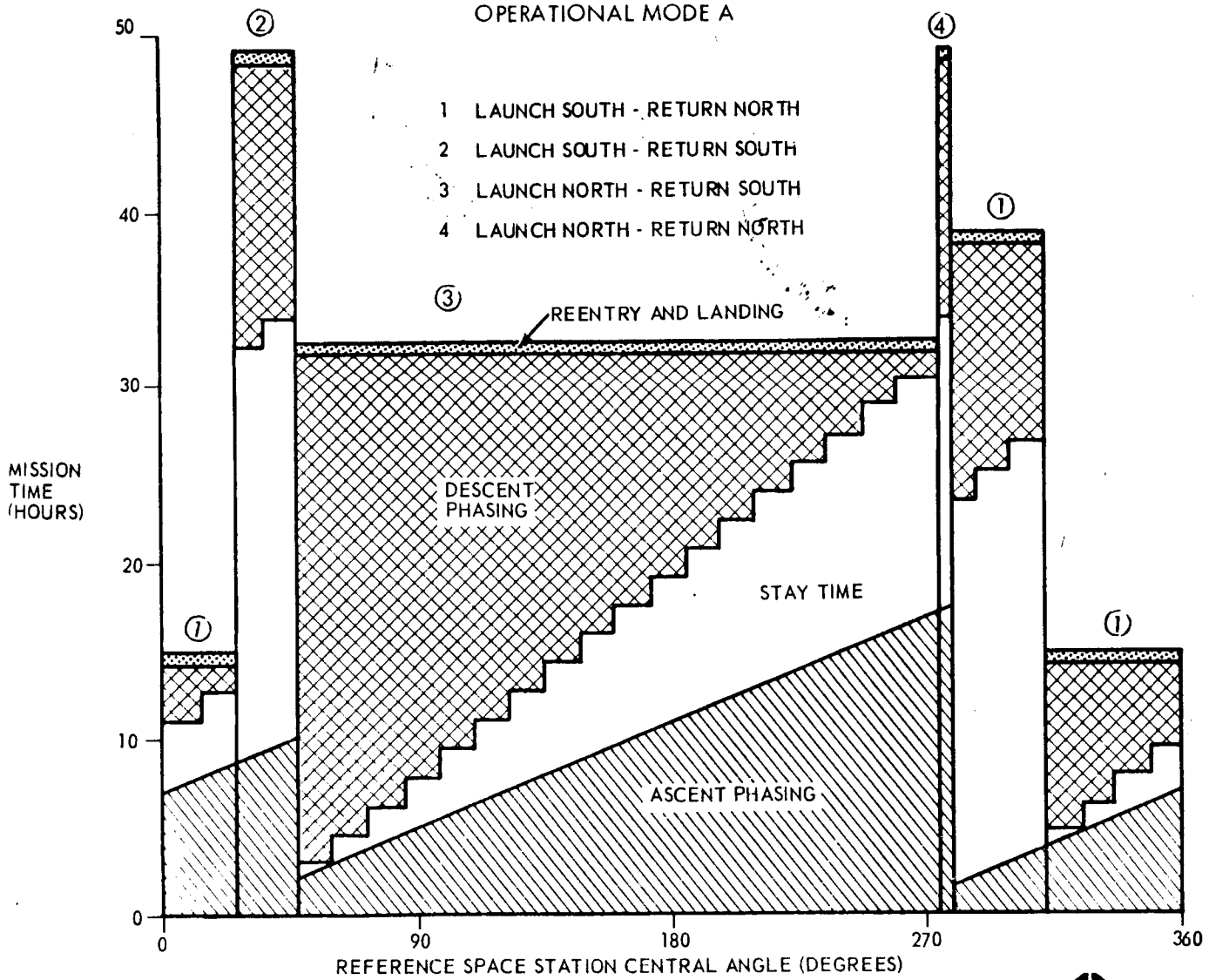

22

SPACE DIVISION CHRYSLER CORPORATION

3.1.2 MODE B MISSION PHASING REQUIREMENTS

For operational Mode B, where SERV remains in the 110 nm parking orbit while the spacecraft proceeds to the space station, the positional orientation in terms of latitude, longitude for deorbit is independent of the space station central angle at launch. It depends rather on the ascent to orbit characteristics of SERV. It was found that the orbit trace of the selected parking orbit passed through the desired deorbit position once every 16 revolutions of the parking orbit without phasing adjustments. The critical timing associated with this operational mode was related to achieving the rendezvous of the spacecraft with SERV for return. Regardless of the ascent phasing time required for the original rendezvous with the space station, the first opportunity for return to the SERV required a stay time at the station of 22.1 hours after arrival. The total mission time as a function of space station central angle at launch for this mode is presented on the chart for a north launch. A total mission time of 47.4 hours is required for all space station central angles except those from 33 through 41 degrees. For this region, ascent phasing time requirements resulted in missing the first return opportunity. Utilizing a south launch for this region, however, will provide mission times of 47.4 hours throughout the central angle range. For this mode the difference in regression of the orbital planes of the parking orbit and the space station orbit will require a plane change of 0.7 degrees/day to accomplish the SERV/spacecraft rendezvous. Parking orbit maintenance time for this mode is a minimum of 46 hours and increases with mission duration. If required stay time at the station exceeds the 22.1 hours available for the minimum mission time case, additional return opportunities recur every 22.9 hours thereafter.

MODE B MISSION PHASING REQUIREMENTS

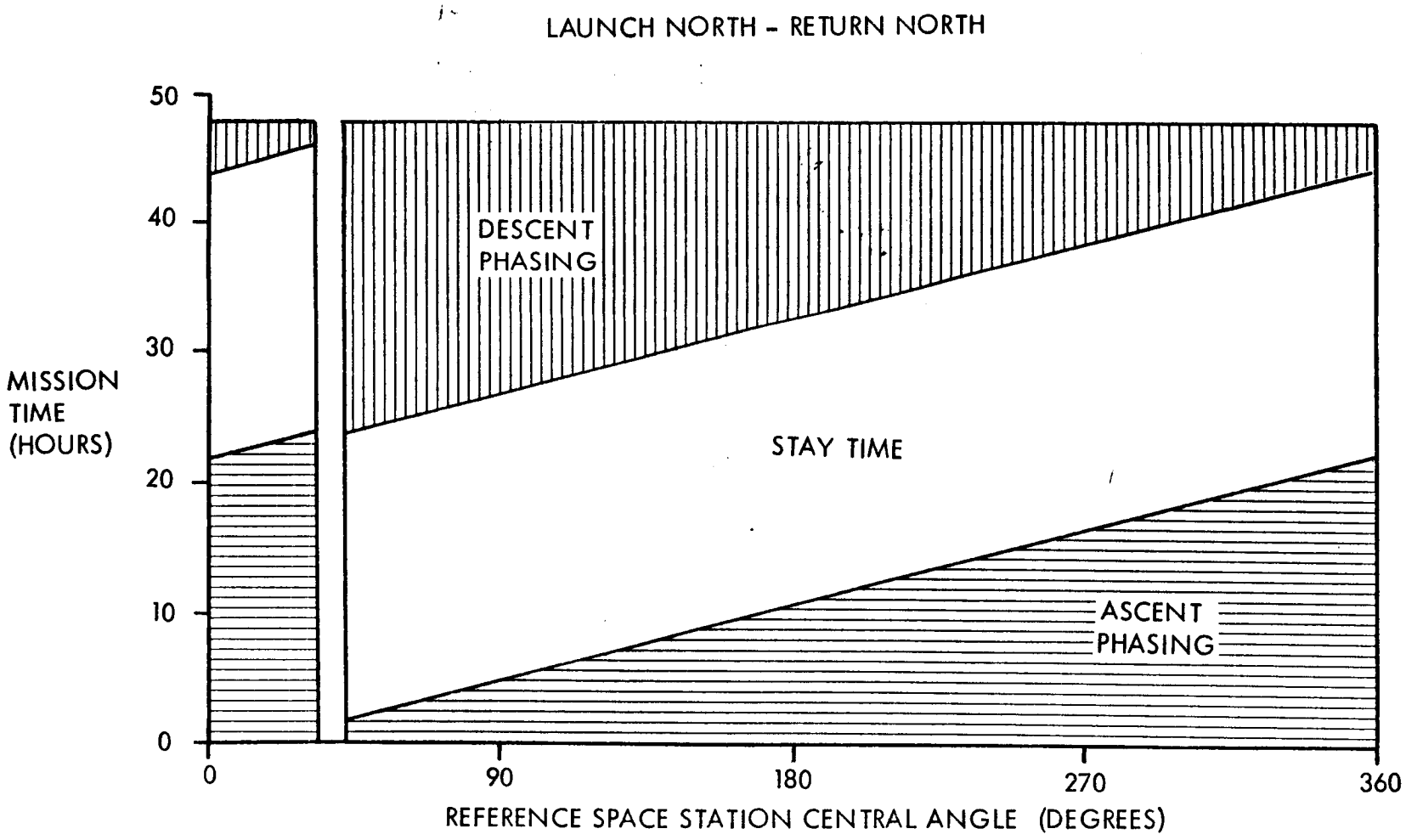

3.1.3 DELIVERABLE CARGO VARIATION WITH MISSION DURATION

Using the appropriate velocity budgets associated with both Modes A and B coupled with the phasing information on these profiles, the deliverable cargo carrying capability for the SERV-PM and the SERV-MURP configurations was determined. The results are presented on the chart as a function of mission duration. Based on the phasing results the minimum duration mission for each mode of operation is noted. The cargo carrying capability of the SERV-PM using either mode exceeds the SERV-MURP capability because of the lower spacecraft weight associated with this configuration.

DELIVERABLE CARGO VARIATION WITH MISSION DURATION

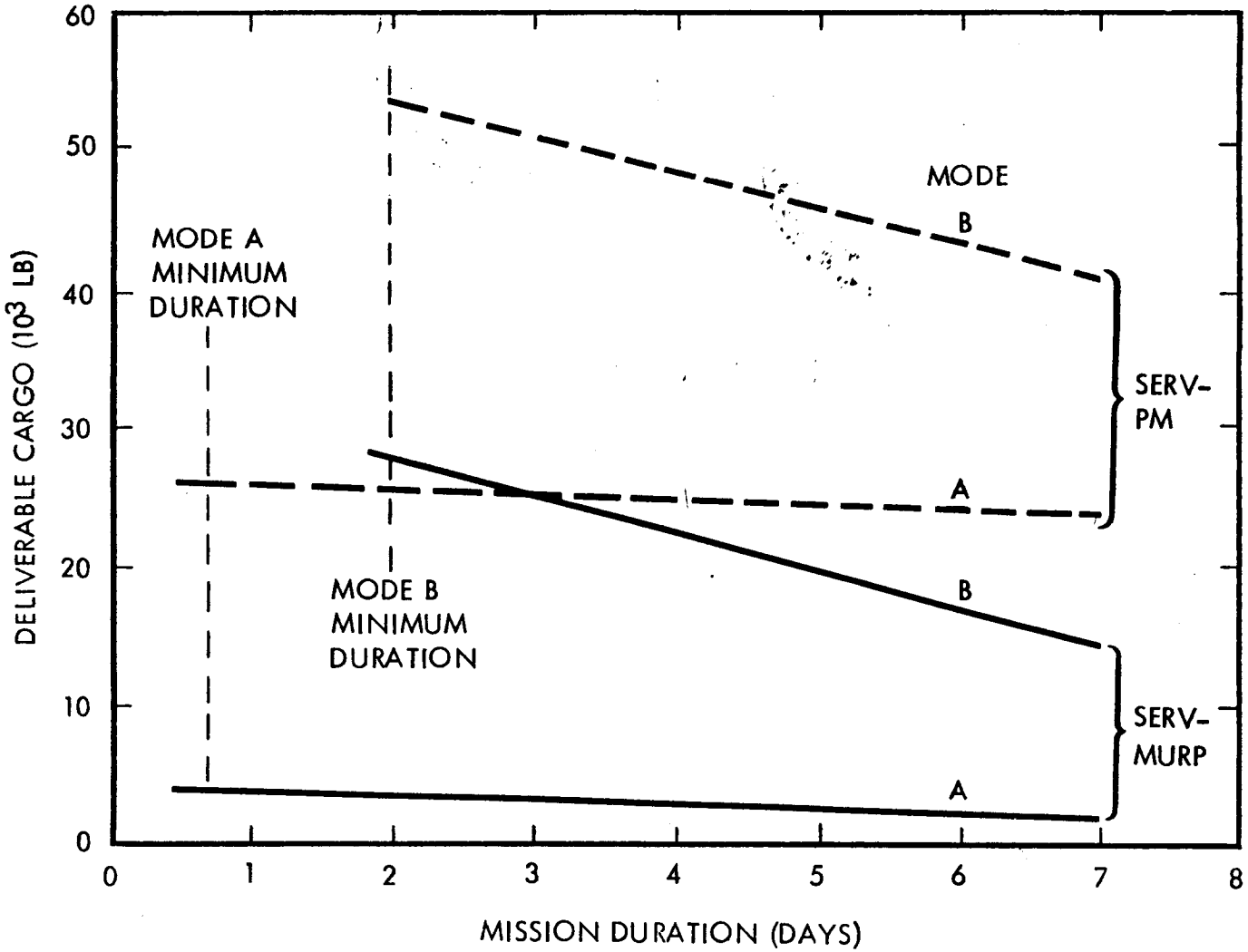

3.1.4 CONFIGURATION/PROFILE ASSESSMENT

For each payload configuration, the performance and operational characteristics associated with both operational modes were examined and the advantages and disadvantages assessed. The results of this assessment are summarized on the chart. Generally speaking, both operational modes have desirable characteristics. Mode B provides a performance advantage, while Mode A has advantages related to phasing flexibility. No single selection needs to be made at this time since the ability to operate in either mode is possible under the current design concept. Indeed the selection of the operational mode to be used can be made for each mission without penalizing other missions. This capability greatly enhances the flexibility of SERV.

CONFIGURATION/PROFILE ASSESSMENT

ITEM	CONFIGURATION AND MISSION PROFILE			
	SERV-PM		SERV-MURP	
	MODE A	MODE B	MODE A	MODE B
PAYLOAD IN PARKING ORBIT (LB)	50,900	86,700	53,600	88,900
CARGO TO SPACE STATION, MIN. DURATION (LB)	25,000	53,200	3,100	27,300
CARGO TO SPACE STATION, 7-DAY MISSION (LB)	23,400	40,900	1,500	14,600
ABILITY TO MEET DESIRED MISSION CHARACTERISTICS:				
• 25,000 POUND CARGO, MIN. DURATION	YES	YES	NO	YES
• 25,000 POUND CARGO, 7-DAY MISSION	NO	YES	NO	NO
• 48-HOUR RESCUE MISSION REACTION TIME	YES	NO	YES	NO
• 1500-NM CROSS RANGE CAPABILITY	NO	NO	YES (MURP)	YES (MURP)

3.2 HAZARDS AND ABORT

3.2.1 ENGINE OUT IMPLICATIONS

The aerospike engine for SERV consists of 12 modules. Each module has a turbopump which feeds into a common manifold. The turbopumps have been designed with an overspeed capability such that should an individual pump fail the remaining pumps can operate above the nominal operating speed to maintain the required thrust level.

The thrust level that can be maintained after the failure of one or more turbopumps is a function of the design overspeed capability of the pumps. This relationship is presented parametrically on the left hand side of the chart which shows the percent of nominal thrust after failure as a function of percent overspeed in the pump design for 1, 2 and 3 turbopumps out. Trajectories simulating failures to various thrust levels occurring at varying times along the ascent trajectory were generated. From these data the curve of failure time was determined, after which a failure to a specific percent thrust could occur without aborting the mission. These results are shown on the right hand side of the chart. The shaded area indicates the thrust level, failure time combinations yielding mission abort situations. To the right of this region is an area of combinations for which the nominal mission can be accomplished utilizing part or all of the flight propellant reserve. This region is bounded on the right by the nominal thrust level versus time.

The current point design of the turbopumps incorporates a 20 percent overspeed capability. The dashed line on the chart reflects this capability. Interpreting the results for this design indicates that the nominal mission can be accomplished with a failure of one or two turbopumps at any time. The nominal mission can be accomplished utilizing the FPR with three turbopumps out if the failure of a third pump occurs after 50 sec.

ENGINE - OUT IMPLICATIONS

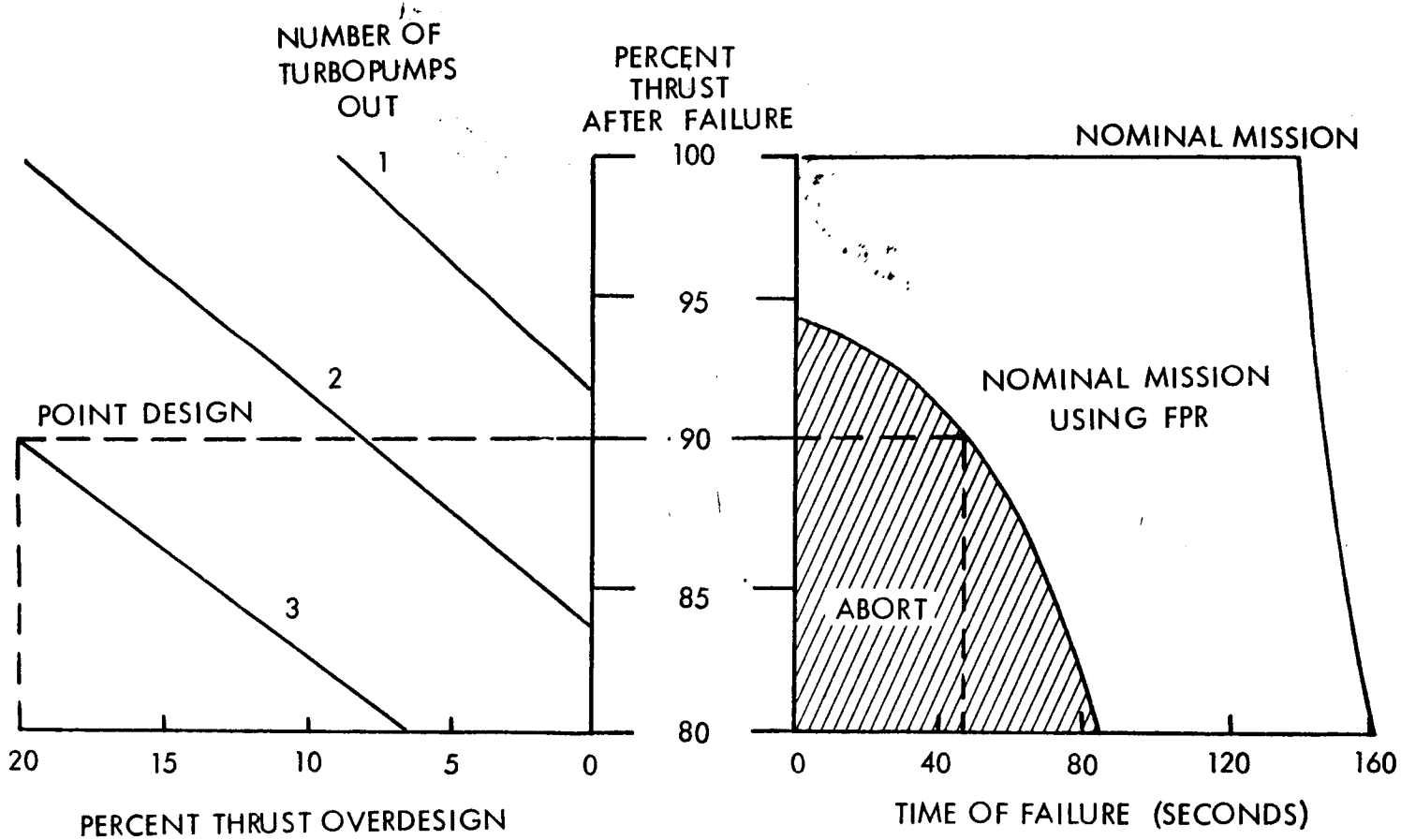

3.2.2 INTACT ABORT IMPLICATIONS

In the event of a catastrophic malfunction of SERV during ascent, abort capability for both the PM and the MURP spacecraft has been provided. Abort for the PM is provided using eight solid rocket motors, which have been sized to give an initial T/W = 5.7 from SERV with all engines shut down. For SERV failures which precipitate moderate rates to structural breakup, this abort system will be adequate. The PM, once aborted, will traverse a parabolic arc trajectory until it reaches 50,000 ft in altitude, at which time a sailwing is deployed and the PM landed on either land or water. Similarly, for the MURP, separation from a malfunctioning SERV is accomplished using solid rocket motors. However, with this spacecraft an aircraft type landing will be used. The abort modes for both the PM and the MURP are shown schematically on the chart.

SERV ABORT MODES

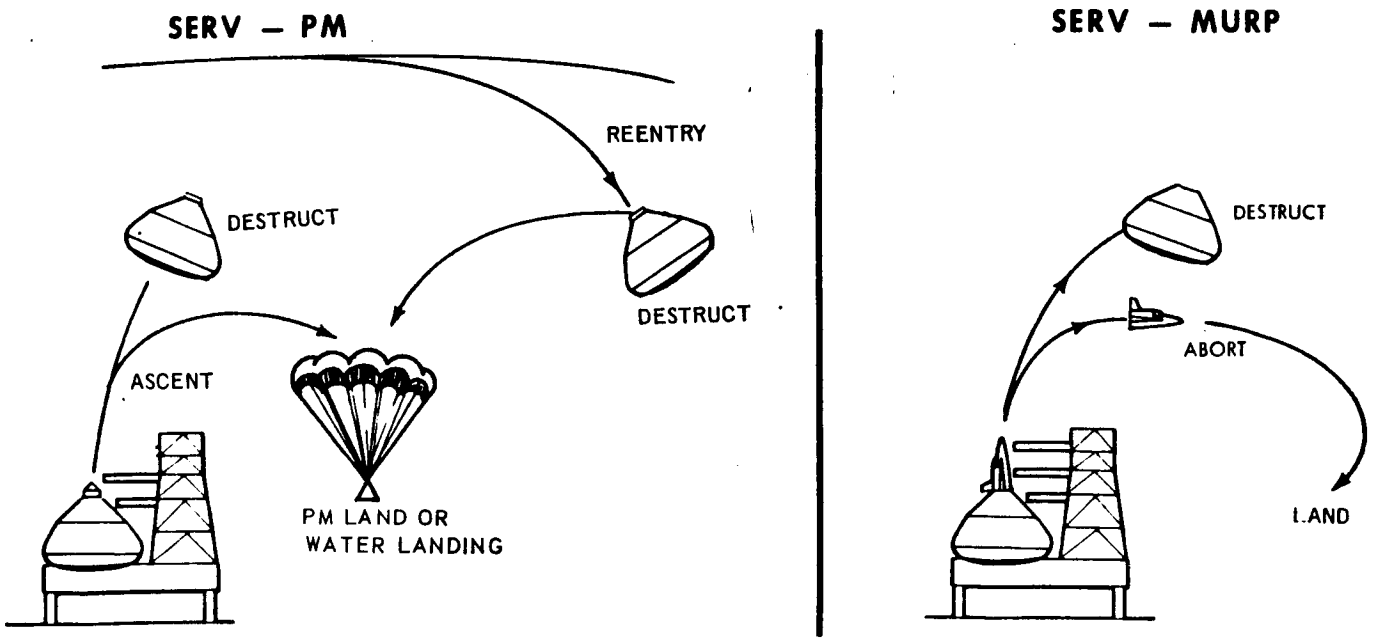

3.3 SERV FINAL PERFORMANCE

The capability of the SERV for a spectrum of missions has been determined and is presented on this chart. Both configurations 2A and 2B vehicles have been evaluated with both a PM and a MURP spacecraft configuration. The numbers presented are gross payload values (i.e., spacecraft plus cargo). For the space station mission the deliverable cargo weights are shown in parenthesis. For this mission, payload and cargo using the two operational modes were examined.

SERV FINAL PERFORMANCE
GROSS PAYLOAD CAPABILITY

SPACECRAFT	MISSION ORBIT (PAYLOAD IN POUNDS) (NM CIRCULAR X DEGREE INCLINATION)				
	110 NM X 28.5 DEG	270 NM X 55 DEG MODE A	270 NM X 55 DEG MODE B	100 NM X 90 DEG	100 NM X 104 DEG
MURP	116,439 (65,912)*	53,577 (3,052)	83,370 (27,282)	NA	NA
PM	112,260 (90,170)	50,873 (25,000)	80,697 (53,223)	42,975 (20,885)	25,819 (3,729)
NOSECONE**	112,260	50,873	NA	42,975	25,819
EXTENDED NOSECONE**	125,000	63,000	NA	54,000	36,000

*VALUES IN PARENTHESES ARE CARGO WEIGHTS

**WEIGHT OF NOSECONE AND EXTENSION INCLUDED IN PAYLOAD

3.4 FIXED HARDWARE SENSITIVITIES

The sensitivity of payload to variations in significant vehicle and mission parameters has been determined for Configuration 2A for three missions of interest. For the space station cargo delivery mission, cargo sentitivities have also been assessed. These data are presented on the chart. These are fixed hardware sensitivities and reflect the expected variation in payload that will result from a known variation in a particular parameter on the ground.

FIXED HARDWARE SENSITIVITIES

(CONFIGURATION 2A)

PARAMETER / MISSION			OPERATIONAL SENSITIVITY*			
			DUE EAST 100 NMI/28.5°	SPACE STATION 110 NMI/55°		RETROGRADE 100 NMI/104°
			PAYLOAD	PAYLOAD	CARGO**	PAYLOAD
WEIGHTS						
INERT WEIGHT		LB/LB	-1.000	-1.000	-0.875	-1.000
INERT WEIGHT		LB/PERCENT	-6012	-6016	-5264	-6001
DRY WEIGHT		LB/LB	-1.003	-1.004	-0.879	-1.008
DRY WEIGHT		LB/PERCENT	-4,958	-4,962	-4344	-4,982
PROPULSION (PERCENTAGE VARIATIONS)						
SPECIFIC IMPULSE	(T CONSTANT)	LB/SEC (VAC)	3,690	3,582	3,134	3,364
SPECIFIC IMPULSE	($\dot{w}$ CONSTANT)	LB/SEC (VAC)	4,214	4,065	3,557	3,777
THRUST	(ISP CONSTANT)	LB/PERCENT		2,038	1,783	1,715
THRUST	($\dot{w}$ CONSTANT	LB/PERCENT	19,570	18,977	16,603	17,632
PROPELLANT LOAD		LB/LB	0.1063	0.1028	0.0899	0.0962
PERFORMANCE						
ASCENT VELOCITY		LB/FPS	-53.7	-51.4	-44.9	-46.2
ON-ORBIT ΔV				-		
SERV/ASCENT PAYLOAD		LB/FPS	-52.0	-49.6	-43.4	-45.4
SERV/RETURN CARGO		LB/FPS	-47.4	-47.4	-41.4	-47.4
SERV		LB/FPS	-43.4	-43.4	-38.0	-43.4
DRAG		LB/PERCENT	-724	-697	-610	-640
ORBIT INCLINATION		LB/DEG	-850	-1125	-984	-1200
LAUNCH SITE ALTITUDE		LB/FT	6.33	6.17	5.38	5.47

*MOST SENSITIVITIES ARE NON-LINEAR AND SHOULD BE USED ONLY FOR SMALL DEVIATIONS.

**CARGO DELIVERED TO 270 N MI

29

SPACE DIVISION CHRYSLER CORPORATION

3.5 REENTRY PERFORMANCE

This chart shows reentry footprint envelopes for constant L/D reentry from an orbital altitude of 110 nm for a retro velocity increment of 400 ft/sec. Footprint size is shown for L/D values of 0.25, 0.30 and 0.35, and the point at which various deceleration values are reached is shown for each L/D value. For SERV, the maneuvering capability is measured from the point of maximum range to the point where a deceleration of 3.0g is encountered. As shown, an increase in maneuvering capability above the nominal provided by an L/D of 0.30 could be provided by either trimming the vehicle to a higher L/D value or by raising the deceleration limit, or by a combination of both.

REENTRY FOOTPRINT FOR CONSTANT L/D REENTRY

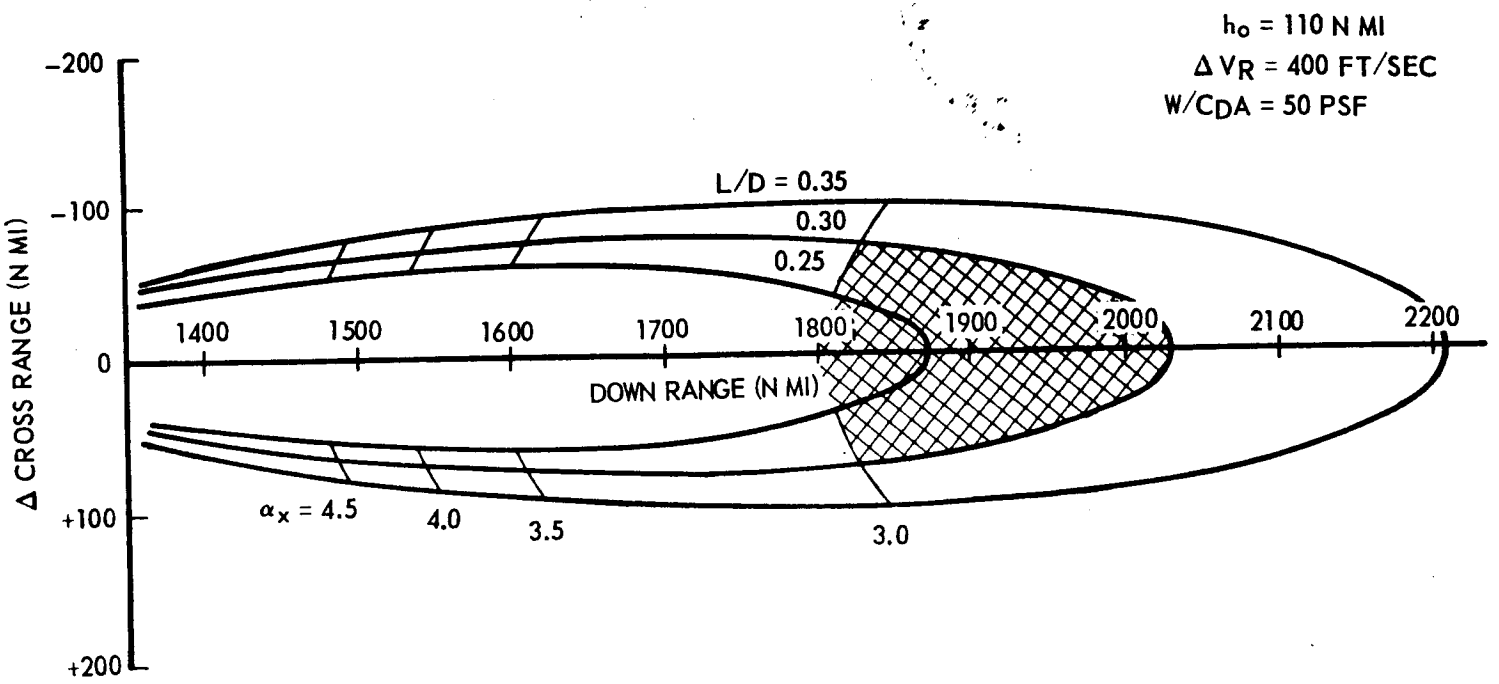

SPACE DIVISION CHRYSLER CORPORATION

AEROSPIKE PROPULSION PERFORMANCE

Section 4
AEROSPIKE PROPULSION PERFORMANCE

4.0 GENERAL

To answer this foremost feasibility issue, a series of cold flow tests were performed on a 27-inch-diameter model of SERV at the Arnold Engineering Development Center. Engine characteristics, test procedures, and test results are presented herein.

The model design was based on the 90-ft diameter baseline vehicle, having 12 aerospike modules arranged in a ring of 87.4 ft outside diameter. The engine is fully integrated with the SERV, forming the base closure of the vehicle, and utilizing the entire base of the vehicle. Each of the 12 interconnected modules have a set of 2-stage, turbine-driven pumps; module interconnection is accomplished by use of a common manifold on the high pressure side of the pumps. Individual modules are controlled by oxidizer and fuel valves downstream of the common manifold. The module turbopumps are capable of emergency operating levels in such a manner that in the event of a failure of one of the 12 units, the remaining 11 can maintain all 12 modules at their normal operating level. Protective doors are provided to protect the aerospike ramp during reentry operations, as shown in cross section on this chart.

Data for the baseline engine were supplied by Rocketdyne and subsequently resubmitted to reflect a revised integration with SERV. This integration resulted in an engine with a larger overall diameter, a higher area ratio (483), and interconnected modules to allow turbopump-out capability. Rocketdyne also incorporated an improved turbopump in the system. The resultant engine specific impulse was improved by 3.2 sec at vacuum conditions and 1.4 sec at sea level, while engine weight increased by 7,345 lb. The weight increase was due primarily to module interconnection plumbing and the increase in diameter (1.3 ft). The revised data were used as the baseline for subsequent trade study tasks.

Although the engine area ratio changed from 465 to 483 during the design integration, the fabrication schedule of the cold flow model dictated use of the earlier baseline engine at ϵ of 465.

AEROSPIKE ENGINE INTEGRATED WITH SERV

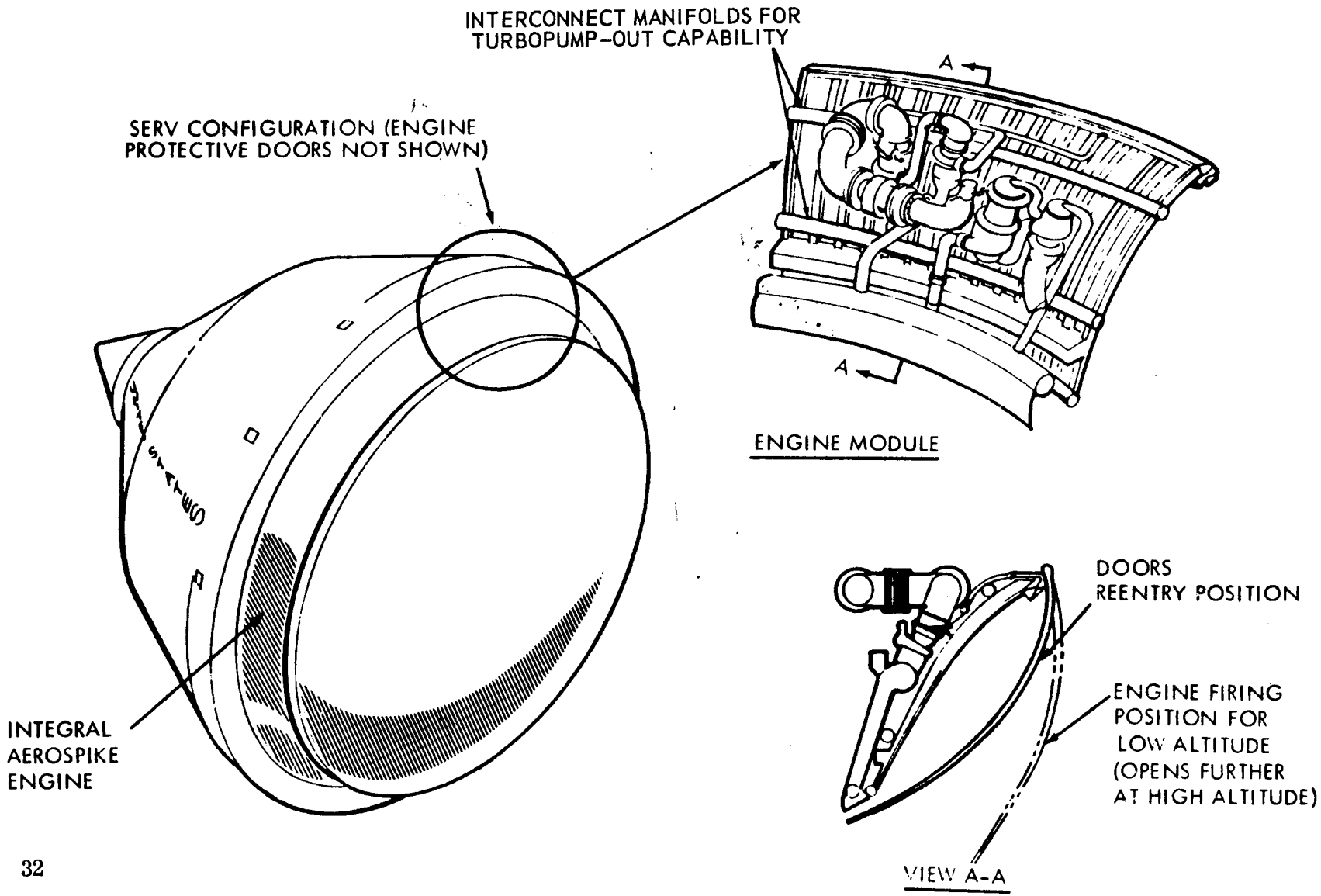

32

Rocketdyne
North American Rockwell

SPACE DIVISION CHRYSLER CORPORATION

4.1 COLD FLOW MODEL TESTING

4.1.1 PRIOR STATUS OF AEROSPIKE TESTING

A summary of prior aerospike nozzle testing is shown plotted in normalized form. Note that different area ratios (ϵ), nozzle lengths (%L), gas properties (γ), and secondary flow rates (W_S/W_P) are presented. The range of interest for SERV is shown in the lower left corner. Although the data appears to scatter, it must be emphasized that it is a basic characteristic of the aerospike nozzle to follow a "humping" or "roller coaster" type curve during recompression at low pressure ratios. Thus, the data spreading shown is the result of superimposing the recompression characteristics of many different configurations.

It is readily apparent from the indicated range of interest that insufficient information was available for accurate prediction of the SERV engine performance. In addition, no test information existed for slipstream operations with blunt bodies and high nozzle expansion ratios. Hence, the cold-flow test program was implemented to provide this information.

STATUS OF AEROSPIKE TESTING PRIOR TO SERV COLD - FLOW TESTING

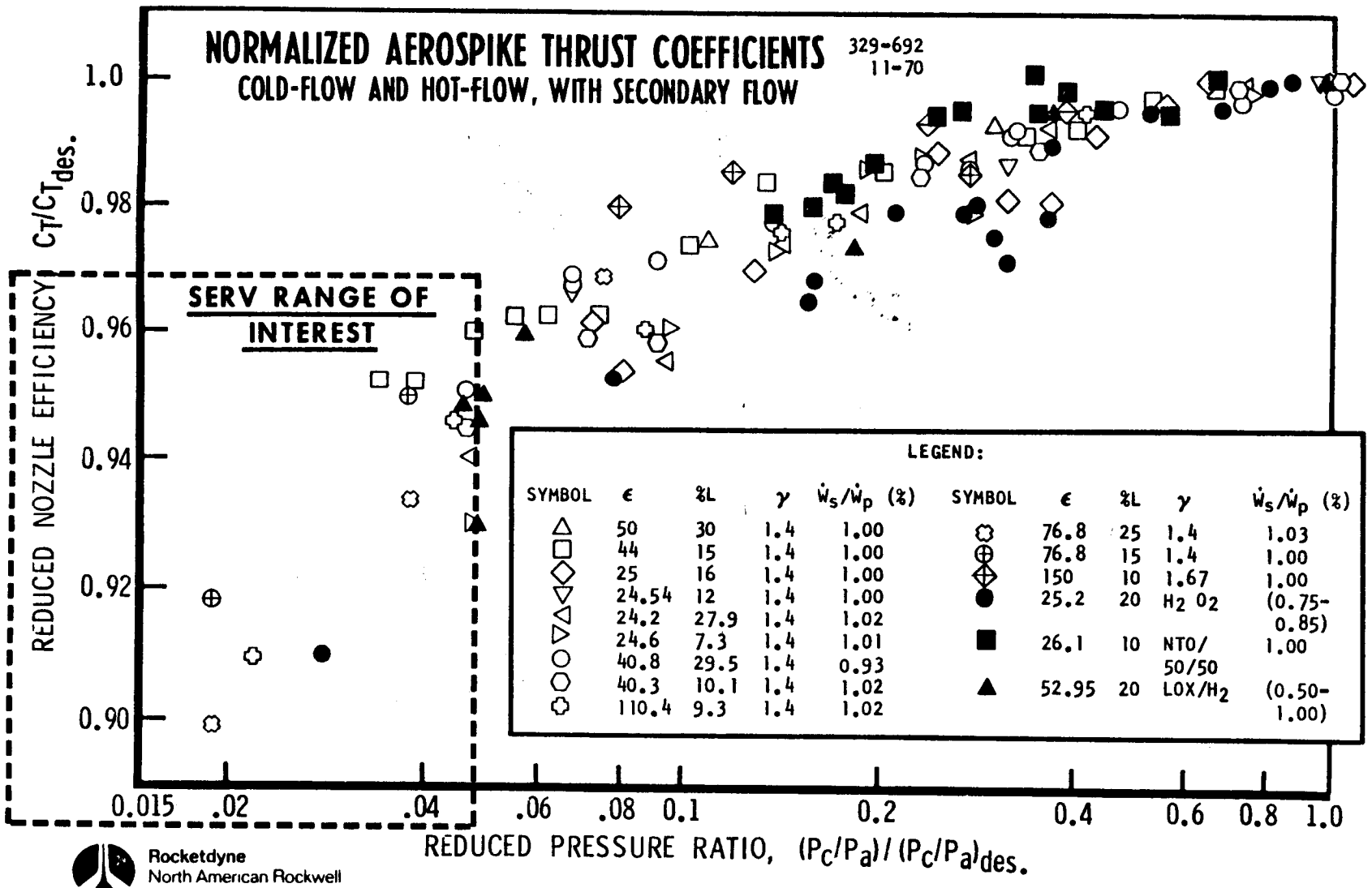

Rocketdyne
North American Rockwell

33

SPACE DIVISION CHRYSLER CORPORATION

4.1.2 TEST DESCRIPTION AND DATA ANALYSIS PROCEDURE

The objective of the cold flow test was to determine performance and base flow characteristics of a high area ratio (465) aerospike engine at flight Mach number and simulated altitude conditions. A cold flow (air) test model was selected to minimize model cost, minimize test cost, and maximize geometric model accuracy. The final status of model design, fabrication, and test is as follows:

1) The model was designed jointly by Chrysler and Rocketdyne (completed 8-22-70).
2) It was fabricated, assembled, and static checked by Rocketdyne (completed 11-10-70).
3) It was tested at AEDC 16T PWT on 12-1-70 through 12-8-70.

The model scaling method used was by direct scaling of the aerospike engine area ratio ($AR_{FS} \approx 465$; $AR_{MS} \approx 417$) and an isentropic compression ramp designed for air ($\gamma = 1.4$).

The essential part of the procedure for predicting hot-firing performance from cold-flow tests lies in the normalization procedure indicated in this chart. The relative simplicity of the technique belies the amount of theoretical and experimental effort expended to prove its usefulness. Shown at the top of the chart are the performance curves for two nozzles with different design pressure ratios and design point thrust coefficients. These values can be different because parameters such as area ratio, gas properties, nozzle length, or contour shape are generally different. If the thrust coefficient and pressure ratio for each case is divided (normalized) by its respective design point value, then both curves tend to map onto a single curve as shown in the lower figure. The inverse of this procedure, that is, mapping from a normalized curve to a hot-flow curve was applied in this test program.

Thus the procedure used for the data analysis was as follows for each Mach number:

1) Values of model C_T vs. pressure ratio were obtained from test data and correlated with respect to $C_{T\infty}$, C_{TBV}, and C_{TBVO}.
2) Using these data, normalized curves of $C_T/C_{TDESIGN}$, vs. $(Pc/P_\infty) / (P_c/P_\infty)_{DESIGN}$ were prepared; model and full scale performance were then correlated by this relationship.
3) Finally, C_T and I_S vs. pressure ratio were obtained for the full scale engine using the normalized C_T - pressure ratio relationship.

NORMALIZATION OF AEROSPIKE THRUST COEFFICIENTS

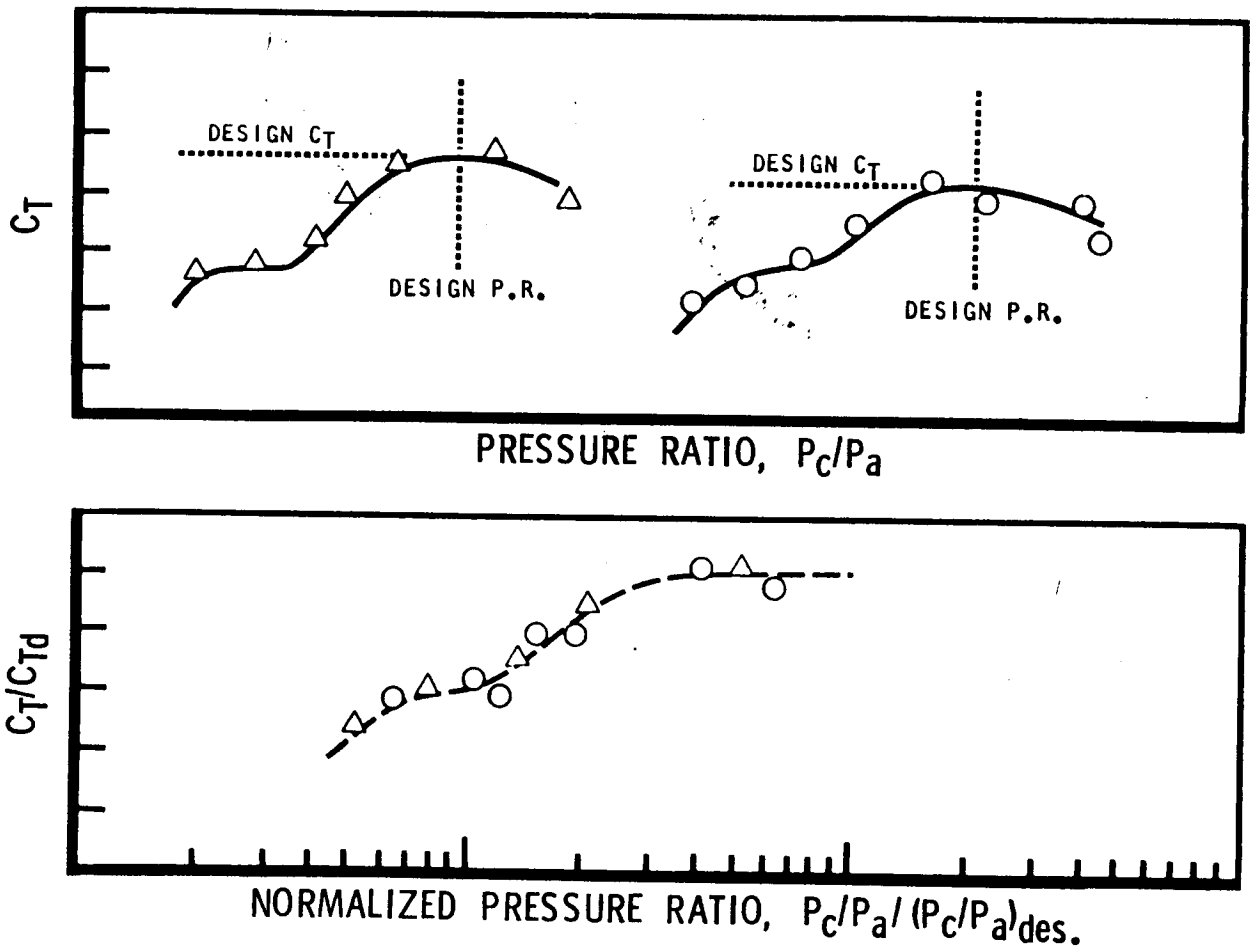

Rocketdyne
North American Rockwell

SPACE DIVISION CHRYSLER CORPORATION

4.1.3 PROPULSION WIND TUNNEL INSTALLATION

This view shows the 2-1/2 percent model (approximately 27 inches in diameter) installed in the 16-foot Transonic Propulsion Wind Tunnel at the Arnold Engineering Development Center. The model is forward-strut-mounted to eliminate obstructions and disturbances in the base region. Four tether cables are secured to the forward sting to prevent dynamic buffeting. The minor aerodynamic disturbances in the base flow created by forward protuberances were well within the accuracy of the measured test data.

Before shipment to AEDC, static checkout of the model was performed in the Rocketdyne Rocket Nozzle Test Facility. The model pressure system was certified to 1080 psi and system leak and proof tests were performed.

PROPULSION WIND TUNNEL INSTALLATION

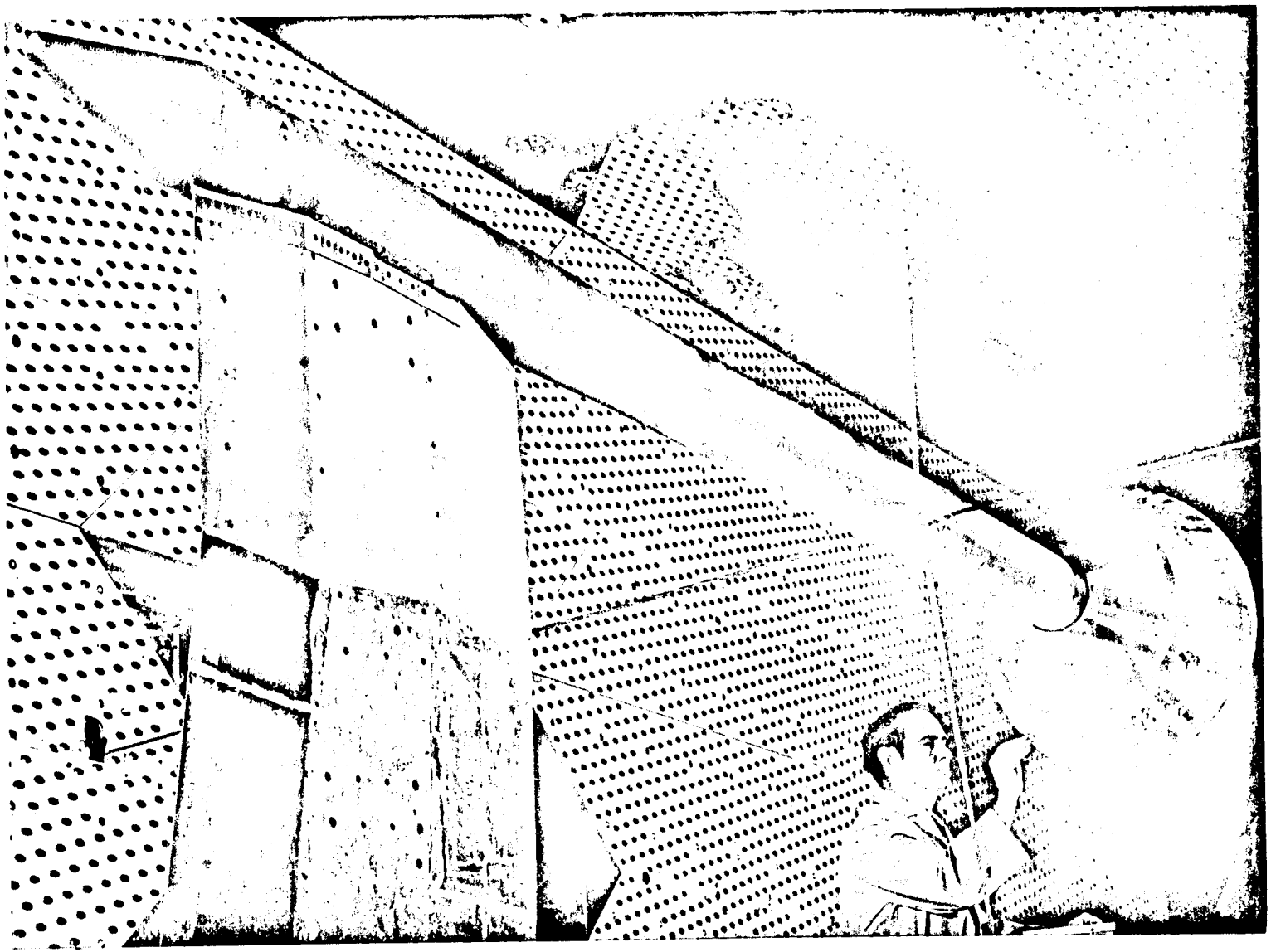

35

Rocketdyne
North American Rockwell

SPACE DIVISION CHRYSLER CORPORATION

4.1.4 TEST CONDITIONS AND DATA

The scaling procedure developed by Rocketdyne dictates that the model geometric area ratio should be approximately equal to the full-scale geometric area ratio. Contours on the nozzle expansion surface are then designed for the corresponding ratio of specific heats of 1.4 for cold flow and 1.2 (approximately) for hot flow. Test conditions and test data are summarized as follows:

1) P_c for the model was 400 psia.
2) P_c/P_∞ was varied from 100 to 1000.
3) M_∞ was varied for a range of values: 0, 0.6, 0.8, 0.9, 1.1, and 1.25.
4) Data taken were:
   a) Force For Engine-on, Engine-off.
   b) Static pressures on forebody, doors, cowl, ramp, base.
   c) Engine primary and secondary flow rates.

A typical Schlieren to illustrate test operation is shown here. Test conditions were: doors off, pressure ratio of 600, and Mach number of 0.9. For a more complete description of test operations there is a motion picture which further documents the cold-flow test.

SCHLIEREN OF COLD FLOW TEST RUN

DOORS OFF, PRESSURE RATIO=600, MACH=0.9

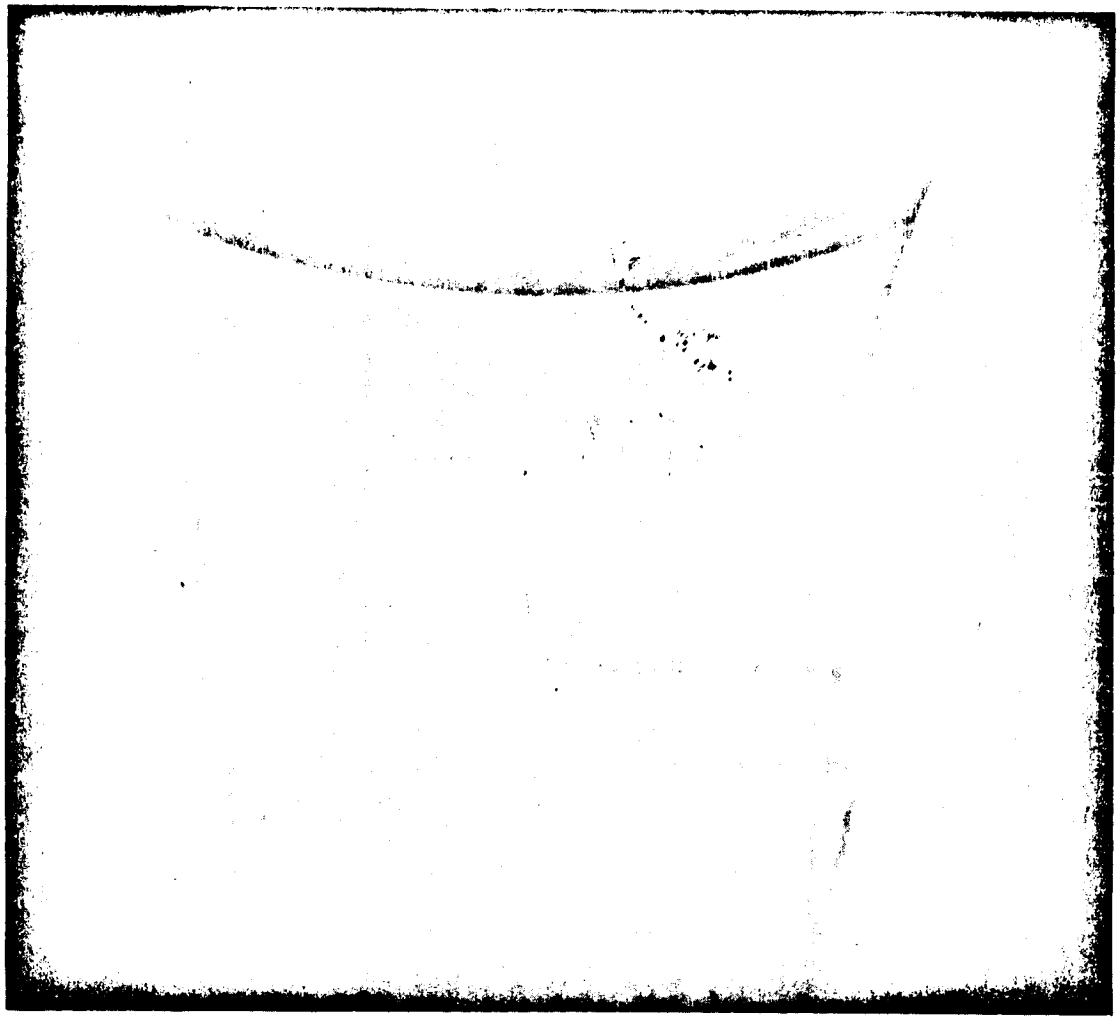

4.1.5 MODEL INSTALLED NOZZLE EFFICIENCY

The installed nozzle efficiency is a measure of nozzle performance including the effect of the nozzle on the vehicle drag:

$$C_{T_I} = C_{T_\infty} - \Delta C_{T_D}.$$

For high pressure ratios, the net effect of the protection doors was a decrease in installed nozzle efficiency. The particular door configuration selected for the model tests did not behave as predicted. The results from these tests indicate that optimization of the door configuration has the potential for a significantly improved installed nozzle efficiency.

Consequently, only doors-off performance was used; but in vehicle design analysis, the door drag was incorporated as a part of the total aerodynamic drag, and the mechanical design of the doors included a means for ventilating the inside cone region, if required after further investigation.

MODEL INSTALLED NOZZLE EFFICIENCY

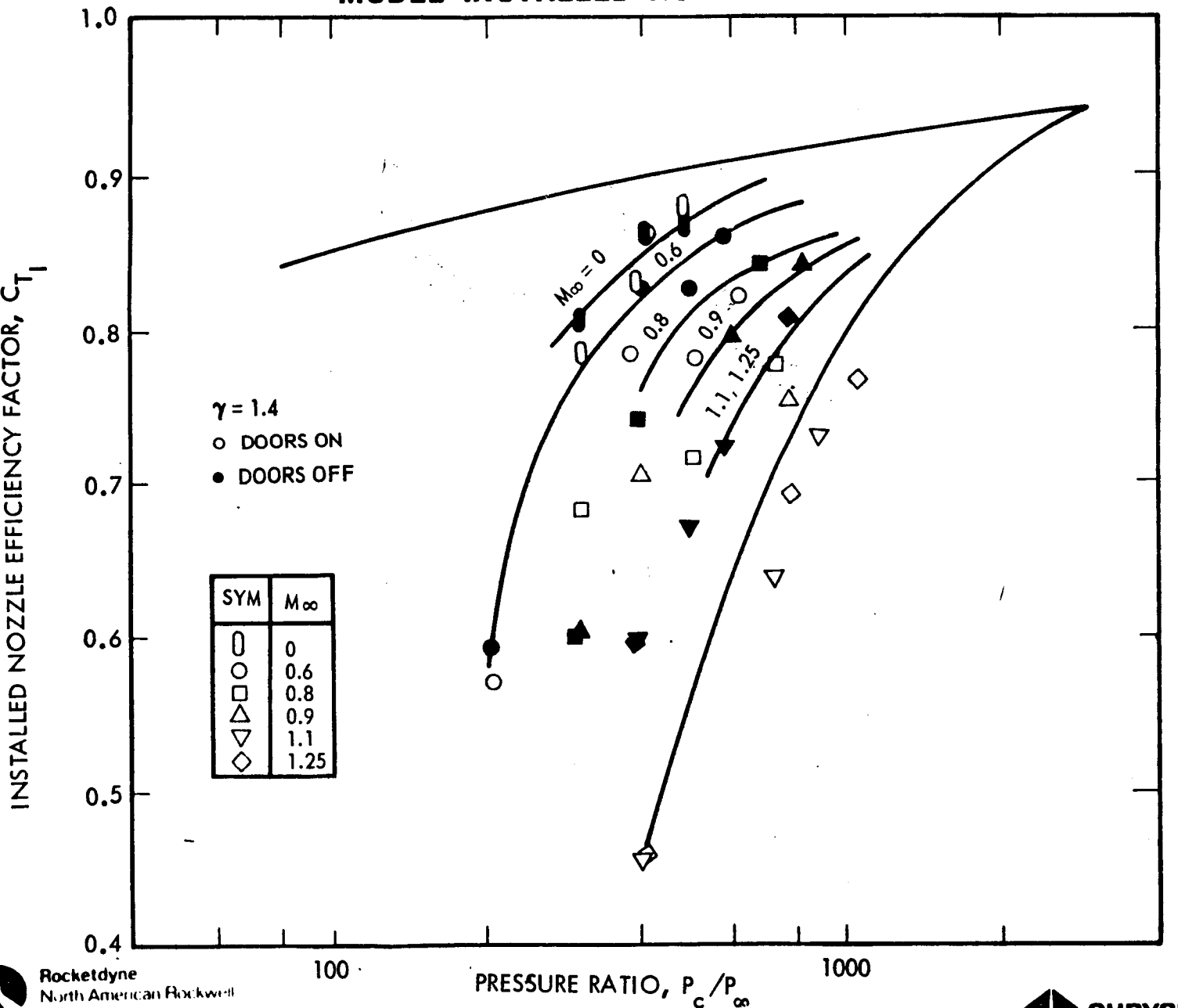

37

Rocketdyne
North American Rockwell

SPACE DIVISION CHRYSLER CORPORATION

4.1.6 FULL SCALE NOZZLE EFFICIENCY FROM MODEL DATA

Having located the point of departure from the uncompensated curve for each flight Mach number, the C_{T_∞} data were extended to the range of pressure ratios corresponding to the SERV operating conditions. The installed efficiency C_{T_I} was computed for C_{T_∞} minus ΔC_{T_D} for the same conditions, the ΔC_{T_D} (drag due to engine operation) being extrapolated from the model data. The full scale installed efficiency was then computed:

$$C_{T_I\ \text{FULL}} = (C_{T_I\ \text{MODEL}}) \quad \frac{C_{T\ \text{DESIGN, FULL}}}{C_{T\ \text{DESIGN, MODEL}}}$$

at the full scale pressure ratio:

$$PR_{\text{FULL}} = (PR_{\text{MODEL}}) \quad \frac{PR_{\text{DESIGN, FULL}}}{PR_{\text{DESIGN, MODEL}}}$$

The range of pressure ratios covers the expected range of pressure ratio and Mach number operating conditions for the SERV mission.

FULL-SCALE NOZZLE EFFICIENCY FROM MODEL DATA

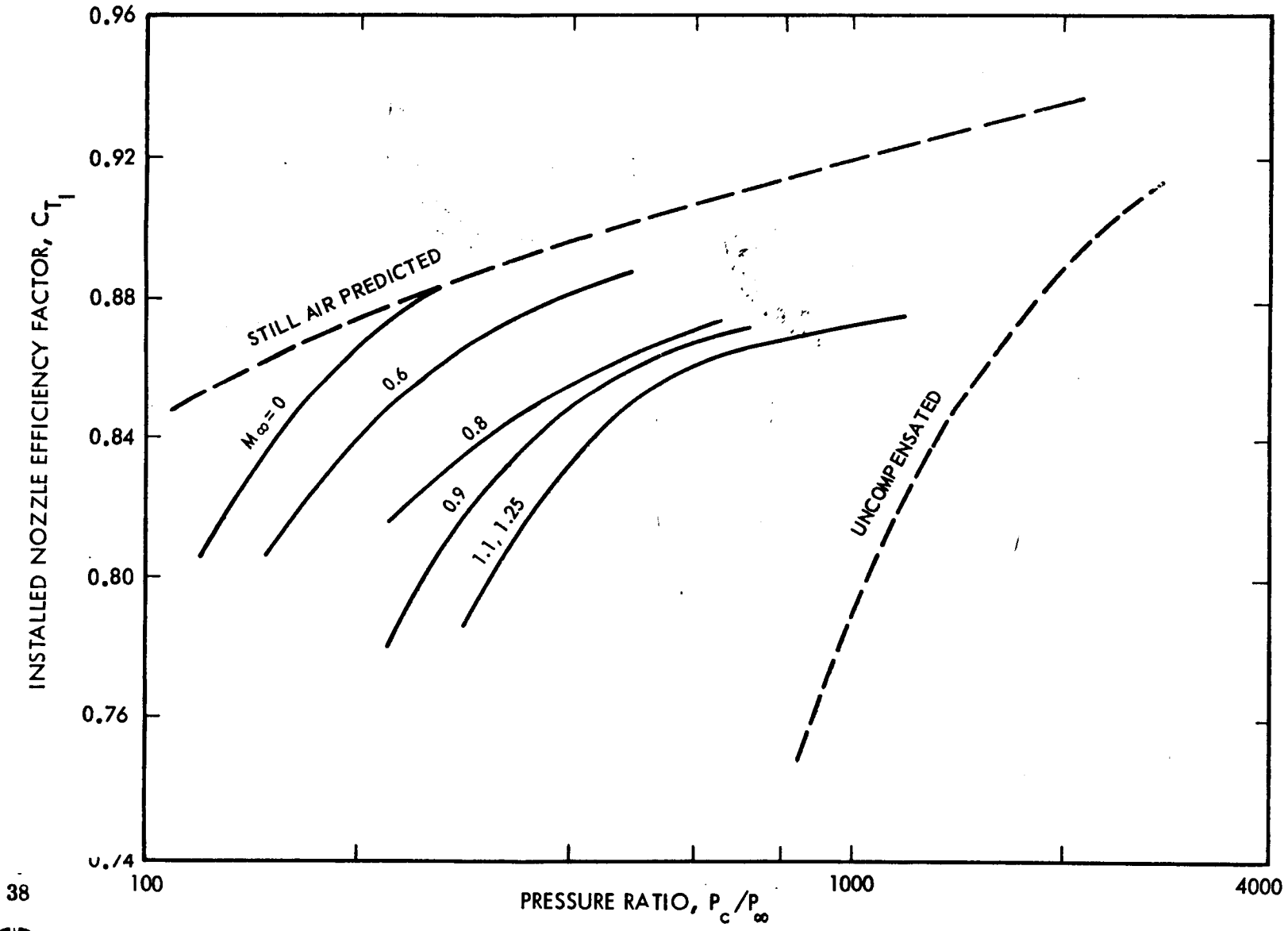

Rocketdyne
North American Rockwell

SPACE DIVISION CHRYSLER CORPORATION

4-15

4.1.7 FULL SCALE ENGINE PERFORMANCE BASED ON MODEL DATA

Specific impulse vs. altitude follows directly from the C_{T_I} vs. pressure ratio data:

$$I_s = C_{T_I} \cdot \eta_{c^*} \cdot I_{s_{IDEAL}}$$

For P_c = 2000 psia, ambient pressure (P_∞) is obtained from pressure ratio, P_c/P_∞, and altitude is known, having P_∞.

FULL-SCALE ENGINE PERFORMANCE BASED ON MODEL DATA

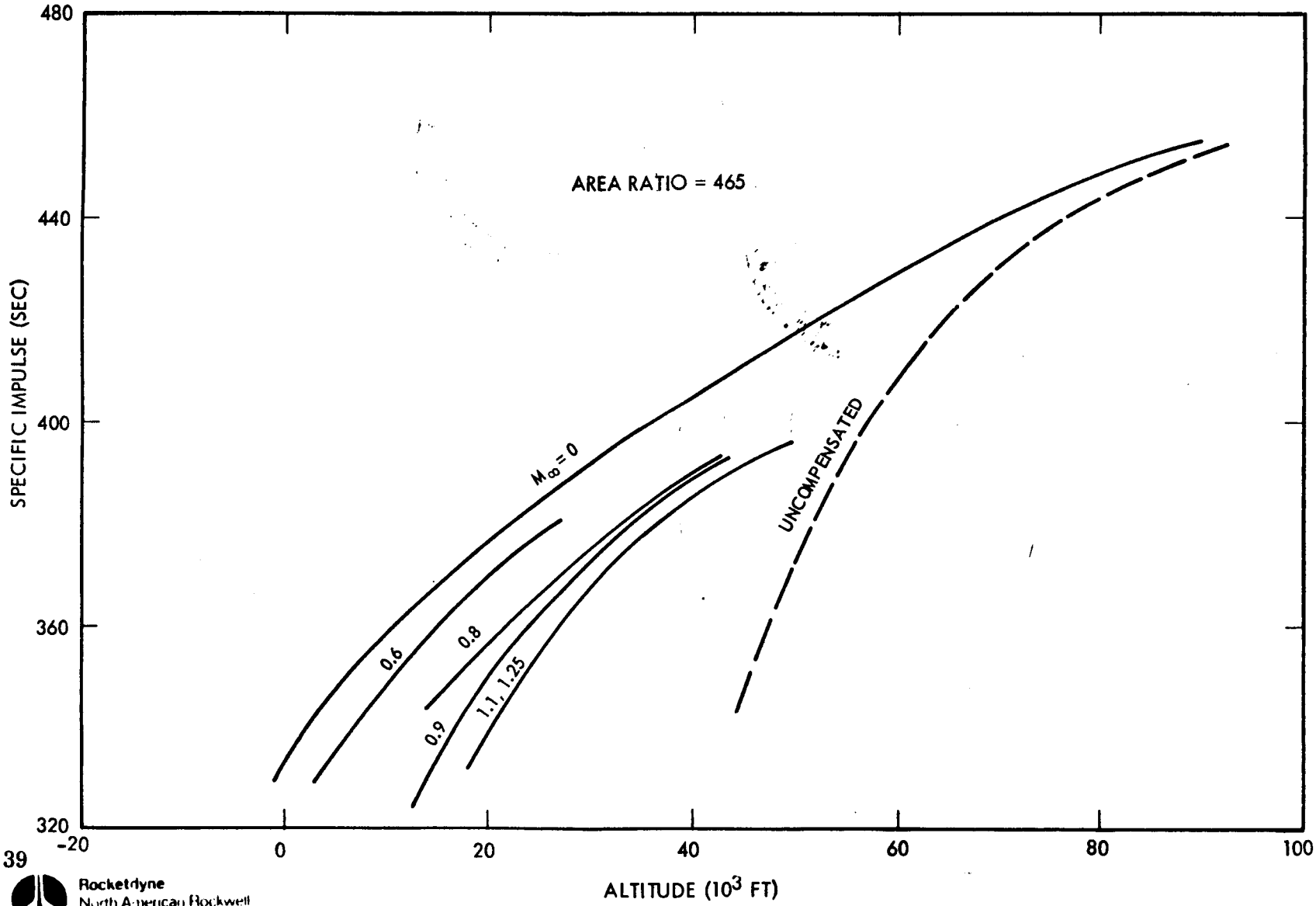

39

Rocketdyne
North American Rockwell

SPACE DIVISION CHRYSLER CORPORATION

4.2 INTEGRATED ENGINE PERFORMANCE

Point design engine performance is presented and overall conclusions of the analysis are listed.

4.2.1 NOMINAL PERFORMANCE OF POINT DESIGN ENGINE

Nominal performance of the point design engine developed by Rocketdyne in the latter portion of the study is shown here. This performance also makes use of the model test data as did the performance presented on last chart. The values of specific impulse as a function of Mach number and altitude shown on this graph were input to the sizing program to perform final configuration sizing. Performance values for a typical SERV trajectory are indicated by the dashed line on the carpet plot.

NOMINAL PERFORMANCE OF POINT DESIGN ENGINE

(AREA RATIO = 433.7)

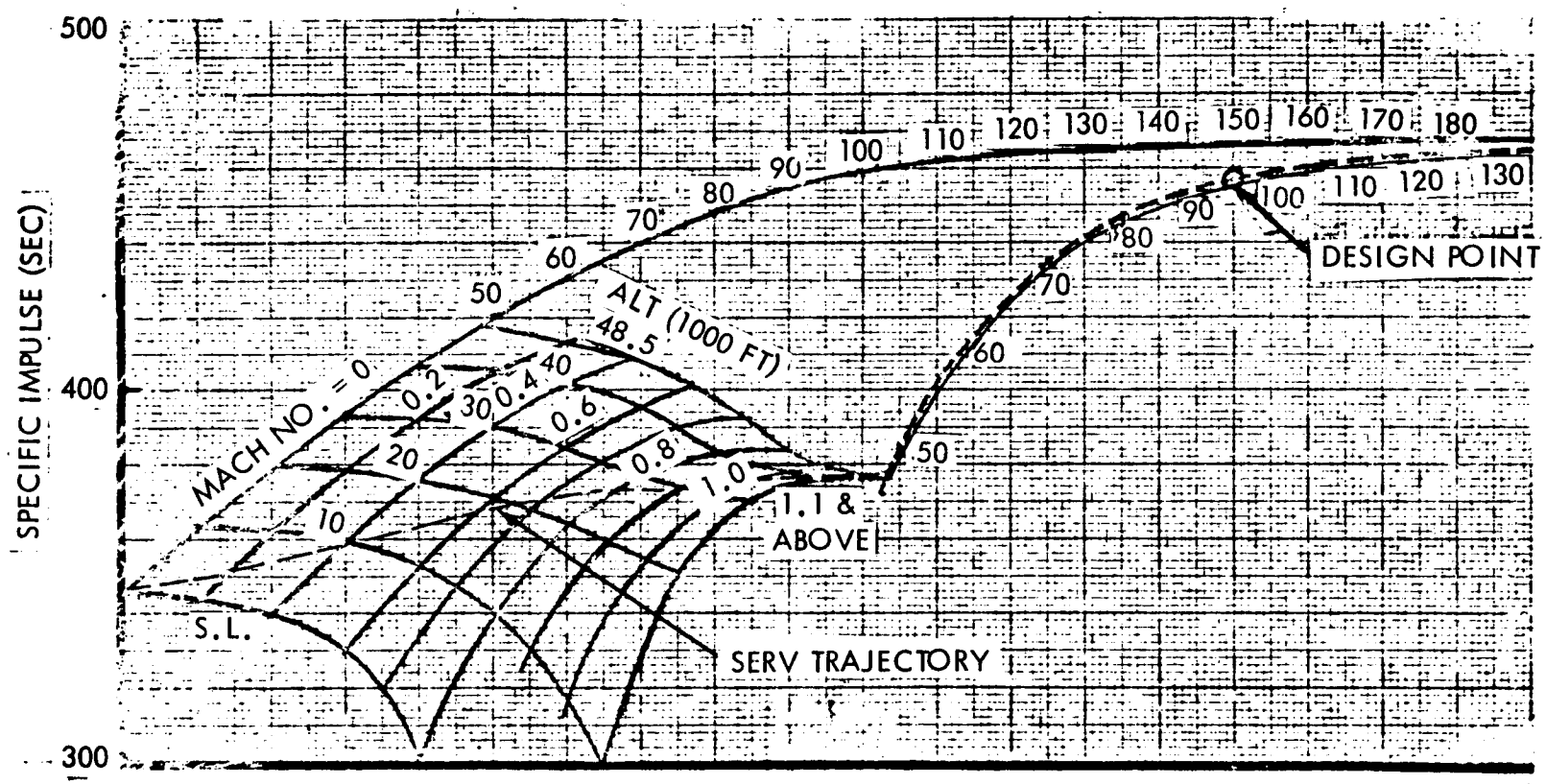

SPACE DIVISION CHRYSLER CORPORATION

4.2.2 CONCLUSIONS - AEROSPIKE PROPULSION PERFORMANCE

Three principal conclusions may be drawn from the analysis:

1) The behavior of the SERV aerospike nozzle was as expected. The base pressures were lower than anticipated but the integrated SERV-aerospike performance was as predicted. No fundamentally new phenomena were observed.

2) Feasibility has been demonstrated within limitations of current tests.

3) Further optimization of engine/vehicle geometry should be explored to improve performance.

CONCLUSIONS - AEROSPIKE ENGINE PROPULSION PERFORMANCE

COLD FLOW TEST RESULTS SHOW -

- BEHAVIOR OF THE SERV AEROSPIKE CONFIGURATION WAS AS EXPECTED
- FEASIBILITY HAS BEEN DEMONSTRATED WITHIN LIMITATIONS OF CURRENT TESTS
- OPTIMIZATION OF ENGINE/VEHICLE GEOMETRY WILL IMPROVE VEHICLE PERFORMANCE

AERODYNAMIC CHARACTERISTICS

Section 5
AERODYNAMIC CHARACTERISTICS

5.0 GENERAL

This section describes drag and stability characteristics for both the ascent configuration and the descent configuration. In addition, reentry trim angle of attack and lift-to-drag ratio are described for the descent configuration. This presentation includes a discussion of test results.

5.1 ASCENT CONFIGURATION

To resolve this feasibility issue, four major tasks of aerodynamic analysis and testing were completed:

1) Investigation of sensitivity of aerodynamic performance to geometric parameters.

2) Definition of preliminary stability and drag characteristics by analytical methods.

3) Performance of preliminary wind tunnel test programs:

   a) Aerospike engine and base flow tests at the AEDC 16-foot Transonic Propulsion Wind Tunnel for a Mach range of 0 to 1.25 (completed 12-8-70).

   b) Force tests at the ARC 6-foot Supersonic Wind Tunnel for a Mach number range of 0.4 to 2.0 (completed 11-10-70).

   c) Force tests at the LaRC 4-foot Unitary Plan Wind Tunnel for a Mach number range of 2.6 to 4.64 (completed 1-12-71).

4) Application of wind tunnel data for definition of full-scale characteristics.

ASCENT AERODYNAMICS

- INVESTIGATE SENSITIVITY OF AERODYNAMIC PERFORMANCE TO GEOMETRIC PARAMETERS
- DEFINE PRELIMINARY BASELINE STABILITY AND DRAG CHARACTERISTICS BY ANALYTICAL METHODS
- CONDUCT PRELIMINARY WIND TUNNEL TEST PROGRAM
  - AEDC 1T PWT BASE FLOW PILOT TEST FOR MACH = 0.6 → 1.3 (COMPLETED 9-1-70)
  - AEDC 16T PWT BASE FLOW TEST FOR MACH = 0 → 1.25 (COMPLETED 12-8-70)
  - ARC 6-FOOT SUPERSONIC WIND TUNNEL FORCE TEST FOR MACH = 0.4 → 2 (COMPLETED 11-10-70)
  - LaRC 4-FOOT UNITARY PLAN WIND TUNNEL FORCE TEST FOR MACH = 2.6 → 4.64 (COMPLETED 1-12-71)
- APPLICATION OF WIND TUNNEL DATA FOR DEFINITION OF FULL SCALE CHARACTERISTICS

5.1.1 INTRODUCTION - NET AXIAL FORCE

Net axial force during ascent flight is defined by three force components acting on the vehicle. These are:

1) Forebody drag composed of pressure and friction drag over the forward surfaces of the vehicle from the payload nose apex rearward to include the outside of the engine doors;

2) the base drag exerted over the inside of the engine doors and exterior flange inward to the engine nozzle, determined by the pressures acting over these surfaces with main stage propulsion on; and

3) effective aerospike engine thrust including compression ramp and base heat shield pressure forces.

The first two of these force components are typically expressed in aerodynamic coefficient form as a function of the flight Mach number at altitude. Forebody and base drag analysis and testing will be discussed in this section. Aerospike engine performance was covered in the previous section.

NET AXIAL FORCE = THRUST – FOREBODY DRAG – BASE DRAG

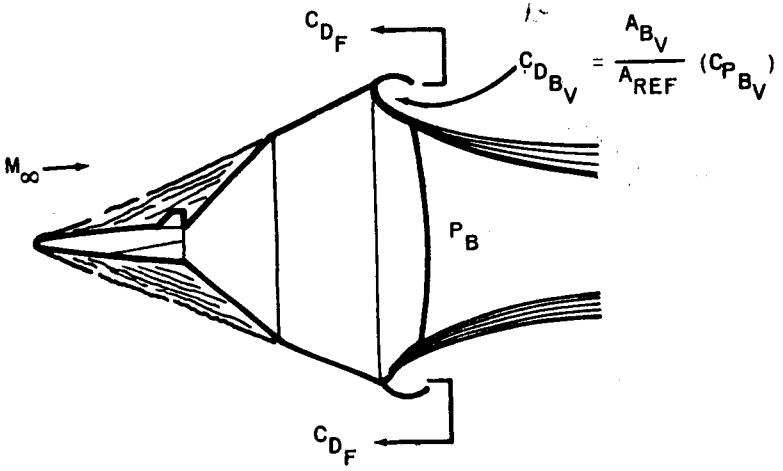

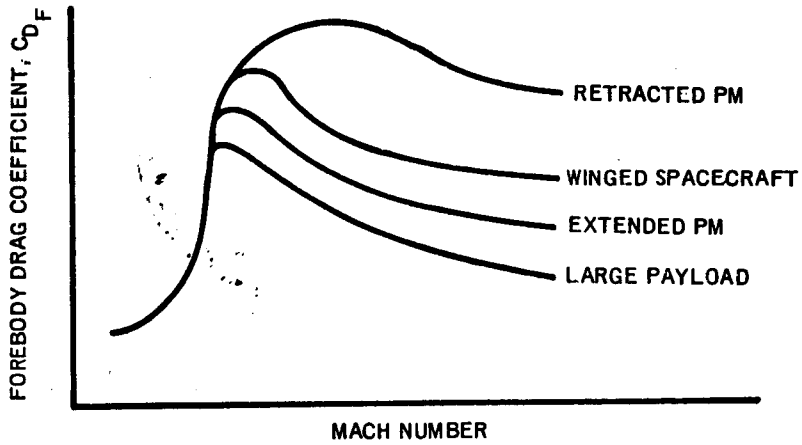

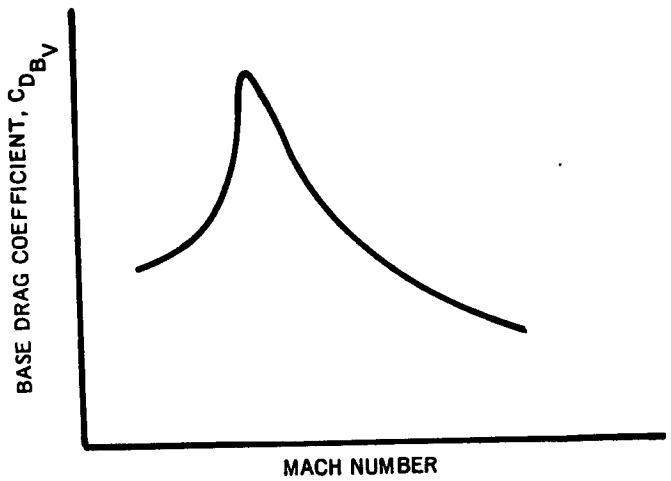

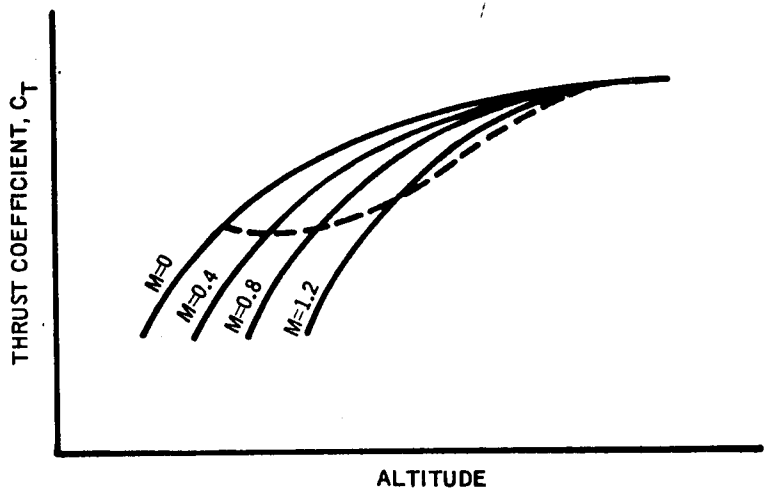

5.1.2 FLOW FIELD SCHLIERENS

Wind tunnel tests of 0.55 percent scale models were conducted at the NASA Ames Research Center and Langley Research Center to define preliminary values of the forebody aerodynamic drag and stability forces for the SERV ascent configuration with various payload geometries.

Shown on this chart are typical schlieren photographs of the aerodynamic flow around the various payload/vehicle configurations from an Ames transonic test. Test conditions are freestream Mach number of 1.4 at zero degrees vehicle angle-of-attack.

FLOW FIELD SCHLIERENS AT MACH 1.4 AND $\alpha = 0$

(FROM ARC TRANSONIC TEST 66-552)

RETRACTED PERSONNEL MODULE (PM-2)

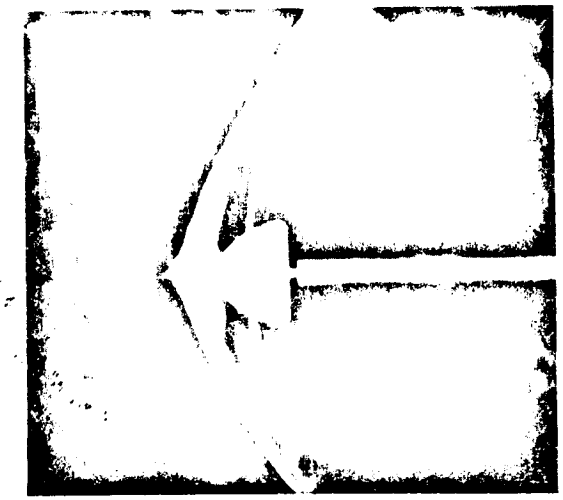

WINGED SPACECRAFT (WP-1)

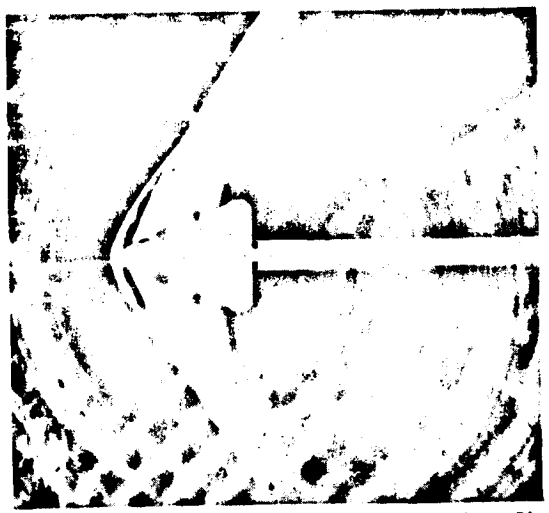

EXTENDED PERSONNEL MODULE (PM-1)

LARGE PAYLOAD (LP-1)

5.1.3 AERODYNAMIC DRAG

Vehicle forebody and base drag coefficients are defined in this chart as a function of flight Mach number. The solid curves present data evaluated from the various scale model wind tunnel tests compared to the preliminary predicted values presented by the dashed curves. The reductions in forebody drag for the various payloads are a result of the aerodynamic spike effect of the longer and larger payloads. Such payloads produce more conical flow pressure fields over the forebody surface as opposed to the high pressure blunt body level of the retracted personnel module configuration. The increase in drag of the winged payload above Mach 2 is caused by a decrease in the separated region and oblique shock attachment on the 45-degree cone. These trends are influenced by local Reynolds number.

The base drag coefficient includes base pressures acting on the engine doors and base cowl area outside of the engine nozzle perimeter. This incremental term provides a total drag coefficient for the vehicle with the correct engine door opening angle consistent with the definition of installed thrust performance presented in the previous section.

AERODYNAMIC DRAG

$\alpha = 0$, $A_{REF} = 6079\ FT^2$

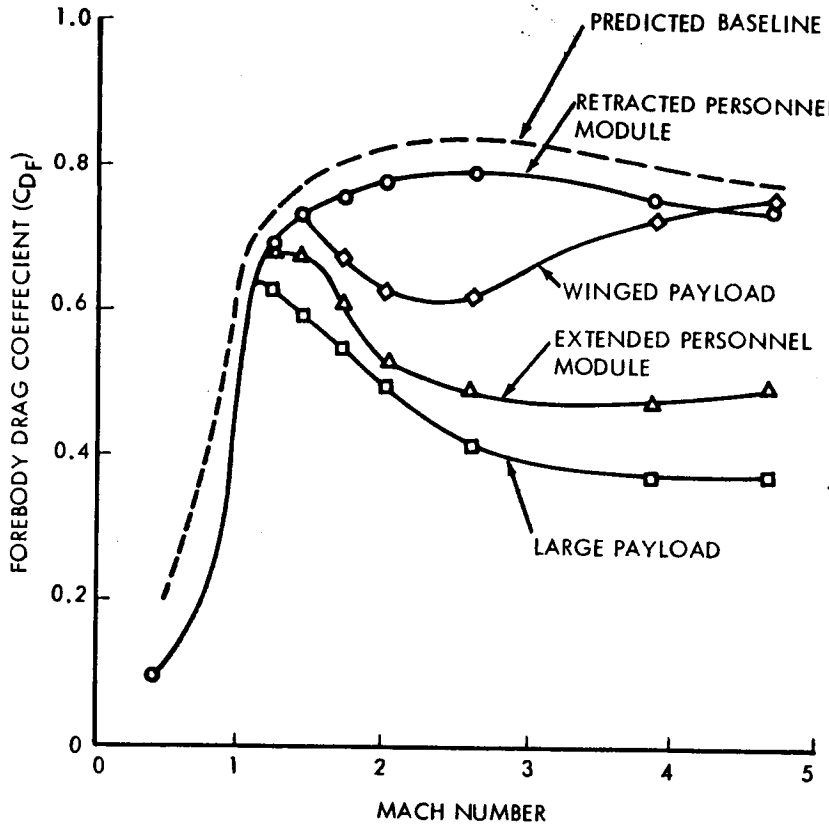

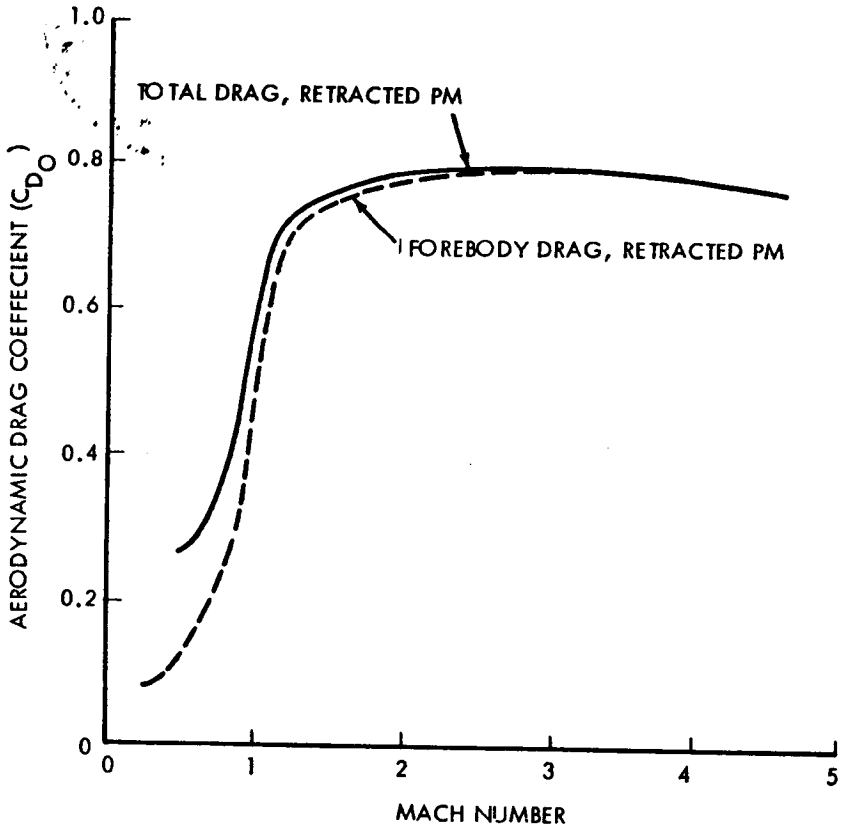

46

SPACE DIVISION CHRYSLER CORPORATION

5.1.4 STABILITY CHARACTERISTICS

Aerodynamic stability characteristics, as determined from the scale model wind tunnel force tests, are presented and compared with the preliminary predictions. The various payload configurations are not all statically stable (i.e., aerodynamic center of pressure (CP/D) aft of the center of gravity); however, the centers of aerodynamic moment are sufficiently close to the nominal center of gravity to not require excessive control forces for directional steering and attitude stability.

ASCENT AERODYNAMIC STABILITY

$-5° < \alpha < +5°$; $A_{REF} = 6079\ FT^2$; $D_{REF} = 88\ FT$

..... PREDICTED BASELINE
——— APPLICATION OF ARC AND LaRC TEST DATA

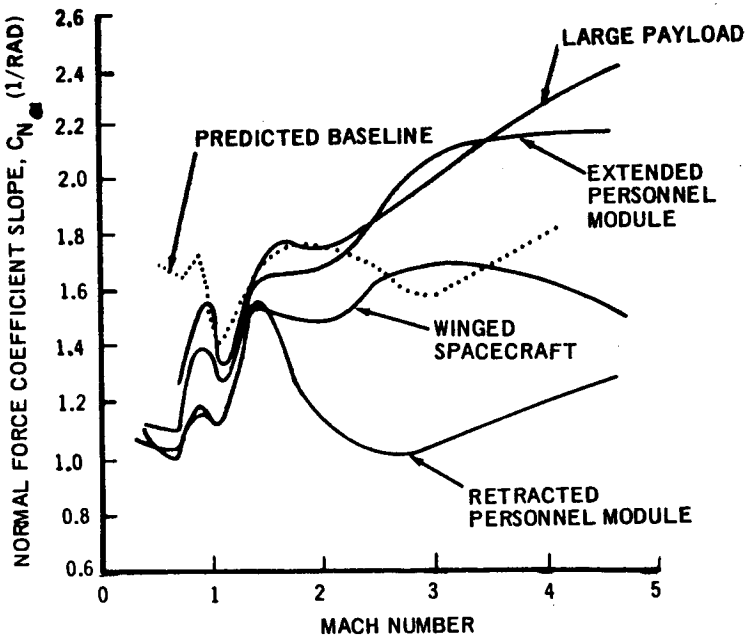

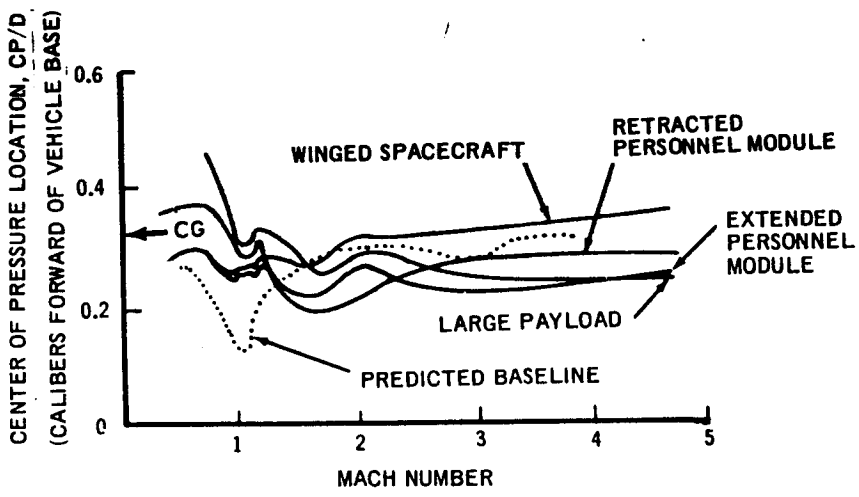

5.1.5 CONCLUSIONS - ASCENT AERODYNAMICS

In summary, for the ascent vehicle, the retracted payload configuration demonstrates high forebody drag characteristics typical of blunt bodies.

The extended payload configurations have lower characteristic drag due to the induced flow separation and equivalent conical flow fields over the forebody above Mach 1.2.

The aerospike engine doors are approximately 10 percent of the total aerodynamic drag. Base drag is induced both by the ambient slipstream flow and the aerospike engine jet exhausts.

All payload configurations have sufficient neutral stability from the standpoint of minimum control force requirements.

CONCLUSIONS – ASCENT AERODYNAMICS

- RETRACTED PM VEHICLE DEMONSTRATES BLUNT BODY DRAG CHARACTERISTICS
- EXTENDED PAYLOADS INDUCE FLOW SEPARATION RESULTING IN DRAG REDUCTION AND EQUIVALENT CONICAL BODY CHARACTERISTICS ABOVE MACH 1.2
- AEROSPIKE ENGINE DOORS APPROXIMATELY 10 PERCENT OF TOTAL DRAG
- ALL PAYLOAD CONFIGURATIONS ADEQUATELY STABLE

5.2 DESCENT CONFIGURATION

SERV descent characteristics were first estimated by preliminary design analytical methods utilizing available Apollo data. These characteristics include reentry drag, stability, trim angle of attack, and lift-to-drag ratio. A minimum-scope preliminary wind tunnel test program was then defined to verify the predicted characteristics and determine those characteristics in the transonic and subsonic Mach range for which prediction methods are not adequate.

The test program consisted of testing a 0.55 percent (6 inch diameter) scale model of SERV parametric configurations through the deceleration Mach range of 4.64 to 0.4. It was concluded from indications of the reference Apollo data that the high Mach number aerodynamic data could be extrapolated to the reentry hypersonic Mach range with adequate accuracy for this feasibility study.

High Mach range tests were conducted in the 4-foot supersonic leg of the Langley Unitary Plan Wind Tunnel and were completed on January 12, 1971. Testing in the lower subsonic and transonic Mach range was completed in the Ames 6-foot Supersonic Wind Tunnel on November 10, 1970. These data were then analyzed to define the full scale hypersonic reentry and deceleration characteristics for vehicle definition.

DESCENT AERODYNAMICS

- INVESTIGATE SENSITIVITY OF AERODYNAMIC PERFORMANCE TO GEOMETRIC PARAMETERS
- DEFINE PRELIMINARY BASELINE REENTRY AND TERMINAL DECELERATION AERODYNAMIC CHARACTERISTICS BY ANALYTICAL METHODS AND AVAILABLE APOLLO DATA (SCALE MODEL TESTS AND FLIGHT)
  - DRAG
  - LIFT-TO-DRAG RATIO (L/D)
  - STABILITY AND TRIM CHARACTERISTICS
- CONDUCT PRELIMINARY WIND TUNNEL TEST PROGRAM
  - LaRC 4-FOOT UNITARY PLAN WIND TUNNEL FOR MACH = 4.6→2.6 (COMPLETED 1/12/71) HIGH MACH NUMBER DATA INDICATIVE OF HYPERSONIC REENTRY VALUES
  - ARC 6-FOOT SUPERSONIC WIND TUNNEL FOR MACH = 2→0.4 (COMPLETED 11/10/70
- ANALYZE TEST DATA FOR DEFINITION OF FULL SCALE HYPERSONIC REENTRY AND TERMINAL DECELERATION AERODYNAMIC CHARACTERISTICS

5.2.1 REENTRY TRIM AERODYNAMICS

The SERV reenters with heat shield forward and with a negative wind angle of attack to achieve the required lift-to-drag ratio (similar to the Apollo spacecraft). To obtain static trim at this negative angle of attack, a center of gravity offset from the vehicle geometric centerline may be employed. Shown here are the static trim angle of attack (α_{TRIM}) and the lift-to-drag ratio (L/D) at trim angle of attack for the SERV baseline reentry vehicle, with and without engine doors. These values are presented as a function of CG offset in feet for reentry flight Mach numbers varying from 9.0 to 0.4. As defined in the legend, the solid lines represent predicted values for the SERV baseline vehicle with engine doors. These predictions were determined by use of empirical application of Apollo reference data. The data symbols reflect SERV wind tunnel test data acquired in the Ames Research Center and Langley Research Center scale model force tests. By application of Apollo data trends, these values can be extrapolated to the hypersonic reentry Mach range with adequate accuracy for this level of feasibility study.

Removal of the aerospike reentry protection doors lowers α_{TRIM} and respective L/D by approximately 30 percent below that with doors on. These data show that an approximate 4-foot CG offset will be required for the SERV baseline with engine doors to statically trim at an angle of attack in the hypersonic Mach range sufficient to attain an L/D of 0.3. With this constant CG offset, the static trim angle of attack and respective L/D will increase and then decrease as the vehicle decelerates through the supersonic and transonic Mach ranges.

Also illustrated are Schlieren photographs showing the aerodynamic flow around the two configurations at $M_\infty = 2.0$ and $\alpha = -22$ degrees; these are typical of the photographs taken during the ARC and LaRC tests.

REENTRY TRIM AERODYNAMICS

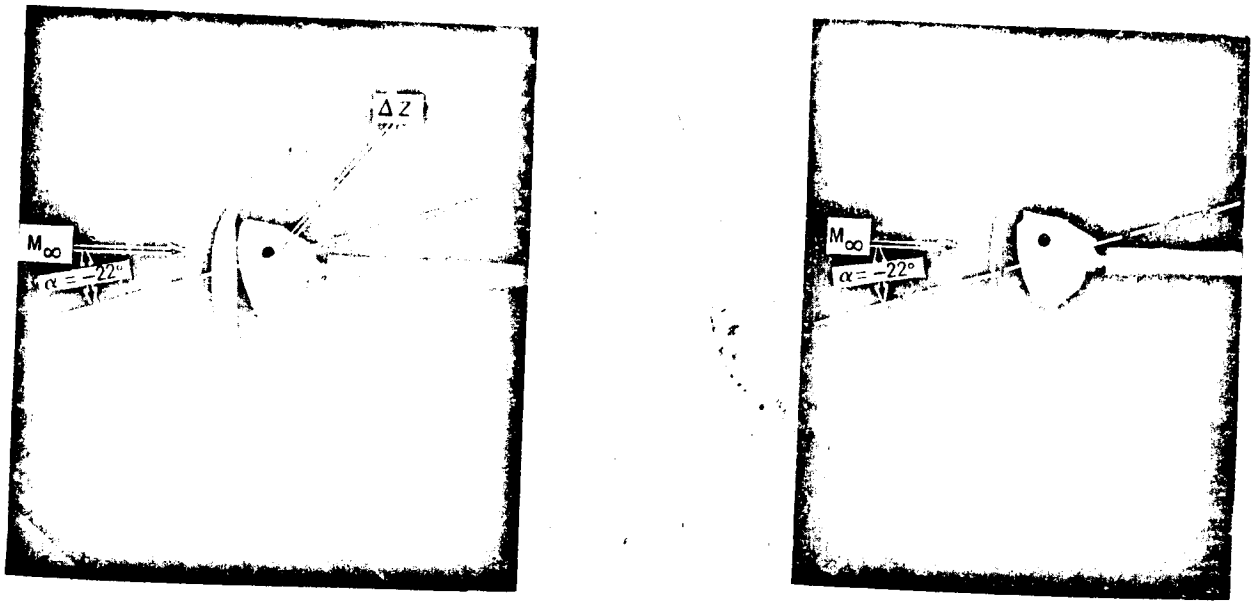

ARC TEST FLOW SCHLIERENS AT $M_\infty = 2.0$

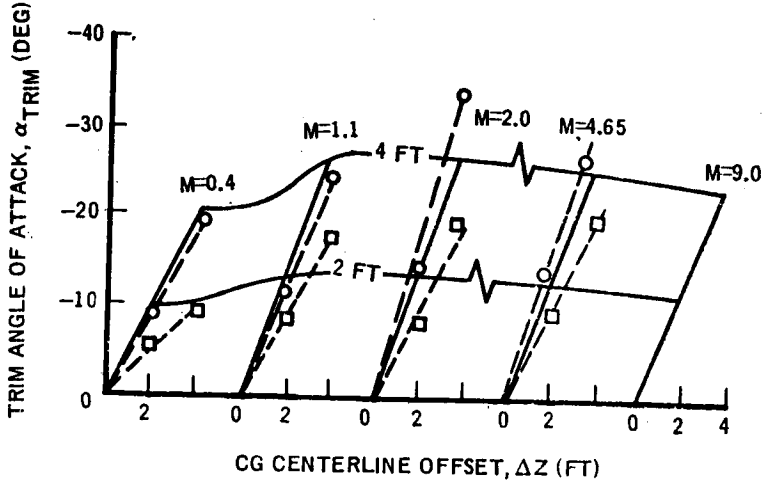

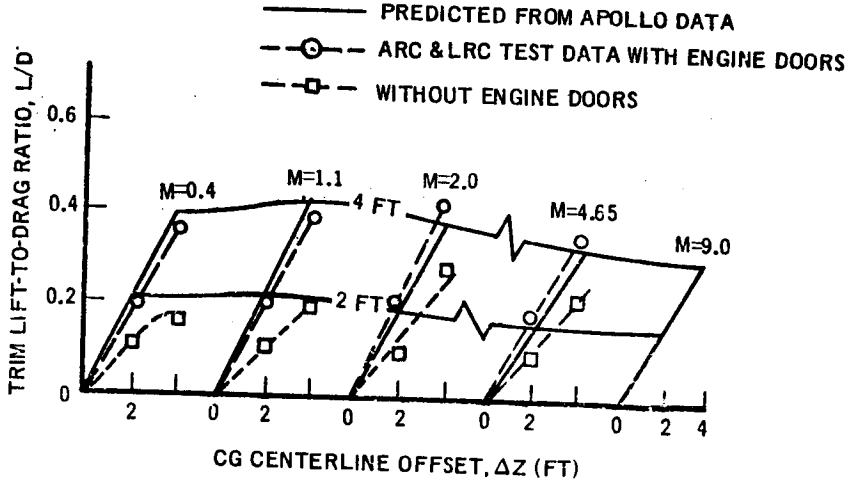

5.2.2 STABILITY AND DRAG

Employing a vehicle center-of-gravity offset above the vehicle geometric centerline will result in the vehicle aerodynamically trimming at a heat shield facedown angle of attack. This is illustrated by the left hand figure of the chart which shows aerodynamic pitching moment coefficient as a function of wind angle of attack (α) for the vehicle center-of-gravity offset. For each Mach condition, the static aerodynamic trim angle of attack is that point at which the aerodynamic pitching moment is equal to zero. The continuous near-linear negative slope of the pitching moment with angle of attack indicates that the reentry configuration is stable within ± 10 degrees of the trim angle of attack and will have a favorable restoring moment when disturbed by winds.

As illustrated in the right of this chart, the aerodynamic drag coefficient at α_{TRIM} is nearly constant from hypersonic reentry through supersonic deceleration for a specific offset of the center of gravity from the vehicle geometric centerline. These values decrease below Mach 1.0, following the trend expected for a hemispherically blunt body such as SERV.

Aerodynamic lift-to-drag ratio (L/D) at trim angle of attack increases with decreasing deceleration Mach number, down to Mach 1.5 and becomes irregular through the transonic speed regime.

AERODYNAMIC TRIM CHARACTERISTICS FOR TASK 4 BASELINE DESCENT VEHICLE

REFERENCE CG LOCATION: $\Delta X = 21.6$FT , $\Delta Z = 3.39$ FT

$A_{REF} = 6079$ FT^2 $D_{REF} = 88$ FT

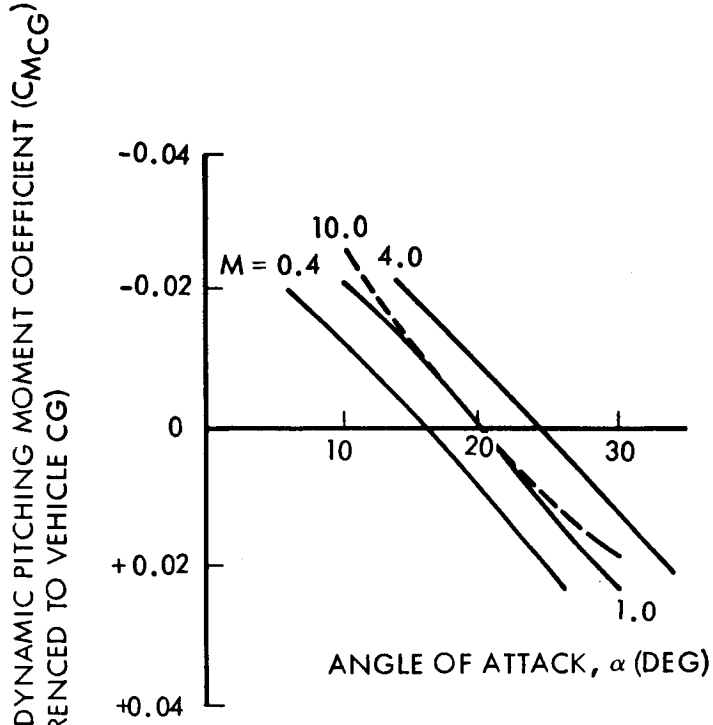

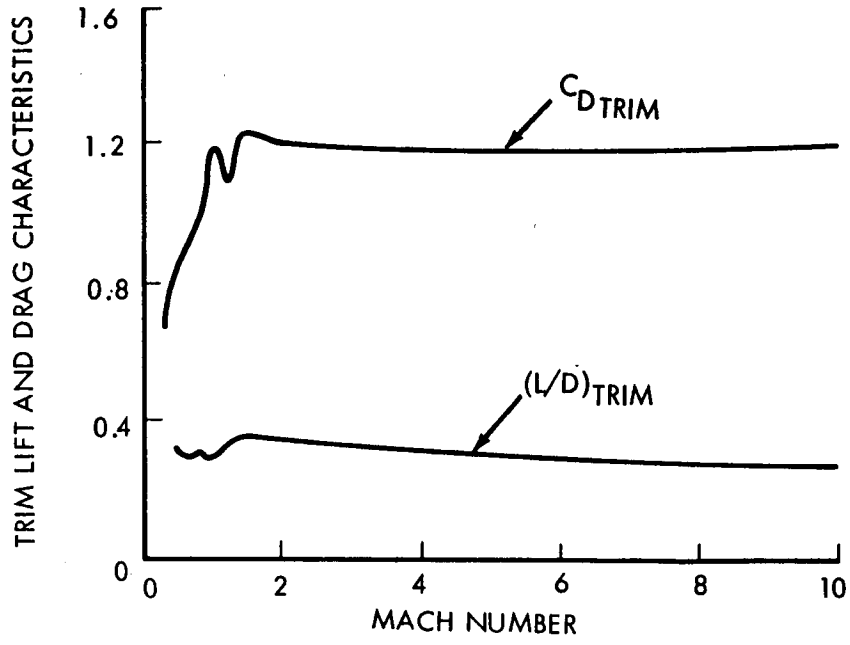

51

SPACE DIVISION CHRYSLER CORPORATION

5.2.3 CONFIGURATION TRIM CHARACTERISTICS

Descent vehicle static aerodynamic trim characteristics are very sensitive to the reentry heat shield corner geometry. Illustrated here are the trim angle of attack (α_T) and lift-to-drag ratio at α_T for four different corner geometries at Mach 4.64 as a function of lateral center of gravity position for a specific longitudinal location. There is no appreciable change in α_T by decreasing the heat shield corner radius from the baseline 11 percent to 5 percent, but there is an approximate 10 percent increase in L/D at trim angle of attack. Removing the aerospike engine thermal protection doors results in a 20 percent reduction in α_T and over a 30 percent decrease in the trim L/D. A very favorable increase in both α_T and $(L/D)_T$ is obtained by reducing the corner radius on just the lower side of the heat shield. A 11 percent / 5 percent combination was tested which indicated that at this Mach number a trim angle of attack of 10 degrees and a trim lift-to-drag ratio of 0.15 could be obtained with no lateral CG offset; and for all feasible CG locations, there would be a sizable increase in the trim lift-to-drag ratio primarily due to the increase in α_T.

CONFIGURATION TRIM CHARACTERISTICS

NOTE:

- LOGITUDINAL CG LOCATION, X/D = 0.2459 REFERENCED TO VEHICLE STA (O)
- ΔZ REFERENCED TO VEHICLE CENTERLINE (FT)
- M_∞= 4.64

——— 11% HEAT SHIELD CORNER RADIUS
- - - - 5% HEAT SHIELD CORNER RADIUS
——— 11% UPPER, 5% LOWER HEAT SHIELD CORNER RADIUS
—·— NO DOORS

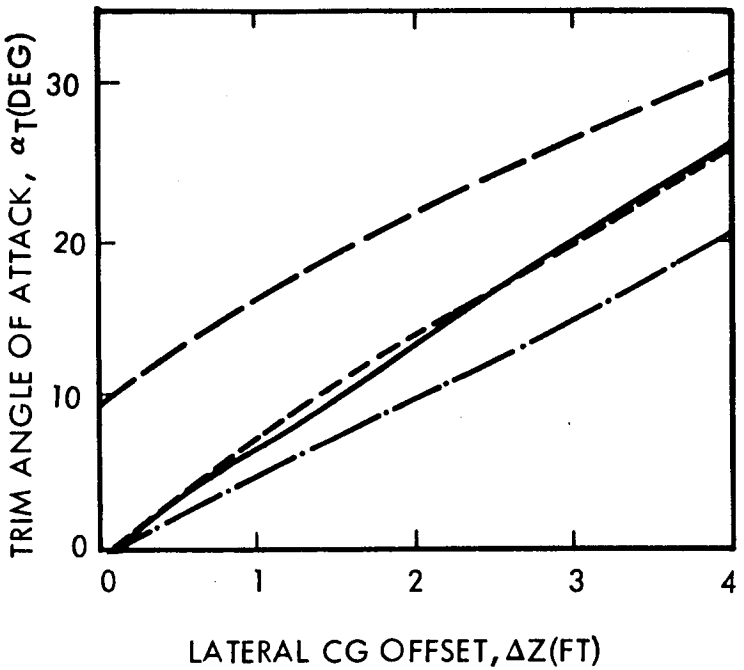

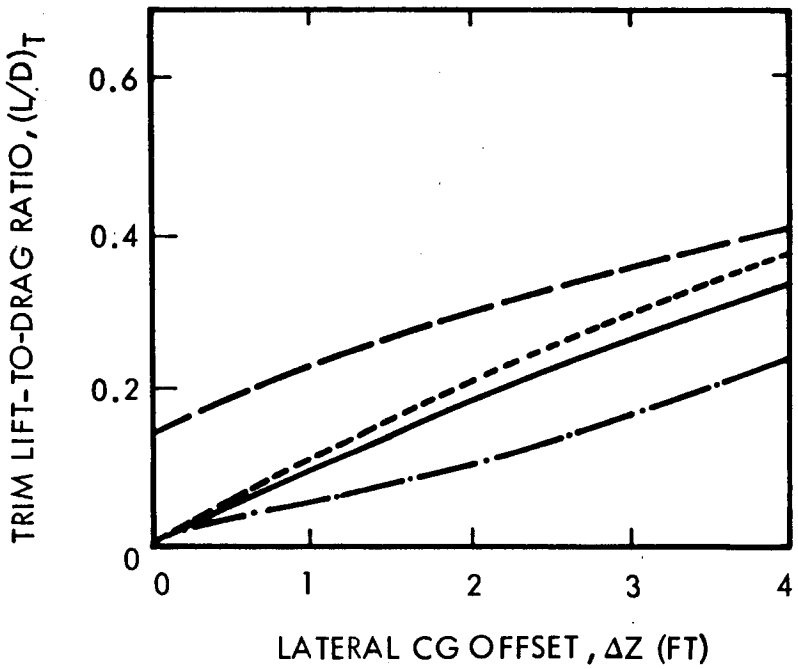

5.2.4 EFFECT OF HEAT SHIELD DIFFERENTIAL CORNER RADIUS ON AERODYNAMIC TRIM CHARACTERISTICS

The Mach 4.64 SERV test data have been extrapolated to Mach 7.3 by application of Mach number trends of reference Apollo data. This chart compares SERV trim characteristics at Mach 7.3 with Apollo data and other geometric reference data from the Apollo design studies. Trim angle of attack (α_T) and trim lift-to-drag ratio $(L/D)_T$ are presented as functions of the upper and lower reentry heat shield corner radii. SERV compares well with the Apollo data, though somewhat lower in values for the same corner radii combination. This is due primarily to the shallower afterbody angle of the SERV and partly to the conservatism in extrapolating the SERV test data. The trim conditions shown here are for a nominal CG location of 25 feet axially from the center of the face of heat shield and 2.5 feet of lateral offset from the vehicle centerline. This center of gravity location should not be difficult to attain. At this flight Mach number, the 11-percent/5-percent heat shield corner radii combination should provide more than the trim L/D of 0.3 desired.

EFFECT OF HEAT SHIELD DIFFERENTIAL CORNER RADIUS ON AERODYNAMIC TRIM CHARACTERISTICS M≈7.3

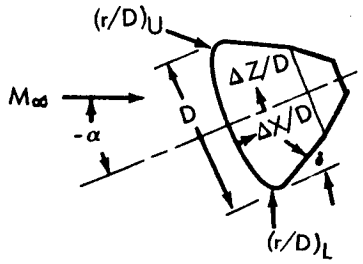

SYM	(r/D)L	(r/D)U	δ(DEG)	REFERENCE
⊙	0	0	33	NASA-TM-X588
⊡	0	0.05	33	NASA-TM-X588
◈	0	0.10	33	NASA-TM-X588
◬	0.05	0.05	33	APOLLO, NASA-TM-X588
◣	0.10	0.10	33	NASA-TM-X588
◢	0.15	0.15	33	NASA-TM-X588
◈	0.05	0.11	25	SERV
◈	0.11	0.11	25	SERV

NOTE: CG LOCATED AT X/D = 0.28, Z/D = 0.028

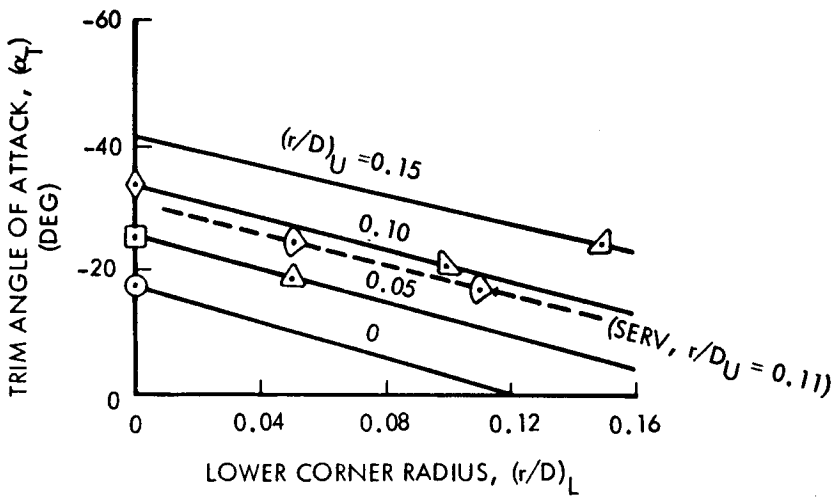

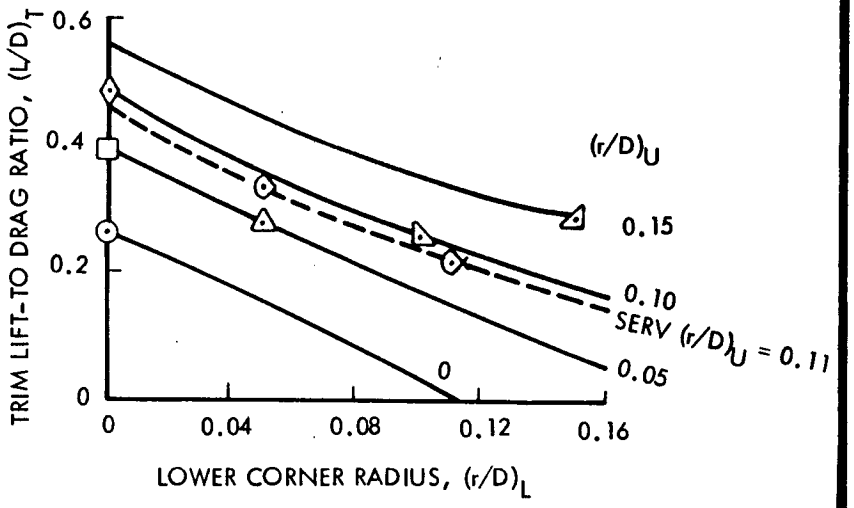

SPACE DIVISION CHRYSLER CORPORATION

5.2.5 DESCENT AERODYNAMIC TRIM CHARACTERISTICS FOR RECOMMENDED VEHICLE

To achieve the desired reentry L/D of 0.3 with minimum CG offset requirement, it was recommended that aerodynamic trim augmentation be utilized by employing different corner radii on the upper and lower perimeter of the heat shield. This chart illustrates trim conditions which the recommended vehicle, having an upper corner radius of $(r/d)_u = 0.11$ and a lower corner radius of $(r/d)_L = 0.05$, would fly from reentry through supersonic deceleration. The vehicle would be statically stable throughout this range and continue to be stable through transonic and subsonic deceleration.

Reentry trim angle of attack would be held to less than the afterbody angle to minimize afterbody heating, by decreasing the lateral CG offset if necessary. A resultant α_T of approximately -22° would adequately provide the reentry L/D of 0.3 desired. Both α_T and $(L/D)_T$ would increase with decelerating Mach number in the supersonic range below the flight regime of maximum aerodynamic heating.

The differential corner radii can easily be achieved by contouring the upper three quarters of the heat shield circumference to the larger radius and employing the smaller corner radius on only the lower quadrant. Effects of this heat shield corner radiusing would hardly be significant to the ascent aerodynamic characteristics of the vehicle, particularly if the radii were confined to the aerospike engine protection doors, which are open during ascent flight.

DESCENT AERODYNAMIC TRIM CHARACTERISTICS FOR RECOMMENDED VEHICLE

- $A_{REF} = \frac{\pi D_{REF}^2}{4}$
- $D_{REF} = D_{MAX}$
- CG LOCATED AT $\Delta X/D = 0.28$, $\Delta Z/D < 0.028$
- $(r/D)_U = 0.11$, $(r/D)_L = 0.05$

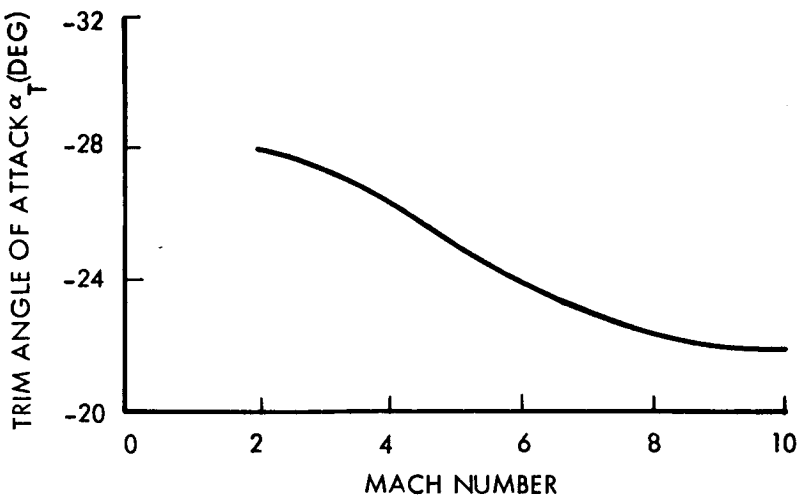

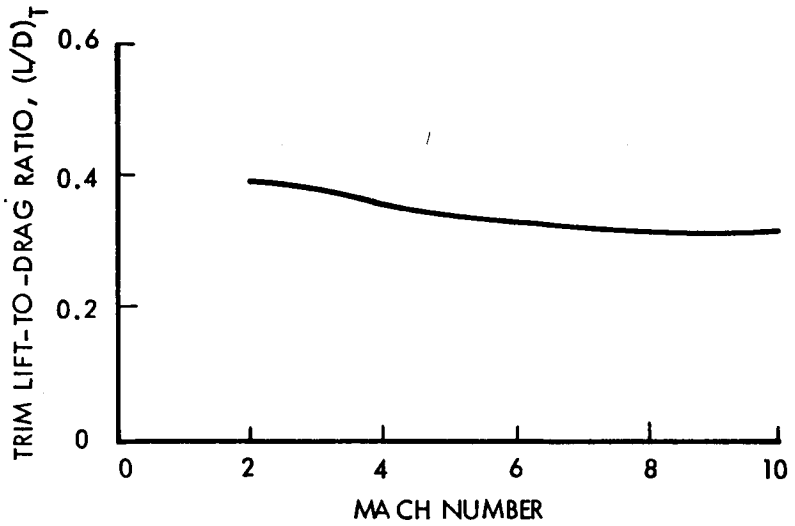

54

SPACE DIVISION CHRYSLER CORPORATION

5.2.6 CONCLUSIONS - DESCENT AERODYNAMICS

The desired hypersonic reentry trim L/D of 0.3 can be obtained for the baseline vehicle with a CG offset of approximately 4 ft. Trim angle of attack would be $\alpha \approx -22$ degrees. The vehicle is statically stable within ± 10 degrees of the trim angle of attack from hypersonic reentry through transonic deceleration.

Removal of the aerospike engine thermal protection doors would result in over a 30 percent reduction in reentry trim L/D. This is due to both the reduction in reentry trim angle of attack and L/D at angle of attack.

Differential corner radiusing of the heat shield is recommended to minimize CG offset required to achieve the desired trim lift-to-drag ratio.

CONCLUSIONS – DESCENT AERODYNAMICS

- HYPERSONIC REENTRY ($(L/D)_{TRIM} = 0.3$) ATTAINABLE FOR BASELINE VEHICLE WITH APPROXIMATELY 4 FT OF CG OFFSET ($\alpha_{TRIM} \approx -22°$)
- VEHICLE IS STATICALLY STABLE WITHIN $\pm$ 10° OF α_{TRIM} FROM HYPERSONIC REENTRY THROUGH TRANSONIC DECELERATION
- REMOVAL OF AEROSPIKE ENGINE DOORS REDUCES $(L/D)_{TRIM}$ APPROXIMATELY 30 PERCENT
- DIFFERENTIAL CORNER RADIUSING OF HEAT SHIELD RECOMMENDED TO MINIMIZE CG OFFSET REQUIRED TO ACHIEVE DESIRED $(L/D)_{TRIM}$

THERMAL PROTECTION CHARACTERISTICS

Section 6

THERMAL PROTECTION CHARACTERISTICS

6.0 GENERAL

The thermal environment and protection requirements for ascent and reentry are presented and the effect of cryogen boil-off is discussed.

SERV reenters the atmosphere at an attitude very similar to the Apollo spacecraft. Because the SERV shape is also similar to, though larger than Apollo, extensive use was made of Apollo experimental and flight data in the SERV reentry heating predictions.

6.1 ASCENT HEATING RATE COMPARISON

The ascent trajectory of SERV would result in lower aerodynamic heating than the trajectories flown by the Saturn IB vehicles. However, the aerodynamic flow field caused by the SERV's 45°0′ and 22°40′ frustums results in higher aerodynamic heating than the smaller frustum angles on the Saturn IB. Convective thermal environments that occur on the SERV frustums are compared with Saturn IB heating rates in the chart. It is seen that the heating rates on the upper and lower frustums of the SERV structure are more severe than the Saturn IB heating rates on the 9-degree LEM shroud.

The ascent thermal environment on these structures, assuming no thermal protection, will result in temperatures of the exposed surfaces that are well below the temperature limit of Inconel 718, which is approximately 1250°F. However the temperature differential across the basic honeycomb panels during ascent and reentry were not acceptable from a structure design standpoint. Therefore, methods of reducing the temperature differential were investigated. On the 45-degree frustum, maximum temperature gradients will occur at a location that is an integral part of the hydrogen tank. The gradients are, therefore, the result of extremely cold (-420°F) hydrogen on one side of the honeycomb, ambient air on the other side of the honeycomb, and the excellent insulative properties inherent to a honeycomb structure.

ASCENT HEATING RATE COMPARISON

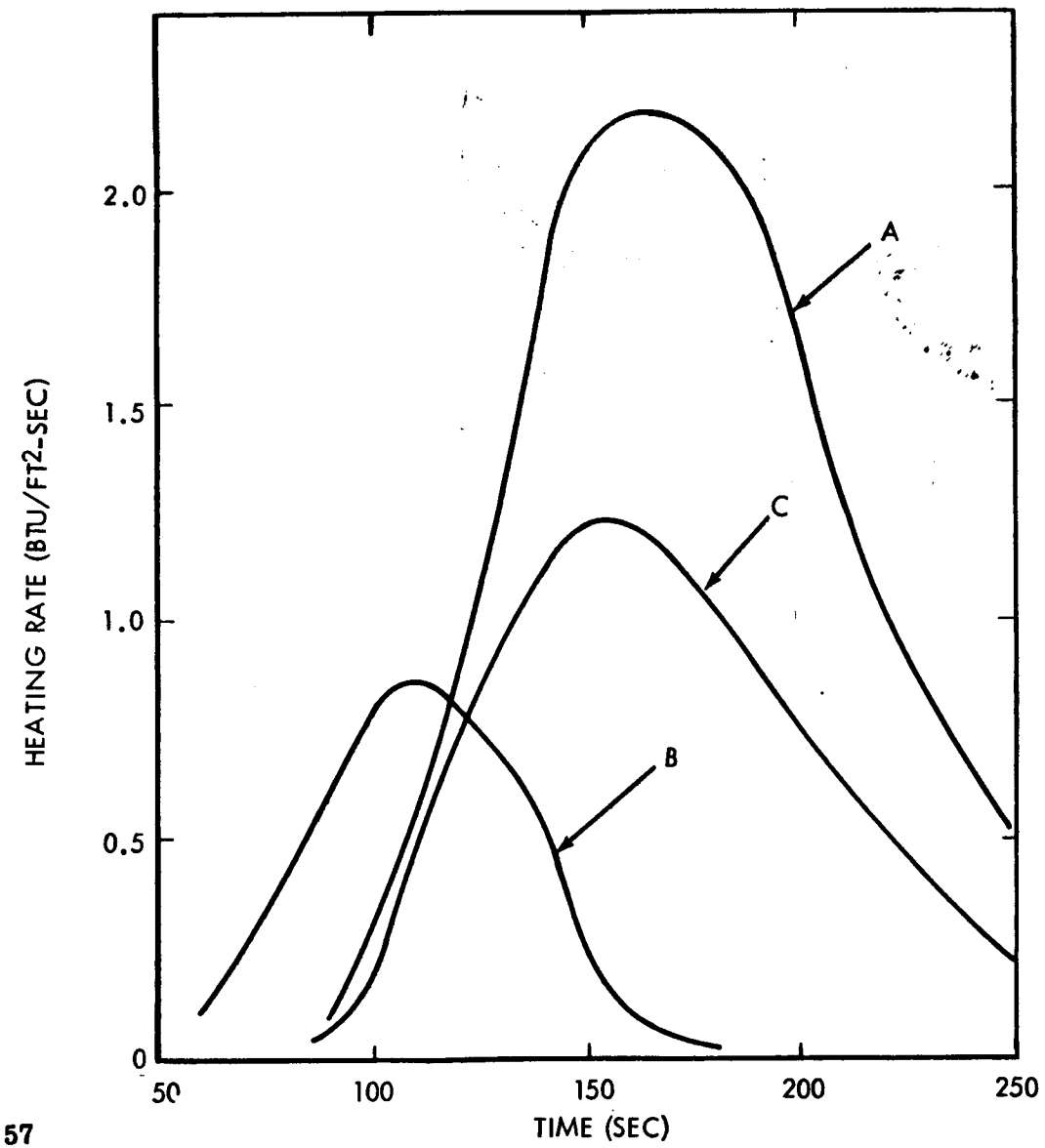

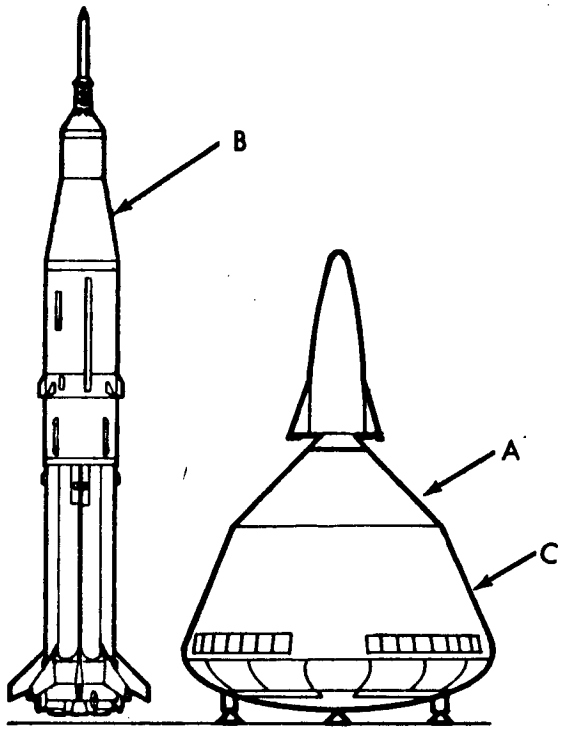

57

SPACE DIVISION CHRYSLER CORPORATION

6.1.1 CRYOGENIC TANK THERMAL PROTECTION

The chart presents the SERV tank arrangement and the structural configuration in each area. The external wall configurations for the 45°0′ and 22°40′ frustums consist of a double honeycomb. The inner honeycomb is a structural load carrying honeycomb. The exterior honeycomb is light weight and non-load carrying and is designed to reduce the temperature gradient across the primary honeycomb.

CRYOGENIC TANK THERMAL PROTECTION

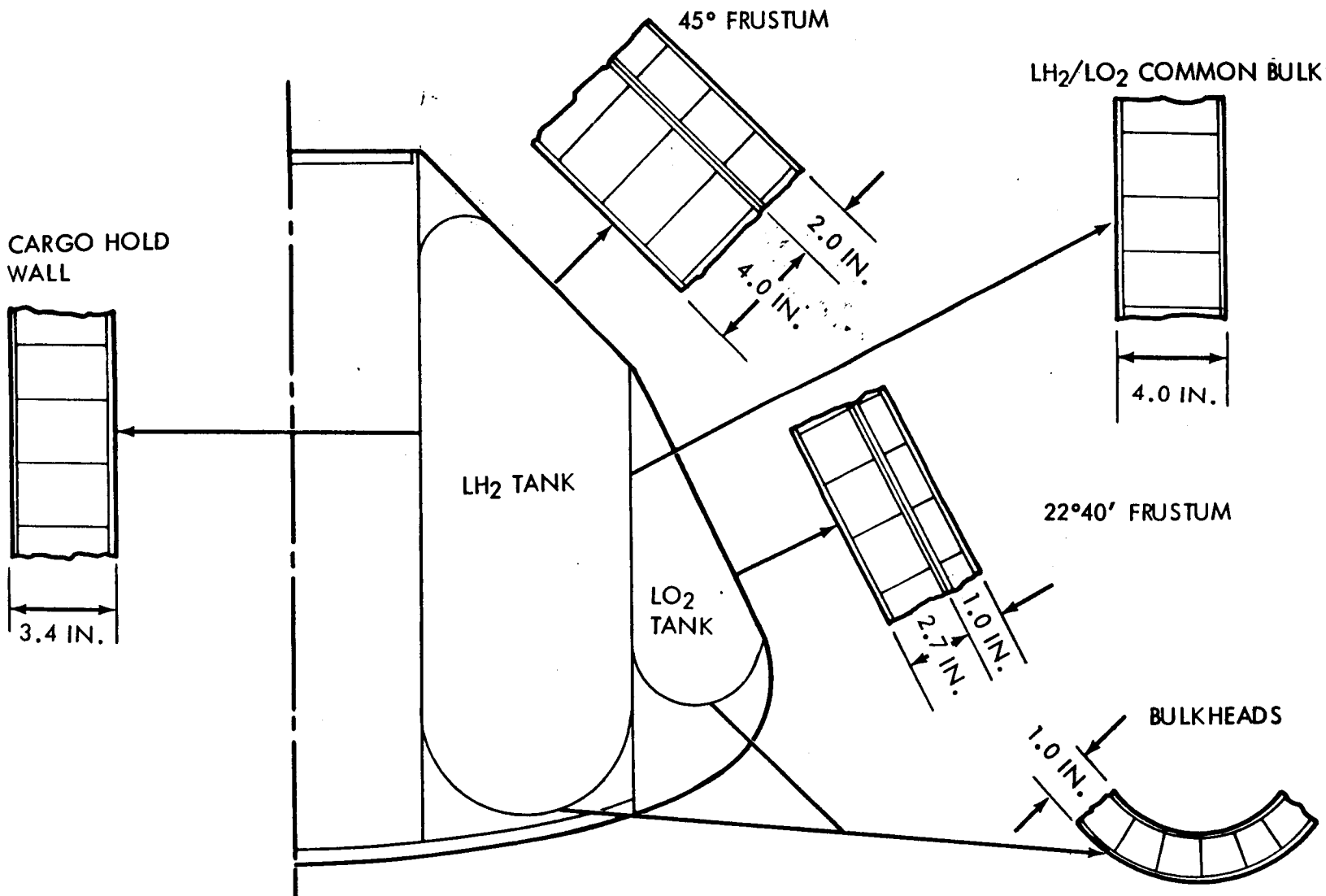

58

SPACE DIVISION CHRYSLER CORPORATION

6.1.2 ASCENT TEMPERATURE HISTORIES

Temperatures for each face of the double honeycomb configuration are presented on the left. The outer face of the TPS panel reaches a maximum temperature of 890°F at 185 sec. The inner face of the TPS honeycomb reaches 160°F at 300 sec. The inner face of the structural panel is in contact with LH_2 prior to liftoff and, because the honeycomb panel is a good insulator, it remains very cold during ascent. The figure on the right presents the transient temperature differential across both the TPS panel and the structural panel for the 45-degree frustum. As shown, a maximum differential of 910°F occurs across the 2.0-inch TPS panel at 185 sec. Since this panel will not be a load carrying member, a differential of this magnitude is acceptable. A maximum differential of 540°F is shown across the 4.0-inch-thick structural panel at 300 sec after liftoff. At this time, aerodynamic loads are negligible and the magnitude of this differential is also acceptable. A similar analysis was conducted on the 22°40′ frustum. The outer face of the TPS panel reached a temperature of 650°F. The maximum temperature gradient for the structural panel is 400°F.

ASCENT TEMPERATURE HISTORIES

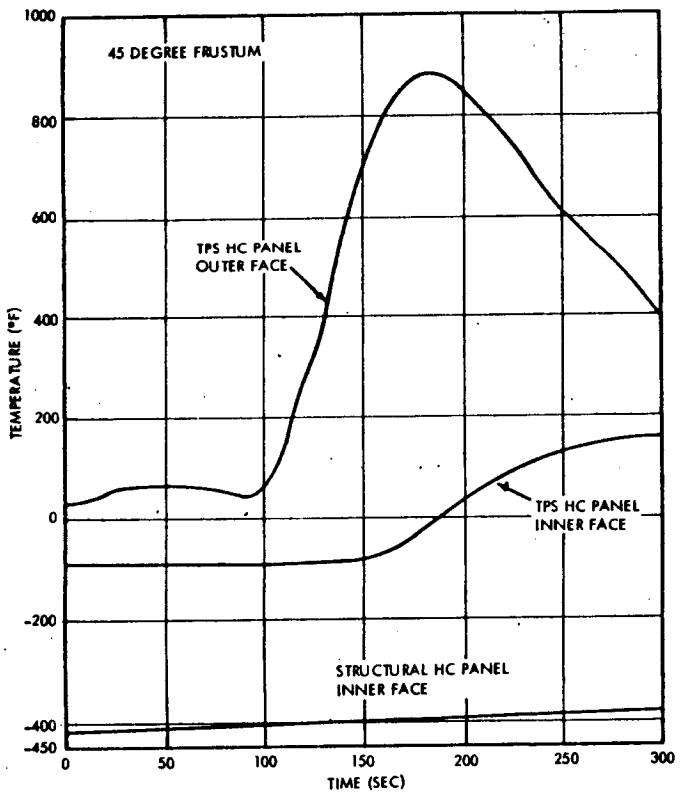

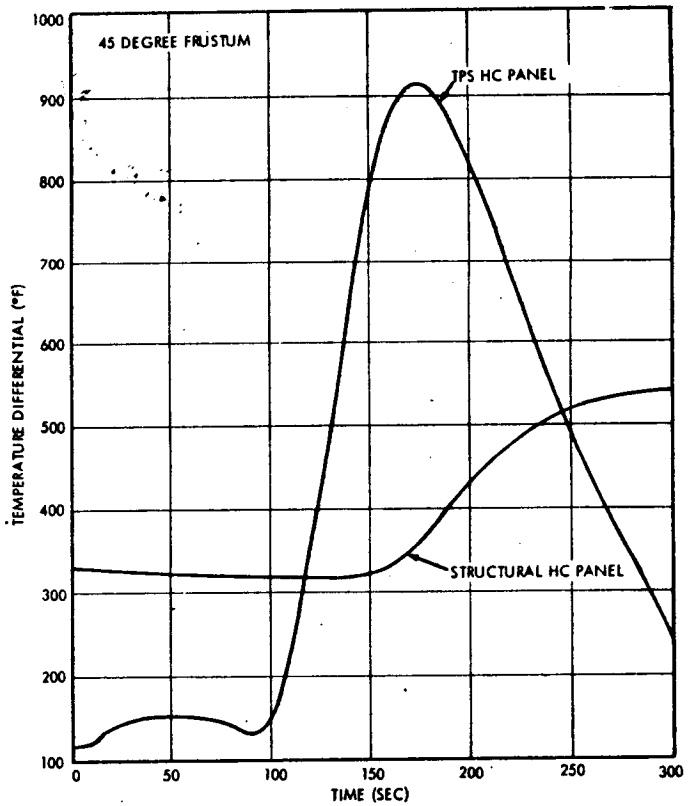

6.2 REENTRY TEMPERATURE HISTORIES

Heating rates and the outer face structural temperatures on the 45-degree frustum will be lower during reentry than during ascent. The chart shows transient temperatures for all faces of the double honeycomb panel configuration at the point of maximum heating on the 45-degree frustum. The temperature of the exterior face of the TPS panel is seen to reach 800°F. Peak temperatures of the inner face of the TPS panel and the inner face of the structural panel is 385°F and 170°F, respectively. The maximum temperature gradient across the TPS panel and the structural panel are 600°F and 280°F, respectively. These temperature gradients are much lower than during boost because there is no temperature gradient at the start of reentry; whereas, there is a large gradient prior to liftoff due to LH_2 being in contact with the inner wall. A similar analysis was conducted for the 22°40′ frustum during reentry. The peak temparature on the outer skin of the TPS honeycomb is 1420°F.

REENTRY TEMPERATURE HISTORIES

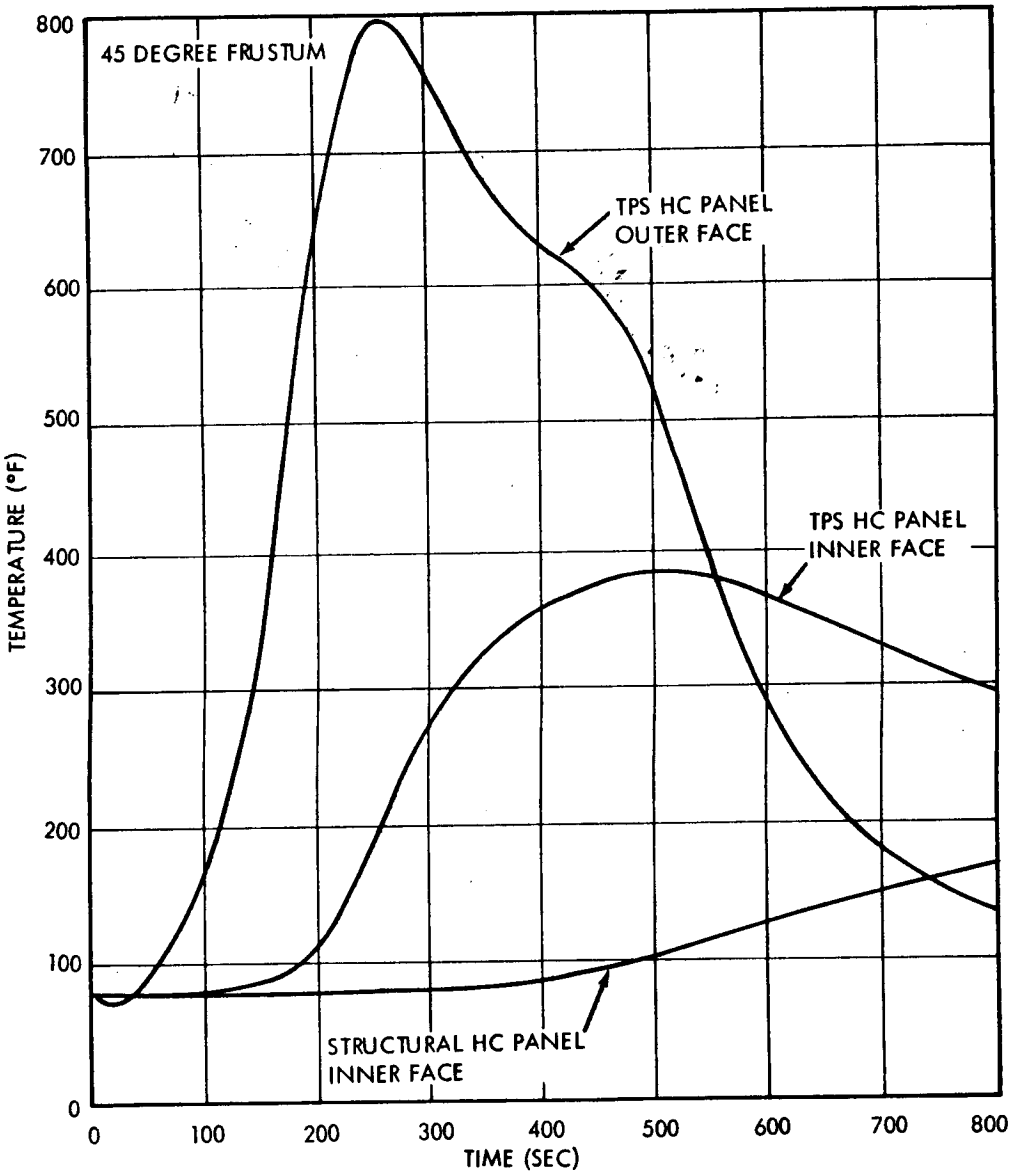

60

SPACE DIVISION CHRYSLER CORPORATION

6.2.1 REENTRY HEAT SHIELD THERMAL ENVIRONMENT

Aerodynamic heating on the SERV heat shield during reentry is the dominant factor in establishing the ablative material requirements and substructure temperature. Reentry aerodynamic heating rates on the heat shield were calculated at the maximum heating location (S = 60 feet) and at the stagnation point (S = 0 feet). This was performed for both the maximum peak heating trajectory and the maximum total heating trajectory. The aerodynamic heating rates for these locations resulting from the maximum total heating trajectory are shown as a function of time. The chart also shows the variation in thermal environments on the heat shield expressed as radiation equilibrium temperatures for the maximum total heating trajectory. It is seen that highest heating rates and consequently maximum ablative thickness will be required approximately 60 ft from the stagnation point.

REENTRY HEAT SHIELD THERMAL ENVIRONMENT

(MAXIMUM TOTAL HEATING TRAJECTORY)

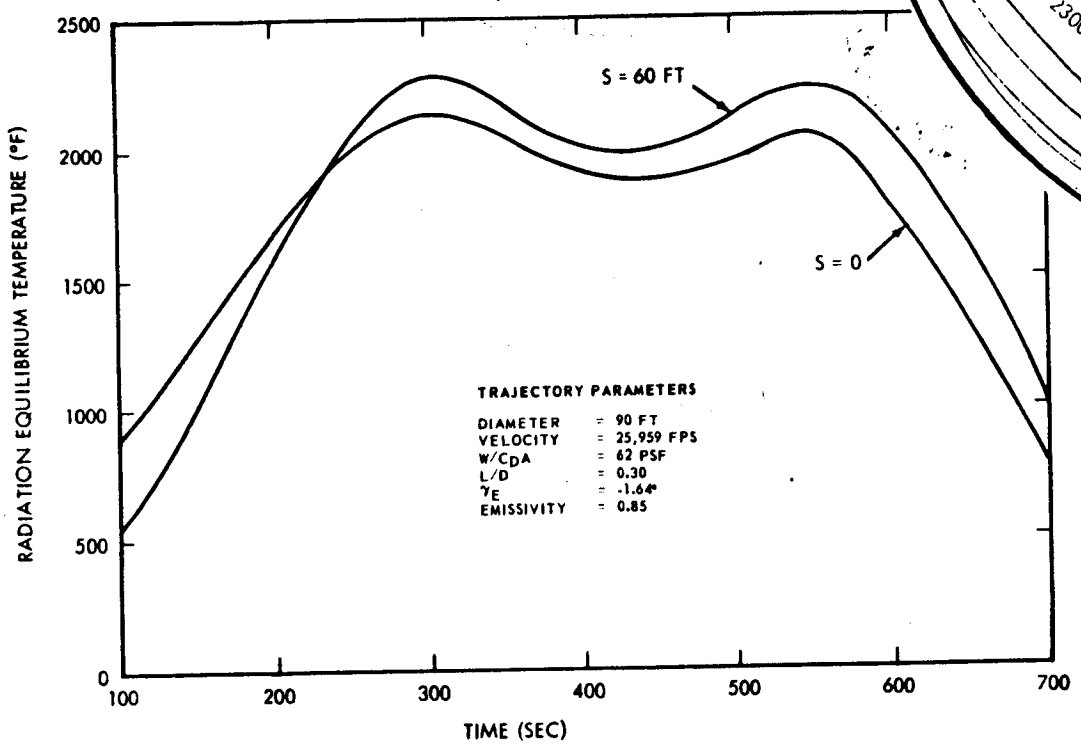

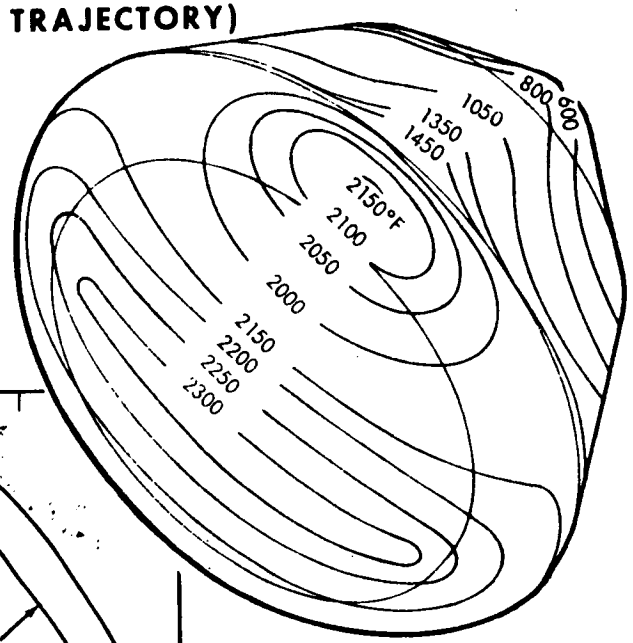

61

SPACE DIVISION CHRYSLER CORPORATION

6.2.2 ABLATION HEAT SHIELD CONFIGURATION

The adiabatic model depicted by Configuration A will result in the most conservative estimate of required ablation material. To determine the influence of a non-adiabatic back-side honeycomb constraint, the two additional configurations, B and C were analyzed. A low density silicone elastomer was analyzed using these models. Ablator-honeycomb interface temperatures and structural honeycomb backside temperatures were determined.

ABLATION HEAT SHIELD CONFIGURATION

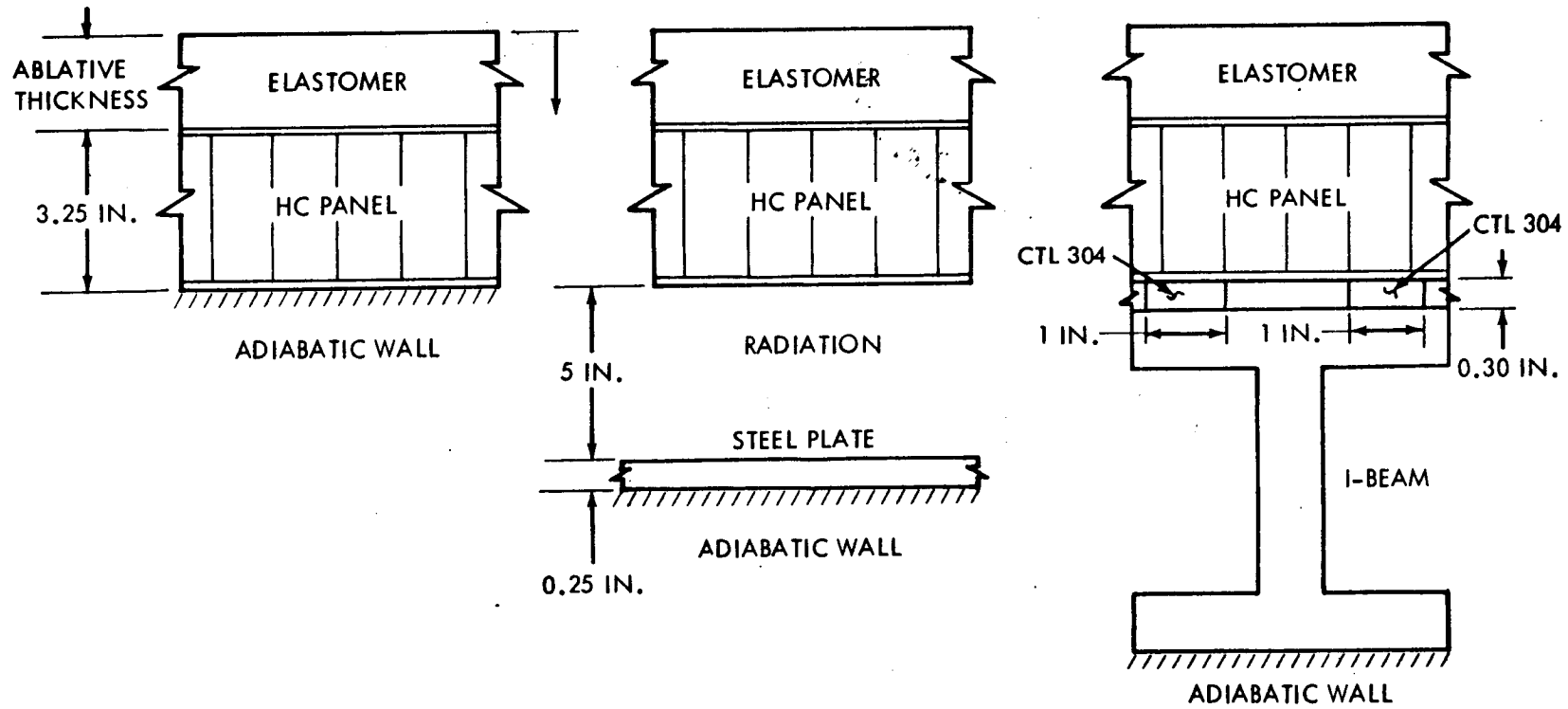

CONFIGURATION A
NO RADIATION

CONFIGURATION B
WITH RADIATION

CONFIGURATION C
I-BEAM WITH INSULATION

6.2.3 INFLUENCE OF SUBSTRUCTURE ON PRIMARY STRUCTURE TEMPERATURE

The influence of internal structure on elastomer-honeycomb interface temperature and honeycomb backside temperature for the three configurations analyzed is shown. As can be seen from these curves, the presence of internal structure decreases the maximum temperatures and increases the structural honeycomb temperature gradient. Peak interface and backside temperatures for the three configurations are shown in the following table:

Peak Interface and Backside Temperatures for Silicone Elastomer

For Maximum Total Heating Trajectory and an Elastomer Thickness of 0.8 inch	Configuration		
	A	B	C
Peak Ablator/honeycomb Interface Temperature (^{o}F)	480	445	380
Peak Structural Honeycomb Backside Temperature (^{o}F)	455	370	230

INFLUENCE OF SUBSTRUCTURE ON PRIMARY STRUCTURE TEMPERATURE

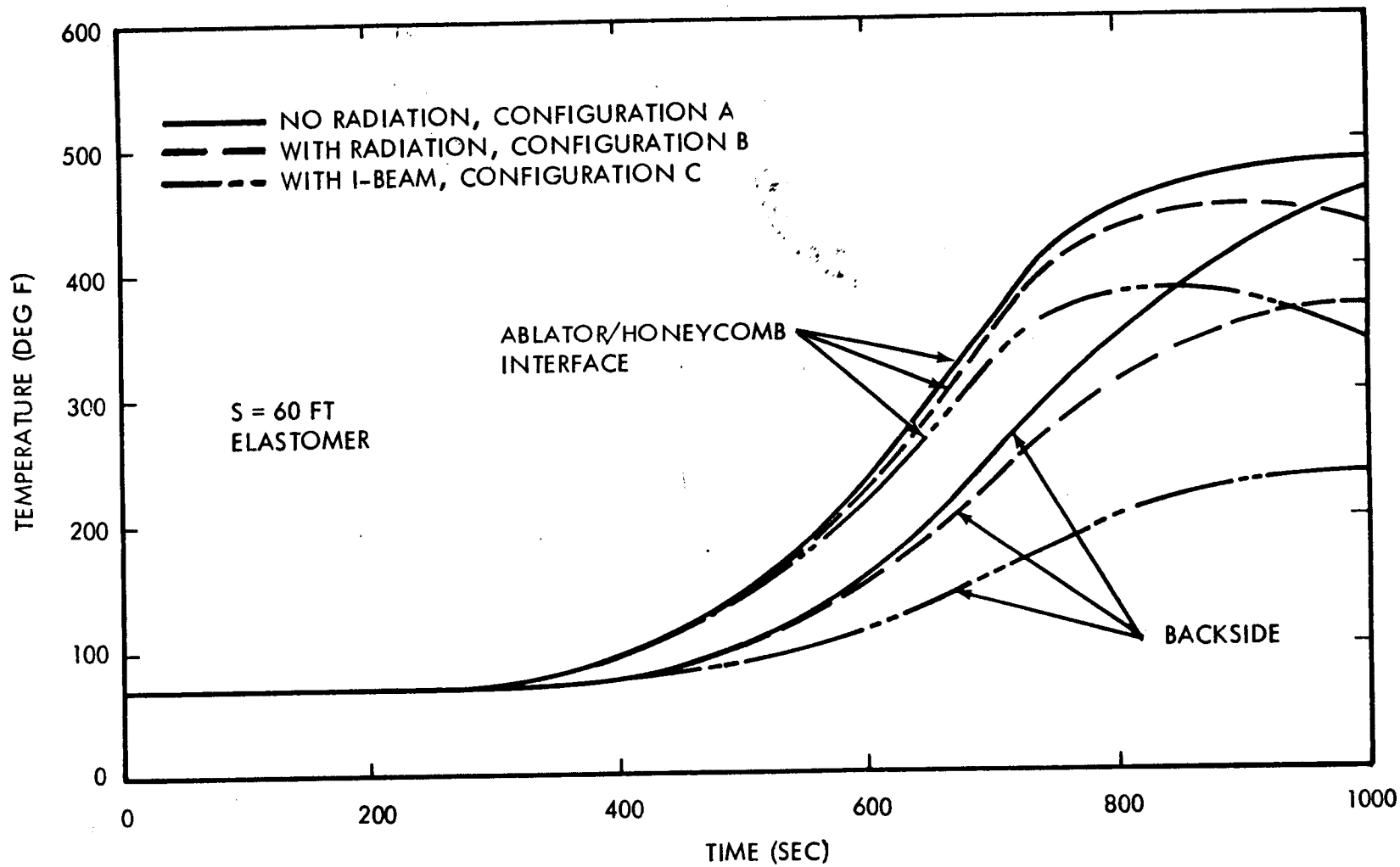

SPACE DIVISION CHRYSLER CORPORATION

6.3 CRYOGEN BOIL-OFF COMPARISON

This chart presents a summary of boil-off comparisons between the S-IB stage LO_2 and S-IVB LH_2 with the SERV propellants.

Heat will enter the LH_2 tank from the 45-degree conical outer wall, the LH_2/LO_2 common bulkhead, the cargo hold wall, and the upper and lower bulkheads. Heat transferred through each of these structures was calculated and the net heat entering the LH_2 tank determined.

The total boil-off rate is 5,161 lb/hr of hydrogen. The total weight of LH_2 in SERV at liftoff is 604,517 lb. Therefore, the boil-off rate per hour expressed as a percentage of loaded weight is 0.85 percent.

For comparison purposes, a loaded S-IVB stage includes 44,300 lb of LH_2 and the boil-off rate on the pad is approximately 2,700 lb/hr, or a rate per hour of 6.09 percent. SERV has a much lower percent boil-off due to the honeycomb panel being a better insulator than the polyurethane foam, which is used on the side walls of the S-IVB, and because of the good area-to-volume ratio permitted by the large SERV size.

Heat will enter the LO2 tank from the 22°40′ lower frustum wall and the lower bulkhead. In addition, the LO_2 will be cooled by the LH_2, but this effect is small and was not considered in the analysis. An analysis was made for each structure similar to that described for the hydrogen tank. The total boil-off rate for the LO_2 tank is 10,047 lb/hr, or approximately 0.30 percent of the total loaded LO_2 weight.

For comparison purposes the LO_2 boil-off from the S-IB stage is approximately 28,470 lb/hr, or 4.5 percent of the loaded LO_2 weight. The LO_2 tanks on the S-IB stage are uninsulated aluminum and have poor surface-area-to-volume relationship, therefore, a higher percent boil-off.

CRYOGEN BOIL-OFF COMPARISON

LOX

STAGE / QUANTITY	S-IB	SERV
TOTAL BOIL-OFF LB/HR	28,470	10,047
TOTAL LOX LB	630,000	3,628,655
PERCENT OF TOTAL BOILOFF/HR	4.5	0.3

LH_2

STAGE / QUANTITY	S-IVB	SERV
TOTAL BOIL-OFF LB/HR	2,700	5,161
TOTAL LH_2 LB	44,300	604,517
PERCENT OF TOTAL BOIL-OFF/HR	6.09	0.85

FLIGHT CONTROL CHARACTERISTICS

Section 7

FLIGHT CONTROL CHARACTERISTICS

The major phases of ascent, reentry and landing are shown in the accompanying charts. Vehicle attitude control during ascent is achieved through a combination of differential throttling of selected quadrants of the aerospike engine and RCS roll control thrusters.

Depending on the SERV mission with either a MURP or PM payload, reentry is by deorbit from either a 110-nm orbit or a 260-nm orbit. Conditions of entry angle and velocity at the 400,000 ft entry interface are determined by constraints imposed by such factors as heating environment, acceleration limits, and the reentry footprint.

During the hypersonic region, maximum dynamic pressure and peak heating temperatures are experienced and vehicle maneuvering is initiated to maintain the desired descent trajectory. The required L/D characteristic for maneuvering is achieved by a vehicle center of gravity (CG) offset of approximately 30 to 36 inches with differential corner radii incorporated.

High altitude winds are encountered in the supersonic/transonic region of flight. During this regime the CG offset is reduced by the transfer of landing propulsion fuel. These factors combine to produce significant dynamic conditions for consideration in the design of the guidance and control systems.

In the subsonic region the landing sequence is carried out with particular attention given to the landing engine operational constraints, winds, and guidance and control requirements for obtaining the necessary range with minimum fuel consumption.

The following charts show some of the more significant results of the ascent, reentry and landing control analyses performed for the SERV vehicle.

ASCENT, REENTRY AND LANDING

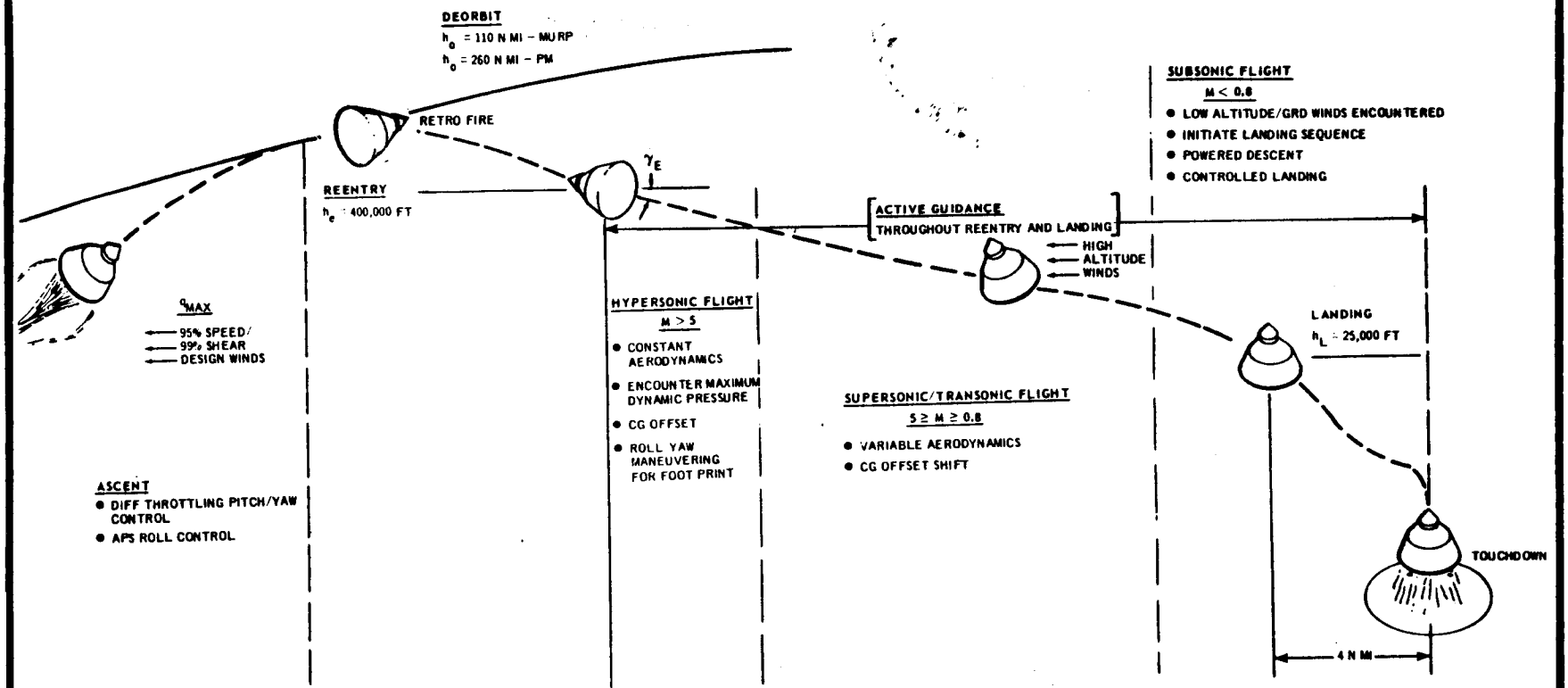

66

SPACE DIVISION CHRYSLER CORPORATION

7.1 ASCENT PITCH/YAW ATTITUDE CONTROL

A block diagram of the pitch/yaw ascent attitude control system is shown on this chart. The control is generated from attitude and attitude rate signals. An attitude error gain of 1.75 percent/degree and an attitude rate gain of 1.40 percent/(deg/sec) provide a control frequency of approximately 2.0 rad/sec and a damping ratio of 0.7 at q_{max}. The control torque is generated by throttling down an appropriate quadrant of the aerospike engine, thereby producing a moment due to the resultant thrust imbalance. Only one quadrant of the engine is throttled for a given control signal polarity (per axis) as symbolized by the diodes in the diagram. The controllability characteristics of SERV in the q_{max} region are also shown. A worst case condition was simulated by flying the vehicle through a 95 percent speed/99 percent shear synthetic wind profile peaking at q_{max} and acting in the yaw plane. Parameter dispersions were also considered in evaluating the controllability characteristics. A six degree-of-freedom simulation of the vehicle was used to compute the nominal responses and a convariance propagation routine was used to establish the effects of parameter dispersions. The resultant angle of attack and control throttle ratio in response to the wind, along with the corresponding dispersion envelopes due to the parameter dispersions, are shown on the chart. Note that the peak control throttle ratio requirement for both wind and parameter dispersions is 11.5 percent; the maximum available is 15 percent.

ASCENT PITCH/YAW ATTITUDE CONTROL

CONTROL GAINS FROM LIFTOFF THROUGH q_{MAX}:

- A_0 = 1.75 PERCENT/DEG
- A_1 = 1.40 PERCENT/(DEG/SEC)

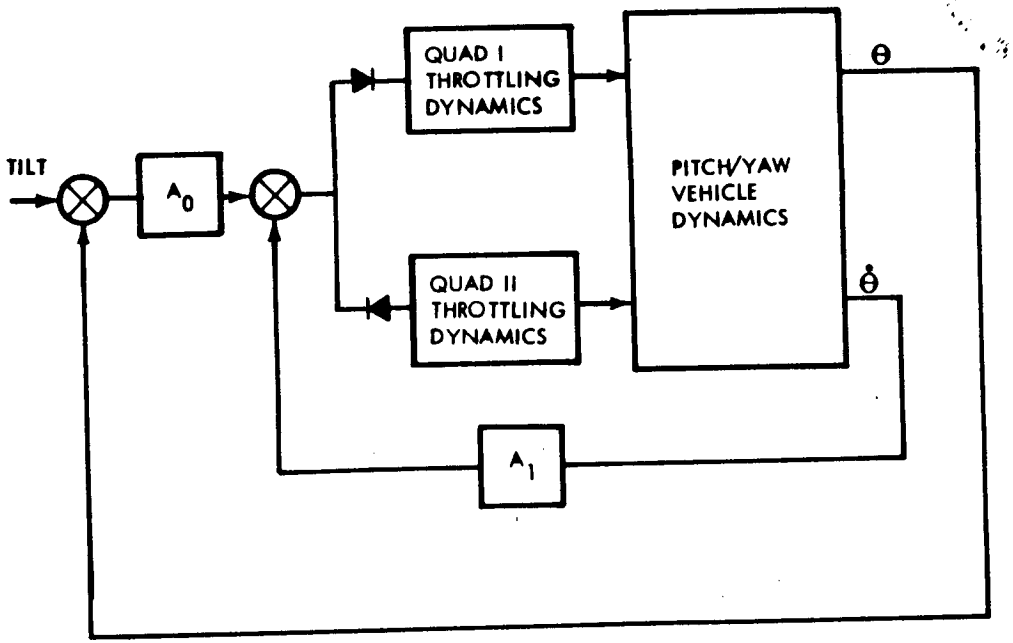

ASCENT PITCH/YAW CONTROL SYSTEM BLOCK DIAGRAM

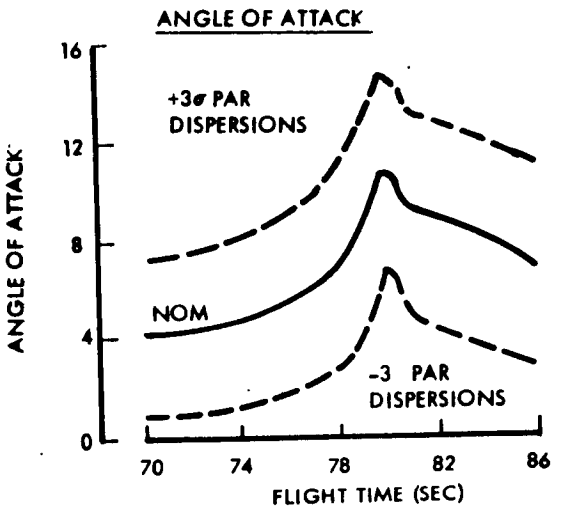

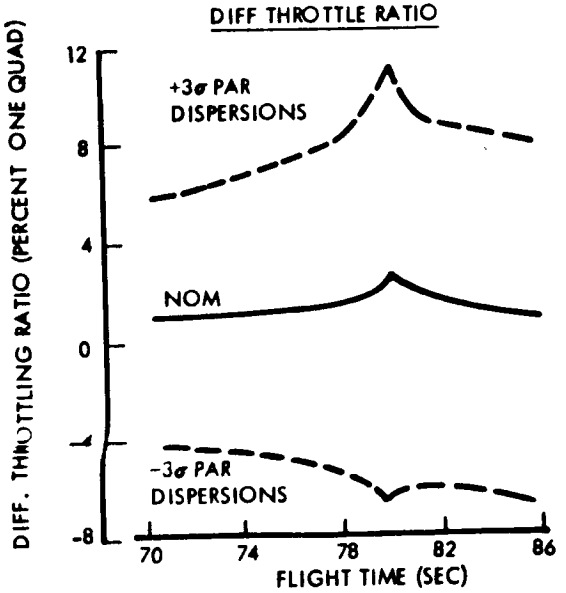

SPACE DIVISION CHRYSLER CORPORATION

7.2 ASCENT ROLL CONTROL

The roll control system for SERV during ascent employs an auxiliary propulsion system (APS) for providing the roll control torques in conjunction with a time optimal control law to minimize the response time during roll maneuver. A one degree dead zone in the switching logic is incorporated to provide a compromise between fuel consumption and an acceptable limit cycle amplitude. Response time and fuel consumption for various roll maneuver attitudes is shown on the chart along with a typical response to a 45 degree roll maneuver.

ASCENT ROLL CONTROL

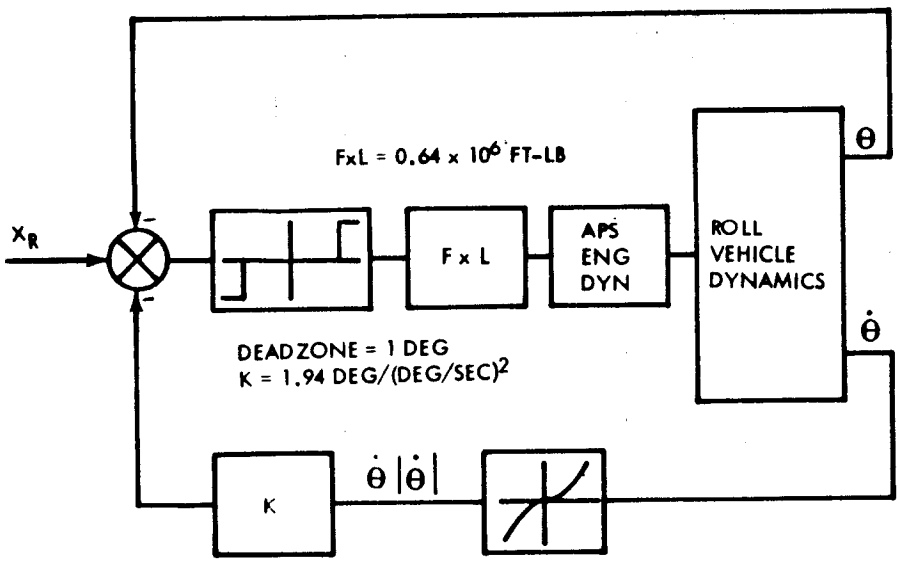

ASCENT ROLL CONTROL
SYSTEM BLOCK DIAGRAM

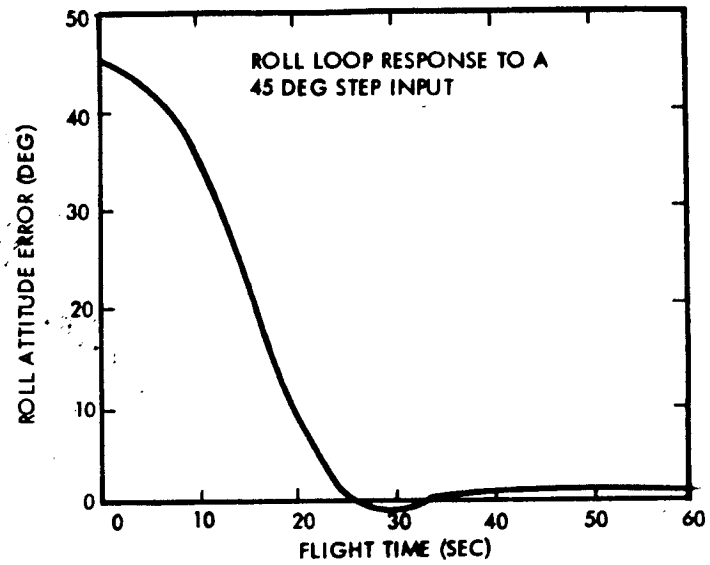

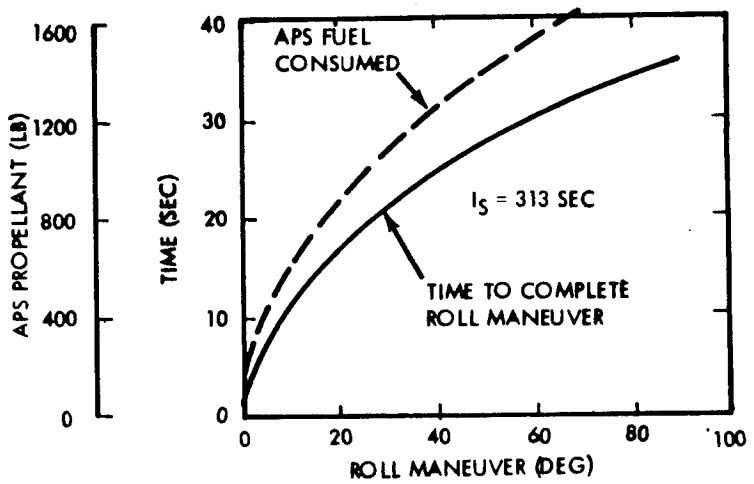

SPACE DIVISION CHRYSLER CORPORATION

7.3 REENTRY ATTITUDE CONTROL

The reentry attitude control subsystem (ACS) for SERV employs the same basic principles and type of hardware utilized in the Gemini and Apollo spacecraft. The basic system is composed of a sensing system, signal conditioners and a set of reaction control thrusters, which function in an automatic mode to provide the necessary three-axis stabilization of SERV from deorbit, through reentry, and down to the landing interface. The system is activated prior to the deorbit maneuver to orient the vehicle in its correct deorbit attitude. Attitude control is maintained throughout the deorbit maneuver. When the vehicle penetrates the atmosphere, the pitch and yaw attitude reference loops are opened to allow the vehicle to attain its aerodynamic trim state which is induced by an offset CG. Rate feedback is maintained in all three axes to damp oscillations which may be started due to perturbations in the trajectory.

Guidance of SERV is achieved by rolling the vehicle about the velocity vector to distribute the direction of the lift vector such that the proper reference trajectory is maintained. To minimize side slip, a portion of the roll rate signal is introduced into the yaw channel to effectively coordinate the turn.

REENTRY ATTITUDE CONTROL

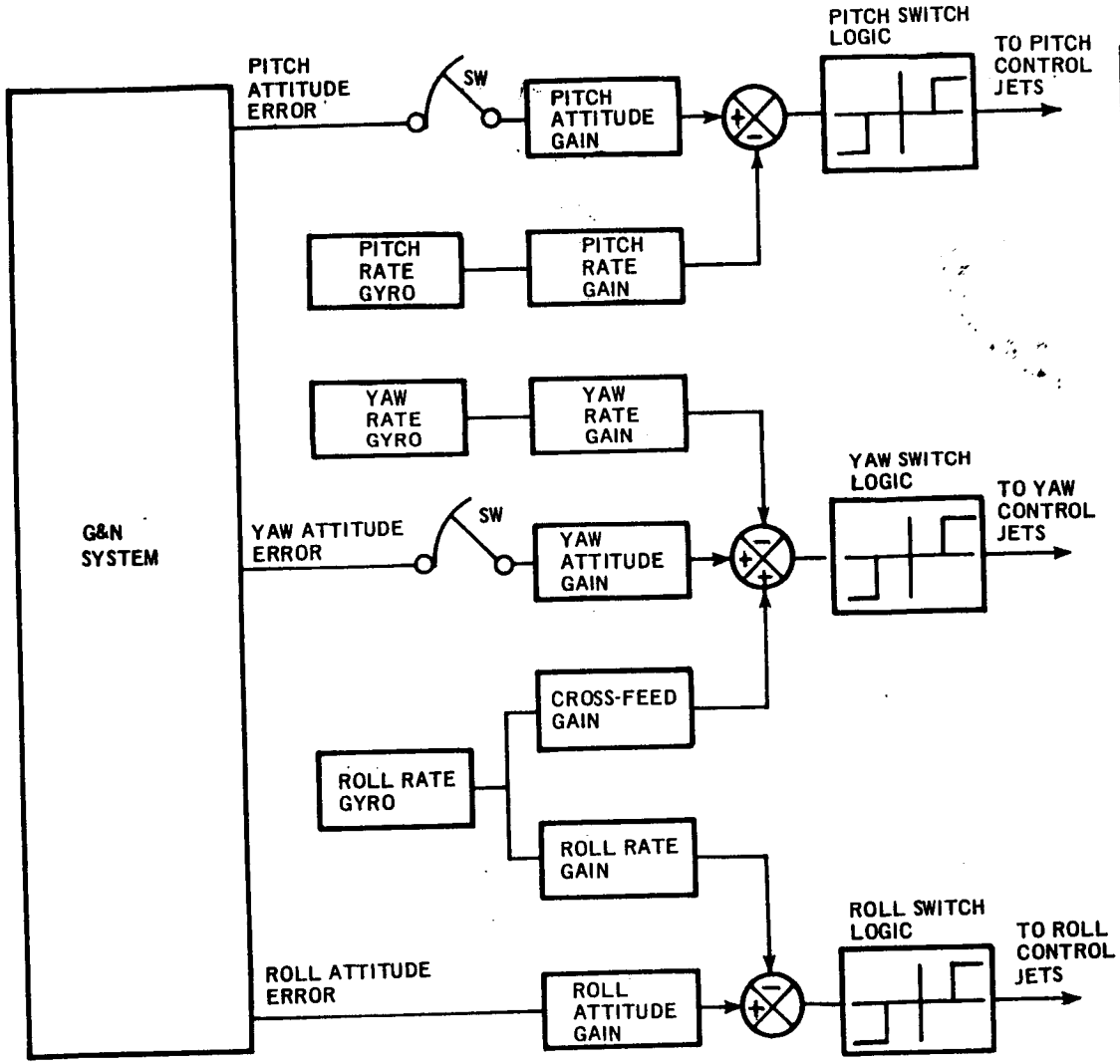

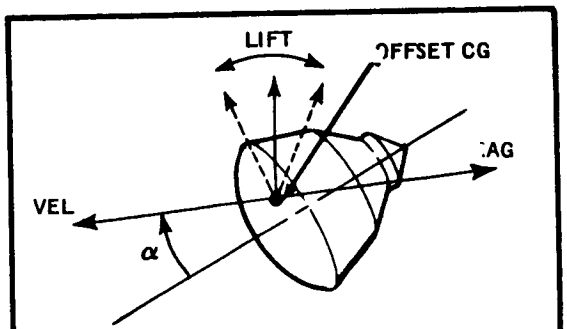

- GUIDANCE ACHIEVED BY ROLLING VEHICLE ABOUT VELOCITY VECTOR

- CONTROL ACCELERATIONS

  ROLL = 1.12 DEG/SEC^2
  PITCH = 1.62 DEG/SEC^2
  YAW = 1.87 DEG/SEC^2

7.4 SUMMARY OF REENTRY WIND RESPONSE ANALYSES

Controllability of the vehicle in response to winds was assessed by investigating the attitude response characteristics for a family of 95 percent speed, 99 percent shear buildup and backoff wind shear profiles peaking in the altitude range between 46,000 to 26,000 ft. Results of the wind response analyses are summarized in the chart which shows the nominal no wind angle of attack along with superimposed responses to representative cases of the wind profiles considered. The envelope of peak wind induced angles of attack indicates that the maximum deviation from that of the no wind case is approximately 7 degrees. This occurs for a wind profile peaking at approximately 28,000 ft. Also shown is the stability boundary for allowable angles of attack in the worst case direction (nose down). It is concluded from the results that the vehicle has adequate stability margins for the assumed trim condition and that higher trim L/D in the transonic/subsonic regions can be allowed if more maneuver capability is required.

SUMMARY OF REENTRY WIND RESPONSE ANALYSIS

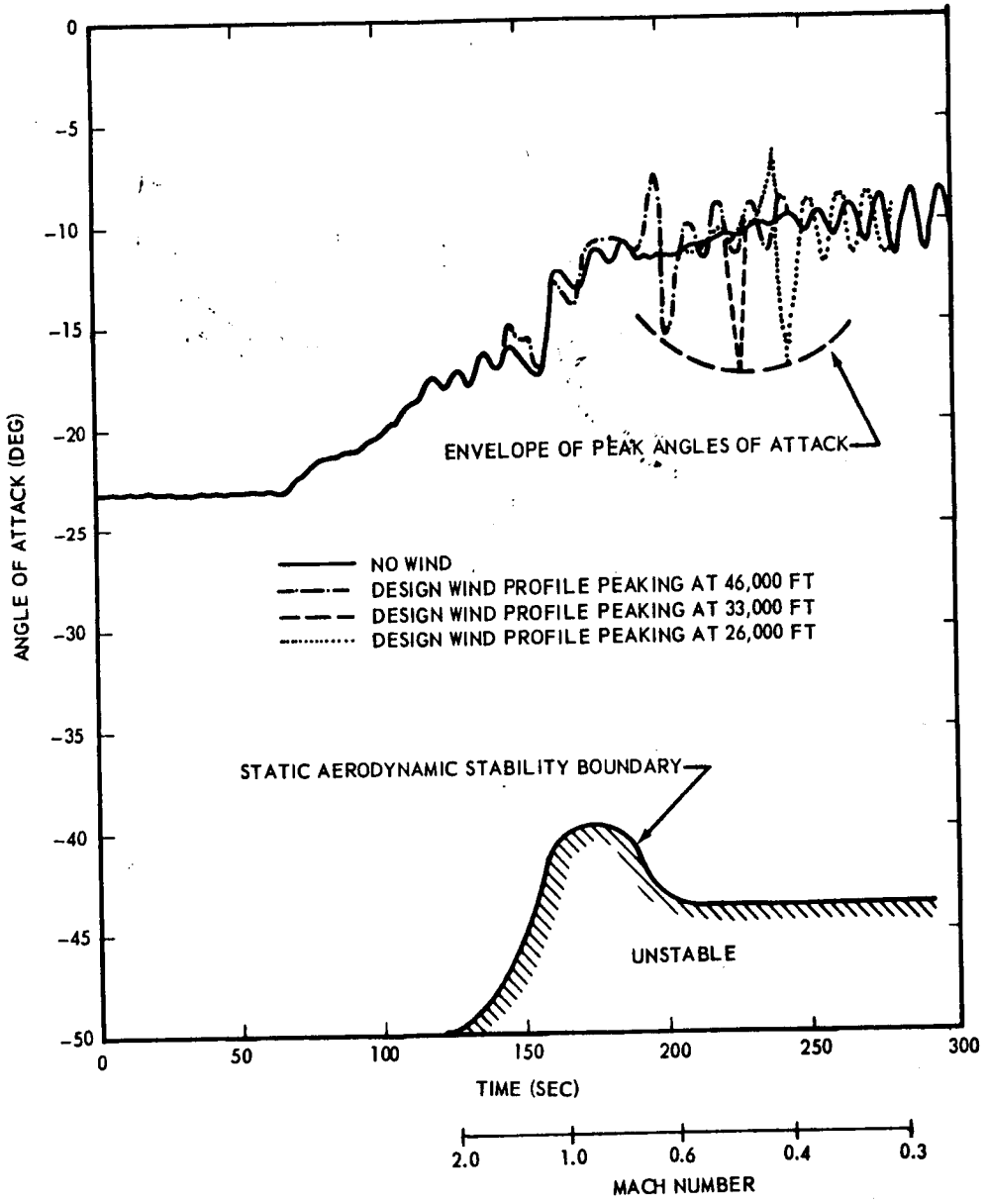

7.5 REENTRY ATTITUDE AND TRAJECTORY TIME HISTORIES

Pitch attitude and trajectory time histories for the nominal maximum lift condition resulting from a zero roll angle are shown on the chart. These time histories represent the vehicle response characteristics starting at an altitude of 159,000 feet down to the landing interface at 25,000 ft. The CG shift trim maneuver starts at approximately 66 sec (at which time the Mach number is 5.5) and is completed at 116 sec (Mach 2.5). The responses to the trim maneuver are smooth and well damped. Maximum activity occurs during the transonic region. This region is characterized by highly varying aerodynamic characteristics which produce the relatively high amplitude oscillation between 120 and 220 sec. The oscillations, however, are maintained within the control deadbands.

REENTRY ATTITUDE AND TRAJECTORY TIME HISTORIES

INITIAL CONDITIONS:
- ALTITUDE = 159,313 FT
- MACH = 10.504
- FLIGHT PATH ANGLE = -2.1612 DEG

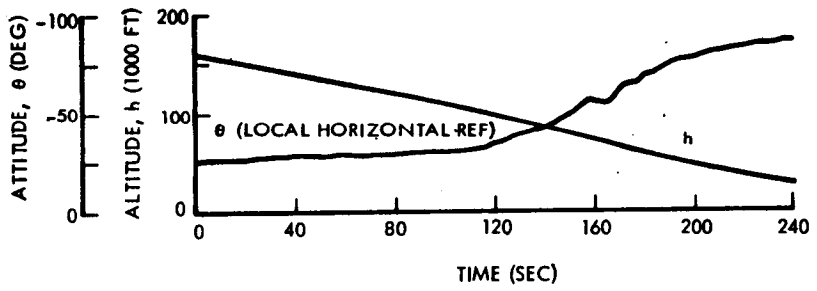

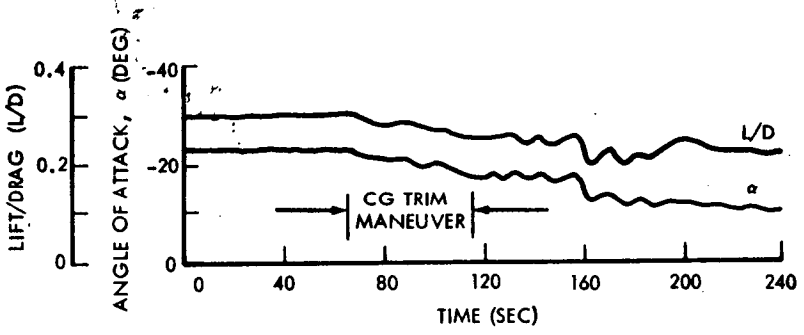

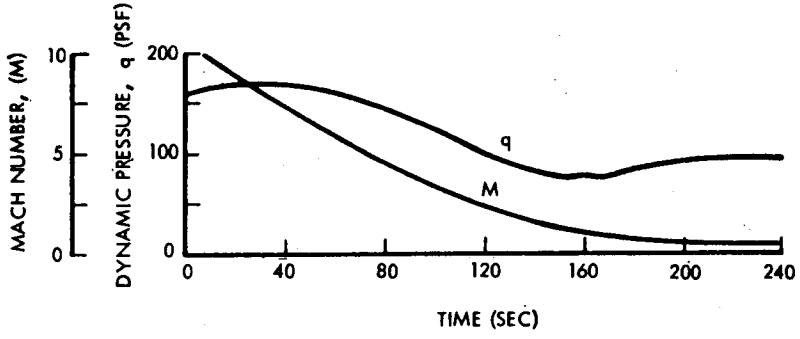

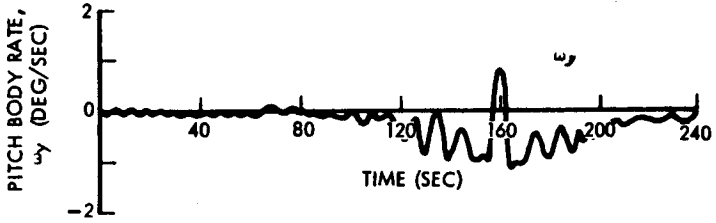

71

SPACE DIVISION CHRYSLER CORPORATION

7.6 RESPONSE CHARACTERISTICS TO ROLL COMMANDS

Control of the reentry trajectory for SERV is achieved by modulating the L/D about the vehicle velocity vector. Modulation of L/D in the pitch plane controls the range, while modulating the lift vector in the roll plane controls the crossrange. The maneuver commands, which are in the form of roll commands, are generated by the guidance and navigation subsystem. The control system accepts the roll commands and translates them directly into roll body axis commands, achieving turn coordination by crossfeeding roll rate into the yaw damper loop.

Typical responses of the point design vehicle to maneuver commands were obtained for the hypersonic/supersonic region and for the transonic/subsonic region. Step inputs of 20 degrees roll command were assumed in the hypersonic/supersonic region to simulate the vehicle response to typical bank angle commands which would be generated by the guidance and navigation subsystem for the purpose of maintaining a reference trajectory. The responses are smooth and well damped. Good turn coordination is achieved by the crossfeed method as can be seen by observing that the yaw angle of attack (sideslip) remains small during the response.

Response in the transonic/subsonic region shows a constant roll rate command of 10 deg/sec from Mach 3 down to approximately Mach 0.65. The constant roll rate is employed to effectively average out the lift so that an effective ballistic trajectory is maintained in this region. The purpose of doing this is to provide equal maneuver capability in any direction for controlling drift due to winds. The roll rate for this example is commanded to stop at approximately Mach 0.65 at which time the commanded roll angle is 90 degrees to represent a typical crossrange error correction. Just prior to reaching the landing interface, the roll angle is commanded to zero to illustrate the roll loop response characteristics for a typical landing preparation maneuver. In general, the responses, like that in the hypersonic/supersonic region, are shown to be well damped and the limit cycle amplitudes are small. Here again it is seen that good coordination of the roll maneuvers is provided by observing that the yaw angle of attack remains small during the response.

RESPONSE CHARACTERISTICS TO ROLL COMMANDS

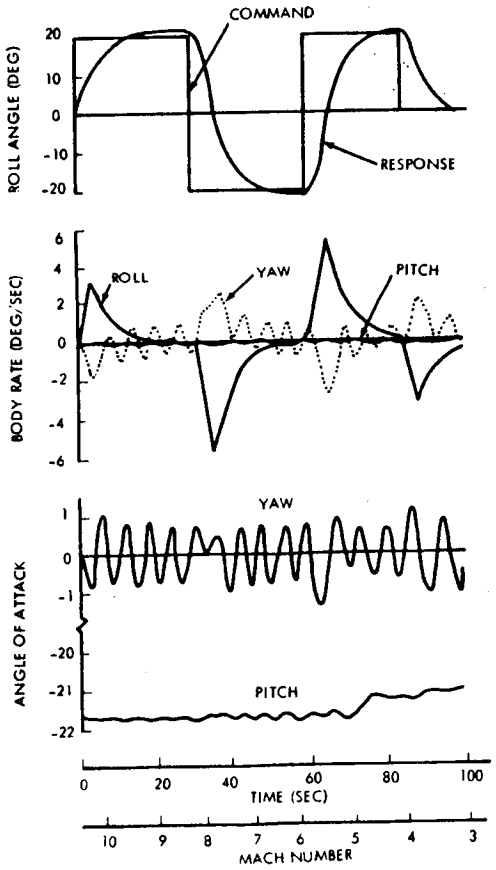

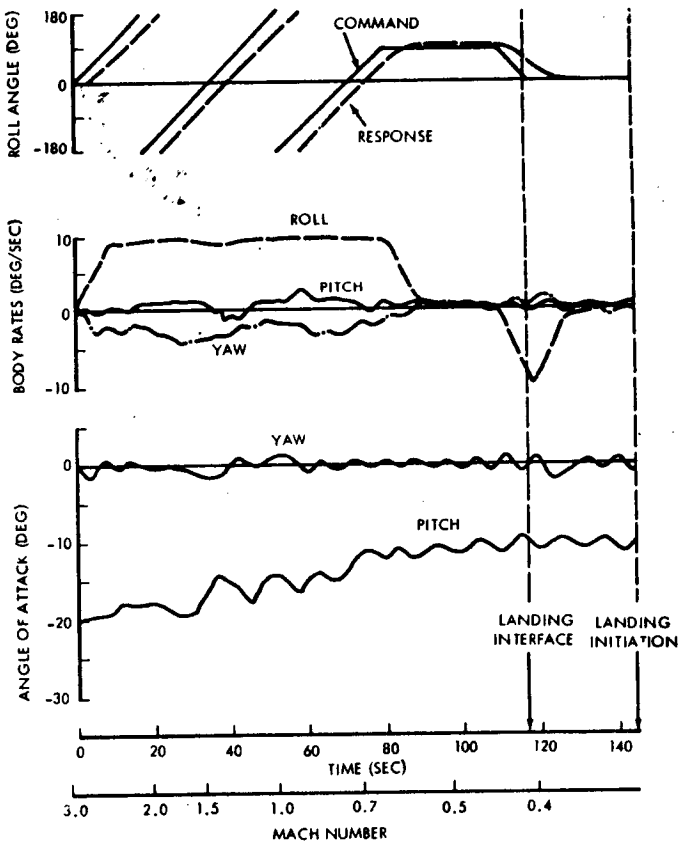

7.7 LANDING CONTROL REQUIREMENTS

The landing mode of SERV will be initiated when SERV approaches an altitude of 25,000 feet, at which time its velocity is approximately 325 ft/sec. At that point in the trajectory the lift engine doors are opened and the engines started, with the ignition sequence taking approximately 8 sec of an available 40 sec. The vehicle will continue to descend with the propulsion subsystem at idle thrust (approximately 20 percent of maximum), down to 15,000 ft altitude at which point the controlled descent is initiated.

The controlled descent is achieved by an automatic system capable of landing SERV at the preselected landing site from any point within a 4 nm radius. The landing system is sized to safely land SERV through a 95 percent speed, 99 percent shear wind and with one engine out. Translation control is achieved by simultaneously pitching the vehicle and throttling the propulsion subystem. Attitude control in the pitch/yaw planes is provided by differentially throttling the landing propulsion subsystem, and roll control by the same reaction control subsystem used during reentry.

To provide the maximum safety for a manned landing, a manual override capability will be added to the fully automatic system. Manual override will be used in an emergency mode in the event SERV fails to reach the vicinity of the primary landing site due to improper reentry. During the manual mode the pilot will utilize an optical display system along with an onboard navigation system to select an alternate site for landing without hazard to life.

LANDING CONTROL REQUIREMENTS

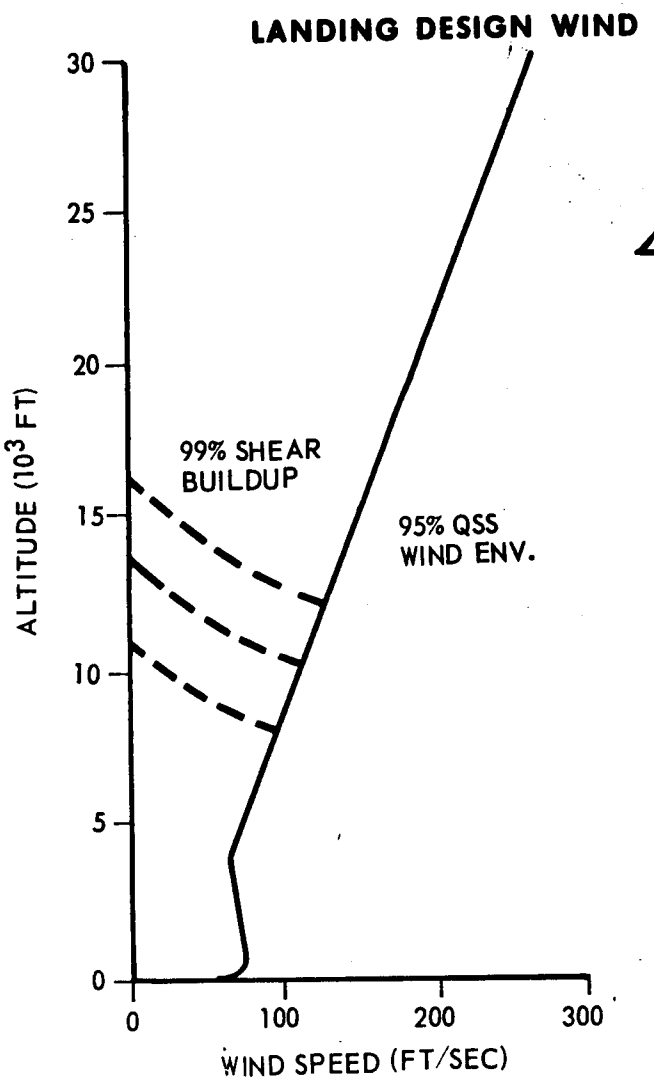

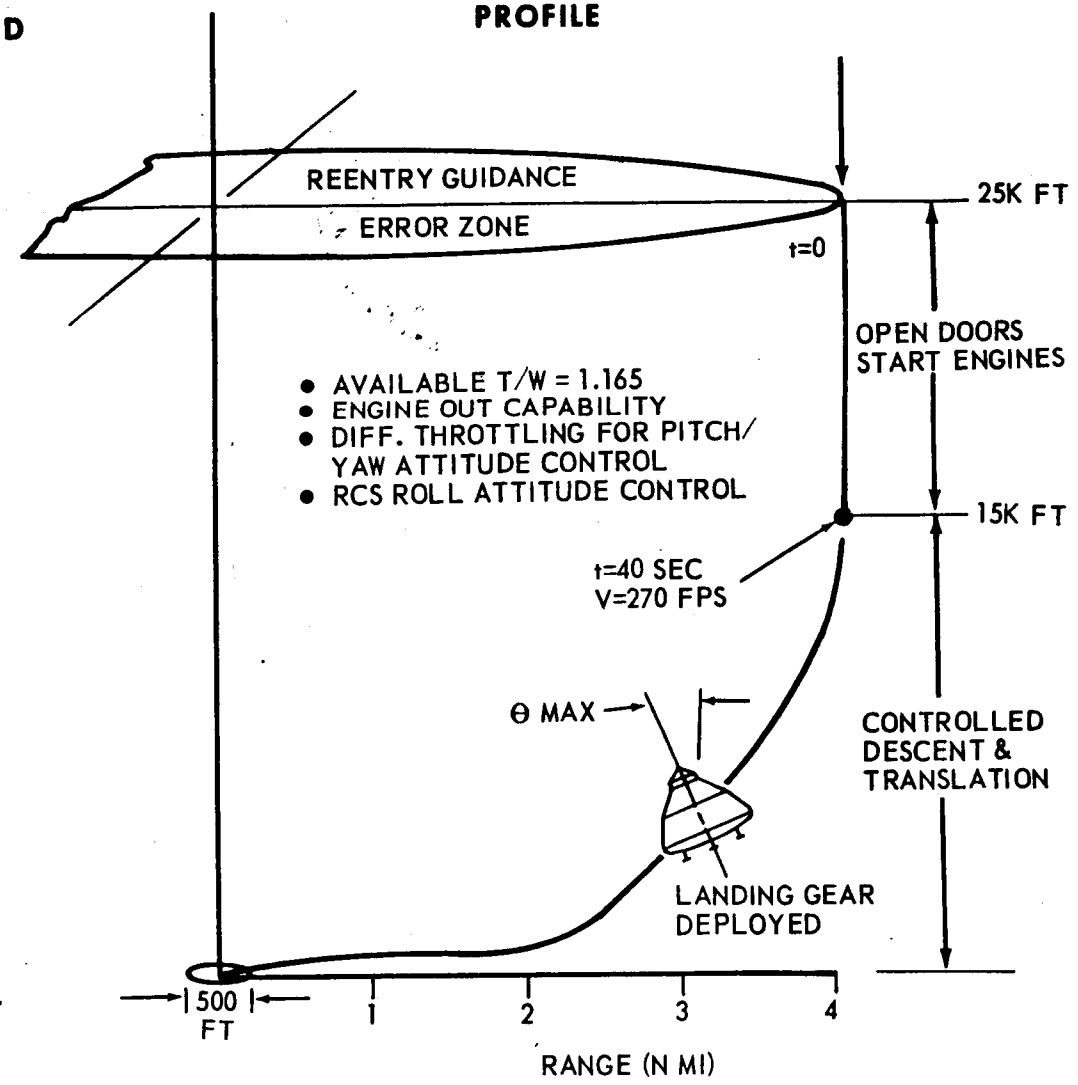

73

SPACE DIVISION CHRYSLER CORPORATION

7.8 LANDING G&C SYSTEM DIGITAL COMPUTER SIMULATION

Because of the complex nature of the landing control dynamics, it was necessary to develope a detailed landing simulation in order to adequately design and evaluate a functional system. The simulation, developed on a digital computer, computes the motion of the vehicle in three coupled degrees of freedom: vertical translation, horizontal translation, and rotation; an uncoupled roll degree of freedom is also included. The simulation contains a detailed representation of the propulsion system and incorporates nonlinear aerodynamics.

LANDING G&C SYSTEM DIGITAL COMPUTER SIMULATION

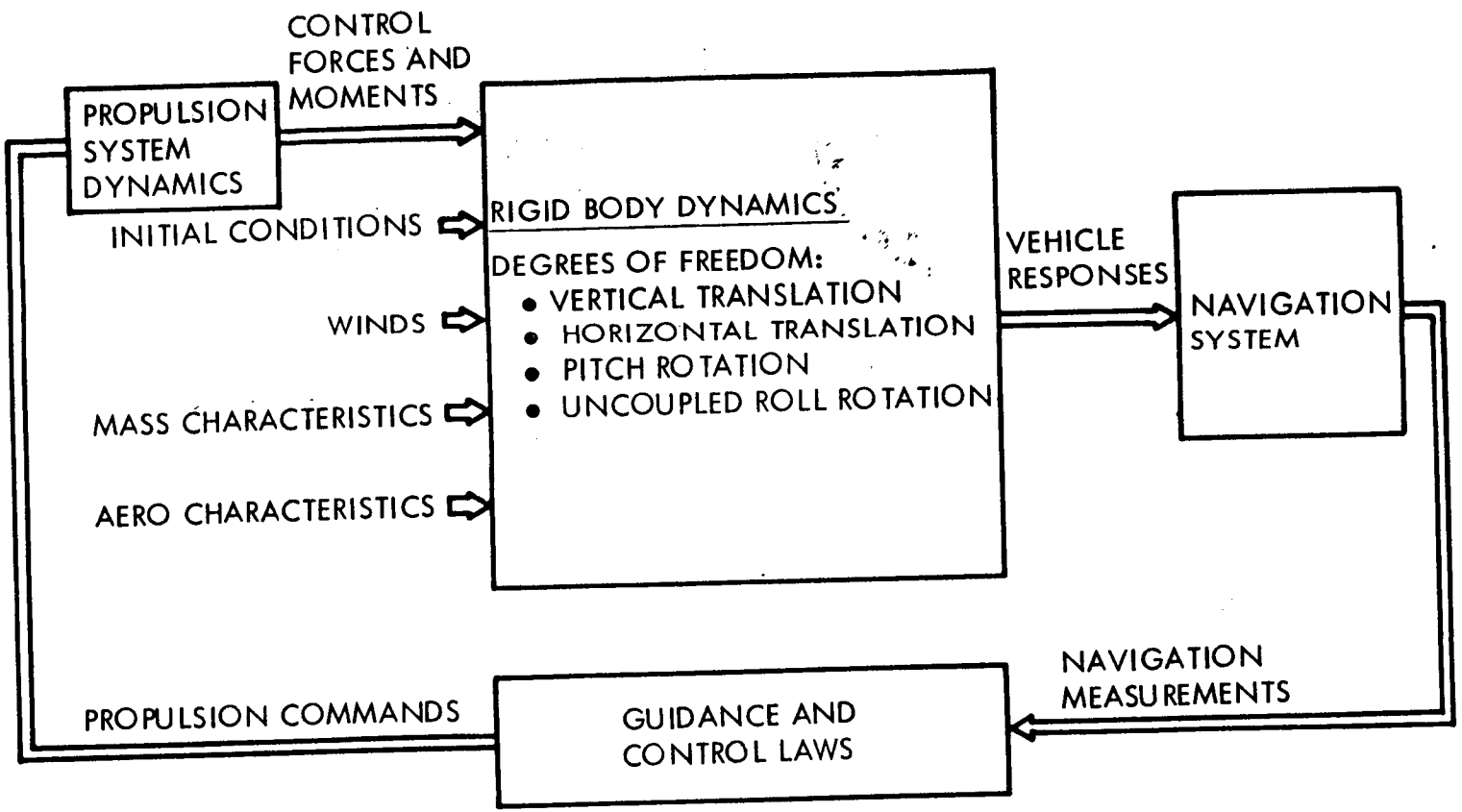

7.9 LANDING G&C SYSTEM

The primary landing concept for SERV employs a fully automatic landing guidance and control (G&C) system which controls the descent of the vehicle to the preselected landing site. Inputs to the system consist of a set of measurements of the vehicle states obtained from an onboard navigation subsystem augmented by a set of suitable ground based navigation aids located near the landing site.

A functional diagram of one plane of the landing subsystem is shown on the chart. There are three basic loops: altitude, range, and attitude. The altitude loop controls the vertical descent by commanding an altitude rate issued by the guidance subsystem. The commanded altitude rate is compared to the sensed altitude rate to form the error signal. This signal is then processed to form the control command, which is routed to the propulsion subsystem. In a similar manner the range is controlled by commanding a range rate issued by the guidance subsystem. This signal is compared to the sensed range rate to form an error signal, which is then processed to form an attitude command. The attitude command signal is combined with the sensed attitude and attitude rate to form the final control signal, which is subsequently routed to the differential throttles of the direct-lift gas turbine engines, causing the vehicle to rotate to the desired attitude, and thus provide the originally commanded range rate.

Guidance is achieved from a set of precomputed profiles stored in the guidance computer. These profiles are established to satisfy the propulsion subsystem constraints while minimizing fuel consumption. Functionally, the guidance profiles represent a set of nonlinear gain functions that relate the instantaneous measured altitude and range to the altitude rate and range rate commands.

LANDING G&C SYSTEM

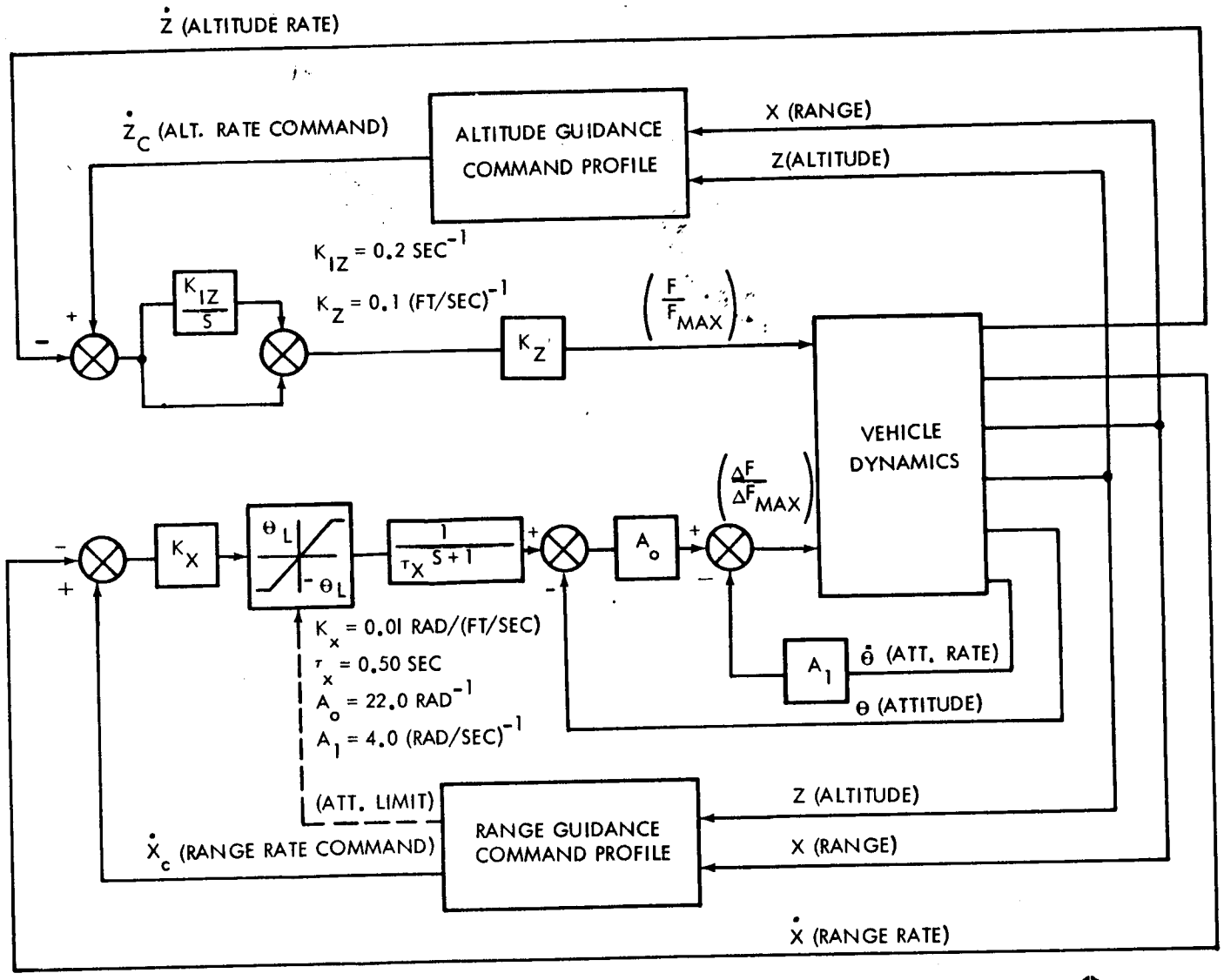

75

SPACE DIVISION CHRYSLER CORPORATION

7.10 TYPICAL LANDING CONTROL RESPONSES

A typical set of nominal responses for the maximum design condition is shown on the chart. This case represents a condition where the vehicle is 4 nm from the landing pad and encounters a 95 percentile speed, 99 percentile shear KSC design head wind profile peaking at 12,000 ft. The 3 degree-of-freedom digital computer landing simulation was used to generate the response.

The controlled descent starts at 15,000 ft with touchdown occurring some 200 sec later. As the vehicle descends, its velocity vector is forced from an almost vertical direction to horizontal. At the same time the attitude is controlled to within $\pm$ 22 degrees from the local vertical to ensure that the vertical propulsive forces can counteract gravitational forces. With these conditions the vehicle angle of attack ranges from zero to approximately 105 degrees. The peak aerodynamic disturbing moment during the landing maneuver has been minimized by appropriately shaping the altitude guidance command profile so that the dynamic pressure is reduced at the point where the vehicle total aerodynamic moment coefficient is maximum. This is illustrated by the dip in the dynamic pressure at approximately 10 sec after landing initiation. The resultant peak disturbing moment (not shown) for this maximum design condition is only 50 percent of the available control, indicating that adequate controllability is available. Total fuel consumption for this case is 27,900 pounds, which is used as the design fuel loading for vehicle weight computation. The peak translation velocity during the landing is 170 ft/sec referenced to the ground, which is 240 ft/sec relative to the wind. Final lateral deceleration occurs when the vehicle is approximately 800 ft from the center of the landing pad. Deceleration is shown to be smooth and well damped. The attitude response during the final deceleration is well damped, with the attitude error close to zero at touchdown.

TYPICAL LANDING CONTROL RESPONSES

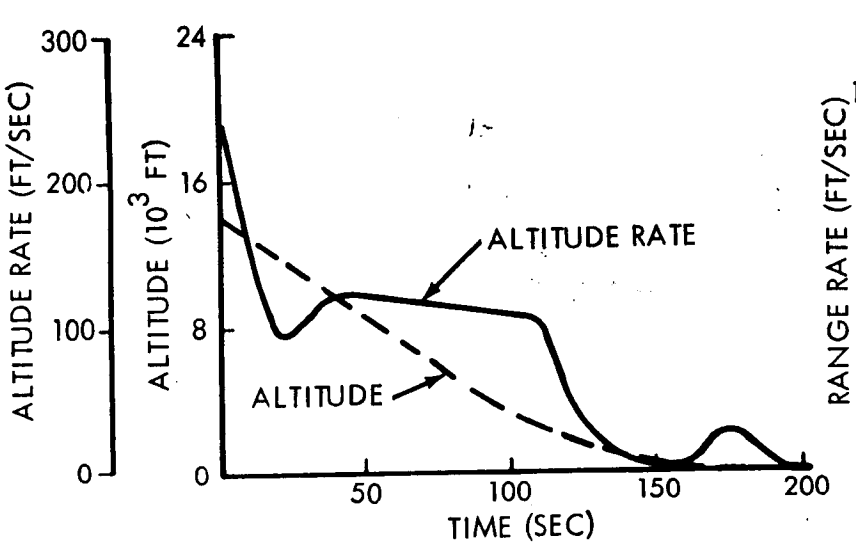

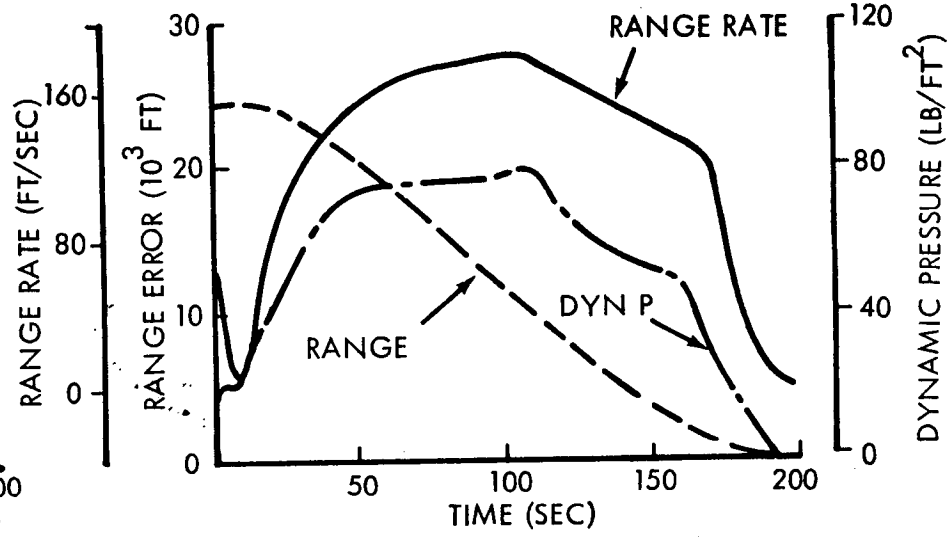

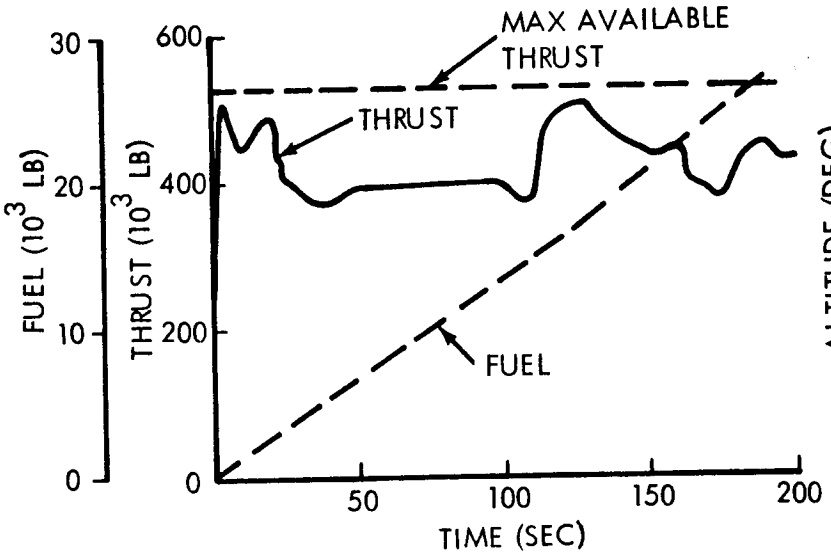

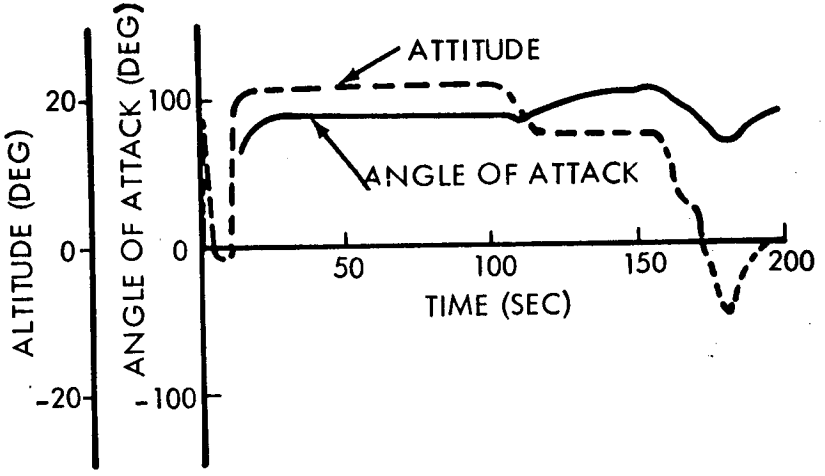

SPACE DIVISION CHRYSLER CORPORATION

7.11 FINAL APPROACH AND TOUCHDOWN CHARACTERISTICS WITH PERFECT NAVIGATION

The most critical phase during a fully automatic instrument landing is the approach and touchdown. Accurate guidance, navigation, and control must be provided during this phase so that the vehicle touches down with conditions within the design limits of the vehicle. During the design of the guidance and control system, special emphasis was placed on achieving satisfactory touchdown characteristics by designing well damped, high accuracy control loops. The accompanying chart shows the final approach trajectories for various combinations of initial range errors and winds with the assumption that perfect navigation is available. The summary table on this chart shows that the touchdown characteristics for all combinations of winds and initial conditions analyzed are well within the design requirements.

FINAL APPROACH AND TOUCHDOWN CHARACTERISTICS

(PERFECT NAVIGATION)

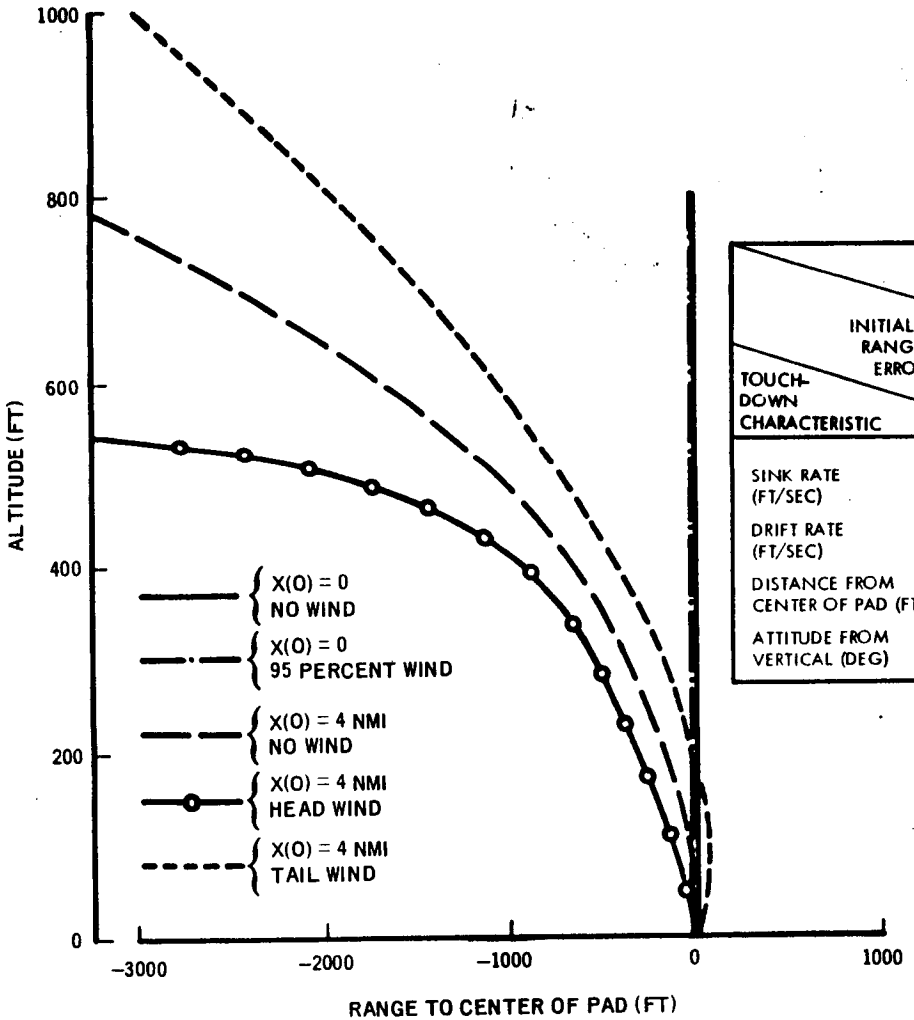

WIND / INITIAL RANGE ERROR / TOUCHDOWN CHARACTERISTIC	NO WIND		95 PERCENT HEADWIND	95 PERCENT HEADWIND	95 PERCENT TAILWIND
	0	4 NMI	0	4 NMI	4 NMI
SINK RATE (FT/SEC)	0.31	0.26	0.26	0.22	0.18
DRIFT RATE (FT/SEC)	0	0.41	0	0.35	0.48
DISTANCE FROM CENTER OF PAD (FT)	0	2.60	1.90	7.30	8.70
ATTITUDE FROM VERTICAL (DEG)	0	0.03	0	0.25	0.32

77

SPACE DIVISION CHRYSLER CORPORATION

7.12 EFFECT OF LANDING NAVIGATION ERRORS ON TOUCHDOWN CHARACTERISTICS

The previous chart illustrated landing touchdown characteristics of SERV for the ideal case of perfect navigation. During an actual landing, however, there will be some measurement errors present. A sensitivity analysis was therefore performed to establish the relationship between navigation errors and touchdown dispersions. This was accomplished by calculating a sensitivity matrix that transforms an appropriate navigation error model to a corresponding set of SERV touchdown dispersions. The 3 degree-of-freedom digital computer landing simulation developed during the landing studies was used to evaluate the sensitivity matrix.

Application of the sensitivity matrix method was made in analyzing a navigation scheme currently being studied by the NASA Ames Research Center. The Ames System, called RAINPAL (Recursive Aided Inertial Navigation for Precision Approach and Landing), consists of an IMU, a barometric altimeter, a set of ground based navigation aids, and employs a Kalman filter algorithm programmed in an onboard digital computer for optimally combining data from the various sources. Preliminary error models of the RAINPAL system for two different ground based navigation aids are shown in the table on the left. The first set of data is for the precision ranging system (PRS) ground based navigation aid, and the second set is for the microwave scan beam (MSB) ground based navigation aid. The latter system is being currently considered as the future standard for commercial aviation. The 3 σ landing touchdown dispersions of SERV corresponding to the two navigation error models along with the maximum allowable for SERV are shown in the table on the right. Note that both navigation error models provide touchdown characteristics which surpass the requirements.

EFFECT OF LANDING NAVIGATION ERRORS ON TOUCHDOWN CHARACTERISTICS

ASSUMED NAVIGATION ERROR MODELS

MEASUREMENT	RMS ERRORS AT TOUCHDOWN	
	PRECISION RANGING SYSTEM (PRS)	MICROWAVE SCANNING BEAM (MSB)
RANGE	1.5 FT	30 FT
RANGE RATE	0.5 FT/SEC	0.60 FT/SEC
ALTITUDE	1.5 FT	2.0 FT
ALTITUDE RATE	0.03 FT/SEC	0.03 FT/SEC
ATTITUDE	0.0466 DEG	0.0466 DEG

SERV TOUCHDOWN CHARACTERISTICS

TOUCHDOWN PARAMETER	3-σ TOUCHDOWN DISPERSIONS FOR 95% HEADWIND/ 4 NAUT MILE INITIAL RANGE ERROR		MAX ALLOWABLE FOR SERV
	PRS	MSB	
RANGE ERROR	7.91 FT	94.7 FT	180 FT
DRIFT RATE	1.88 FT/SEC	2.58 FT/SEC	5 FT/SEC
SINK RATE	1.42 FT/SEC	1.89 FT/SEC	12 FT/SEC
ATTITUDE	0.487 DEG	0.749 DEG	2 DEG

SUBSYSTEM DESIGN

79

SPACE DIVISION CHRYSLER CORPORATION

Section 8
SUBSYSTEM DESIGN

8.0 GENERAL

Subsystem design and analysis began with the baseline vehicle development (Task 1), progressed through a series of trade studies under concept evaluation (Task 3), was supported by model testing (Task 2), and was concluded under the final vehicle definition (Task 4). Vehicle subsystems investigated during this course of study will be discussed here under the headings of structural, mechanical, propulsion, avionics and power. In addition, a subsystem weight summary is given by way of introduction and summary.

8.1 SUBSYSTEM WEIGHT SUMMARY

The basic structural components analyzed are indicated diagramatically on this chart. All weight analysis results are consistent with the definitions listed here.

BASELINE STRUCTURAL ARRANGEMENT

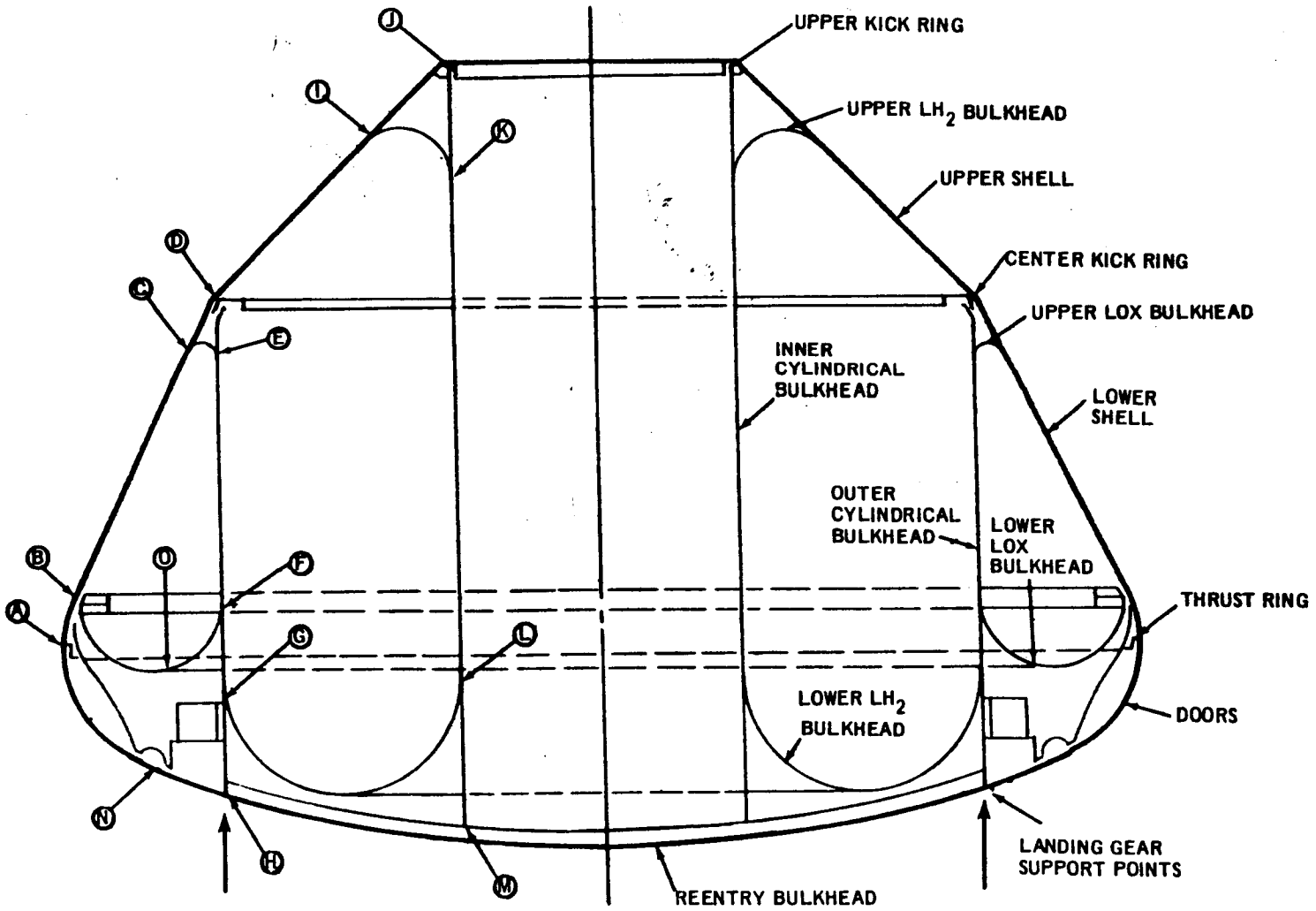

SPACE DIVISION CHRYSLER CORPORATION

8.1.1 SUBSYSTEM WEIGHT COMPARISON

The total design analysis effort can be summarized grossly by considering the delta weight of 41,201 lb between the initial baseline dry weight used for the trade study and the final design dry weight used as input to the final sizing. This delta represents the weight growth not only due to expanded visibility into design details, but also the growth due to the incorporation of shuttle ground rules and the hybrid concept.

The 41,201 lb weight change resulted from both trade study and detailed analysis during the vehicle definition period. This chart summarizes the changes by subsystems, and highlights of the analyses include the following:

1) Structural changes were due to a continuing detailed analysis throughout the study; a further breakdown of these changes is given later.

2) The types of base thermal protection were evaluated and an elastomeric ablative material was selected over the Avcoat ablator and the coated columbium alloy reradiator.

3) Thermal protection for the frustum sections was changed from jacketed microquartz on localized areas to Inconel welded honeycomb on all areas.

4) The revised design of the landing gear and door actuators caused their respective weight changes.

5) Reduced turbojet thrust efficiency and engine-out capability caused a substantial weight increase.

6) Better definition of propulsion subsystems and propellant feed hardware caused a weight increase.

7) The incorporation of turbopump-out capability caused the aerospike engine weight to increase.

8) Other weights increased due to better definition; note that all weights were affected, either directly or indirectly, by dimensional and configuration changes as required throughout the study.

SUBSYSTEM DESIGN WEIGHT CHANGE SUMMARY

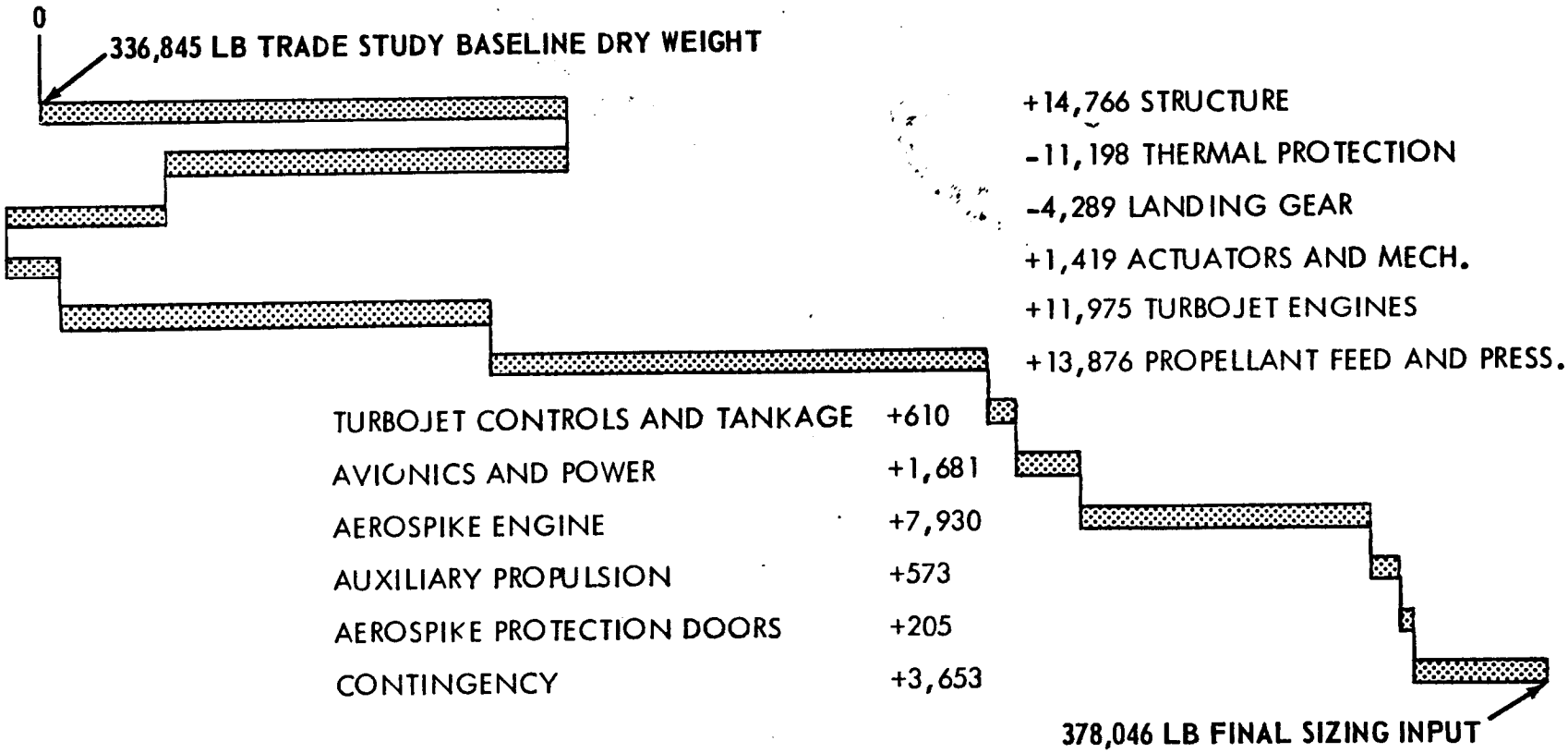

8.1.2 STRUCTURAL WEIGHT COMPARISON

A similar comparison of weights for the structural items identified in the previous diagram is presented in this chart. Here, structural analysis results may be summarized by examining the delta weight of 14,766 lb between the initial baseline for the trade study and the final design value used as input to the final sizing. The chart summarizes changes by major assembly to yield the 14,766-lb delta:

1) Increased depth of thrust ring and incorporation of weight items related to turbojet inlet doors, aerospike protection doors, and the joints and baffles item below.

2) The kick rings were resized after stress analysis.

3) The lower shell was reinforced due to revised analysis which included consideration of thermal gradients and discontinuity bending moments.

4) The inner and outer cyclindrical bulkheads were reinforced to accommodate revised analysis including consideration of concentrated landing loads and discontinuity bending moments.

5) The lower LO_2 bulkhead and upper and lower LH_2 bulkheads were resized after stress analysis and changed from membrane to honeycomb construction to provide insulation.

6) The upper shell was reinforced to consider thermal gradients and equipment penetrations.

7) The reentry bulkhead was resized after stress analysis including a lower value for dynamic load factor.

8) Lift engine supports were resized after stress analysis, and air intake ducts were added.

9) Miscellaneous weights were reallocated from the joints and baffles item, and ring-type baffles were added.

STRUCTURES DESIGN WEIGHT CHANGE SUMMARY

THRUST RING	+6,153
KICK RINGS	+286
LOWER SHELL	+10,203
OUTER CYLINDRICAL BULKHEAD	+6,701
LOWER LO_2 BULKHEAD	+270
UPPER SHELL	+609
INNER CYLINDRICAL BULKHEAD	-1,332
UPPER LH_2 BULKHEAD	-189
LOWER LH_2 BULKHEAD	+2,054
REENTRY BULKHEAD	-4,892
LIFT ENGINE SUPPORT	-3,317
JOINTS, BAFFLES, ETC.	-1,780

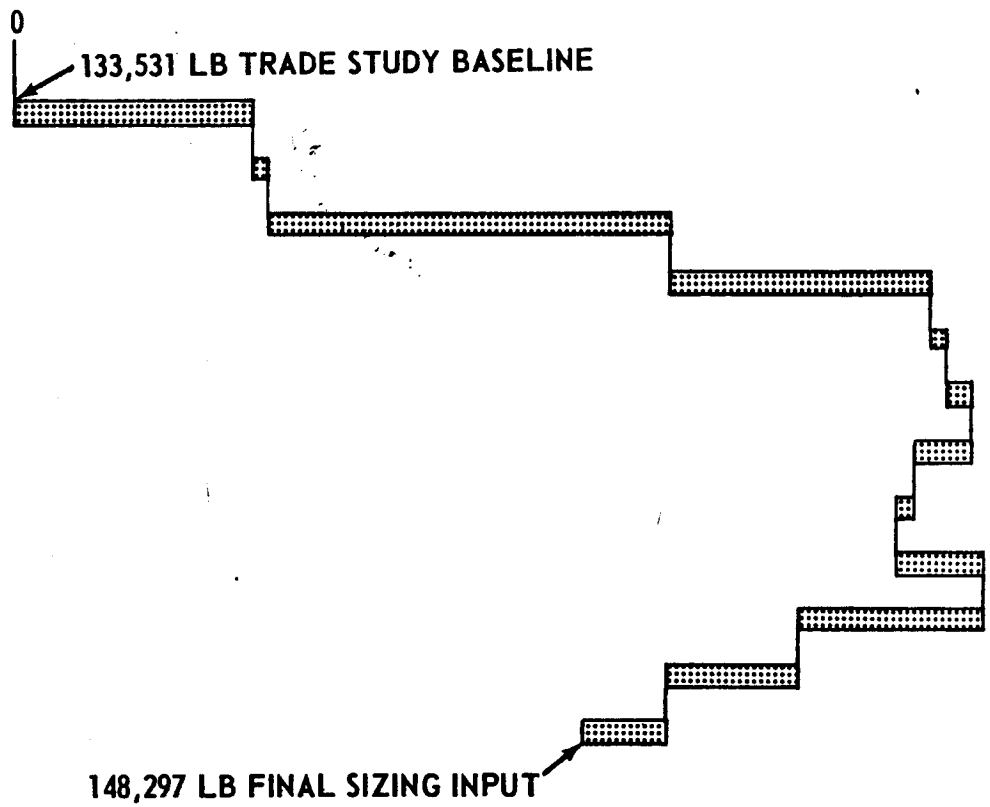

82

SPACE DIVISION CHRYSLER CORPORATION

8.1.3 VEHICLE SIZING GROWTH FACTORS

In addition to establishing the final configuration, the vehicle sizing program was utilized to determine the effects of parametric variations in aerodynamic characteristics, aerospike engine performance, contingency factor and inert weights on vehicle size. These effects are reflected as resizing for propellant load, and vehicle subsystem weight.

VEHICLE SIZING GROWTH FACTORS

(FIXED PAYLOAD)

INDEPENDENT VARIABLE (X)	∂GLOW/∂X	
INERT WEIGHT	+ 20.4	LB/LB
CONTINGENCY	+ 95,470	LB/PERCENT
SPECIFIC IMPULSE FOR NOMINAL THRUST	- 84,534	LB/SEC
SPECIFIC IMPULSE FOR NOMINAL FLOW RATE	-107,912	LB/SEC
THRUST FOR NOMINAL SPECIFIC IMPULSE	- 49,825	LB/PERCENT
THRUST FOR NOMINAL FLOW RATE	-503,733	LB/PERCENT
INITIAL THRUST TO WEIGHT ($\Delta = 0.1$)	- 69,486	LB/0.1
PERCENT ULLAGE	+ 62,590	LB/PERCENT
ASCENT VELOCITY REQUIREMENT	+ 621	LB/FPS
AUXILIARY VELOCITY REQUIREMENT	+ 780	LB/FPS
DRAG	+ 14,413	LB/PERCENT
LIFT FUEL	+ 16.2	LB/LB

53

SPACE DIVISION CHRYSLER CORPORATION

8.2 STRUCTURAL SUBSYSTEM

The structural analysis approach adapted for sizing the primary structural components is discussed in this section.

8.2.1 STRUCTURAL ANALYSIS APPROACH

Major design criteria and required inputs used in the analysis of the SERV structure are summarized. The inputs were extracted from technical reference documents or calculated, using study ground rules and baseline vehicle data. The structural analysis criteria were developed by cognizant personnel in a series of design review meetings or obtained from the "Space Shuttle Design Criteria Document". These data vary from those used during the trade studies as follows: The factor applied to the dynamic pressures on the reentry bulkhead was reduced from 1.5 to 1.1 because of use of actual wind tunnel data in the determination of design pressure distribution. The landing impact of a 3g limit was reduced to a 2g limit as the result of a more refined analysis of the landing phase.

STRUCTURAL ANALYSIS APPROACH

CRITERIA	INPUTS
• 1.4 STRUCTURAL FACTOR OF SAFETY • 1.1 LOADING FACTOR APPLIED TO DYNAMIC PRESSURES ON REENTRY BULKHEAD (NOTE 1) • 3G MAXIMUM ACCELERATION FOR ASCENT AND 3G MAXIMUM DECELERATION FOR DESCENT • SHOCK IMPINGEMENT LOADING APPLIED OVER UPPER FRUSTUM • 10 PERCENT WEIGHT CONTINGENCY • LANDING IMPACT OF 2G LIMIT, 12 FPS VERTICAL, AT 2 DEGREE ATTITUDE (NOTE 1) • ALLOWABLE BUCKLING STRESSES COMPUTED PER NASA PROCEDURE USING EQUIVALENT MONOCOQUE TECHNIQUE	• ASCENT AND REENTRY TRAJECTORY DATA - WEIGHT, THRUST, DRAG - AMBIENT PRESSURE - DYNAMIC PRESSURE • ENGINE PERFORMANCE DATA - THRUST - BASE PRESSURE • AERODYNAMIC DATA - LOCAL SURFACE PRESSURE COEFFICIENT • VEHICLE CONFIGURATION DATA - GEOMETRY - DEAD WEIGHT DISTRIBUTION - INTERNAL PRESSURE

NOTE 1: THESE CRITERIA DIFFER FROM THOSE USED IN TRADE STUDIES

8.2.2 MATH MODEL IDEALIZATION OF UPPER FRUSTUM

The shell structure of the vehicle, which includes the upper and lower frustums and the inner and outer cylindrical bulkheads, was synthesized as a series of conical and cylindrical segments jointed at circumferential node lines. The chart shows the idealization of the upper frustum and is typical of the remaining shell structure. The heat shield bulkhead consisted of a series of sandwich panels supported by a spider beam assembly of major radial beams, short radial beams and cross beams. Attachment of the heat shield bulkhead to the inner and outer cylindrical bulkheads renders the complete vehicle structure redundant. In order to include the heatshield bulkhead in the math model, it was synthesized as an equivalent shell structure whose thickness and modulus of elasticity closely approximated the radial stiffness of the actual assembly.

The computer program was used to analyze an axisymmetric shell structure by the finite stiffness method. A stiffness matrix for each segment is constructed, based on the six degrees of freedom illustrated in the auxiliary sketch on the chart, and on the simple plate characteristics, which are equivalent to the actual sandwich. These segmental stiffness matrices are then assembled, in the same manner as the actual structure is connected, to produce a total stiffness matrix for the vehicle. The stiffness matrix is then inverted, resulting in the vehicle flexibility matrix. A load column is then constructed corresponding to each design condition (or critical mission time point) for which the vehicle is to be analyzed. Multiplying the flexibility matrix by the load column results in a compatible set of nodal deflections for this landing. The deflections at the nodes, forming the end boundaries of an individual segment, are then extracted and multiplied by the segmental stiffness matrix. The result is a set of internal loads acting on the segment.

There are two major advantages gained by the application of the finite stiffness method to the analysis of the SERV primary structure. First, the discontinuity effects arising from the connection of two dissimilar shells of revolution; i.e., the upper frustum to the inner cylindrical bulkhead, are fully evaluated in each shell provided the nodal spacing in each shell, adjacent to the joint, is kept small enough to define the rapidly damped bending moment distribution. Second, since loads are distributed as a function of component stiffnesses, unique solutions are obtained for redundant structures.

MATH MODEL IDEALIZATION OF UPPER FRUSTUM

1. MATH MODEL INCLUDES INTERACTION CAUSED BY ADJACENT SHELLS (DISCONTINUITY EFFECTS)
2. MATH MODEL SOLVES REDUNDANT LOAD PATHS ON BASIS OF RELATIVE STIFFNESS

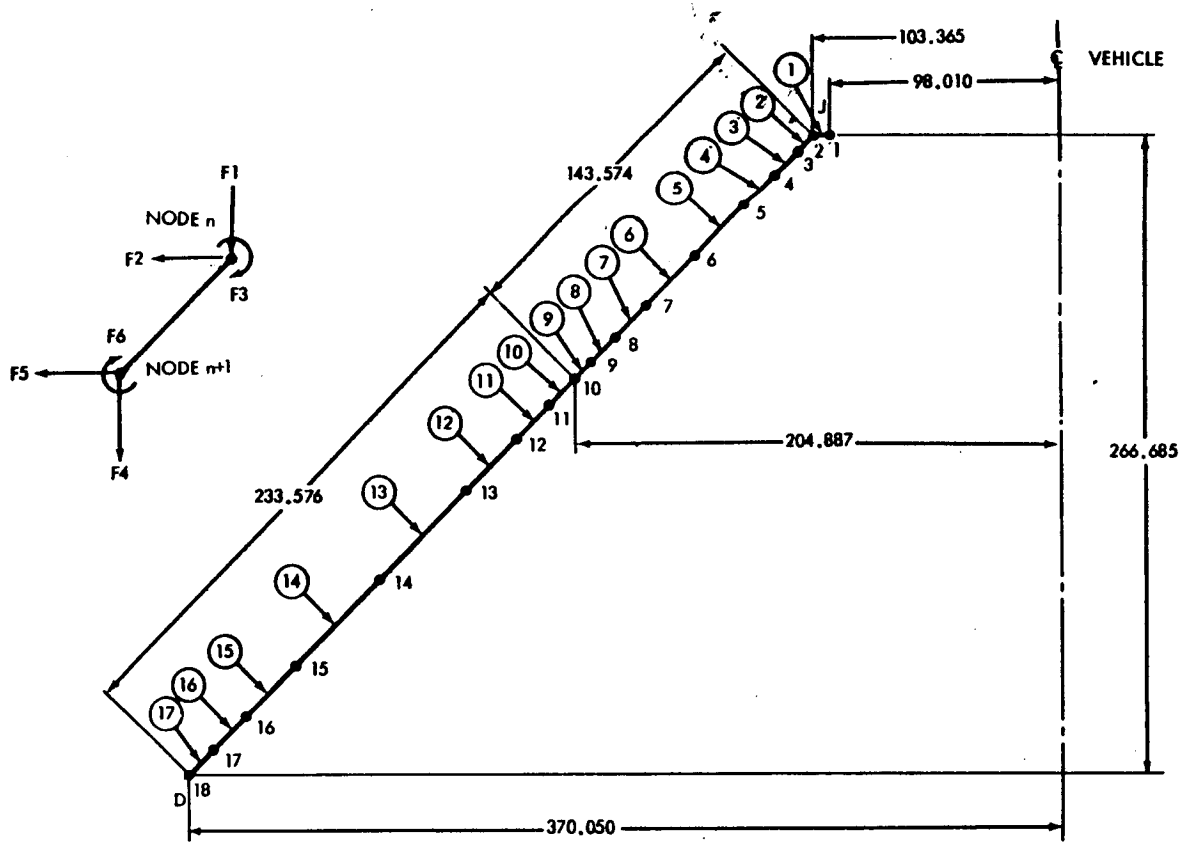

SPACE DIVISION CHRYSLER CORPORATION

8.2.3 FREQUENCIES AND MODE SHAPES

This chart presents the longitudinal normal frequencies for the SERV vehicle, which was derived from a dynamic model constructed by adding the two toroidal lower tank bulkheads to the math model previously discussed. The dynamic model had a total of 116 degrees of freedom and was used to investigate four mass conditions for the free-free case: the fully loaded vehicle at liftoff (T = 0), the vehicle at the maximum dynamic pressure time point (T = 77 seconds), the maximum longitudinal acceleration time point (T = 138 seconds) and the vehicle with propellant tanks empty. The fully loaded vehicle was also investigated for an on-pad condition.

The chart also illustrates the mode shape for a full vehicle in the free-free condition at an omega of 13.154 radians per second, and is presented as a typical example of the results. In general, it was found that the membrane bulkheads were quite flexible compared to the primary structure and that the bulkhead modes predominate at the lower frequencies.

FREQUENCIES AND MODE SHAPES

MODE	FREE - FREE				SUPPORTED
	FULL t = 0	MAX Q t = 77	MAX.ACCEL t = 138	EMPTY	FULL t = 0
1	4.904	5.916	7.405	82.155	4.893
2	8.252	9.955	12.462	123.507	8.196
3	10.276	12.215	15.053	132.122	10.269
4	13.154	15.748	19.471	139.423	11.281
5	16.209	19.345	23.812	218.161	15.889
6	19.721	23.555	29.030	219.653	17.890
7	22.711	27.347	34.124	231.731	20.976
8	29.399	35.282	43.583	271.782	28.542

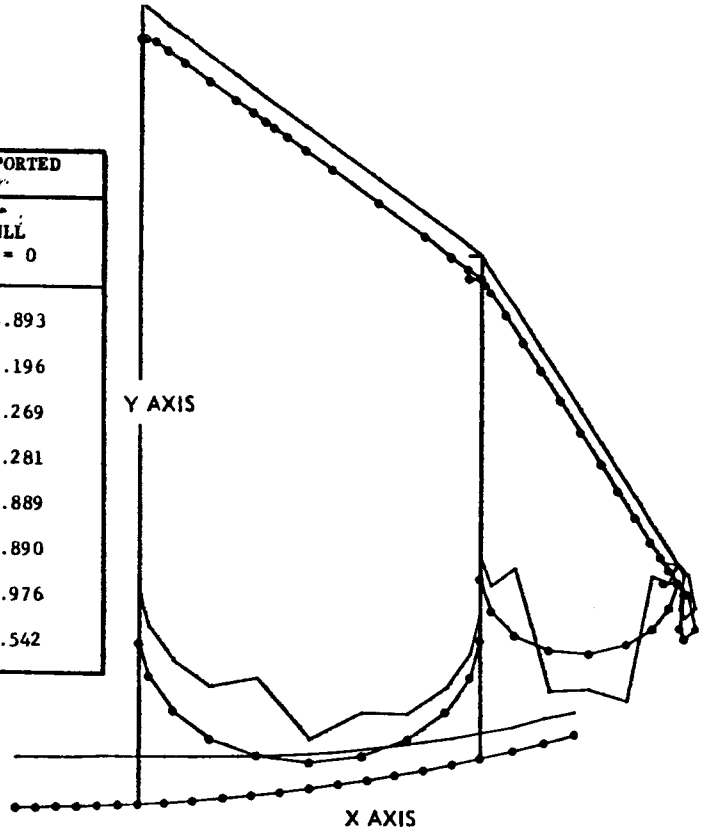

86

8.2.4 PAYLOAD FREQUENCY RESPONSE

This chart shows the results of a preliminary appraisal of the structural/liquid dynamic model, which reveals no significant payload structural gain factor for a sinusoidal forcing function at the thrust vector. Examination of the frequency/mode shape data such as that illustrated on the previous chart, also showed no significant payload displacement relative to the tank bulkheads. Nothing was found in this very preliminary type analysis to indicate that the SERV configuration would be susceptible to POGO type instability, but a much more detailed analysis is recommended for future study.

PAYLOAD FREQUENCY RESPONSE

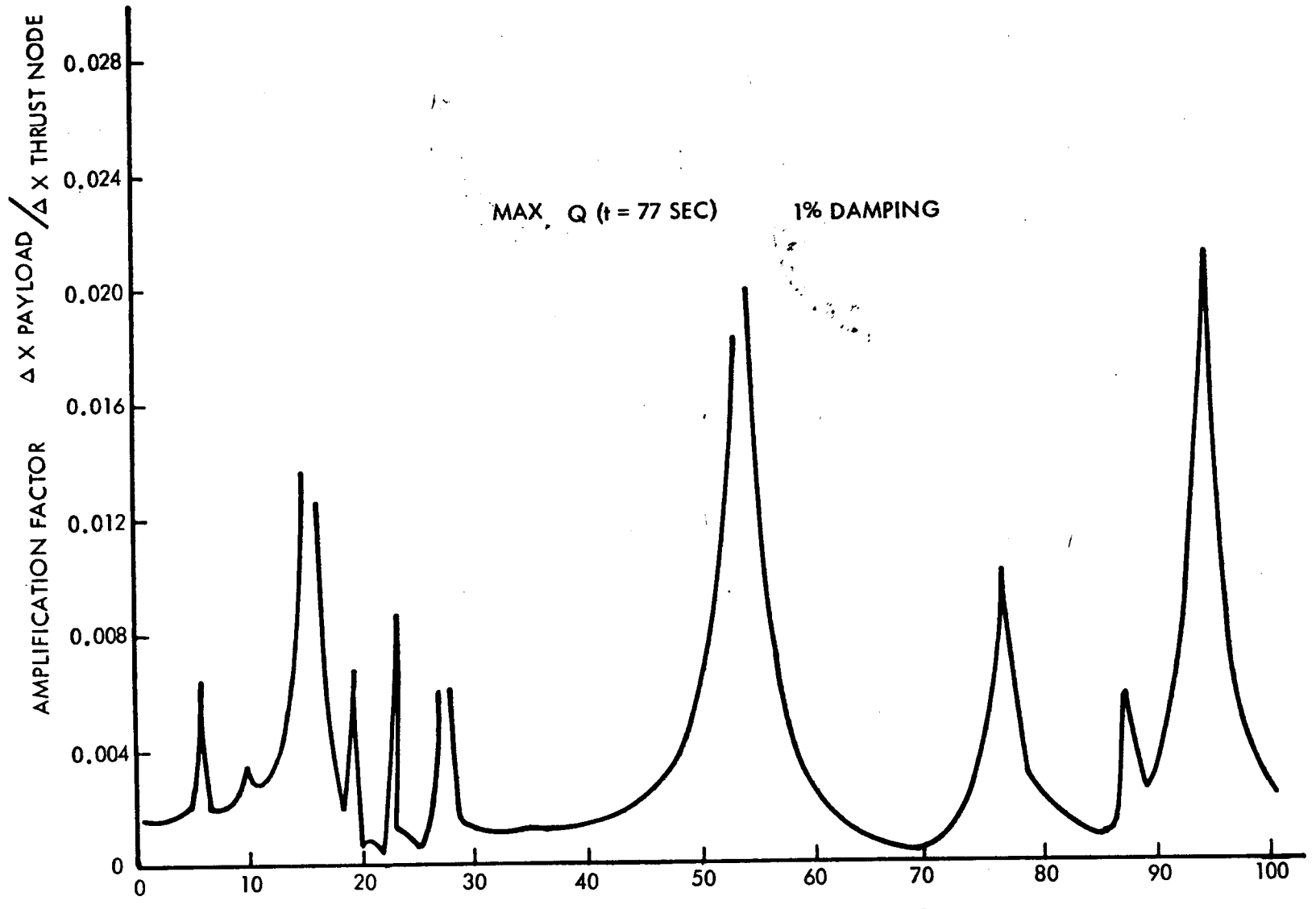

87

SPACE DIVISION CHRYSLER CORPORATION

8.2.5 THERMAL GRADIENT EFFECTS

The sizing of the shell structure previously discussed is based on the use of room temperature material properties. However, the weight of the thermal protective system that would keep the structure at room temperature would be prohibitive. This chart illustrates the method employed in arriving at the combination of thermal protective system weight vs structural weight increase due to an actual thermal gradient that would minimize the increase in total vehicle weight.

The diagram at the left of the chart illustrates the points on the lower frustum at which the analysis was made. These points reflect changes in face thickness. Using theory developed for long sandwich cylinders, the meridional and hoop thermal stresses in both the inner and outer faces of the sandwich were calculated for a given temperature gradient. The difference between the minimum allowable stress and the thermal stress is thus equal to the magnitude of the stress that is available to carry primary airframe loads. For a given ascent design condition, for which the internal loads were known, the required thickness of each face could then be calculated. The percentage increase in sandwich weight of the hot sandwich over that at room temperature was then determined. Repeating this procedure for various temperature gradients provided one curve as shown in the chart under the "structure only" label. Only the worst case portions of the curves are drawn, so when in some cases the failure mode changed from tension to intercell buckling, a discontinuity in the slope of the curve appears as in that for Point Y.

The weight of the thermal protection system, calculated as a percentage of the unit weight of the primary sandwich structure, was also determined in terms of the temperature gradient permitted to exist in the primary sandwich structure. These curves are presented in the chart under the "insulation only" label.

At any value of temperature gradient, the percentage weight of the combined thermal protection system and the structure was evaluated and plotted as the fish hook curves under the "structure plus insulation" label. The minimum total vehicle weight increase obviously results when the "structure plus insulation" curve is at the lowest point. In general, it can be seen that, for the lower frustum, this occurs when only that amount of insulation is provided which results in a temperature gradient in the structure of approximately $400^{o}F$.

Data from analyses such as is illustrated in this chart was used to estimate the weight of the thermal insulation system and the required structure in the upper and lower frustum for subsequent use in the vehicle sizing program.

THERMAL GRADIENT EFFECTS

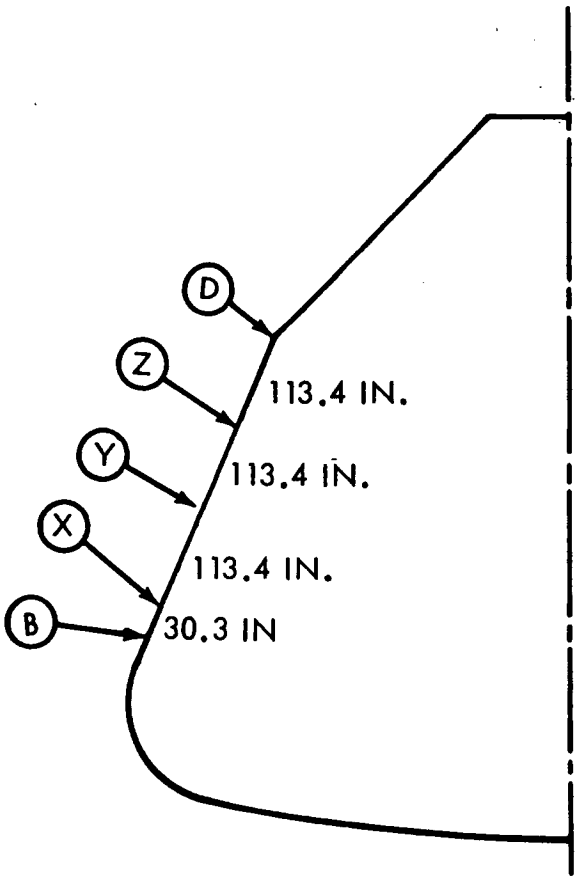

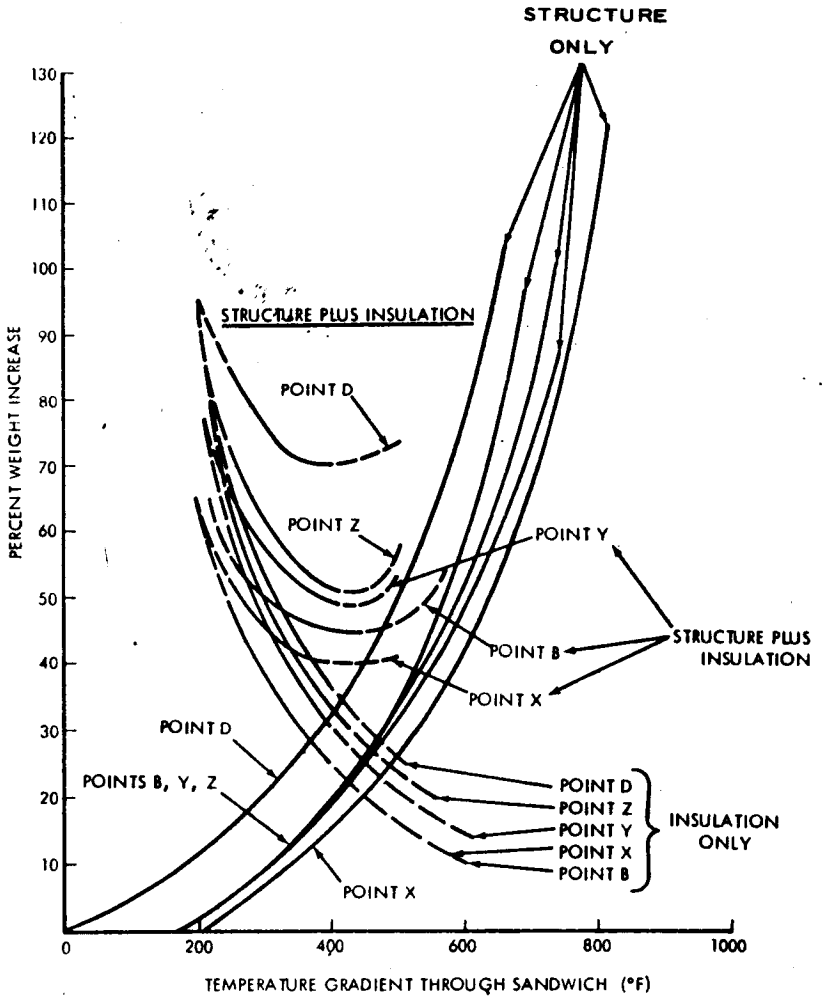

8.2.6 SERV STRUCTURAL ARRANGEMENT

Each of the primary structural components of the vehicle, with the exception of the heatshield bulkhead, was sized on the basis of overall stability. Due to the refinement in analysis made possible by use of the math model, the depth of analysis of the shell structure was increased. The effects can be seen in the added structural detail shown in this chart. The local areas in which the foil thickness of the core is other than earlier target thickness of 0.0020 in. reflect regions where high transverse shear loadings due to shell discontinuity effects has made it necessary to increase the core strength. These same areas, without exception, also exhibit increases in face thickness when compared to neighboring regions. These increases in face thickness were also dictated by discontinuity effects.

SERV STRUCTURAL ARRANGEMENT

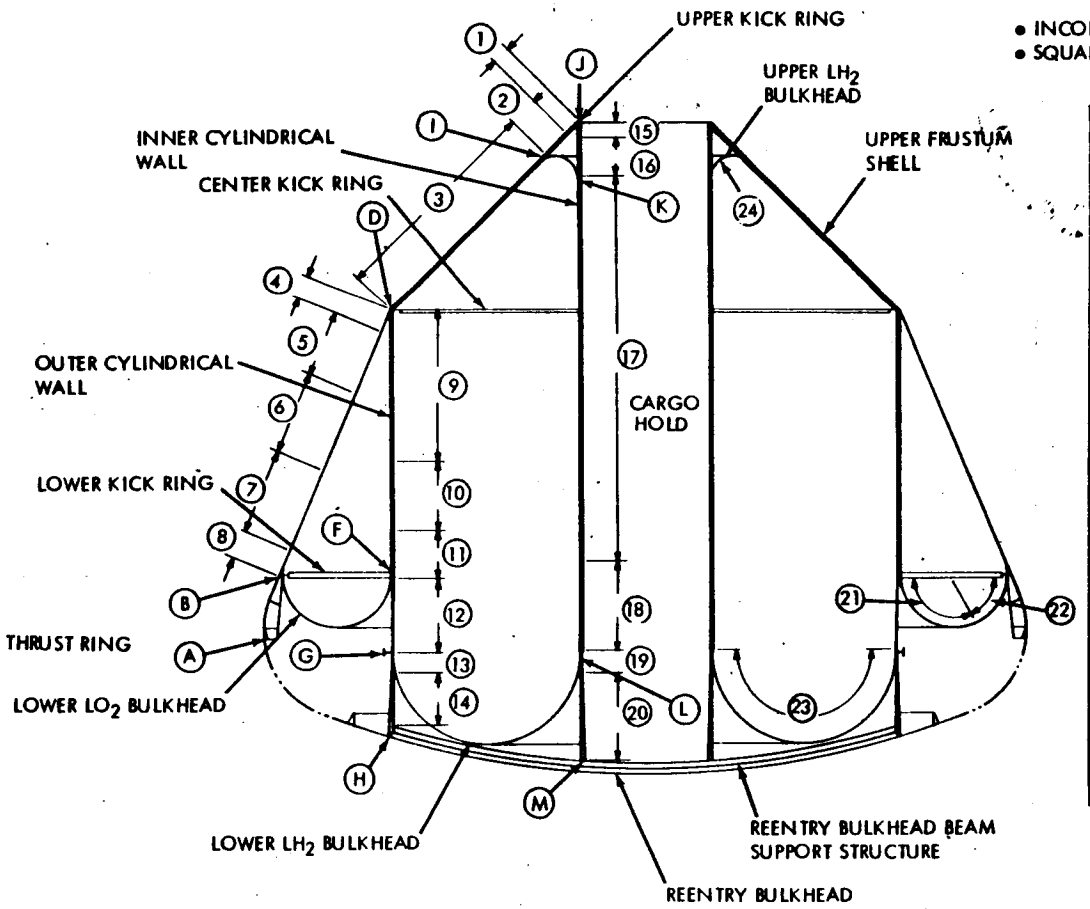

- INCONEL 718 SANDWICH PANEL
- SQUARE CORE CELL

LOCATION	PANEL THICKNESS (IN.)	FACE SHEET THICKNESS (IN.)	CORE SHEET THICKNESS (IN.)	CORE CELL SIZE (IN.)
1	1.60	0.026	0.0025	0.500
2	1.60	0.018	0.0020	0.500
3	4.00	0.020	0.0020	0.500
4	2.70	0.038	0.0030	0.500
5	2.70	0.020	0.0020	0.500
6	2.70	0.018	0.0020	0.500
7	2.70	0.020	0.0020	0.500
8	2.70	0.027	0.0020	0.500
9	5.00	0.024	0.0020	0.500
10	5.00	0.036	0.0020	0.500
11	5.00	0.050	0.0020	0.500
12	0.680	0.014	0.0020	0.500
13	0.680	0.016	0.0020	0.500
14	0.680	0.014	0.0020	0.500
15	0.375	0.030	0.0040	0.500
16	0.375	0.010	0.0020	0.500
17	3.40	0.010	0.0020	0.500
18	3.80	0.010	0.0020	0.500
19	0.375	0.014	0.0035	0.500
20	0.375	0.010	0.0020	0.500
21	1.00	0.014	0.0020	0.750
22	1.00	0.014	0.0020	0.375
23	1.00	0.006	0.0020	0.750
24	1.00	0.006	0.0020	0.750

8.2.7 REENTRY HEAT SHIELD PRESSURE DISTRIBUTION

The heat shield assembly consists of honeycomb panels supported by a spider beam arrangement of structural beams. The heat shield configuration with the panel design pressures superimposed is shown on the left. The panel design pressures were calculated by averaging the node point pressures, which were calculated using pressure coefficient data extracted from the preliminary aerodynamic criteria generated for use in the sizing program. Using these pressures, the honeycomb panels were idealized as circular sectors and rectangular shapes. The assumed pressure distribution on the structural beams is shown at the left of the chart. At 500°F operating temperature was considered in the panel analysis A 200° temperature gradient across the panels yielded a 10 percent weight penalty.

REENTRY HEAT SHIELD PRESSURE DISTRIBUTION

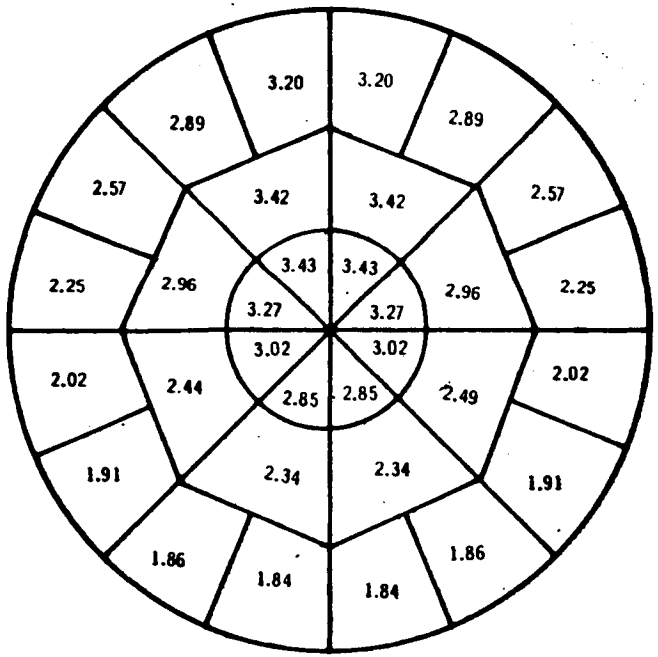

PANEL DESIGN PRESSURES

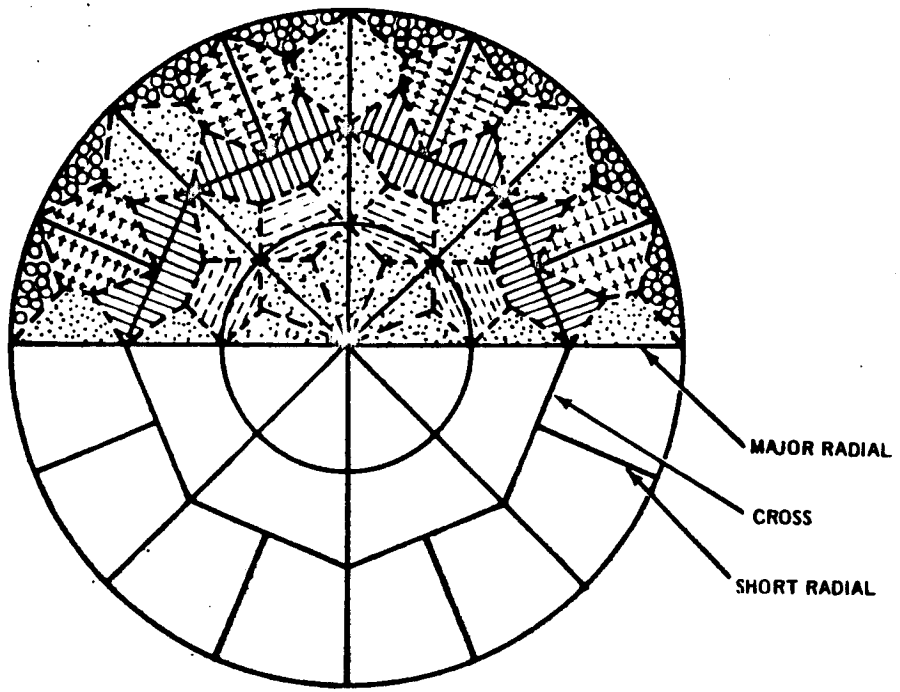

PRESSURE DISTRUBUTION TO BEAMS

8.2.8 REENTRY HEAT SHIELD STRUCTURAL ARRANGEMENT

The chart illustrates the reentry heat shield beam structure and presents panel thickness details of interest.

REENTRY HEAT SHIELD STRUCTURAL ARRANGEMENT

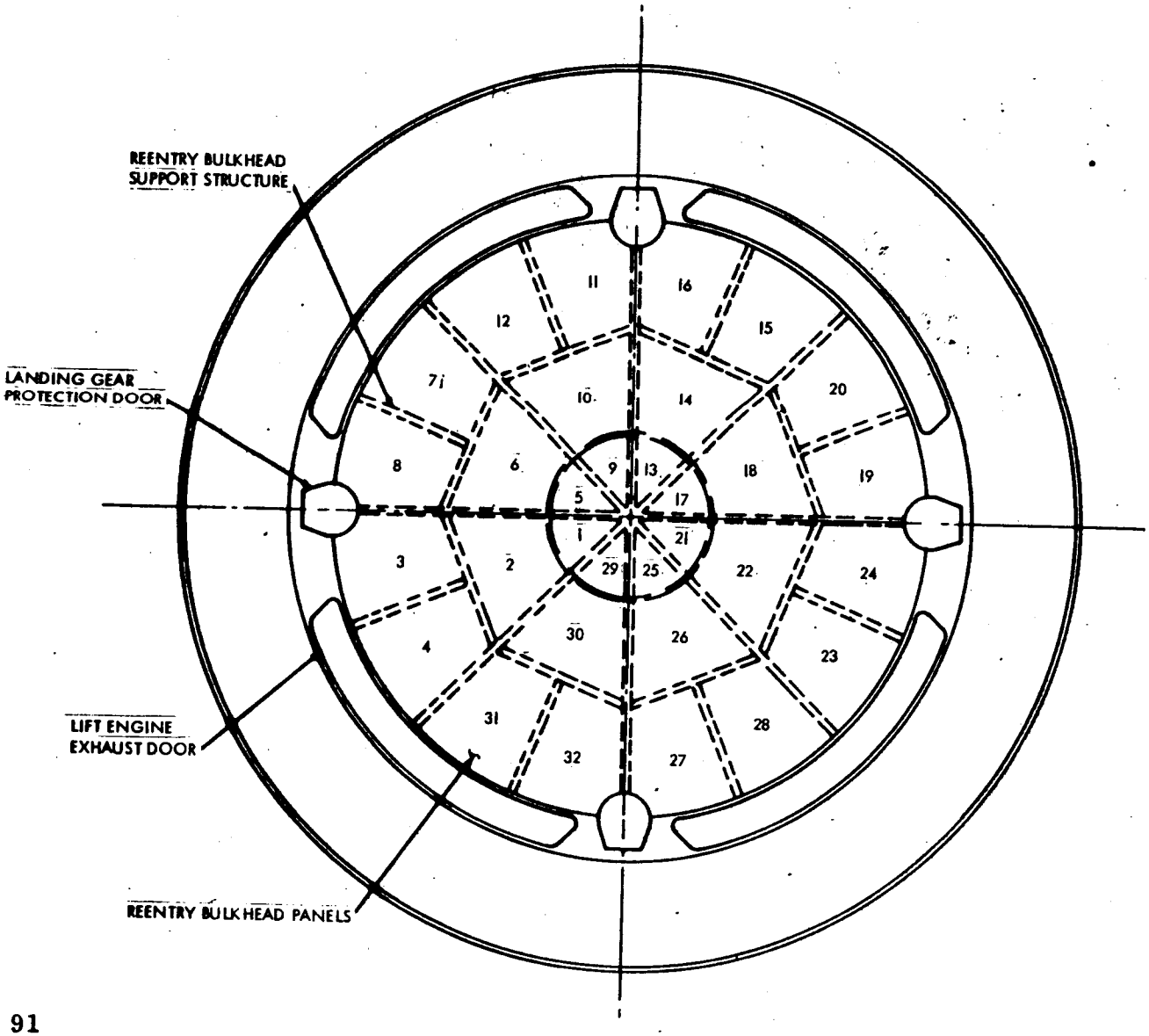

- PH15-7 Mo WELDED SANDWICH PANEL
- 0.50-IN. SQUARE CORE CELL
- 0.002-IN. CORE SHEET THICKNESS

PANEL NO.	PANEL THICKNESS (IN.)	FACE SHEET THICKNESS (IN.)
1,21	1.55	0.010
2,22	2.12	0.015
3,24	1.72	0.015
4,23	1.63	0.015
5,17	1.69	0.010
6,18	2.49	0.015
7,20	2.19	0.015
8,19	1.92	0.015
9,13	1.77	0.010
10,14	2.85	0.015
11,16	2.73	0.015
12,15	2.46	0.015
25,29	1.47	0.010
26,30	1.98	0.015
27,32	1.58	0.015
28,31	1.58	0.015

91

SPACE DIVISION CHRYSLER CORPORATION

8.3 MECHANICAL SUBSYSTEMS

The method of actuation and sealing of the aerospike protection doors and the gas turbine inlet and exhaust doors are discussed in this section. Details of the four landing gear assemblies are presented.

8.3.1 AEROSPIKE DOOR ACTUATION

The aerospike door system comprises 16 doors arranged circumferentially around the SERV, interfacing with the vehicle at the forward and aft ends, and interfacing with each adjacent door at the door sides.

Sixteen linear actuators are positioned at the optimized one third door length point with one actuator located at each door interface. Actuation of the mechanism generates circumferentially in-line loads along the door diameter. This axial load is sufficient in magnitude to effect a radial inboard or outboard force to overcome the flight load at the time point in question. The result is an inboard or outboard door movement caused by a diameter change at the actuator line.

Support beams to take the axial loads generated by the actuation mechanism in opening and closing the doors are installed circumferentially in line with the actuator forming a hoop.

The aerospike door actuation system is formed by the actuator/beam combination and is essentially an expanding hoop when opening, and a shrinking hoop when closing.

AEROSPIKE DOOR ACTUATION

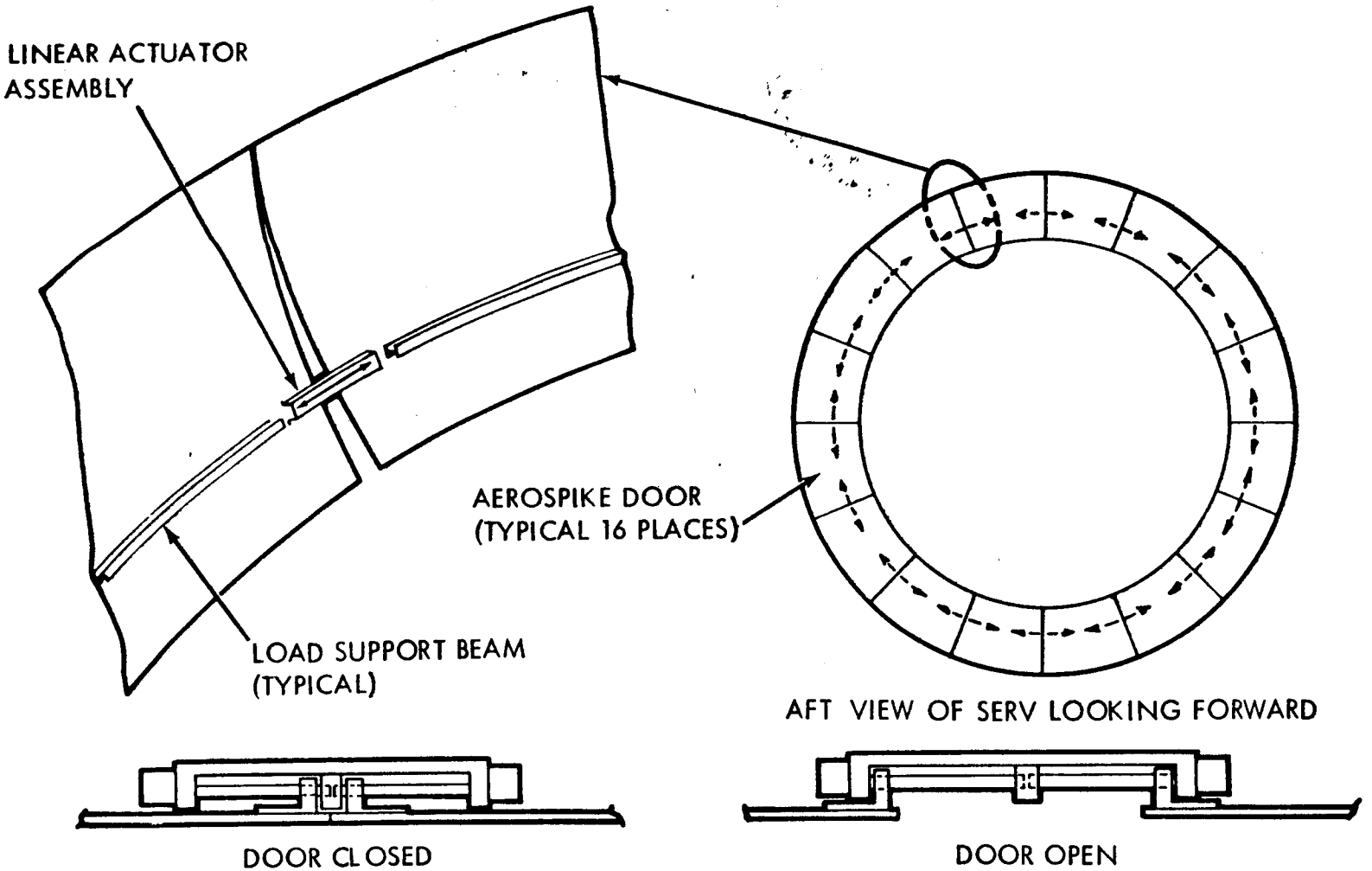

92

SPACE DIVISION CHRYSLER CORPORATION

8.3.2 AEROSPIKE DOOR SEALING

The aerospike door seal is effected by utilization of a door geometry and a high temperature silicone (RTV 560) in combination.

The door-to-door interface seal is made by employing a tongue and groove design such that when the door is drawn to the closed position, the silicone is compressed and wedged to the conformity of the door.

The door forward hinge seal is accomplished by the door forward edge compressing the silicone seal as the door approaches the closed position. The silicone seal is a continuous band installed on the vehicle structure at the door forward interface.

The door aft interface lock and seal arrangement includes a high temperature silicone seal along the aft end and inboard corner of the door panel. The SERV structure is designed to receive the door by implementing a groove and step design to ensure a seal over any imperfections or uneveness in the seated interface between the door and the structure. All of the door seal configurations have the wedging and compressing characteristics to effect a positive seal over imperfections in the interface structure.

A positive lock and seal compression effect on the aft interface is accomplished by means of a spring lock actuation device installed in a structure cavity. As the door closes, a trunion attached to the door structure engages with the locking device, activating the spring causing the door to be snugged into place. Six locking devices per door ensures a uniform interface seal.

AEROSPIKE DOOR SEALING

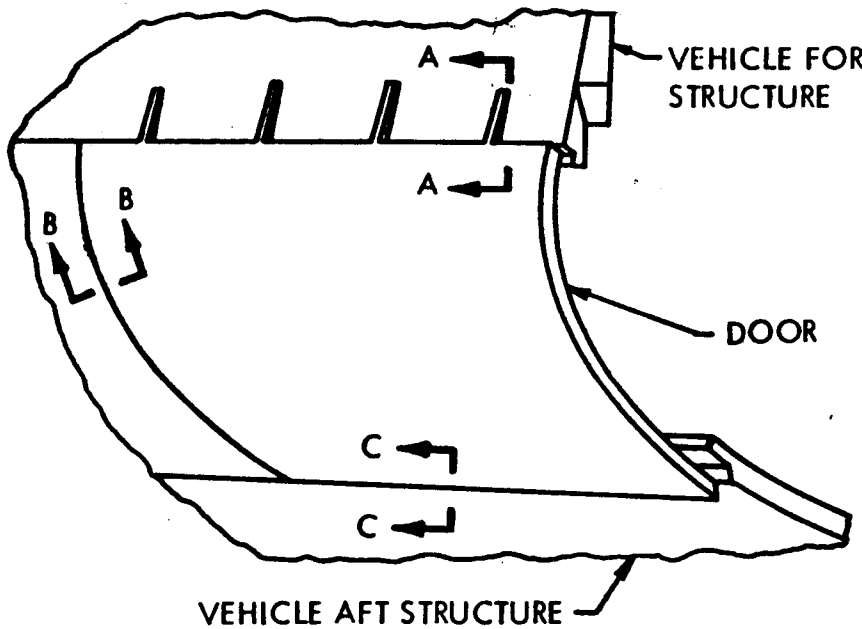

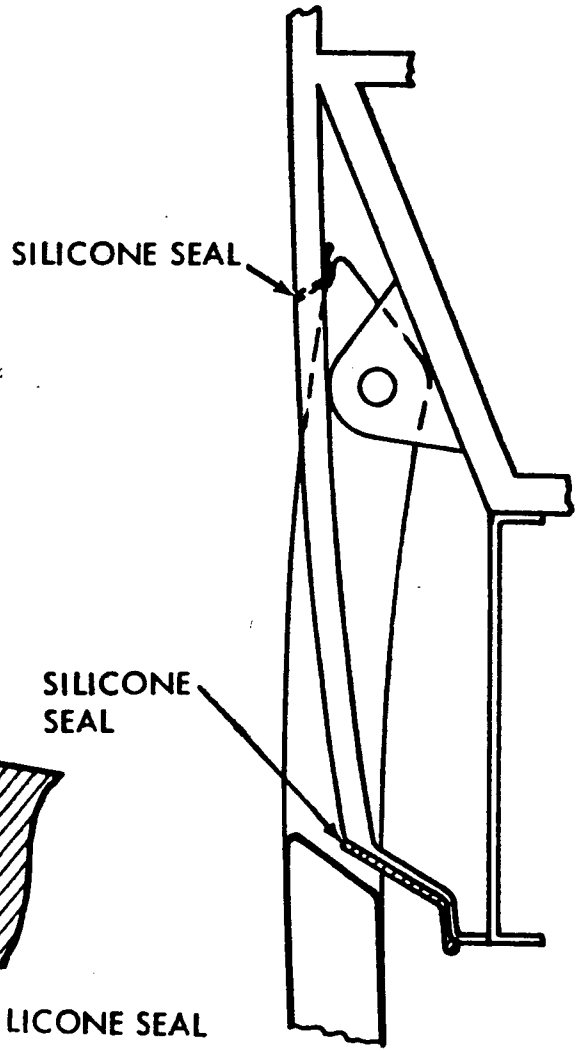

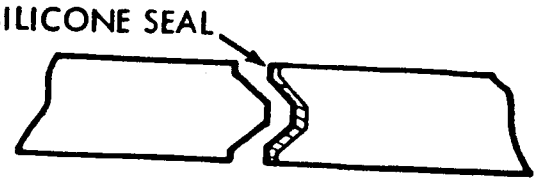

SECTION B-B
DOOR SPLICE

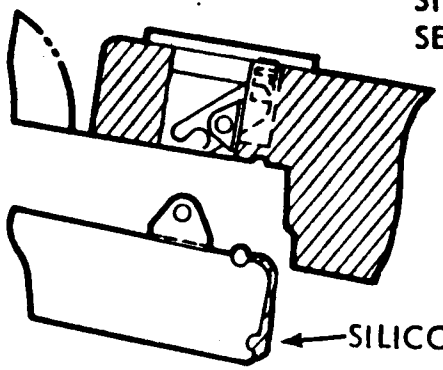

SECTION C-C
DOOR AFT LOCK AND SEAL

SECTION A-A
DOOR FORWARD HINGE AND SEAL

93

SPACE DIVISION CHRYSLER CORPORATION

8.3.3 ACTUATION AND SEALING OF LIFT ENGINE AIR INTAKE DOORS

The lift engine air intake doors are located forward of the aerospike engine and in the thrust ring. Spring actuation coupled with solenoid activation is used as the opening system. The solenoids activate a spring loaded cannister and release positive door locks, thrusting the door open to the air flow. The air flow causes the door to open to the fully extended position, the opening speed being controlled by a snubber device. The snubber device consists of a screw jack rod with a ratchet and shock absorbing lock to prevent the door from closing or slamming open.

Silicone seals (RTV 560) are employed on the perimeter of the door frame. The typical frame and door interface is set at a 45-degree slope with a step groove to ensure compression of the silicone seal in effecting a proper fit over any imperfections in the structure.

ACTUATION AND SEALING OF LIFT ENGINE AIR INTAKE DOORS

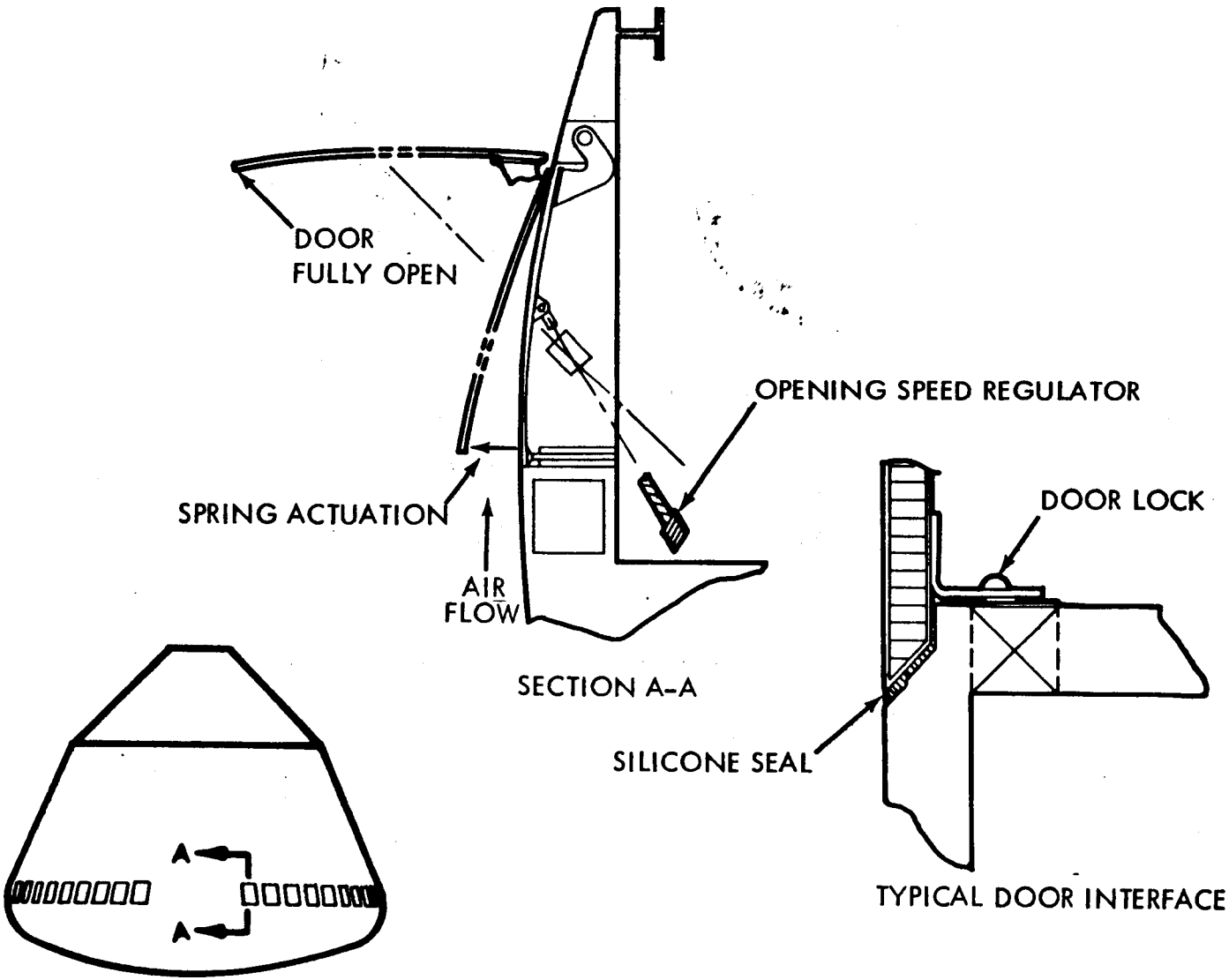

94

SPACE DIVISION CHRYSLER CORPORATION

8.3.4 ACTUATION AND SEALING OF LIFT ENGINE EXHAUST DOORS

The engine exhaust doors employed for the four banks of lift engines are located in the reentry base shield radially equidistant in four quadrants. Electrically powered screw jacks are used to push the door downward into the air flow maintaining an even plane. A cable pulley system subsequently causes each door to move laterally inboard on a track system, exposing the lift engine banks.

Four one half horsepower motors and two one horsepower motors per bank are employed for the door downward and inboard movements. A silicone seal (RTV 560) is installed along the door perimeter and aft corner; the seal interfaces with the vehicle at a 15-degree stepped slope. Positive locking action is employed by a spring latching system that lifts the door against the seal interface, thereby effecting a compressing, wedging action.

ACTUATION AND SEALING OF LIFT ENGINE EXHAUST DOORS

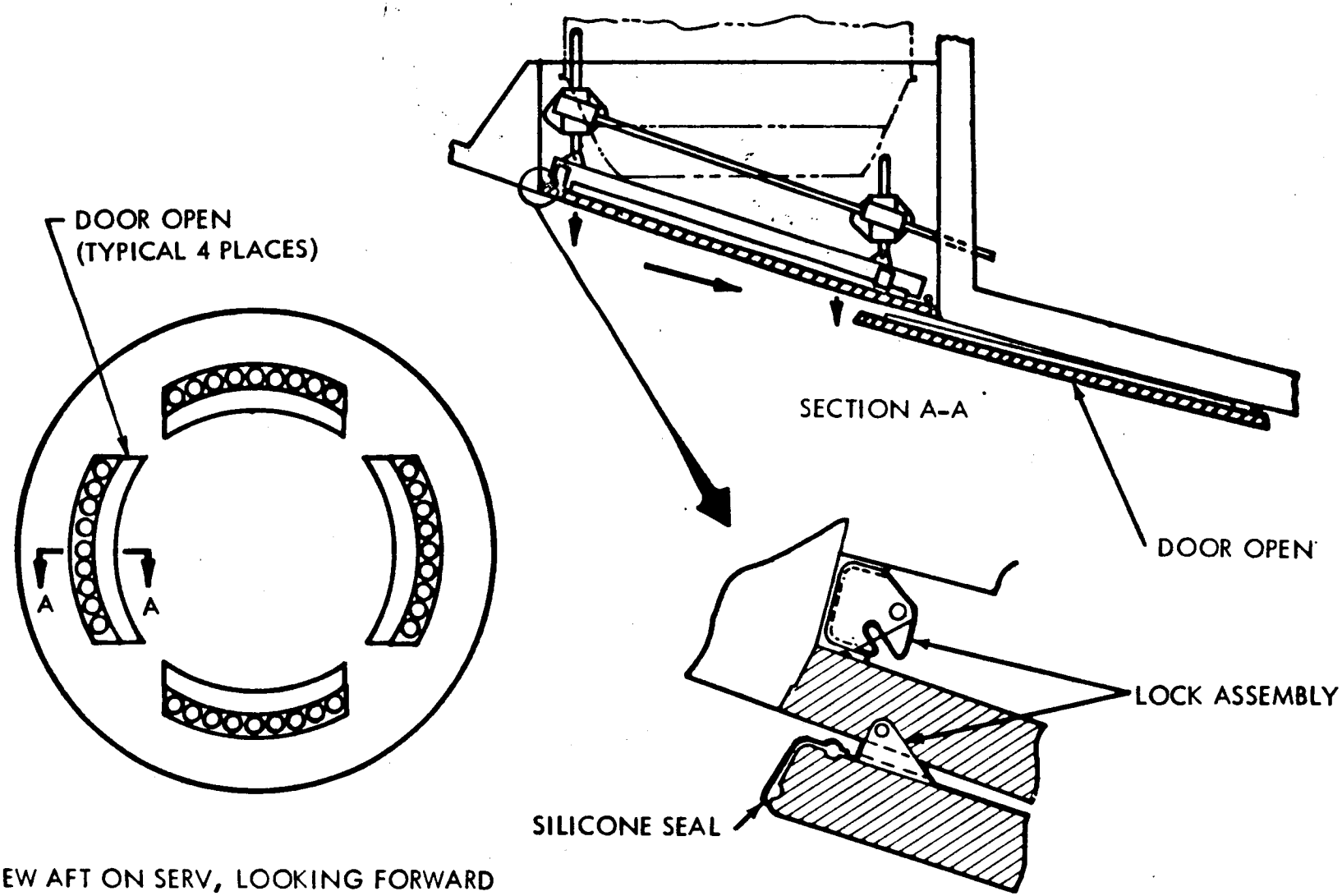

VIEW AFT ON SERV, LOOKING FORWARD

95

8.3.5 LANDING GEAR/DOOR SUBSYSTEM

The selected landing gear system is essentially a linear actuator arrangement enclosed in a cannister mounted in the LO_2/LH_2 common skirt. The system is actuated mechanically and effects opening of the base shield door and extension of the gear housing. An electric motor is used to supply power. After full housing extension, a hydraulic accumulator replenishes the shock absorber cylinder, causing it to extend to the active position and give full extension to the landing gear assembly. At touchdown, oil is bled back into the accumulator by means of the shock stroke. The gear is designed to accept a 2g decelleration, and a 12 ft/sec vertical velocity at a 2g degree attitude.

The gear assembly support is achieved by locating the main gear housing (cannister) within the SERV outer cylindrical bulkhead skirt. The skirt takes the vertical load and a percentage of moment. An attachment is also made to the side wall of the main gear housing by means of a structural tie to the base shield support beams. This provides the remaining resistance to gear moment at touchdown and support for the base shield beams during flight.

LANDING GEAR/DOOR SUBSYSTEM

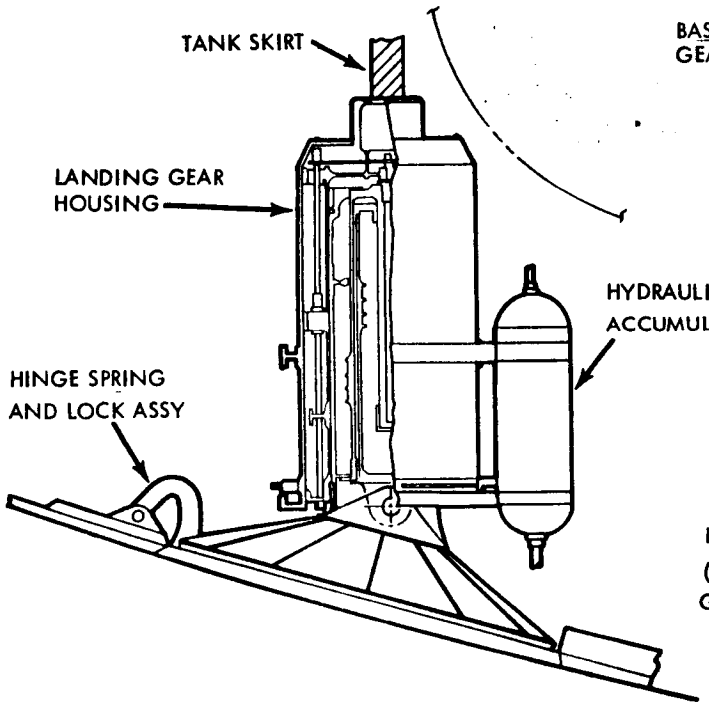

LANDING GEAR STOWED

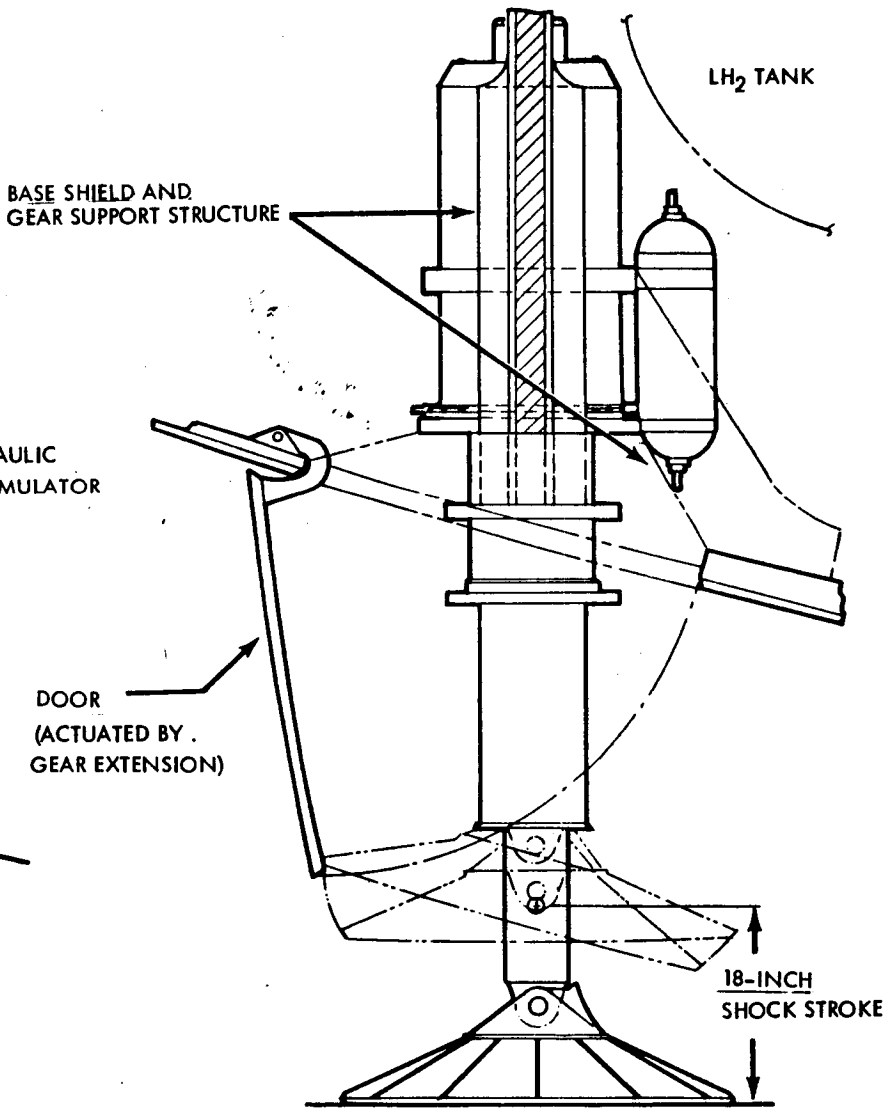

LANDING GEAR EXTENDED

96

SPACE DIVISION CHRYSLER CORPORATION

8.4 PROPULSION SUBSYSTEMS

Design and analysis of these subsystems were performed in sufficient detail to support the investigation of the key feasibility issue of weights. Six subsystems have been identified; the first four make up the ascent main propulsion subsystem group:

1) Twelve-module aerospike engine
2) Main propellant feed, fill and drain
3) Main propellant pressurization and vent
4) Main propellant recirculation and engine purge
5) Auxiliary propulsion
6) Landing main propulsion

8.4.1 ASCENT MAIN PROPULSION

The four ascent main propulsion subsystems are shown on this chart. The 12-module aerospike engine has several special features including interconnection of engine modules on the high pressure side of the turbopumps and a turbopump overspeed capability to provide for turbopump failures without deterioration in engine performance. In addition, the engine is capable of throttling to a minimum thrust level of 18 percent of nominal and differential throttling of ± 15 percent without exceeding minimum thrust level. (The SERV flight trajectory limits vehicle acceleration to 3g, which requires primary throttling of the aerospike engine to approximately 20 percent of nominal thrust.)

Propellant flow to the 12 modules from 24 sumps, 12 in each of the main tanks. Level sensors are provided in each tank at several locations to ensure a fuel-rich depletion cutoff. However, the depletion cutoff provision is a backup method because normal cutoff (fuel-rich) is commanded when orbital velocity is attained. Fluid residuals include propellants trapped in engine lines, main feed lines and recirculation subsystem lines, as well as liquid residuals and pressure gases in the main tanks.

Prevalves are located in each feed line to eliminate the possibility of draining either main propellant tank in the event of a feed line rupture and to allow for propellant shutoff in the event of a turbopump failure. A double-redundant recirculation system is installed on each main tank for propellant conditioning during launch operations. Propellant fill and drain is provided by means of four lines for each propellant. Double-redundant valving is provided to vent the fill lines during flight. The aerospike engine is provided with an inert gas purge prior to introducing liquid propellants. Purge gas is supplied from the same high-pressure helium supply used to fill a pressurant tank in the APS.

The pressure and pressurant requirements for the Task 4 baseline vehicle were used to size the pressurization subsystem, a constant gauge pressure system at 5 psig for LH_2 and 10 psig for LO_2. The autogenous concept was chosen for each propellant and utilizes heat exchangers in main engine turbine exhaust lines, a gaseous pressurant collector, redundant distribution lines and flow control valves located at the pressurant distribution locations at the top of each tank.

ASCENT MAIN PROPULSION

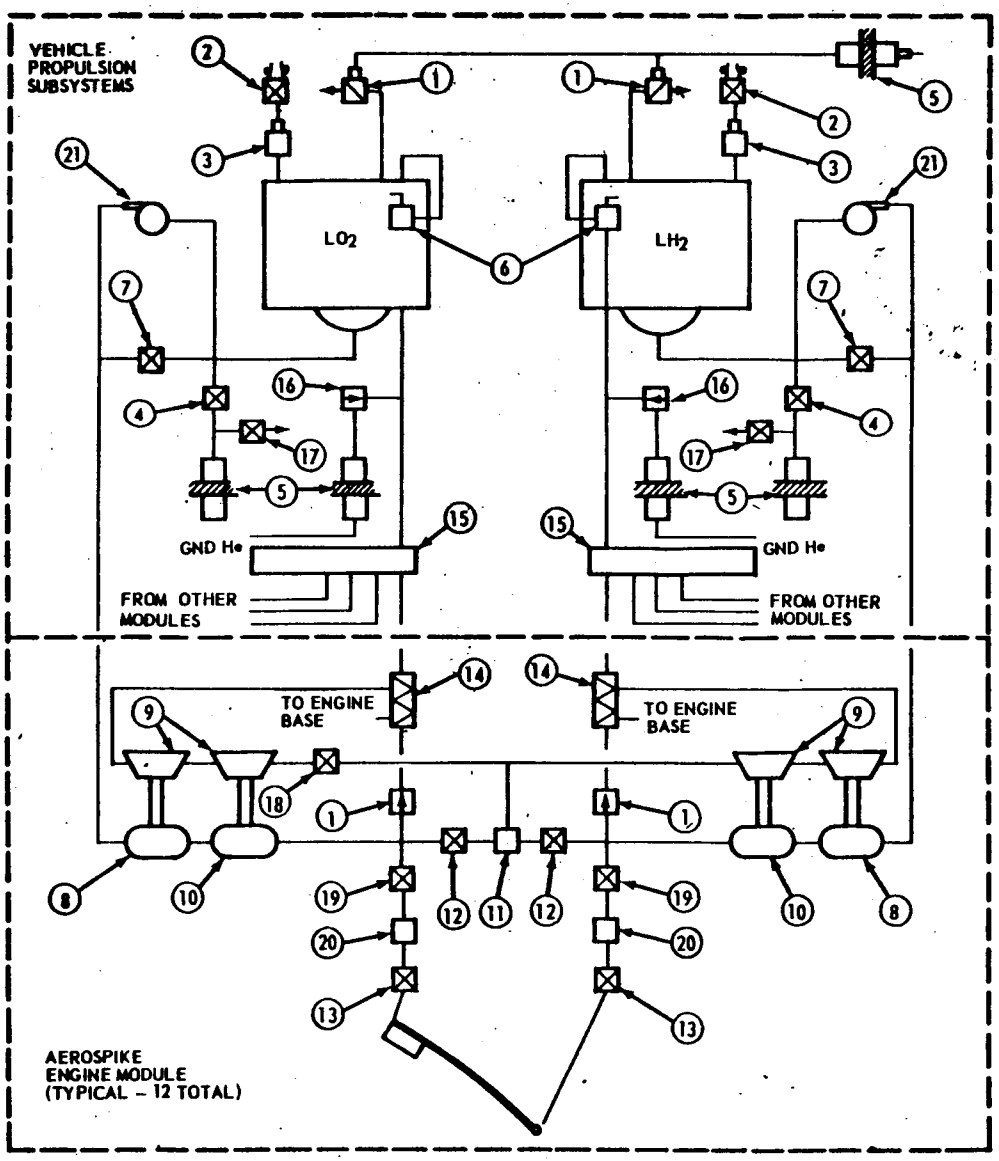

LEGEND

1 VENT VALVES (4)
2 CONTROL VALVES (4)
3 RELIEF VALVES (4)
4 FILL AND DRAIN VALVES (8)
5 QUICK DISCONNECT (12)
6 PRESSURANT FLOW CONTROL VALVES (4)
7 PRE-VALVES (24)
8 LOW PRESSURE PUMPS (12)
9 TURBINE DRIVES (12)
10 HIGH PRESSURE PUMPS (12)
11 GAS GENERATOR (12)
12 GG CONTROL VALVES (48)
13 MAIN VALVES (12)
14 HEAT EXCHANGER (24)
15 PRESSURANT COLLECTOR (2)
16 CHECK VALVES (26)
17 FILL AND DRAIN LINE VENT (8)
18 MIXTURE RATIO CONTROL VALVE (12)
19 PUMP OUT VALVE (12)
20 COMMON MANIFOLD (CONNECTING ALL MODULES)
21 RECIRCULATION PUMP (6)

8.4.2 AUXILIARY PROPULSION

The auxiliary propulsion subsystem serves multiple functions of ascent roll control, orbit circularization, on-orbit station keeping, orbit-to-orbit maneuvering, attitude control for orbit-to-orbit maneuvering, deorbit, reentry attitude control, main propellant tank repressurization during reentry, and propellant supply for fuel cells.

The subsystem is made up of four basic assemblies: propellant tankage, pressurization and acquisition; propellant conditioning; propellant distribution; and thrusters. All components except for tankage, distribution lines and thrusters are triply redundant since crew safety is dependent on its operation. Each component function will be operational after two failures of that component.

Performance and propellant requirements for the APS are based on a thruster I_s of 460 sec and an equivalent system I_s of 400 sec. APS propellant tankage is located on the interior of the SERV main propulsion tanks. A gaseous helium pressurant is incorporated for the oxidizer, while an autogenous hydrogen pressurant is employed. Hydrogen pressurant conditioning is accomplished by coiling tubes around the propellant conditioning gas generator to vaporize the cryogen. Approximately 2 percent of the hydrogen is required as pressurant.

Each APS propellant conditioning assembly consists of two sets of independent gas generators, one feeding a turbopump and the other providing hot gases for input to a heat exchanger for vaporizing and heating the cryogenically stored propellant. The turbine outlet gases are also used as secondary inputs to the heat exchanger. Oxidizer and fuel conditioners operate independently on a demand basis when the propellant accumulator pressure drops below a specified minimum value. Propellant distribution is accomplished via high pressure accumulators and ring line distributors.

APS thrusters are located in four modules of five nozzles at equidistant points around the maximum vehicle diameter. Two thrusters in each module are pointed forward, parallel to the vehicle longitudinal axis, one is pointed downward and the remaining two oppose each other in a tangential direction for roll control. Redundant operation is supplied for all axis maneuvers in pitch, yaw or roll. The eight forward-facing thrusters (two in each module) are used to provide the impulse necessary for orbital maneuvers and SERV deorbit.

A connecting link with redundant valving is supplied between the APS gaseous hydrogen accumulator and the main tank gaseous hydrogen pressurant collector. During reentry, the APS hydrogen conditioner is utilized to provide pressurant for repressurization of the main hydrogen tank.

Additional connecting links join the APS gaseous propellant accumulators and vehicle fuel cell units with redundant regulators and valving. Fuel cell propellant supplies are stored in the APS tanks.

AUXILIARY PROPULSION

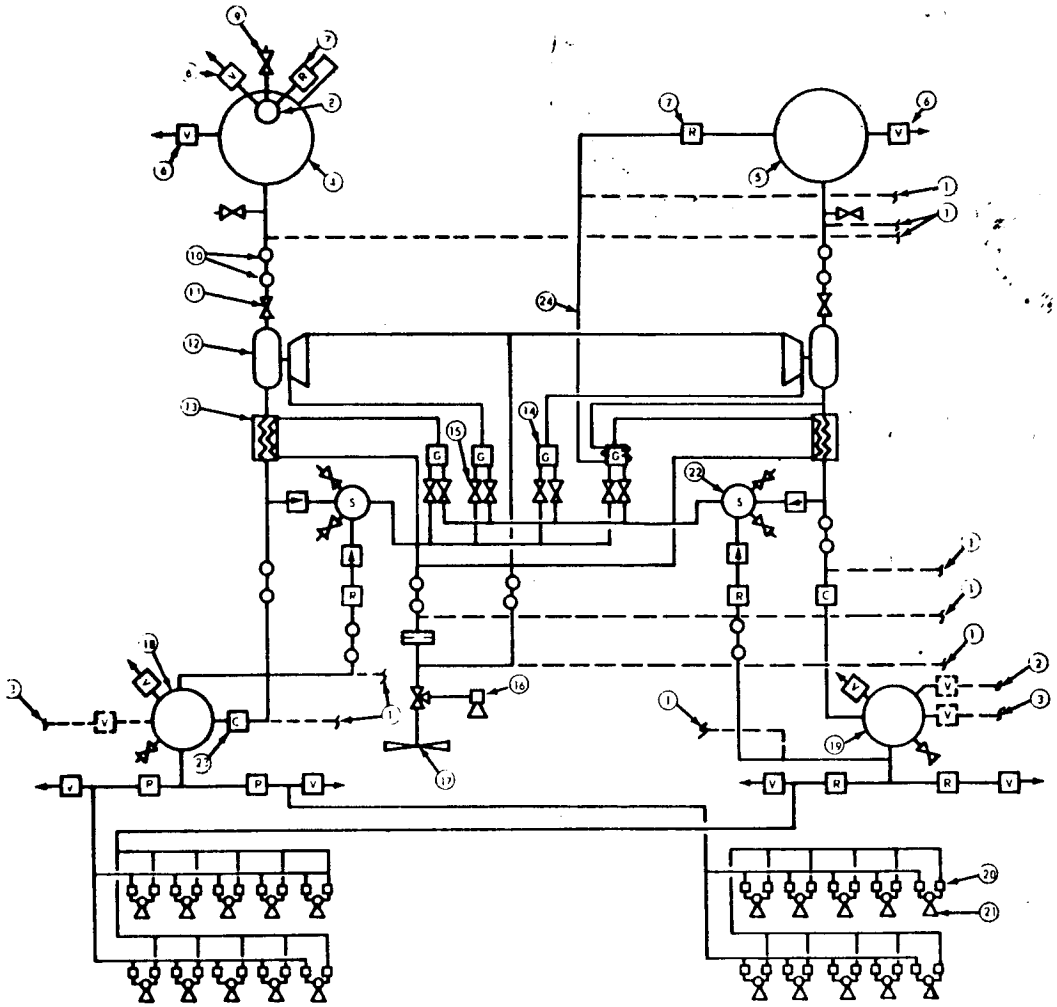

1. CONNECTIONS TO TWO ADDITIONAL IDENTICAL PROPELLANT CONDITIONING UNITS, ONE DOUBLY ISOLATED, ONE SINGLY ISOLATED
2. CONNECTION TO GH_2 PRESSURANT COLLECTOR
3. FUEL CELL PROPELLANT SUPPLY CONNECTIONS
4. LO_2 STORAGE
5. LH_2 STORAGE
6. VALVE ASSEMBLY (TYP)
7. REGULATOR ASSEMBLY (TYP)
8. HELIUM PRESSURANT STORAGE
9. RELIEF VALVE (TYP)
10. ISOLATION VALVES (TYP)
11. SHUTOFF VALVE FOR CONDITIONING UNIT (TYP)
12. TURBOPUMP ASSEMBLY (TYP)
13. HEAT EXCHANGER (TYP)
14. GAS GENERATOR (TYP)
15. GAS GENERATOR CONTROL VALVE (TYP)
16. NON-BURNING PROPULSIVE VENT
17. NON-PROPULSIVE VENT
18. GASEOUS OXYGEN ACCUMULATOR
19. GASEOUS HYDROGEN ACCUMULATOR
20. THRUSTOR CONTROL VALVE, FILTER AND ISOLATION ASSY (TYP)
21. THRUSTOR (TYP)
22. CONDITIONING UNIT START ACCUMULATOR (TYP)
23. CHECK VALVE ASSEMBLY (TYP)
24. HYDROGEN PRESSURIZATION LOOP

98

SPACE DIVISION CHRYSLER CORPORATION

8.4.3 LANDING MAIN PROPULSION

This subsystem is made up of turbojet lift engines and associated tankage, feed lines, and start and control equipment.

The turbojet lift engines identified for SERV are based on development work done by the Detroit Diesel Allison Division of General Motors Corporation in collaboration with Rolls-Royce. An engine with a thrust of 10,000 to 25,000 lb and a thrust-to-weight factor in the range of 17 to 20 is within present technology capabilities.

Jet engine thrust requirements are based on worst operating conditions for translation by differential throttling through maximum opposing winds with one engine out and maximum aerodynamic forces. This worst condition combination sets a required thrust equal to 115.6 percent of SERV weight, occur during a portion of the flight when approximately 80 percent of the loaded jet fuel is still on board the vehicle. A thrust efficiency factor of 80 percent is also applied to account for inlet pressure loss and air temperature effects.

Jet fuel and tankage requirements are based on flight simulation for the worst operation conditions as defined in the foregoing paragraph; an all-nominal flight would leave a jet fuel residual of approximately 12, 000 lb. Fuel tankage is arranged so that all of the fuel is on one side of the vehicle at the beginning of reentry, thereby supplying an additional cg offset. The fuel can be moved to the opposite side prior to the landing phase to minimize thrust unbalance requirements. Fuel transfer is provided via 6-inch lines with a tank pressure driving force.

The fuel transfer lines serve as fuel distribution lines during engine operation, with feeder lines to each engine that are flow controlled by electro-pneumatic devices.

LANDING MAIN PROPULSION

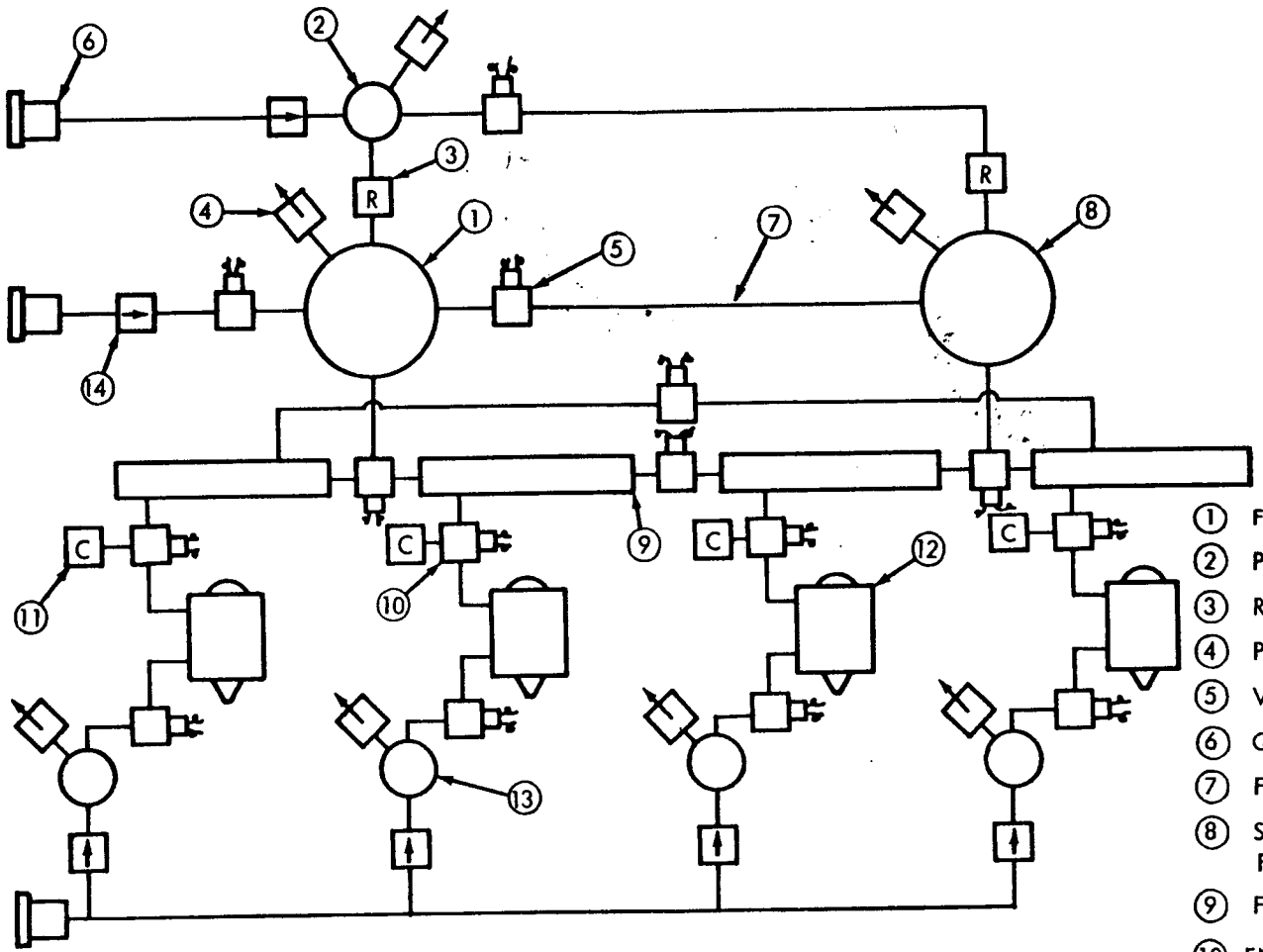

1. FUEL TANK
2. PRESSURANT TANK
3. REGULATOR ASSEMBLY
4. PRESSURE RELIEF VALVE
5. VALVE ASSEMBLY
6. QUICK DISCONNECT
7. FUEL TRANSFER LINE
8. SECONDARY TANKAGE FOR FUEL (FOR CG OFFSET SHIFT)
9. FUEL DISTRIBUTION MANIFOLD
10. ENGINE THROTTLE VALVE
11. THROTTLE CONTROLLER ASSEMBLY
12. TURBOJET LIFT ENGINE
13. STARTER ASSEMBLY
14. CHECK VALVE

99

SPACE DIVISION CHRYSLER CORPORATION

8.5 AVIONIC AND POWER SUBSYSTEMS

The SERV integrated avionics subsystem (IAS) includes all vehicle subsystem operations as an integrated scheme with an on-board digital computer as the focal point of operation. Most of the components considered for the system are either a direct fallout of the Saturn/Apollo program or are available "off-the-shelf". No major development is required to design components not currently available since current technology is sufficient. Error analyses have shown that the selected components for IAS are capable of meeting the imposed SERV performance accuracy requirements for flight and terminal landing.

A gimballed platform has been selected because of the large amount of experience with such platforms. Sun sensors, star trackers and horizon seekers will be used to provide attitude reference while the SERV is in orbit.

The IAS was subdivided into the following functional elements:

- Guidance and Navigation
- Vehicle Flight Control
- Data Management
- Communications
- Power Generation and Control

The functional relationship of these elements is shown on the chart.

The data management (DM) subsystem includes a digital computer, signal interface units, a data distribution network and a digital recorder.

The data analysis unit (DAU) scheme of interfacing can be considered a form of data compression since each of the estimated 60 DAU's will monitor an assigned group of transducers for limit comparison. Normally the only data transmitted from the DAU to the DM Computer would be an out-of-tolerance condition of a flight critical measurement.

An operational communications subsystem will provide SERV with tracking capability for rendezvous and landing, command link for transmission and navigation updates, vehicle status data transmission for remote display, and remote link for vehicle subsystem control.

The RF links required can be implemented using existing aerospace qualified RF communications equipment.

FUNCTIONAL DIAGRAM OF AVIONIC AND POWER SUBSYSTEMS

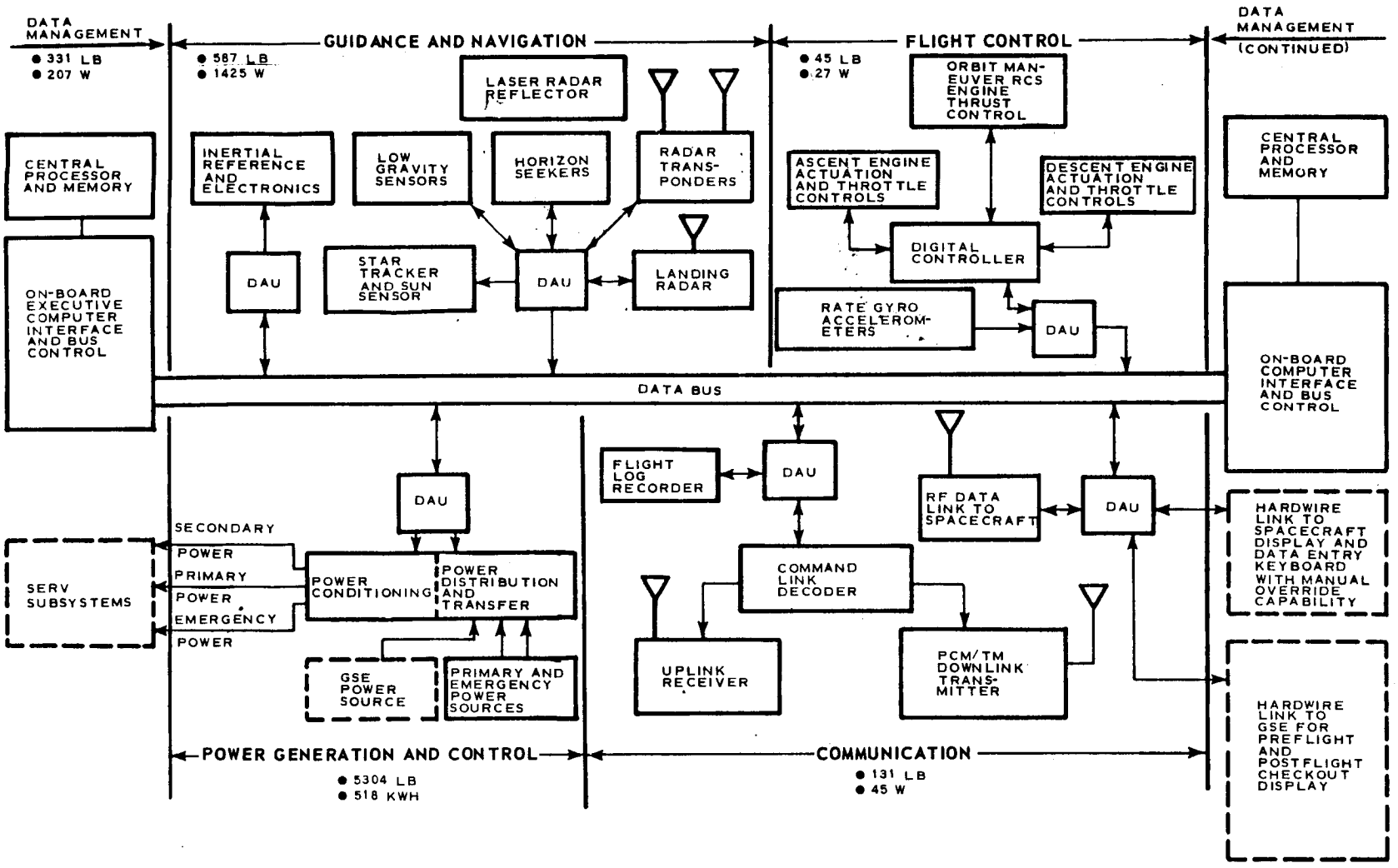

SPACE DIVISION CHRYSLER CORPORATION

8.5.1 FUNCTIONAL DIAGRAM OF POWER SUBSYSTEM

The power subsystem block diagram shows the overall concept. This subsystem supplies: 1) power from the auxiliary source for heavy, short-duration loads; 2) power from the normal source for continuous or intermittent, moderate loads; and 3) power from the emergency source for peak normal or emergency loads.

The primary and secondary power distribution networks includes overload protection devices, buses, bus switching devices, load switching devices, bus transfer devices, and cables.

The power conditioning components include inverters, dc-to-dc converters, regulators, etc., necessary to provide the proper voltages and frequencies to the various loads.

The control processing and distribution network distributes control signals to the various devices of the power distribution network. The network accepts digital multiplexed signals from the internal control logic and the external on-board computer, and provides appropriate signals to power-handling components.

Provisions will be included for connection of a ground power source capable of supplying all power necessary for preflight operations on the ground. While in orbit, the SERV power subsystem is self-supporting and power from external sources is not required.

The weights of power subsystem components are shown in the chart. The power subsystem weight includes plumbing, charge and control units, installation hardware and allowance for structural supports.

FUNCTIONAL DIAGRAM OF POWER SUBSYSTEM

- TOTAL DRY WEIGHT - 5304 LB
- TOTAL ENERGY - 518 KWH

SOURCE \ RATING	S-S (KW)	PEAK (KW)
NORMAL-DC	20	40
AUXILIARY-AC	134	600
EMERGENCY-DC	3	6
TOTAL	157	646

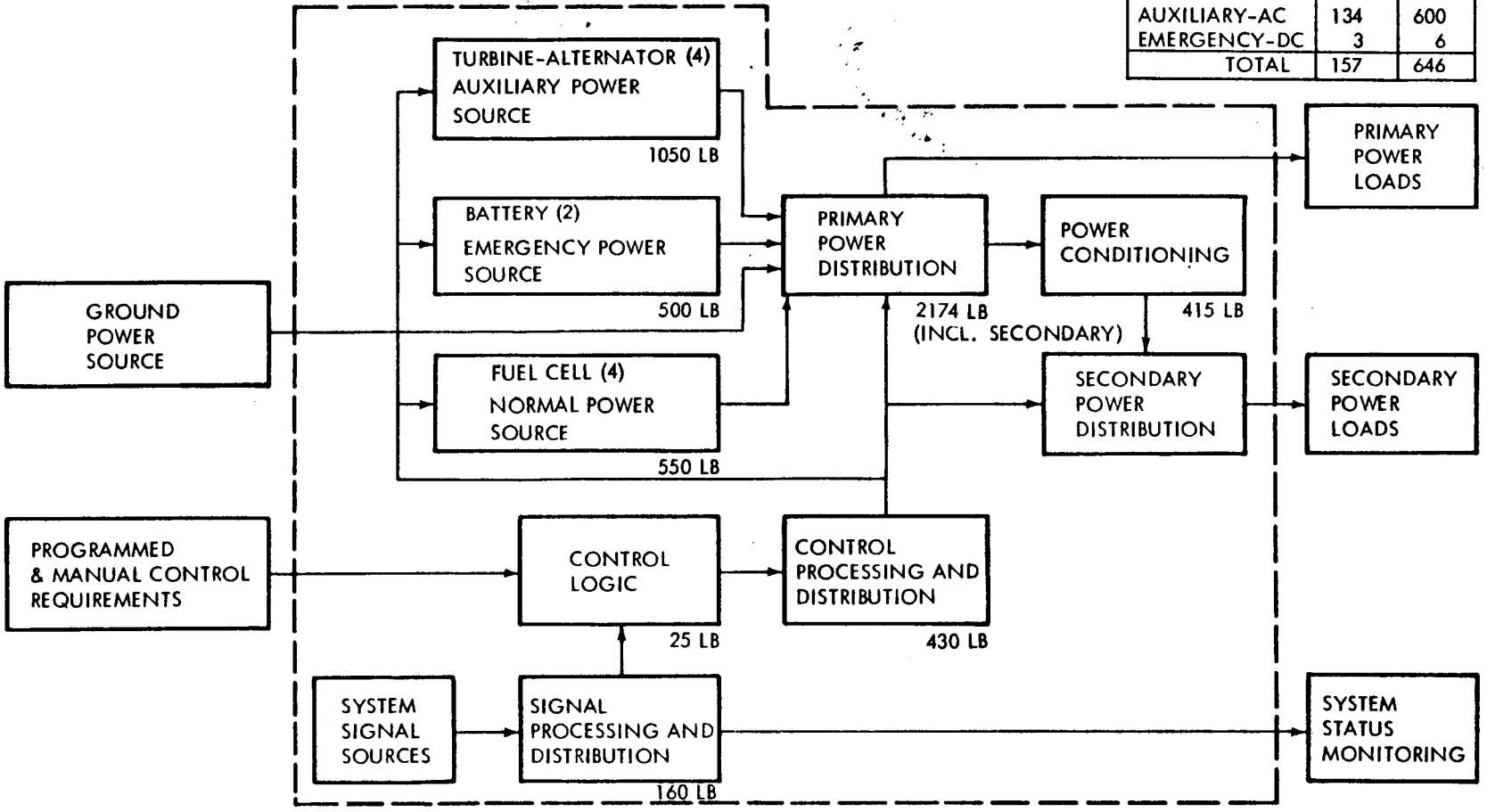

8.5.2 NAVIGATION ERROR ELLIPSES

This chart shows the error ellipses in the downrange and crossrange plane for two different times of IMU update. The worse case (1200 sec before deorbit) shows a downrange error of 1.88 nm and a crossrange error of 2.45 nm. The chart shows that if update can be delayed to 240 sec prior to deorbit, errors can be reduced to approximately one-half.

Further improvement can be made by reducing the IMU navigational error, which was a major contributor to the total error. One of the two large sources of IMU error is that caused by the accelerometer bias. By delaying the processing of accelerometer data until just prior to deorbit (with the exception of the time during reentry) the IMU error can be significantly reduced. Similar improvements could be made if PIGA type accelerometers were to be used, since this type causes bias errors which are an order of magnitude smaller than those specified for the Honeywell platform. The chart shows a comparison of the error ellipses and indicates that in both the downrange and crossrange, IMU errors can be reduced by almost 0.5 nm.

NAVIGATION HARDWARE ERROR ELLIPSES VS "TIME OF IMU UPDATE"

(3-SIGMA RANGE ERRORS AT 25,000 FOOT ALTITUDE)

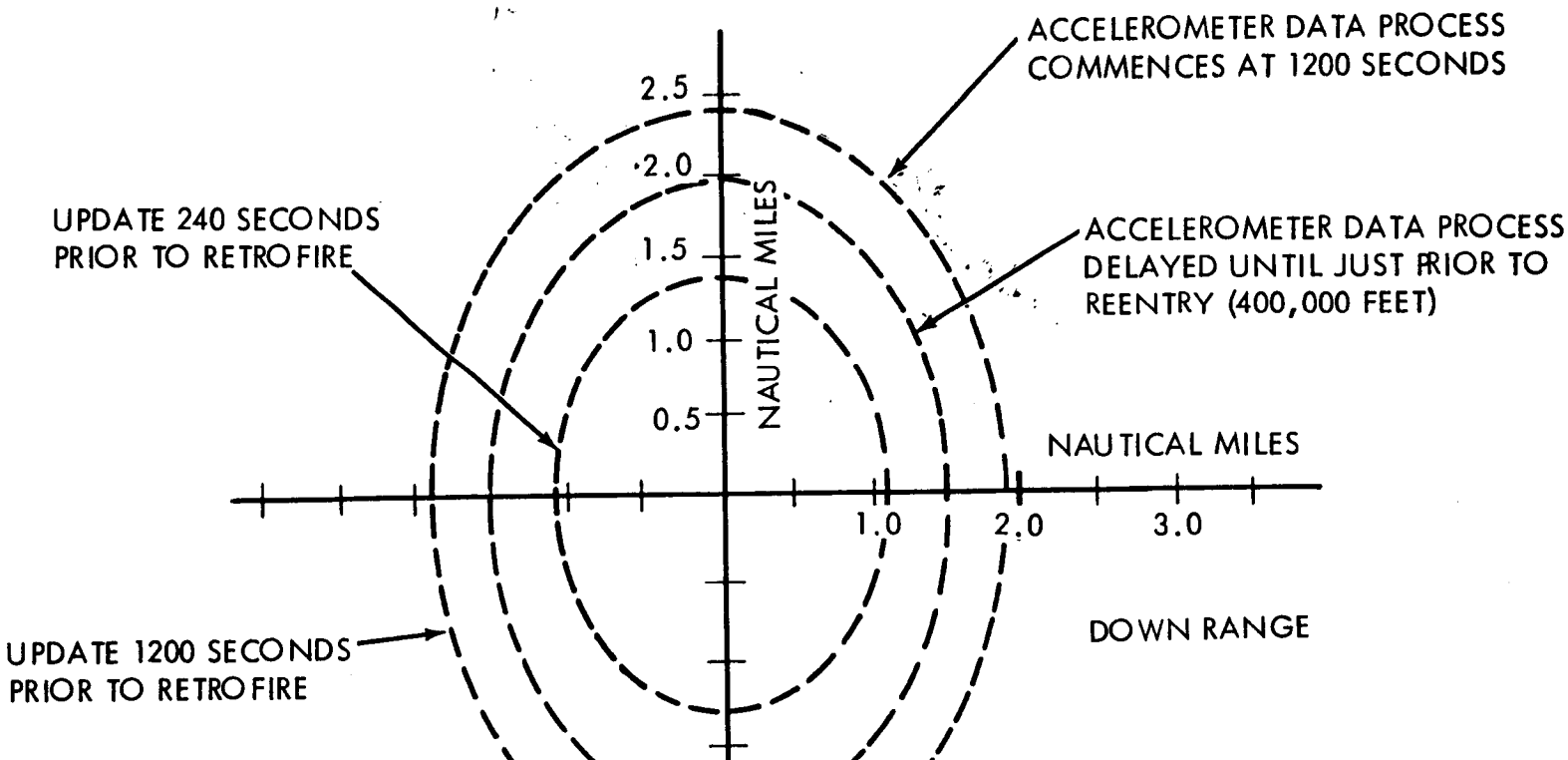

8.5.3 SERV REENTRY ERROR SUMMARY

The chart presents a summary of an error analysis of the SERV guidance and navigation (G&N) system based on the standard 110 nm reference orbit.

The major sources of landing error that cannot be nulled by maneuvering can be attributed to:

- **Inertial measurement navigational errors due to the IMU hardware tolerances. This source is a major contributor to navigation error.**
- **Initial state vector errors (position and velocity) of SERV orbit at the time of last update. The magnitude of these errors considered the Manned Space Flight Network (MSFN) for ground updating.**
- **Guidance or steering laws used.**
- **Bias-type navigation errors resulting from the numerical integration techniques used in the computer navigation logic.**

Each of these error sources are listed on the chart in column 1. An alternate method exists for determining the initial state vectors for the orbit parameters in orbit navigation.

Based on current state-of-the-art accuracy of vertical reference sensors, such as horizon seekers, the navigational error to 25,000 ft will exceed the 4 nm landing maneuver capability. As a result, a supplement is required for this navigational scheme. Orbit state vectors are measured by onboard equipment of SERV and used by the IMU to navigate from deorbit to the reentry interface. When SERV appears near the horizon from the landing site, a ground radar tracks it to establish position. Upon coming out of communications blackout, a radar uplink relays position information to SERV that is designed to reduce the existing navigational errors to within the required $\pm$ 4 nm by the time the landing phase commences (25,000 ft altitude).

If a method for on-orbit navigation is used whose system errors are less than the SERV maneuver capability the SERV can come within 3σ values of 1.71 nm downrange and 1.53 nm crossrange. The table is a summary of all the error sources.

Column 2 presents an estimated increase in landing accuracy if an update of state variables is made using ground tracking located at the landing pad. The update would be made after SERV emerges from the communications blackout region.

SERV REENTRY ERROR SUMMARY

(3 σ RANGE ERROR AT 25,000-FOOT ALTITUDE)

ERROR SOURCE	RANGE ERRORS (N MI) FOR IMU UPDATE			
	(1) PRIOR TO DEORBIT		(2) AT 168,000-FOOT ALTITUDE	
	DOWNRANGE	CROSSRANGE	DOWNRANGE	CROSSRANGE
TRACKING RADAR	0.26	0.86	0.01	0.01
NAVIGATION IMU	1.88	2.47	0.12	0.12
GUIDANCE/STEERING (EST.)	1.50	1.50	1.50	1.50
(a) RSS TOTALS	2.42	3.02	1.51	1.51
(b) NAVIGATION COMPUTATION	0.20	0.02	0.20	0.02
ARITHMETIC SUM OF (a) AND (b)	2.62	3.04	1.71	1.53

8.5.4 DATA ANALYSIS UNIT

A data management technique to reduce data handling in the SERV computers was identified in this study as the Data Analysis Unit (DAU). The DAU is capable of:

1) Asynchonously monitoring all test points assigned to it in a repeating cycle at the DAU clock rate.

2) Making boundary limit comparisons on each measured test point. These comparisons will include high and low limits as well as the action response time within which a measurement should complete its action when stimulated; e.g., thrust buildup of an engine or speed variations of a turbine alternator.

3) Issuance, to the on-board computer, of failure flags when boundary limits are exceeded. These flags would be of varying priority levels to allow for flagging, on a priority basis, of selected measurements related to potential vehicle failure.

The technique of reporting black box failures by exception to the main computer can be considered as a form of data compression.

The DAU memory is addressable from a keyboard or from the on-board computer. Changes to the measurement boundary limits can be made to reflect changes in vehicle mission assignment or in vehicle operational status. Thus, checkout evaluation criteria can be entered into the DAU memory to be compatible with their respective operational phases.

DATA ANALYSIS UNIT

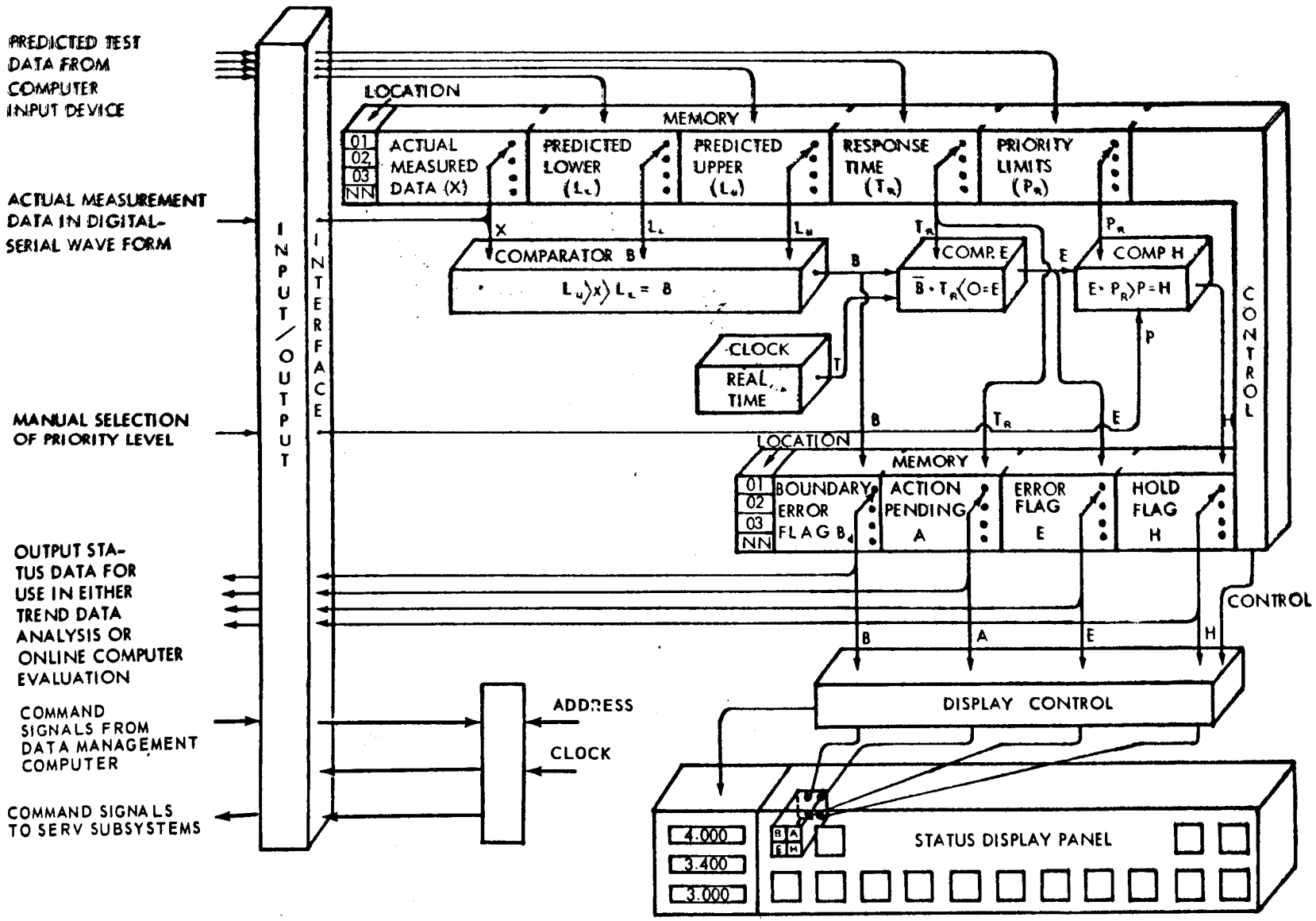

SPACE DIVISION CHRYSLER CORPORATION

OPERATIONS AND FACILITIES

Section 9
OPERATIONS AND FACILITIES

9.0 GENERAL

Major manufacturing operations, manufacturing facilities, transportation and launch operations are discussed in this section.

9.1 MANUFACTURING

9.1.1 MANUFACTURING SEQUENCE

The structural fabrication, assembly, checkout and preparation for shipment will be performed at MAF in buildings 103, 110 (VAB), and 420, stations 1 through 4. Fabrication of structural components and subassemblies such as rings, support beams, inner cylindrical bulkhead, landing gear assembly, doors, reentry bulkhead panels and cargo containers, will be conducted in building 103. Building 110 is used to develop the outer cylindrical bulkhead and the lower and upper outer shell structure. The inner and outer cylindrical bulkheads and the lower and upper outer conical shell subassemblies are fabricated of steel honeycomb panels welded together on a building block approach as a complete circular subassembly. The LO_2 and LH_2 lower bulkheads will be developed as circular segments prior to mainstream assembly. In addition to circular external work platforms, internal suspended work platforms and tooling are required as illustrated in operations 600, 800, 1000 and 1400 on the chart.

All subassemblies in building 103 and 110 are transferred to building 420, station 1 for final assembly as depicted opposite in the mainstream flow sequence. The vehicle is then moved to station 2 for pressure test and cleaning. The LH_2 tank is filled with sealed styrofoam balls and gas pressure tested in conjunction with the LO_2 tank, which is filled with demineralized water to simulate propellant weight and reduce gaseous volume. The vehicle is returned to station 1 for installation of the lower and upper thermal protection shells over the existing structural shell. The vehicle is transferred to station 3 for the installation of electromechanical-hydraulic and avionic and propulsion systems, and final assembly activities. At the completion of these activities the vehicle is moved to station 4 for checkout, weight, CG and optical alignment operations prior to preparation for shipment activities. Total time period for typical manufacture of a vehicle is 93 weeks.

MANUFACTURING SEQUENCE

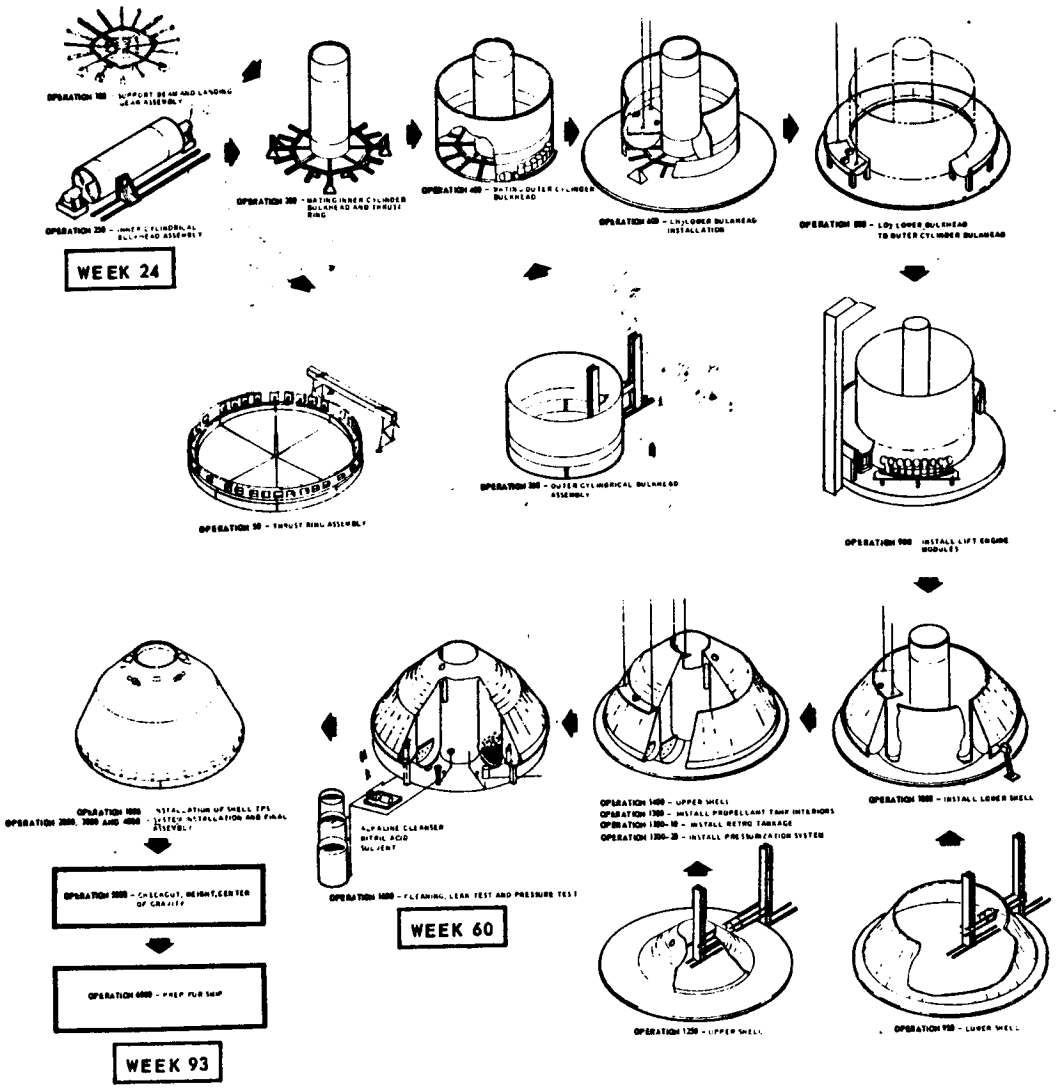

9.1.2 SERV MANUFACTURING SITE PLAN

The major external facility modification at MAF is minimal and limited to enlarging the existing 4-cell building 420 both vertically and horizontally for final assembly, test and checkout. Other external modifications include: widening Saturn Blvd from building 420 to the Michoud Slip; widening of the route between buildings 103, 110 (VAB) and 420; and widening one dock at the Michoud Slip. Modifications to all other buildings involve internal rearrangement only.

Delivery of subcontractor/vendor items can be performed by road, water, or spur rail directly to MAF. The proximity to each other of engineering, manufacture, test and ship loading facilities is notable.

SERV MANUFACTURING SITE PLAN
(MSFC-MAF)

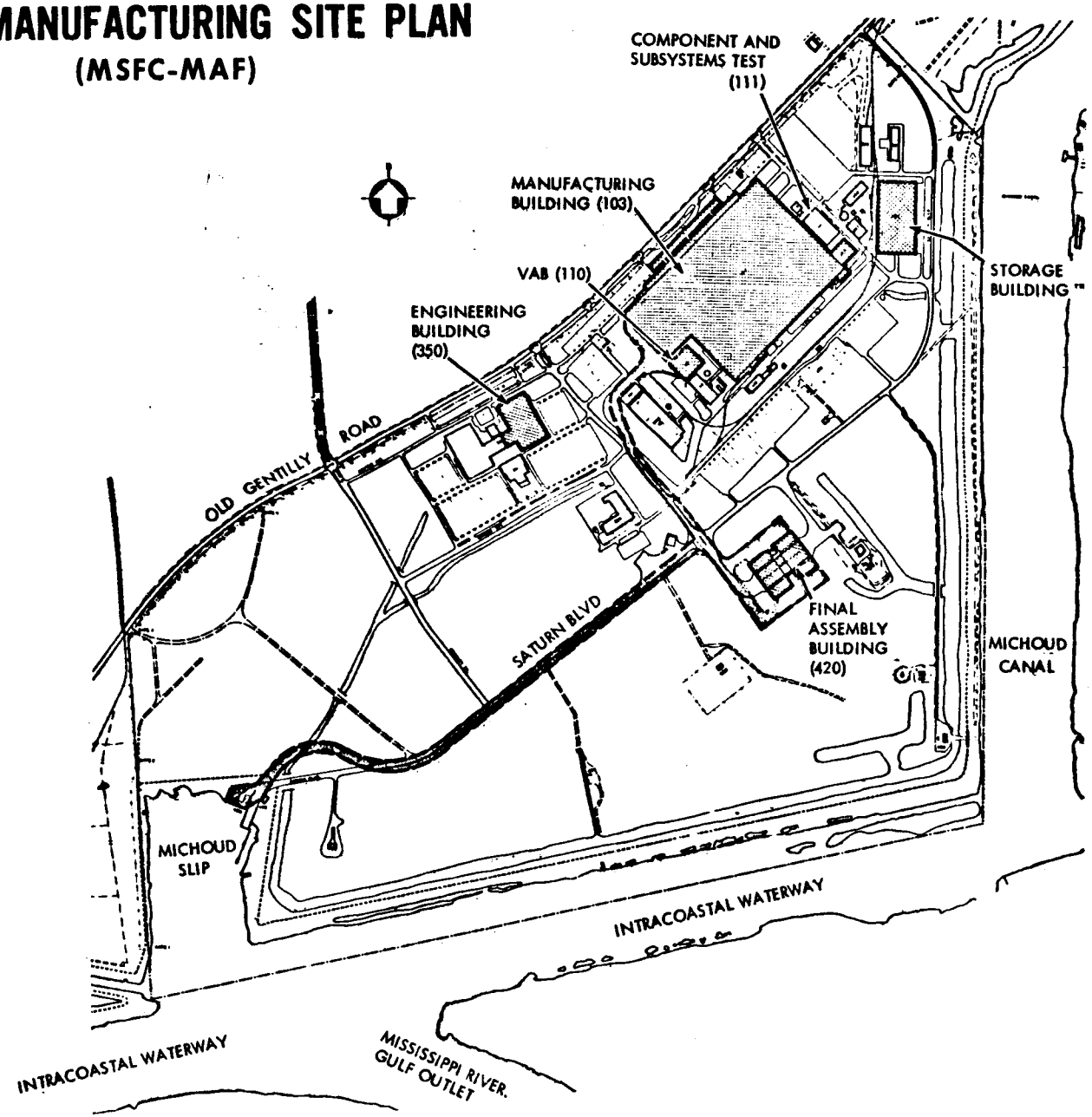

SPACE DIVISION CHRYSLER CORPORATION

9.1.3 FABRICATION AND SUBASSEMBLY OPERATIONS

In addition to the adjacent supporting administration and engineering buildings (101 and 102), the layout chart shows the 1.8 million sq ft building 103 and the adjacent 200-ft high VAB (110). The proximity to each other of all manufacturing direct and supporting operations is very advantageous. In addition to areas for component fabrication and subassembly of vehicle structures, the layout identifies the location of electro-mechanical-hydraulic system components and subassemblies as well as vehicle propulsion and avionic assembly areas.

In addition to normal plant internal rearrangement, the major facility item is the installation of three 90-foot rotary tables in the major subassembly area of building 103, and a single 60-foot rotary table in building 110. No modifications are required to the structure of either building 103 or 110.

It is planned that the more specialized equipment, such as propulsion and avionics, will be received at MAF at the subsystem level of assembly and ready for continued buildup or for final assembly. Flight hardware supporting operations, included in building 103, include various inspection, control, test, checkout, cleaning, machine shops, heat treat, metrology, mock-up and education and training facilities.

FABRICATION AND SUBASSEMBLY OPERATIONS

BUILDING 103 AND 110 (VAB)

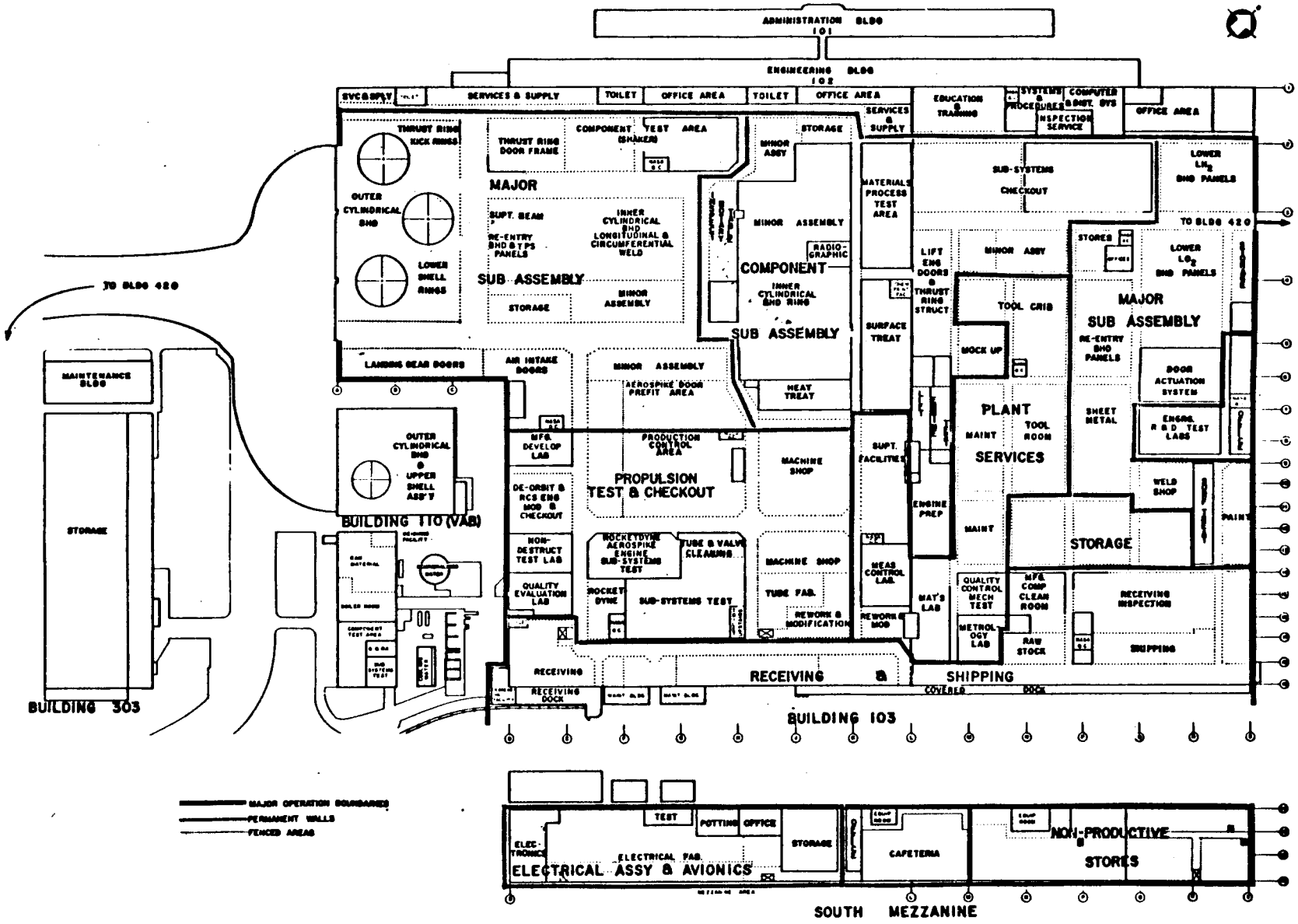

SPACE DIVISION CHRYSLER CORPORATION

9.1.4 FINAL ASSEMBLY AND TEST

Building 420, consisting of four cells, was used for pressure testing the S-IC stage and has corregated steel sheet "blowout" exterior walls with thick concrete inner walls separating the cells. Maintaining the present concrete walls, the plan is to increase the present dimensions of building 420 from 166 ft by 465 ft to 465 ft by 540 ft. The expansion will provide two stations (1A and 1B) for vehicle assembly; pressure test and cleaning in station 2; systems installation in station 3 and checkout, weight, center of gravity and preparation for shipment in station 4. The major internal modification is the installation of 90-ft diameter rotary tables and a telescoping weld fixture-gantry cranes at station 1A and 1B.

The clear truss height in the building must be increased from the current 50 ft to 130 ft over stations 1; however, stations 2, 3 and 4 only require a clear truss height of 90 ft. Localized pavement is required for movement of the SERV on its transporter between stations during final assembly.

FINAL ASSEMBLY AND TEST - BUILDING 420

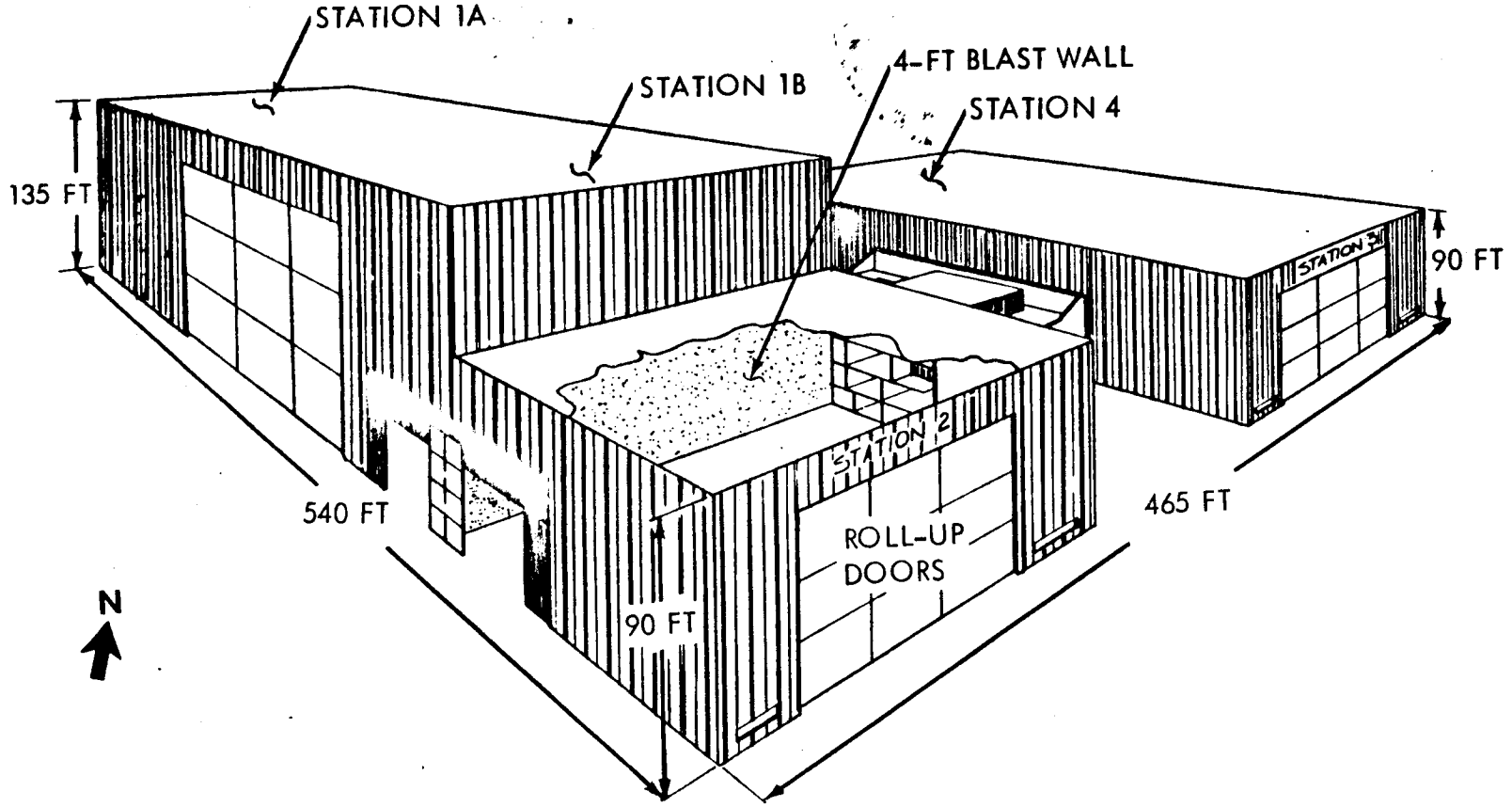

109

SPACE DIVISION CHRYSLER CORPORATION

9-9

9.2 TRANSPORTATION

The chart shows the SERV being transported on the Bay-class vessel owned by the West India Shipping Company. The vessel is 266 feet long with a 51 foot beam and can be ballasted to draw 6-12 feet of water. The pin-on type sponsons would increase the vehicle width to 89 feet. Therefore the vessel can negotiate the locks and bascule bridges between the MAF and KSC-VAB dock with no route modifications or off-loading of cargo. The pin-on sponsons are presently under consideration for other applications by the West India Shipping Company. The vessel deck can presently accept the point loading from the landing gear. However, if the SERV diameter is in excess of 88 feet, the SERV will be supported by a transportation ring (similar to the launch ring) which can pivot vehicles up to 96 feet diameter through 22° to produce an effective width of 89 feet in order to negotiate the bascule bridge and locks at KSC.

This method of transportation is estimated to cost substantially less than the modifcation and upkeep of existing barges.

BAY CLASS VESSEL TRANSPORTER

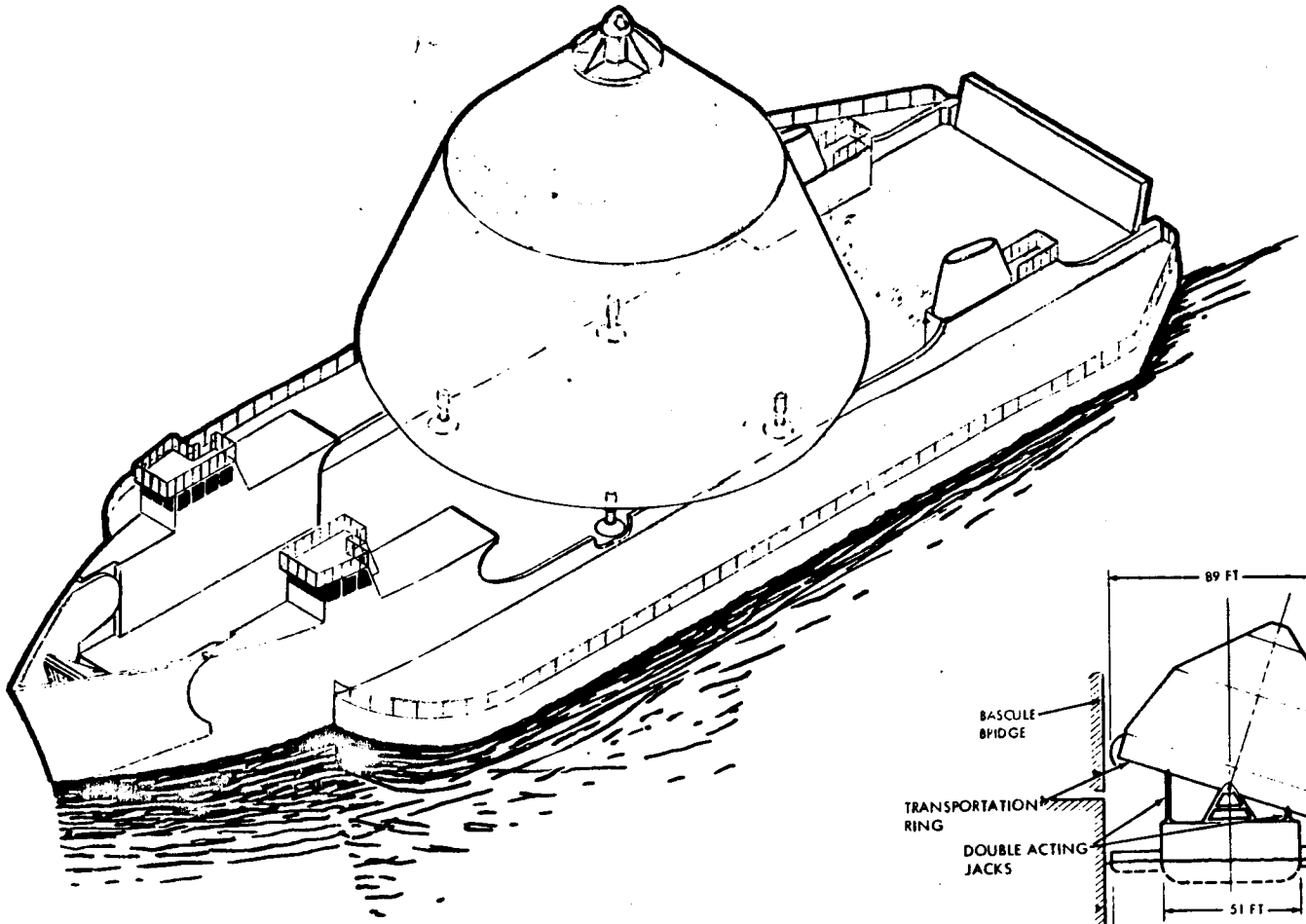

9.3 KSC OPERATIONS

The baseline ground operations approach involves the area between the VAB and launch pads A and B at LC-39. SERV vehicles up to 96-ft diameter can be delivered from MAF through the Port Canaveral 90-ft-wide locks and bascule bridges via the Banana River to the VAB dock. SERV vehicles between 88 and 96 ft in diameter can be transported by tilting the SERV as deck cargo on the Bay-class vessel to reduce the effective width. This water route will also be used for the delivery of the Personnel Modules and Cargo Modules, the latter using modified S-IB stage transporters for overland movement to and from existing barges. The baseline ground operations approach identifies twin 500-1000 ft diameter landing pads for the SERV adjacent to the crawlerway and 1.75 miles from the VAB and LC-39. The 4-mile radius circle identifies the target area at 25,000 ft altitude and centered on the landing pads. The winged MURP spacecraft will land at the existing 10,000-foot landing strip. Transportation of the relatively small MURP spacecraft from the landing strip back to the VAB poses no problems as this vehicle can be tractor towed on existing highways at off-peak congestion hours. The use of the existing VAB for cargo and vehicle assembly, dispersal, storage, servicing and refurbishment provides proximity to road, rail, sea and air methods of transportation from all parts of the nation.

KSC OPERATIONS

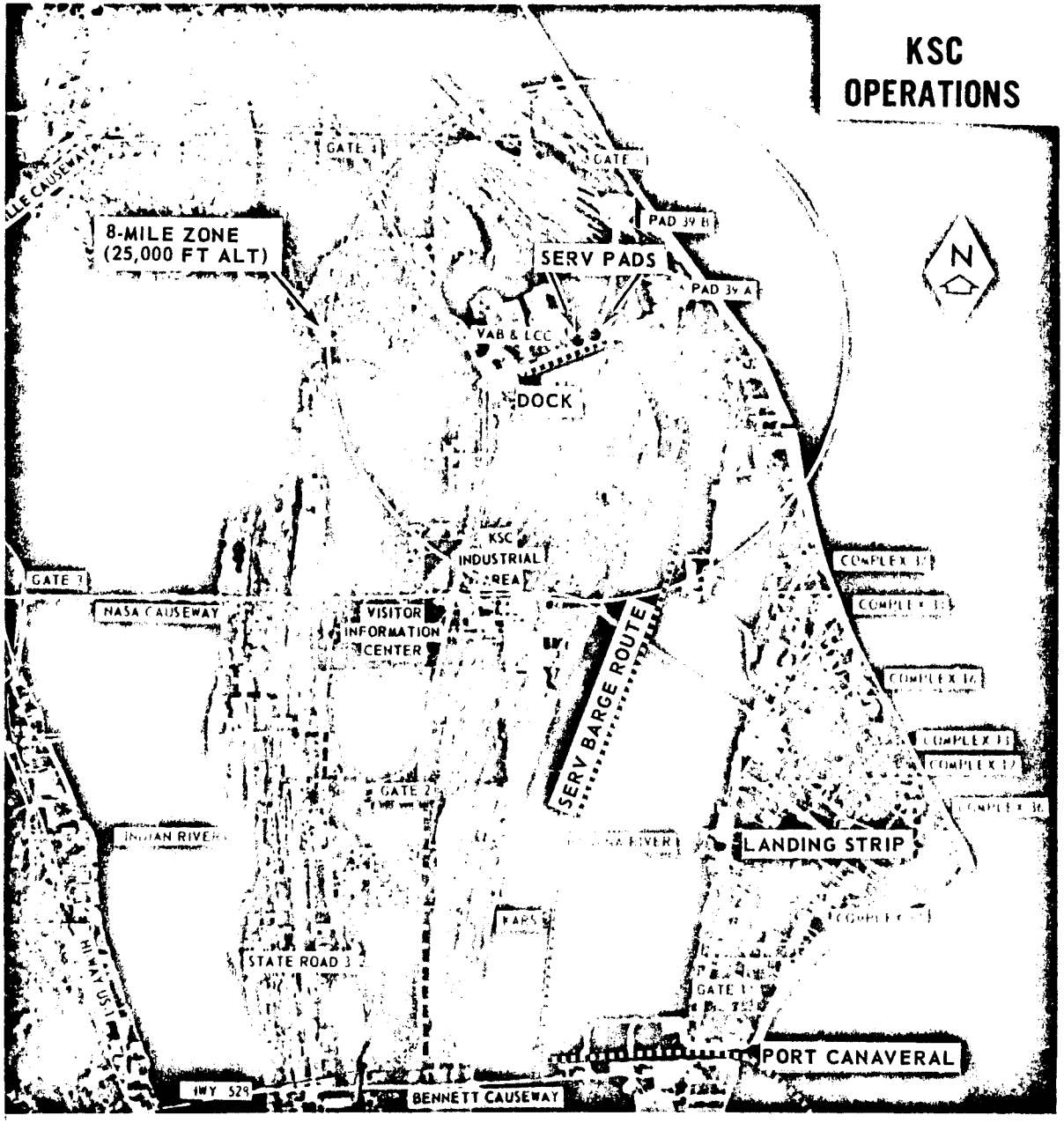

111

SPACE DIVISION CHRYSLER CORPORATION

9.3.1 SERV-SPACECRAFT GROUND OPERATIONS

The flow chart identifies the major facilities and operations involved in the selected operational approach, with special emphasis on the turnaround cycle. Delivery of the test and operational SERV vehicles from MAF to KSC is by a Bay-class vessel. A 200-ton capacity barge crane is used to off-load the SERV onto the operational wheel type transporter, which is then tractor drawn to the VAB.

Following SERV landing in proximity to the VAB and after cooldown, deactivation, and personnel and priority cargo removal operations have been performed, SERV is loaded onto the wheeled transporter used previously for land movement at MAF. The loading of SERV onto the transporter is accomplished by positioning dollies under the landing gear pads and winching SERV up ramps onto the transporter for delivery to the VAB high bay.

The chart identifies major sequential operations required in preparation for vehicle storage, or recycling for launch. The platform enclosure that can be raised and lowered to encompass the SERV assembly in the VAB high bay provides a ready means for personnel access to all levels during disassembly, servicing, refurbishment and assembly regardless of the launch configuration required. During configuration disassembly and assembly operations, hoist capability is provided by an existing 250-ton traveling bridge crane in the VAB. A new LUT and existing crawler-tractor (CT) provide the transportation system to LC-39 in a similar manner to the Saturn V.

The SERV storage, servicing and vehicle assembly and disassembly operations are performed in the VAB high bay area. The cargo module, MURP and Personnel Module, storage, servicing, assembly and disassembly of cargo are performed in the low bay area.

The MURP spacecraft would return to KSC from orbit and land on the existing skid strip. MURP would be tractor towed from the strip via the Orsino Causeway to the VAB low bay for recycling to storage or relaunch as required.

SERV SPACECRAFT GROUND OPERATIONS

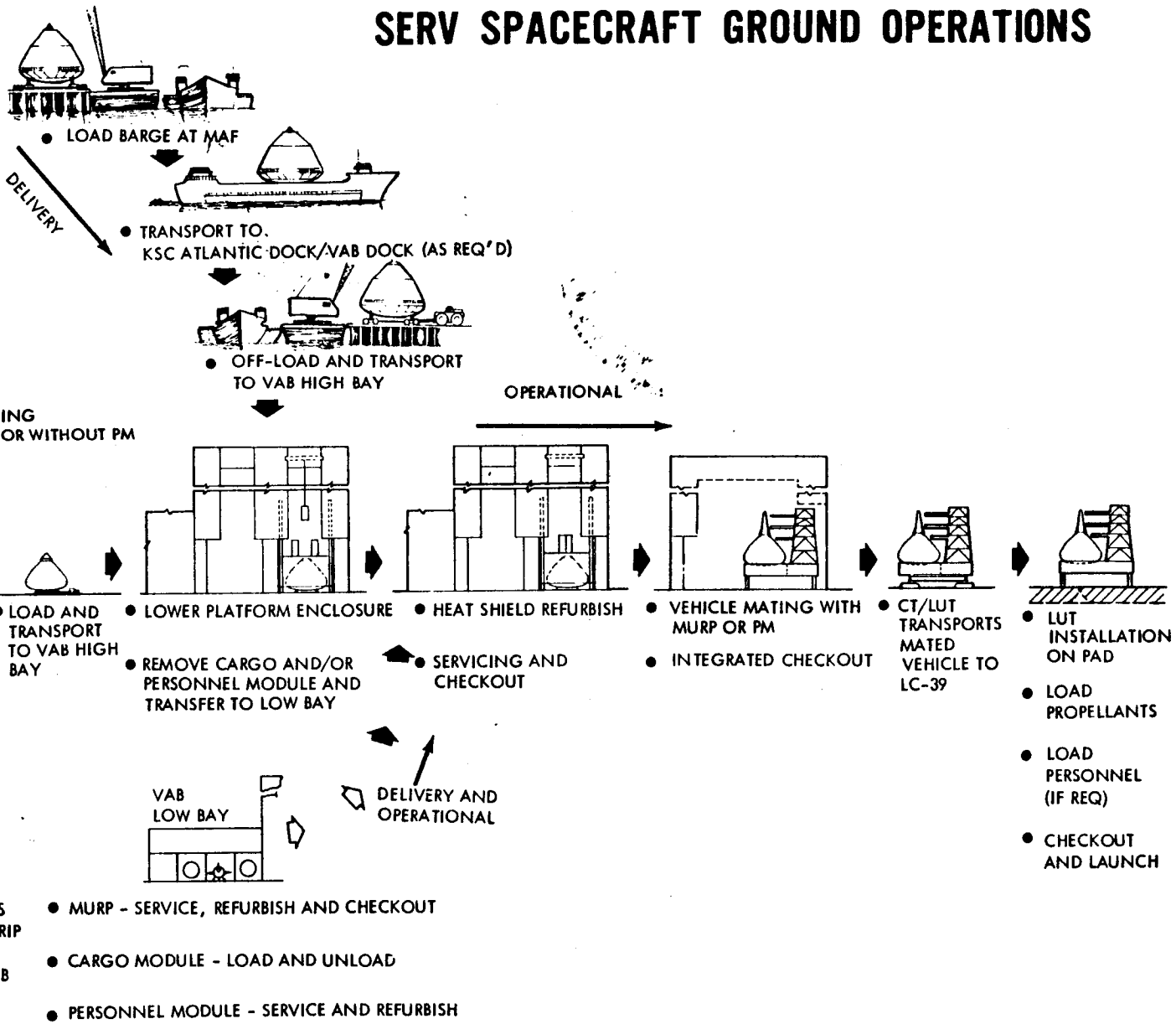

9.3.2 OPERATIONS TIME LINE

The chart identifies in sequential order the major ground operations from landing to launch within a 10-day period. The operation time line assumes an 8-hour work day. If mission demands are such that a continuous 24-hour operation is required, then theoretically the turnaround cycle with three 8-hour crew shifts becomes 3.3 days. However, practical considerations such as safety, or where transporation may be locally restricted or completely limited to daylight movement, could increase turnaround time on an emergency basis to 4 to 5 days.

The chart shows a marked similarity of operations for both the SERV vehicle (with or without the PM) and the MURP spacecraft during the complete ground cycle. The first day after landing (day 10) involves propellant draining and inerting of the vehicle after cooldown, in addition to egress of passengers and unloading of priority cargo via enclosures mounted on cherrypicker vehicles.

Day 9 involves the preparation and transportation of the SERV or MURP to the VAB from the landing pad or existing skid strip, respectively, removal of down cargo and the start of servicing and refurbishment operations on the vehicle (SERV, PM or MURP).

During the period of day 9 to 6 ablative materials will be replaced and any inflight recorded failures or malfunctions will be corrected on a modular remove and replace basis. During these operations the down cargo will be transferred to the low bay, unloaded and dispersed as required.

Day 5 completes all visual and system self-test to ensure operational readiness of each vehicle (SERV, PM and MURP) and their assignment to storage or reuse.

Day 4 and 3 involves the assembly of all vehicles and the cargo module, as mission dictates, on the LUT previously positioned in the high bay, connection of LUT and intervehicle interfaces and self-test of integrated systems. If the cargo is of an explosive or highly flammable nature such as propellants, the loading of such will be conducted at the pad.

Day 2 and 1 involves the transportation of the vehicle assembly on the LUT/CT to LC-39, pad A or B, connection of pad LUT interfaces involving propellant lines, power for monitoring and communications, etc. This would be followed by ingress of personnel (if required), final system self-test and launch.

For an emergency turnaround, the major time consuming period is the 3 days (day 9.5 to 6.5) for replacing the SERV ablative material. This operation can be condensed to 24 hours by manning three 8-hour shifts of four crews (one crew assigned to each quadrant of the heat shield) removing and replacing panels on a continuous basis. In addition, other internal and external servicing, refurbishment and inspections can be performed during this period.

OPERATIONS TIME LINE

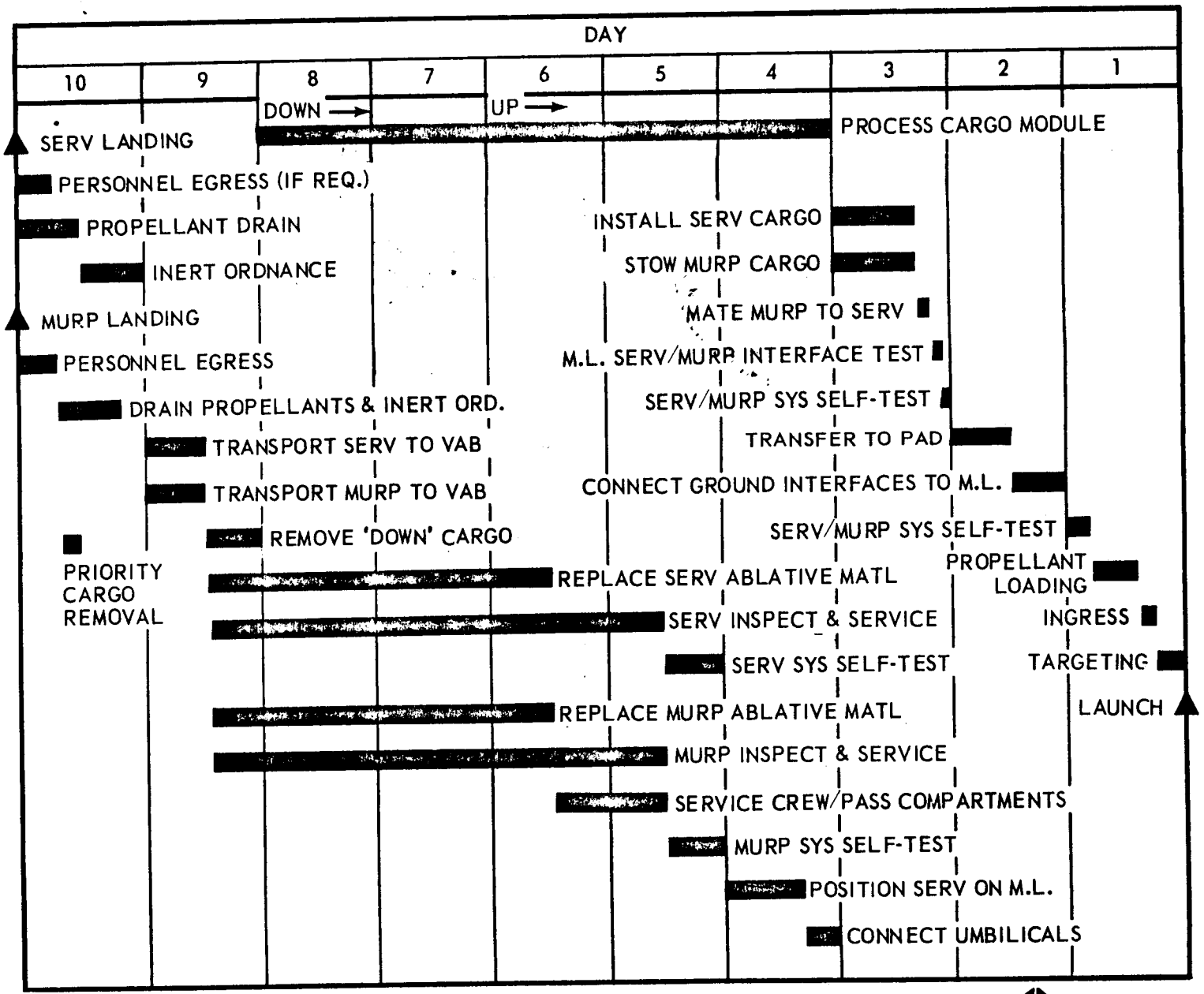

SPACE DIVISION CHRYSLER CORPORATION

9.3.3 VAB UTILIZATION

The chart shows the plan view of operations in the KSC-VAB. All SERV vehicle activities are within the high bay and the MURP spacecraft, Personnel Module and Cargo Modules and associated processing activities are in the low bay.

Following the removal of Saturn V stage equipment and installation of the SERV equipment, additional internal modification to the building is limited to removal of some existing scaffolding up to floor 10, about 115 ft from the ground, in each of the 4 high bay cells to accommodate the SERV diameter when on the LUT.

Using the two existing 250 ton traveling bridge cranes which span the center aisle and two opposite cells, and the 175 ton traveling bridge crane which spans both the high and low bay center transfer aisle, the MURP spacecraft or Personnel Module and the Cargo Module can be moved for assembly, servicing, or refurbishment as required.

VAB UTILIZATION

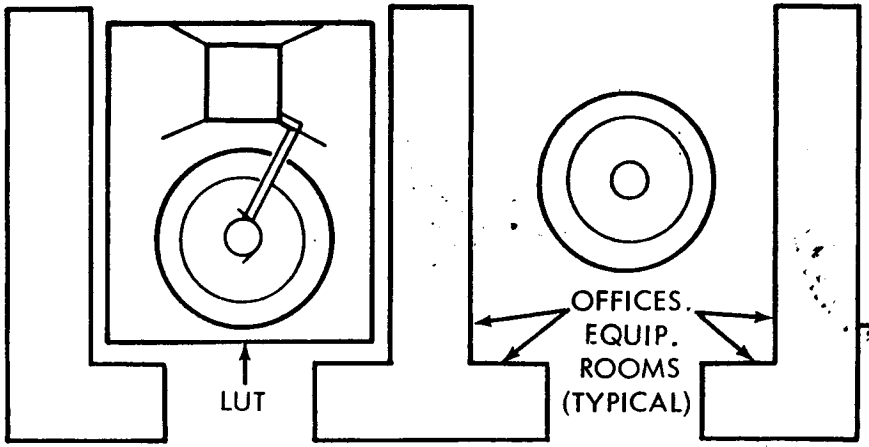

- **HIGH BAYS**
  - REMOVE SATURN V EQUIPMENT
  - INSTALL SERV, SPACECRAFT AND CARGO MODULE EQUIPMENT
- **LOW BAYS**
  - REMOVE S-II AND S-IVB EQUIPMENT
  - INSTALL SPACECRAFT AND MODULAR EQUIPMENT
  - ENLARGE LOW BAY DOOR

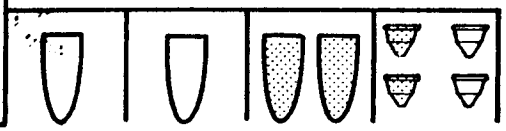

WINGED SPACECRAFT
AND PERSONNEL MODULES

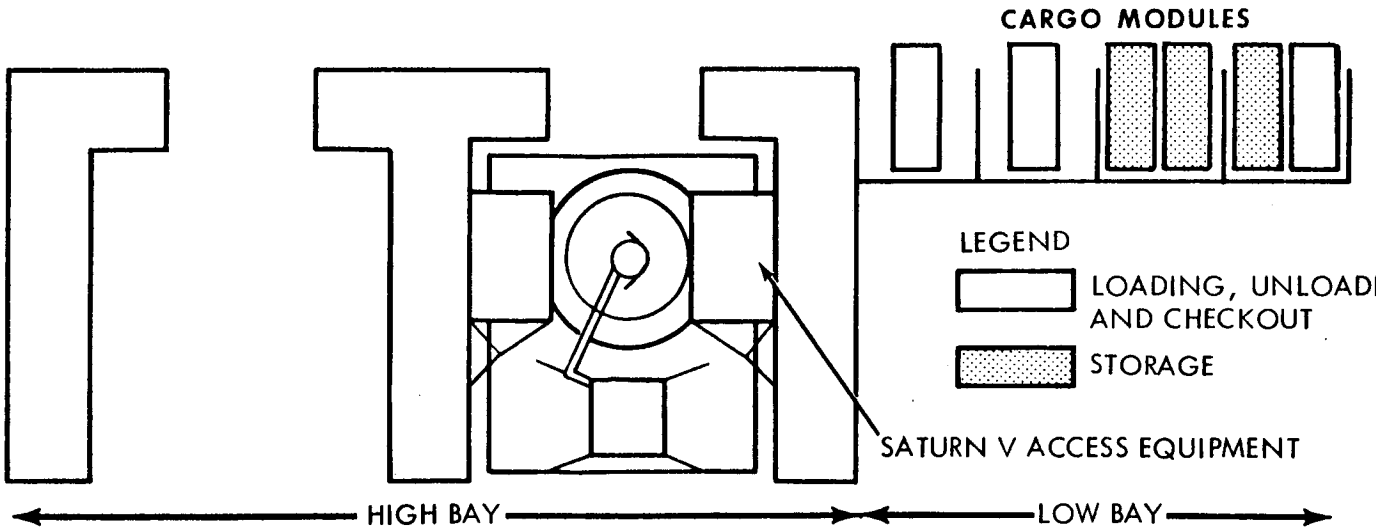

9.3.4 LAUNCH AT LC-39

This chart shows the SERV assembly in the launch position. Interchangeability of launch vehicles involving the SERV, Saturn V and a "pedestalled" Saturn IB at either Pad A or Pad B has been a prime consideration. This capability still exists. Major modifications to either launch complex to achieve this interchangeability are as follows:

1) Installation of an additional 850,000-gallon liquid hydrogen storage tank system for the SERV vehicle.

2) Two portable circular segment flame deflectors for installation between the pad and the undersurface of the mobile base of the LUT and adjacent to either side of the flame trench. The flame deflectors assist, in conjunction with the built-in flame deflectors of the mobile base, to converge the exhaust plume into the 58-ft-wide trench. The flame deflectors require film cooling to reduce refurbishment.

3) The possible need for a new flame deflector of different design in the trench. Further pad-plume impingement studies will establish if this is a necessity.

The size and height of the mobile base of the LUT is identical to that of the Saturn V LUT, consequently the six LUT-to-pad mount mechanisms and the adjacent interfacing towers for propellant loading, electrical connections, etc. can be used without modification. Major LUT modifications involve reducing the Saturn V umbilical tower height by about two-thirds , using 3 of the 9 existing swing arms and increasing the flame hole from 45 ft square to 90 ft diameter.

Pad operations will be limited to interface connections between pad and LUT, propellant loading (including propellant cargo), crew and passenger ingress (if required) and minimum on-board checkout of systems prior to launch.

LAUNCH AT LC-39

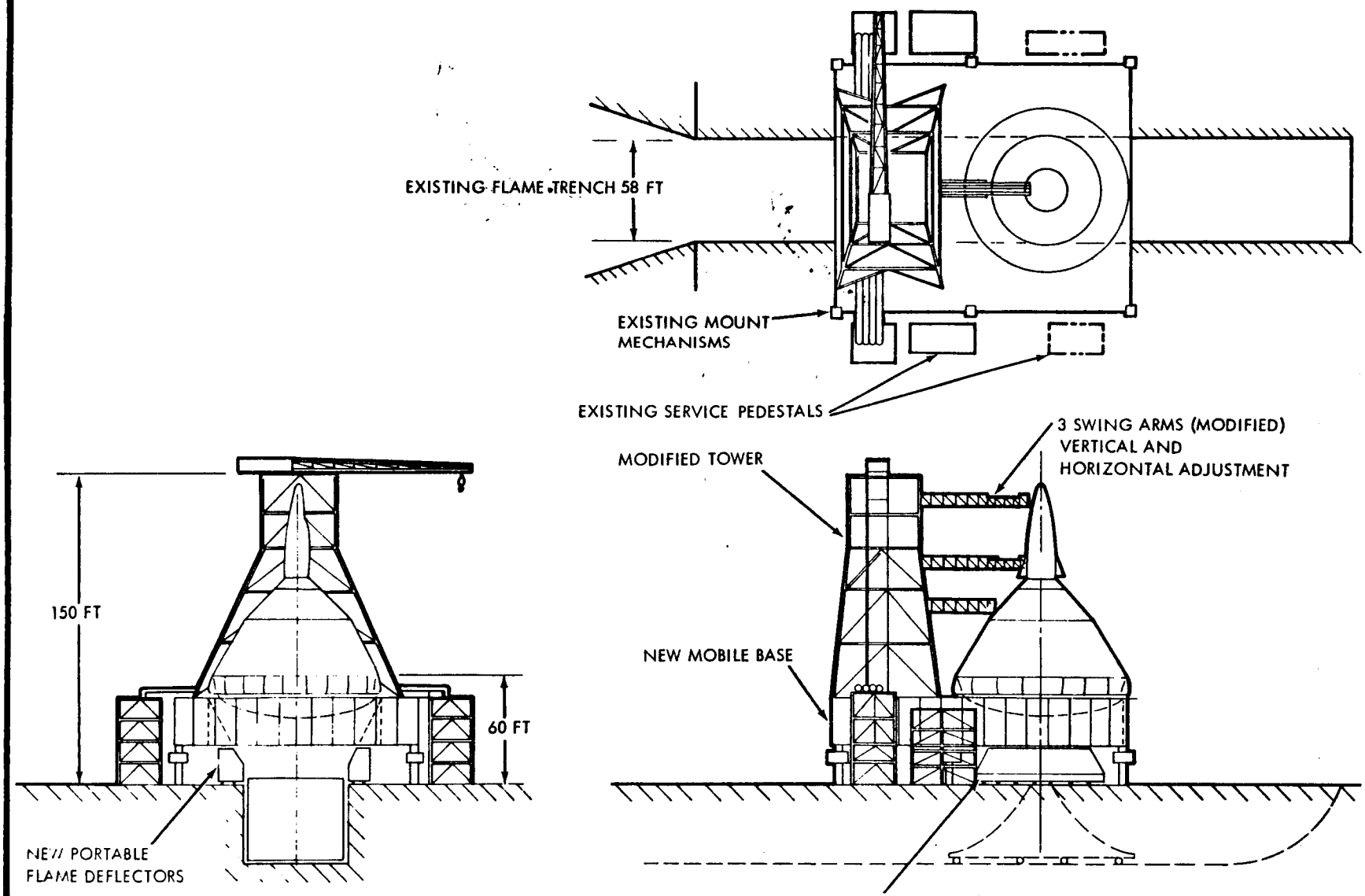

115

SPACE DIVISION CHRYSLER CORPORATION

SCHEDULES AND COSTS

Section 10

SCHEDULES AND COSTS

10.1 SERV PROGRAM

The cost ground rules, program schedule, and ROM program costs are discussed in this section. Since the major emphasis of this study is on SERV, most effort has been concentrated on SERV activities. Cost data for the MURP spacecraft were obtained from NASA reports, and cost data for the PM spacecraft were developed from Chrysler in-house studies supplemented by data from NASA reports. For the purpose of this study, it is assumed that the spacecraft procurement schedule is compatible with the SERV schedule. This assumption is considered reasonable because one feature of the SERV concept is that the spacecraft and booster can be developed independently; thus, SERV is not dependent on the spacecraft to fulfill its capability to deliver payload to orbit.

10.1.1 SCHEDULE AND COST GROUND RULES

Special reference is made to the first ground rule for it highlights an important feature of the SERV concept, namely, that since most projected missions of the baseline 10-year traffic model are of an unmanned nature (e.g., propellant transportation), the procurement of fewer spacecraft is possible. Hence, the investment of four SERV's and three spacecraft is required.

Both flight test vehicles referred to in the second ground rule will be recycled as production vehicles.

SCHEDULE AND COST GROUND RULES

- INVESTMENT OF FOUR SERV'S AND THREE MURP'S OR PM'S
- TWO SERV FLIGHT TEST VEHICLES
- FIRST MANNED ORBITAL FLIGHT IN 2ND QUARTER CY 1978
- IOC IN SECOND HALF OF CY 1979
- 445 OPERATIONAL FLIGHTS
- ONE LAUNCH SITE, LOCATED AT KSC
- 1972 TECHNOLOGY BASE
- PHASE C/D STARTS ON JANUARY 1, 1973
- LEARNING CURVE ON SERV HARDWARE 95 PERCENT, EXCEPT 90 PERCENT ON TPS REPLACEMENT PANELS
- RDT&E FUNDING CONCLUDED 24 MONTHS AFTER FIRST VERTICAL MANNED FLIGHT
- FACILITY COSTS INCLUDED
- CONTRACTOR FEES AND GOVERNMENT MANAGEMENT COSTS EXCLUDED
- COSTS REPORTED IN CONSTANT CY 1971 DOLLARS

10.1.2 PROGRAM SCHEDULE SUMMARY

The program schedule is a projection of activities for those elements having a major impact on the initiation of the program through to the first manned orbital flight (FMOF). The schedule shows a 12-month, Phase B study commencing in the last quarter of CY 1971. This is followed by phases C and D starting at the beginning of CY 1973, with 90 percent engineering release at the end of CY 1974 and 100 percent release 10 months later. Facility modifications are identified at MAF and KSC. Modifications of MAF facilities are scheduled for the start of CY 1973, with emphasis directed toward the modification, tooling and fixtures for building 420. Modifications of KSC facilities can be delayed a year after the start of MAF modifications.

It is proposed to build one structural test vehicle (STV-1), which will be used for handling and transportation equipment checkout, a mode and frequency test and a static loads and life cycle test tollowed by a test to destination. These tests will be conducted at KSC and take approximately 20 months to complete.

A static fire vehicle (SF-1) will be utilized in the program for propellant load, cold flow and static fire tests. Turbojets and other subsystems will not be installed. The tests, of 15 months duration, will be conducted at KSC and after completion the vehicle will be overhauled, refitted and cycled as a production vehicle.

The first flight test vehicle (FT-1) will be fitted with turbojets and associated subsystems and used for horizontal and vertical translation flight tests at KSC. An aerospike engine will not be installed in this vehicle. The translation tests are scheduled to take 6 months and will be completed 3 months before the completion of checkout of the first orbital flight vehicle. Following satisfactory completion of the horizontal and vertical translation tests, the vehicle will be returned to MAF for recycling as a production vehicle.

The second flight test vehicle (FT-2) will be utilized for orbital flight test and will be delivered to KSC 12 months prior to the first manned orbital flight. Prior to the first manned flight, two unmanned orbital tests flights will be accomplished.

Throughout the aforementioned development period, subsystem and component development and qualification tests will be performed at MAF and other government and contractor facilities.

The critical path for the schedule is as follows: 1) complete model tests; 2) initiate MAF and building 420 modifications; 3) commence installment of major tooling and fixtures; 4) MAF facility complete and checked out; 5) 90 percent engineering release, start final assembly of structural test vehicle (STV-1) and static fire test vehicle (SF-1) and start facility installations at KSC; 6) 100 percent installation of major tooling at MAF; 7) 100 percent engineering release and shipment of STV-1; 8) delivery and installation of first aerospike engine modules; 9) delivery and installation of first direct lift gas turbine engines; 10) completion of vehicle static loads, static fire, translation tests and completion of subsystem development and qualification tests; 11) two unmanned orbital flights prior to FMOF; and 12) manned/unmanned flights prior to IOC.

PROGRAM SCHEDULE SUMMARY

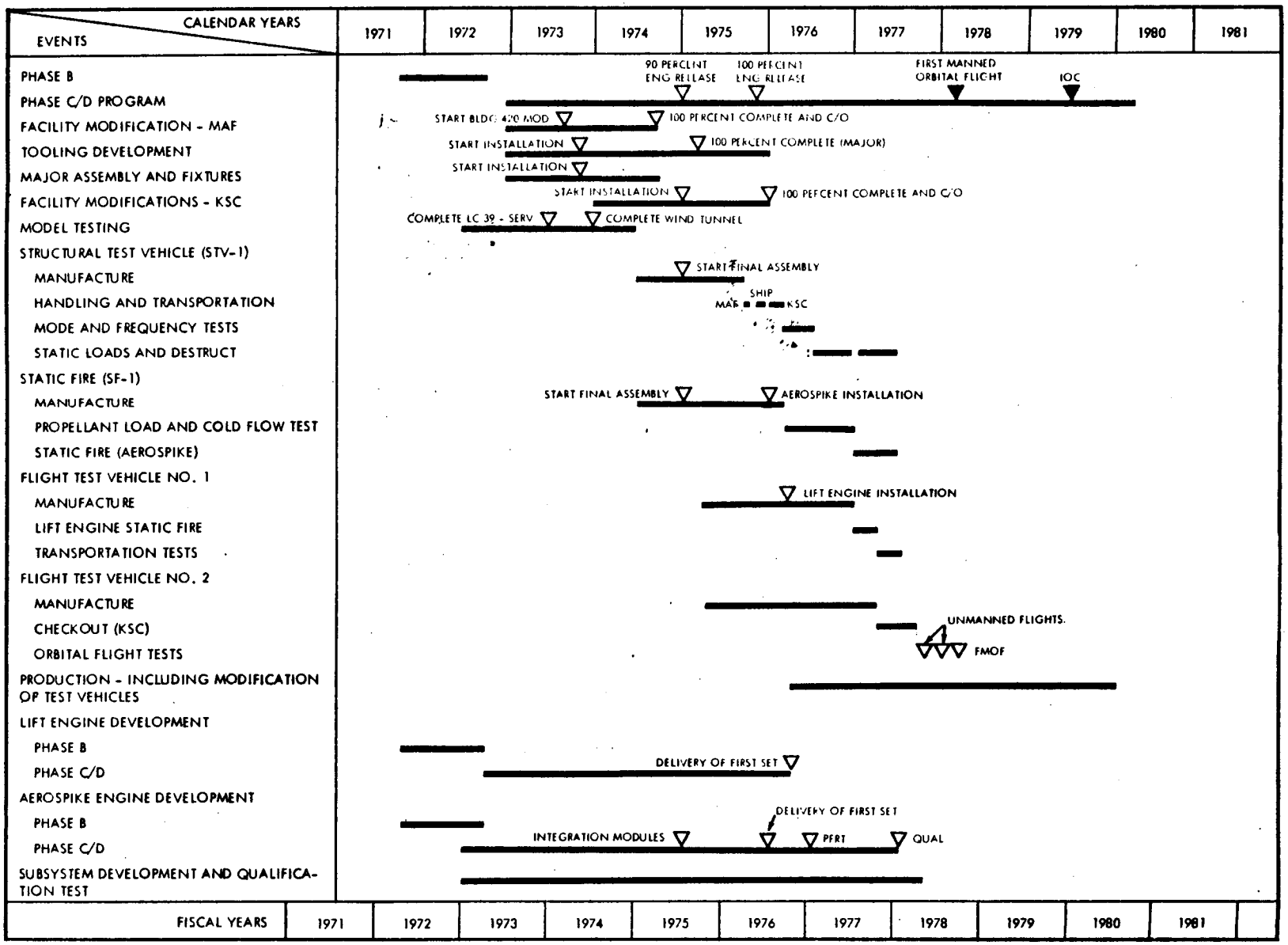

SPACE DIVISION CHRYSLER CORPORATION

10.2 PROGRAM COSTS

In general, costing was accomplished with the aid of a computerized cost model using direct-estimate data or Cost Estimating Relationships (CER's) where estimates were either unavailable or impractical.

10.2.1 PROGRAM COST DISTRIBUTION

Through application of the cost model, program cost distribution curves were developed for a SERV-PM program, SERV-MURP program, and SERV only program.

A program cost summary is also shown on the chart to illustrate the major program cost categories of RDT&E, investment, and operations. The SERV cost breakdown includes the cost for development and operation of SERV only; the spacecraft and program management costs required for accomplishing a total shuttle program are excluded. The SERV-PM and SERV-MURP costs, however, include all costs necessary for the performance of a total program.

The cost distribution curve indicates the peak funding requirement. The SERV-MURP program has the higher peak because of its higher development cost. Any planned delay in program IOC or decoupling of spacecraft and launch vehicle development will reduce the peak funding levels.

PROGRAM COST DISTRIBUTIONS

PROGRAM COST SUMMARY (10^6 $)			
CONFIGURATION	SERV	SERV-PM	SERV-MURP
RDT&E	3890	4714	6530
INVESTMENT	1405	1639	1689
SUBTOTAL	5295	6353	8219
OPERATIONS	1437	1804	1873
TOTAL	6732	8155	10092
TOTAL (LESS MAIN ENG.)	6084	7476	9413

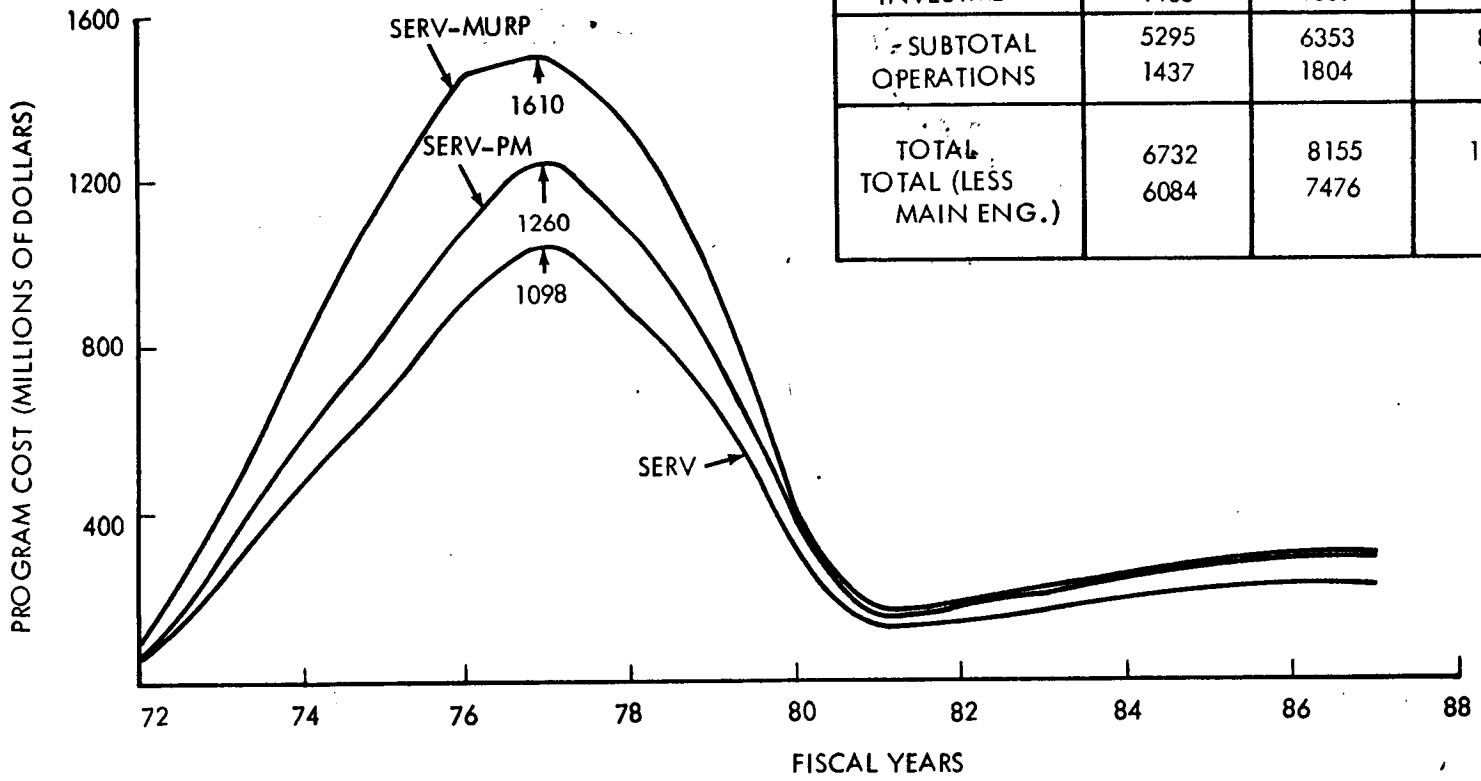

119

SPACE DIVISION CHRYSLER CORPORATION

10.2.2 SERV FIRST UNIT COST

First unit costs for the hardware Work Breakdown Structure (WBS) items are shown and were developed primarily from CER's.

The cost for the advanced reusable aerospike engine was supplied by Rocketdyne. The lift-engine cost was supplied by the Detroit Diesel Allison Division of General Motors Corporation. Attitude control system first unit cost was obtained from CER's for a twenty, 4000-lb thruster subsystem.

The avionics subsystem first unit cost is for a fully automated unmanned system and was developed from CER's.

The first unit cost for the structures was based on an Inconel sandwich structure. The TPS system first unit cost is for an ablative system.

The power system first unit cost includes the cost of batteries, fuel cells and the distribution system, and was developed from CER's. The hydraulic system first unit cost was developed from CER's utilizing system dry weight as the principal variable.

The investment cost for the program was estimated from the SERV first unit cost and a 95 percent learning curve.

SERV FIRST UNIT COST

WBS ITEM		TOTALS
• PROPULSION		
- AEROSPIKE ENGINE	60.0	
- LIFT ENGINES	29.5	
- ATTITUDE CONTROL	8.5	98.0
• AVIONICS		
- GUIDANCE AND NAVIGATION	8.0	
- INSTRUMENTATION	5.6	
- COMMUNICATIONS	1.4	14.8
• AIRFRAME		
- STRUCTURES AND TPS	202.0	
- LANDING	1.0	203.0
• POWER		
- ELECTRICAL	22.7	
- HYDRAULIC AND PNEUMATIC	2.1	24.8
• ASSEMBLY AND CHECKOUT		9.5
• FIRST UNIT COST TOTAL		350.1

(MILLIONS OF 1971 DOLLARS)

10.2.3 OPERATIONS COST

Typical annual operating costs at 75 flights per year and the typical cost per flight for a 445 flight program are shown for both SERV-MURP and SERV-PM programs.

Ground operations costs were developed through detailed analysis and include the cost of manpower necessary to conduct base operations at KSC. These manpower requirements include maintenance, repair, refurbishment, handling, training, propellant loading, overall system tests and checkout, quality assurance, logistics, and administration. The total manning requirement for a 75 flight per year program is 890 personnel.

The cost for flight spares, flight operations, training facility maintenance, program management and payload integration were developed from CER's.

Refurbishment and overhaul costs are based on the requirements for an ablative heat shield, and were obtained from detailed cost estimates. A 90-percent learning curve was applied to derive the replacement heat shield cost.

Fleet amortization was based on a 60-percent unmanned to total flight ratio and a 500-flight vehicle life.

The difference in operations cost between the SERV-MURP and SERV-PM vehicle can be attributed primarily to the return mode of the spacecraft. The MURP spacecraft returns independently of the SERV whereas the personnel module returns with SERV. This important difference in mode of operation results in a decrease in the cost of SERV-PM ground operations, flight spares, and flight operations.

OPERATIONS COST

(MILLIONS OF 1971 DOLLARS)

TYPICAL ANNUAL COST (AT 75 FLIGHTS PER YEAR)	SERV-MURP	SERV-PM
GROUND OPERATIONS	31.9	31.2
PROPELLANTS	31.5	31.5
FLIGHT SPARES	67.7	59.7
FLIGHT OPERATIONS	19.5	16.5
TRAINING	6.5	6.5
FACILITY MAINTENANCE	20.0	20.0
PROGRAM MANAGEMENT	9.7	9.7
PAYLOAD INTEGRATION	30.0	30.0
REFURBISHMENT - OVERHAUL	70.1	70.1
TOTAL ($M/YR)	286.9	275.2

TYPICAL COST PER FLIGHT (445 FLIGHT PROGRAM)	SERV-MURP	SERV-PM
OPERATIONS	4.21	4.05
FLEET AMORTIZATION	0.86	0.83
TOTAL ($M/FLT)	5.07	4.88

10.2.4 PROGRAM HIGH COST AREAS

The cost model calculates the total cost of each work breakdown structure (WBS) element and computes each of these costs as a percent of total program cost. This value has an important function in meaningful cost analysis, as it permits management visibility into the high cost areas of a program. The identification of these areas is an important step in determining where cost savings efforts can best be expended. In addition, the cost model breaks these costs down (lower levels of the WBS) so that WBS elements contributing to the cost of a particular system can be identified as "cost drivers" in each area.

A typical breakdown of the SERV Shuttle Program cost and selected high cost areas are presented. The table identifies the high cost areas by WBS element, percentage of total program cost, and the cost drivers of the WBS element; all other elements have lower percentage costs. Note that the five RDT&E high cost areas identified account for 28.06 percent of the program cost, and this represents 48.3 percent of the total RDT&E cost. Restated, five areas account for approximately 48 percent of the program RDT&E cost.

PROGRAM HIGH COST AREAS

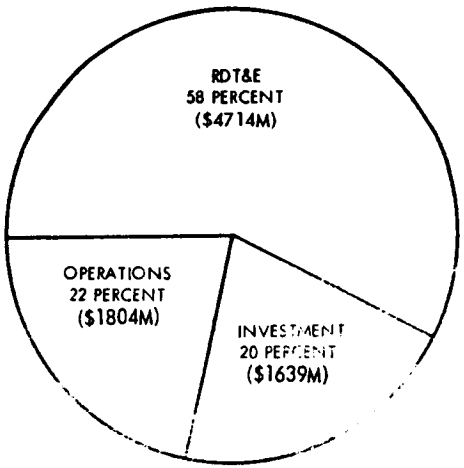

AREA	PERCENTAGE TOTAL PROGRAM COST	COST DRIVERS
SERV FLIGHT TEST - RDT&E	8.21	MONTHS IN FLIGHT TEST PROGRAM, NUMBER OF TEST FLIGHTS, TEST HARDWARE.
STRUCTURES - RDT&E	7.58	DEVELOPMENT OF SANDWICH FABRICATION, EBW WELDING AND NON-DESTRUCTIVE TESTING TECHNIQUES.
MAIN ENGINES - RDT&E	6.82	ENGINE THRUST, CHAMBER PRESSURE, SPECIFIC IMPULSE.
STRUCTURES - INVESTMENT	4.20	FABRICATION OF SANDWICH.
GROUND TEST - RDT&E	3.19	STRUCTURAL TESTING, HOT FIRING, WIND TUNNEL TESTING.
PROGRAM SYSTEM ENG - RDT&E	2.26	ENGINEERING SUPPORT TO INTEGRATION AND DEVELOPMENT ACTIVITIES.

10.2.5 PROGRAM NON-RECURRING COST BREAKDOWN

The following two charts show the SERV-PM Program work breakdown structure (WBS) and associated costs. For each WBS element, the RDT&E cost is in the lower left-hand corner box and the investment cost is in the lower right-hand corner box.

The first chart shows the WBS cost elements to the system level, Level 4. The lower level elements are summed to give the higher order element cost. The one exception to this is for the Level 3 SERV investment cost which includes the cost of modification of R&D vehicles plus the cost of lower element systems.

It is important to note that the costs on this chart are for a SERV-PM program, and no operating costs are shown.

PROGRAM NON-RECURRING COST BREAKDOWN BY WBS ELEMENTS

(MILLIONS OF 1971 DOLLARS)

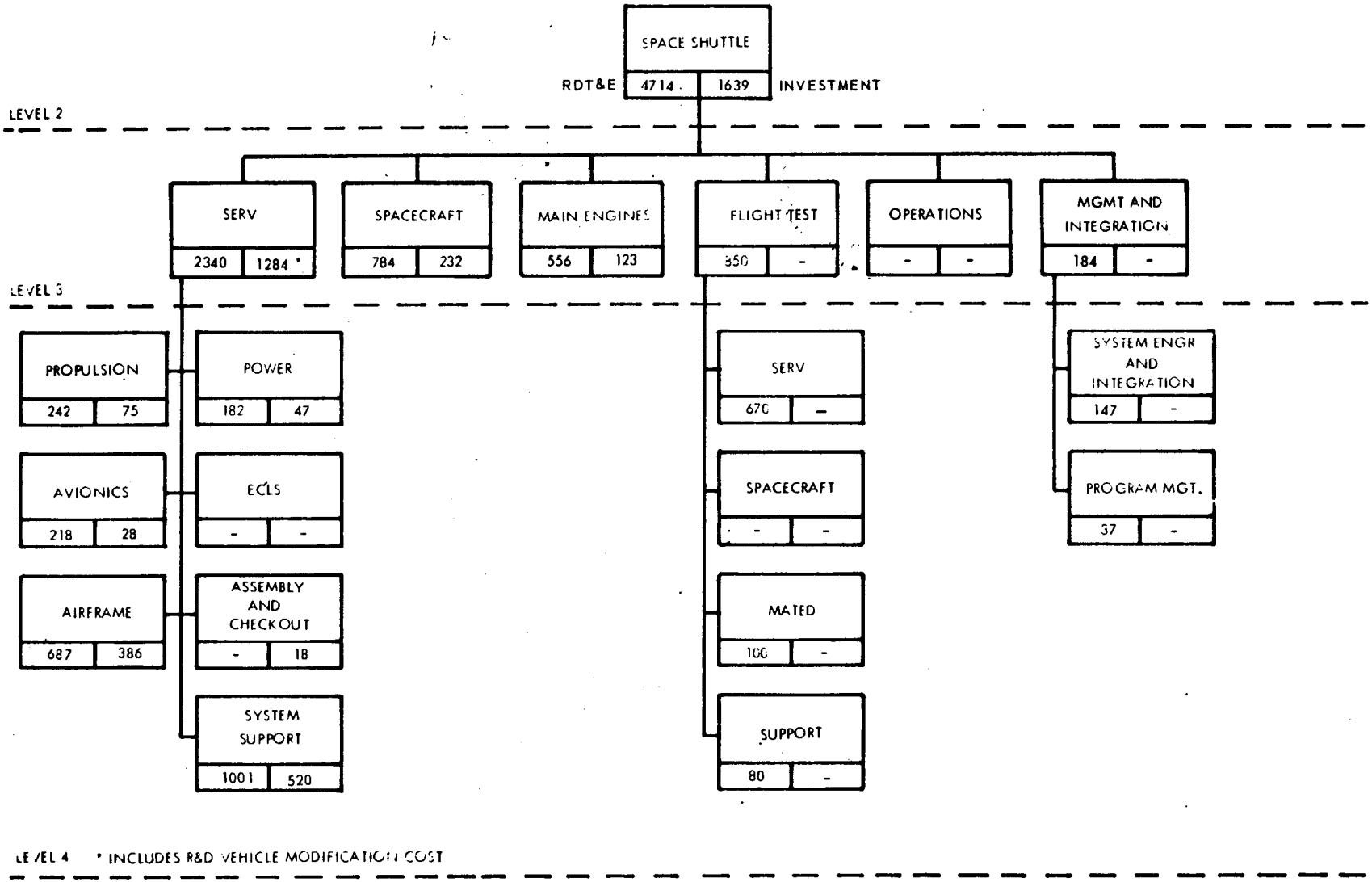

10.2.6 SERV NON-RECURRING COST BREAKDOWN

This chart has the same format as the preceding chart and shows costs to the subsystem element, Level 5.

It should be noted that these costs are for SERV development and investment only and do not include the main engine, flight test, management, and integration, costs which are essential elements of a SERV vehicle program.

SERV NON-RECURRING COST BREAKDOWN BY WBS ELEMENTS

(MILLIONS OF 1971 DOLLARS)

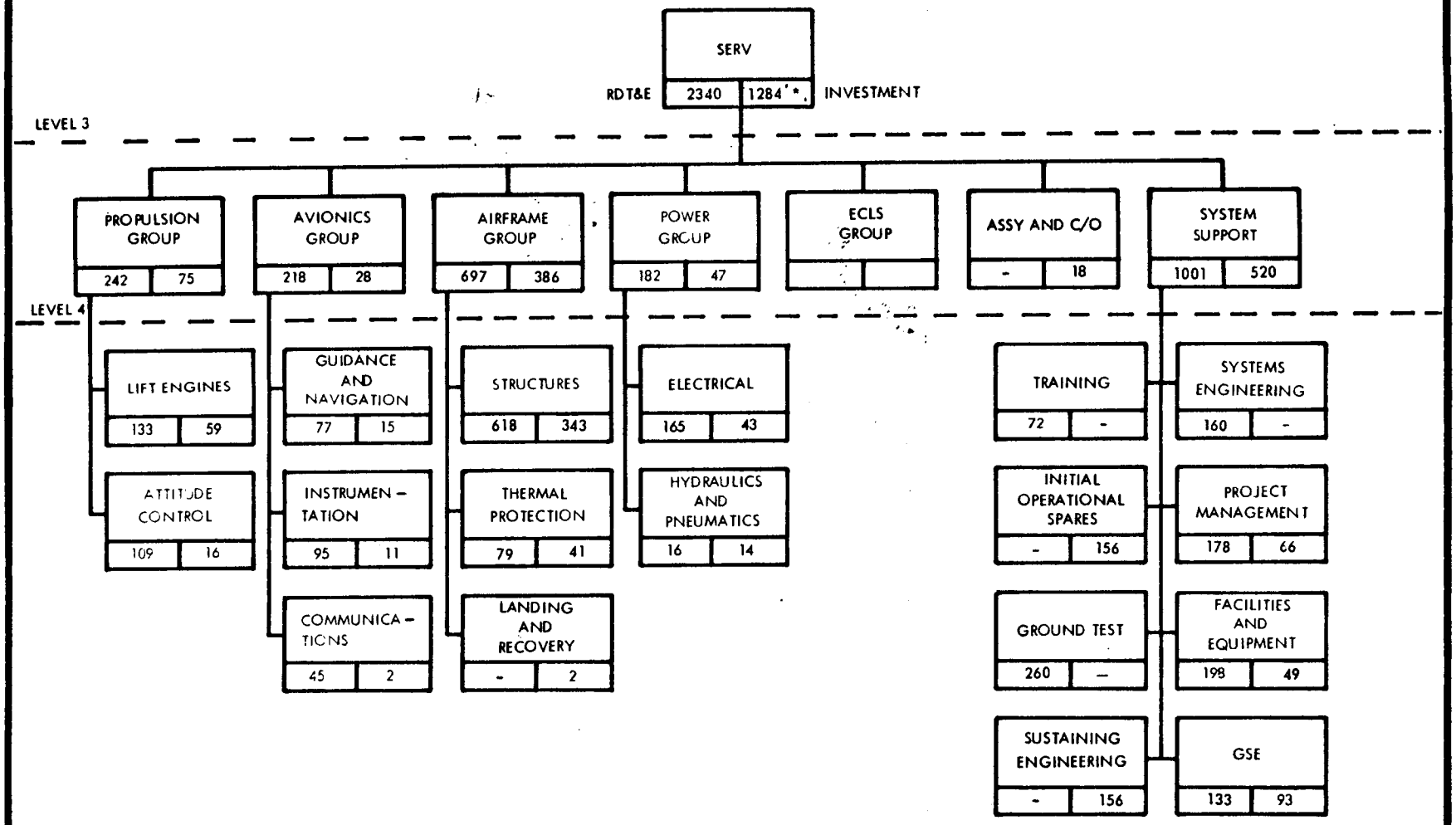

SPACE DIVISION CHRYSLER CORPORATION

CONCLUSIONS AND RECOMMENDATIONS

Section 11
CONCLUSIONS AND RECOMMENDATIONS

11.1 FEASIBILITY ISSUE CONCLUSIONS

Feasibility issue conclusions are listed on this chart. The six key issues are covered within the limitations of the study: performance, weights, ascent aerodynamics, descent aerodynamics, thermal protection, and reentry and landing.

FEASIBILITY ISSUE CONCLUSIONS

- FEASIBILITY OF AEROSPIKE PERFORMANCE FOR SERV APPLICATION CONFIRMED WITHIN LIMITATIONS OF COLD FLOW TESTS
- SSTO WEIGHT FACTORS CONFIRMED BY STRUCTURAL AND SUBSYSTEM ANALYSES
- ASCENT AND REENTRY AERODYNAMIC CHARACTERISTICS ESTABLISHED BY WIND TUNNEL TESTS
- HONEYCOMB FOREBODY TPS AND ABLATIVE HEATSHIELD TPS SELECTED
- VEHICLE STABLE THROUGHOUT REENTRY FROM DEORBIT TO TOUCHDOWN
- FOUR-MILE TARGET RADIUS AT 25,000 FT LANDING INTERFACE ADEQUATE WITH SUITABLE POSITION UPDATE
- AUTOMATIC LANDING PRINCIPLE WITH TURBOJET LIFT ENGINES FEASIBLE
- CAPABILITY FOR INTACT ABORT AND ABORT FOR CREW SURVIVAL IDENTIFIED
- MANUFACTURE AT MAF AND LAUNCH FROM KSC FEASIBLE WITH MINIMAL FACILITY CHANGE

11.2 CONCEPT CONCLUSIONS

Principal conclusions related to the SERV concept are listed here.

CONCEPT CONCLUSIONS

- CONCEPT AS ORIGINALLY CONCEIVED REMAINS FEASIBLE
- CONCEPT IS AN ATTRACTIVE SHUTTLE ALTERNATE EVEN WITH THE HIGH SENSITIVITIES AND ABSENCE OF CARGO CROSSRANGE
- FURTHER SYSTEM/SUBSYSTEM OPTIMIZATION, INCLUDING OPERATION OF LIFT ENGINES DURING ASCENT, CAN REDUCE GLOW
- FURTHER INVESTIGATIONS SHOULD BE UNDERTAKEN TO MAINTAIN SERV AS AN ALTERNATE OR ADVANCED CONCEPT FOR NASA AND DOD CONSIDERATION

11.3 RECOMMENDATIONS FOR FURTHER EFFORT

Recommendations for further effort are listed for two areas: further vehicle investigations (items 1 through 4) and supporting studies of the ascent main engine and the landing main engines (items 5 and 6) .

RECOMMENDATIONS

FURTHER IN-DEPTH INVESTIGATION OF SERV -

- CONFIGURATION AND SUBSYSTEM OPTIMIZATION
- STRUCTURAL DESIGN
- SUBSYSTEM WEIGHTS
- REENTRY AND LANDING CONCEPT
- INTEGRAL AEROSPIKE
- TURBOJET LIFT ENGINE